A Natural Protective Mechanism Against Malaria

The Role of Gut Flora

Bahtiyar YILMAZ

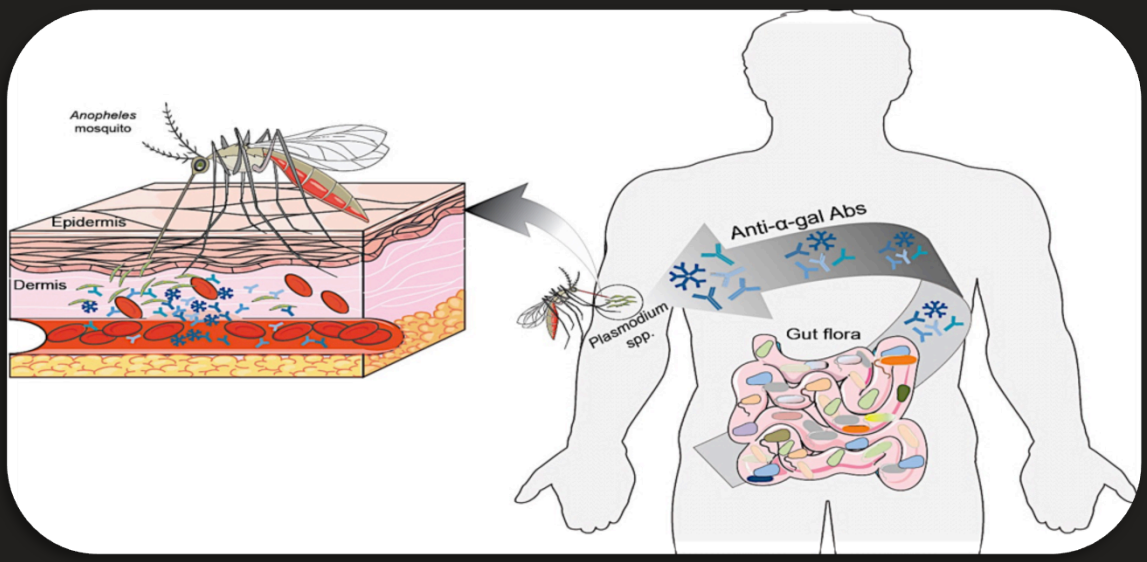

Dissertation presented to obtain the Ph.D degree in Immunology

Instituto de Tecnologia Química e Biológica | Universidade Nova de Lisboa

Oeiras,
February, 2015

INSTITUTO
DE TECNOLOGIA
QUÍMICA E BIOLÓGICA
/UNL

Knowledge Creation

ITQB-UNL | Av. da República, 2780-157 Oeiras, Portugal
Tel (+351) 214 469 100
Fax (+351) 214 411 277

www.itqb.unl.pt

A Natural Protective Mechanism Against Malaria

The Role of Gut Flora

Bahtiyar YILMAZ

Dissertation presented to obtain the Ph.D degree in Immunology

Instituto de Tecnologia Química e Biológica | Universidade Nova de Lisboa

Research work coordinated by:

FUNDAÇÃO CALOUSTE GULBENKIAN
Instituto Gulbenkian de Ciência

Oeiras,
February, 2015

INSTITUTO
DE TECNOLOGIA
QUÍMICA E BIOLÓGICA
/UNL

Knowledge Creation

To my Dear Father…

The study described in this Ph.D. thesis was performed at Instituto Gulbenkian de Ciência (IGC), Oeiras, Portugal and was financially supported by Fundação para a Ciência e a Tecnologia (FCT), Portugal (SFRH/BD/51176/2010).

The work on this thesis resulted in the following publication and some written content of the thesis was introduced into the following publication:

Yilmaz, B., Portugal, S., Tran, T. M., Gozzelino, R., Ramos, S., Gomes, J., et al. (2014). Gut Microbiota Elicits a Protective Immune Response against Malaria Transmission. Cell, 159(6), 1277–1289. doi:10.1016/j.cell.2014.10.053

Acknowledgements

The work obtained during this amazing journey only exists due to the amazing people and their significant amounts of help -no matter it is scientific or not.

First all, my father… Still I remember the day when I was struggling on making a decision to go to Portugal. Your enthusiasm led me here to do this amazing study. Hope you are watching from up there -your true success story.

I'd like to continue expressing my deep appreciation chronologically depending on the time of getting scientific input or help from all of you. While I try my best not to forget any of you, in any case if I forget, please accept my apologies on top of my gratitude. Initially, I would like to thank and express my sincere gratitude to my supervisor, Miguel Che P. Soares, who introduced me this project. Thank you for giving me opportunity to work on this subject. I've learned a lot from you with your guidance and contribution during my PhD study. I appreciate your effort. Later, I would like to thank my thesis committee members, Alekos Athanasiadis and Jocelyne Demengeot. The day that we proposed our PhD project, thesis committee was assigned to help us through this journey with their experiences and scientific inputs. I am indebt to them for their advice – both the scientific and utterly practical. Afterwards, I would like to thank Inflammation Group (past and present members). In the beginning, Ana Ferreira taught me the basics of experimental malaria model. Thank you very much for your patience that you showed during my learning process. Susana Ramos… Soon after I joined to Inflammation Group, she was recruited too. Susana, you are the greatest. My best friend in Portugal... You have borne my all naïve and stupid questions about malaria. You helped me in all critical experiments with your knowledge and experience.

That makes you the greatest! Thank you very much for everything you have done. In addition, I enjoy every small coffee break that I had with you. I will miss that. Raffaella Gozzelino, the master of the Western blots… Your contribution on this study is incredibly crucial. Thanks a lot for your all help and incredibly cheerful friendship. Every lab needs one CC of you. Silvia Cardoso and Sofia Rebelo taught me how to work with murine model. Your patience to me when I was training mice cannot be described. Hope I can teach the same way as you did to me to the future scientists. Thank you guys! Rasmus Larsen… It was a pleasure to work with you. Thank you very much for your initial guidance on gut flora part of the story and the fruitful discussions on that. Virginia de Oliveira Marques, Andreia Cunha and Ivo Marguti… At the beginning of this project, they helped me for all immunological experiments. Guys, I appreciated it all your efforts. Sebastian Weis (a.k.a. Dr. Weis)… I am sorry that our never-ending, fruitful discussions will be over soon. I learned a lot from you about the infectious diseases and I enjoyed our collaborative efforts on a project that is not the part of this thesis. We should definitely repeat this collaboration in future. Lastly, I'd like to thank rest of the past and present Inflammation Group members, specifically Ana Rita Carlos, Jerzy Kotlinowski, Birte Blankenhaus and Ana Ribeiro. You made my days full of joy. I will miss your enjoyable and supportive chats. It was a pleasure to work with all of you.

Many things in this thesis are direct results of good communication and interactions with researchers at IGC. It has been an privilege to work at IGC last few years. Besides that, this thesis also represents the result of good collaborations. The collaborators in this project made some impossible things to be possible for us. Henrique Silveira and Joana Gomes from IHMT provided us mosquitoes every week. This is an incredible effort. If this project went well and smoothly, their labor cannot be ignored at all. I appreciate their all efforts. Silvia Portugal, Tuan Tran and Peter

Crompton… They designed and performed human studies to support our hypothesis. I'd like to thank Peter J. Cowan for providing us the knockout mice and Anita S. Chong for anti-α-gal hybridomas. Here it gives me an opportunity to show my sincere gratefulness to Ana Regalado from Antibody Service at IGC. I owed you a lot. With monoclonal antibodies you produced for us, we did amazing job. Thank you very much, Ana.

Getting through this long journey, it does not only require scientific supports, but it also requires emotional support. I'd like to thank my friends, especially Ali Altintaş, for listening and tolerating me over the past years, although we were away from each other. Ali, hope one day we have a chance to work together again. And of course, Ali Ozgur Argunsah… Hope you learned a lot about malaria and anti-α-gal antibodies through our never ending chat at the end of the tiring days. Thanks a lot for your suggestions and naïve but critical questions.

My Pires… Marta Marialva… You have been in my life more than two years. No words is enough to describe your part in my journey, here in Portugal. I felt your love and support every second. Among all these, I should thank you for your patience regarding to the moments when I was talking about my project without breathing. Life is beautiful with you.

Finally, I wish to express my love and gratitude to my beloved family; for their endless support and love. They taught me the values that have helped me to become the individual that I am today. They also taught me the importance of an education and did everything possible to help me to attain the best education possible.

Bahtiyar YILMAZ
February, 2015

Table of Contents

Preface

This dissertation assembles data obtained during my Ph.D research project, developed at Instituto Gulbenkian de Ciência (IGC) under the supervision of Miguel Che P. Soares from May 2010 to September 2014.

This thesis is structured in 6 chapters, preceded by a summary written in English and Portuguese, outlining the aims of the projects, results and outcomes of the project.

The first chapter provides information about general knowledge on malaria, the importance of naturally occurring anti-α-gal antibodies and immunological aspects of these antibodies. This chapter also includes the specific aims of this work. The second chapter describes the detection of α-gal on the surface of *Plasmodium* sporozoites. Moreover, it shows that *Plasmodium spp.* express α-gal during the exo-erythrocytic stage and erythrocytic stage of the infection in mammals. The third chapter provides insight about the fate of *Plasmodium* sporozoites when facing anti-α-gal antibodies in the dermis of their mammalian host. The fourth chapter provides information about the role of complement system in this protective mechanism driven by anti-α-gal antibodies. The fifth chapter hopefully opens new doors in the field by presenting the role of gut flora in triggering this natural protective mechanism against malaria transmission. The last chapter provides an overall discussions and conclusions of this study. It also contains the future perspectives of the work developed during my Ph.D studies.

Data described in this Ph.D thesis dissertation is the result of my own work. This study has never been submitted for any degree at this or any other universities.

Summary

Malaria is an infectious disease of humans and other animals including birds, reptiles and most mammals. It is transmitted *via* the inoculation of *Plasmodium* sporozoites into the skin through the bite of an infected female *Anopheles* mosquito. Although every year, around 700.000 lives are perished, mainly children under the age of 3-5 years old, to *Plasmodium* infection this deadly parasite has a relatively low efficiency of transmission from mosquitoes into humans. This argues for a natural protective mechanism, which presumably acts during the early stages of *Plasmodium* infection in the human host. Using a rodent model of *Plasmodium* infection to mimic the transmission of disease in humans, this PhD thesis demonstrates that such a mechanism does exists and is mediated through the action of natural antibodies recognizing specifically the Galα1-3Galb1-4GlcNAc-R (α-gal) carbohydrate. It was shown that these T-cell dependent circulating anti-α-gal antibodies can be produced upon antigenic exposure by α-gal expressing specific components of the intestinal microbiota and target *Plasmodium* sporozoites in the skin, immediately after their inoculation by *Anopheles* mosquitoes in mice. Additionally, anti-α-gal antibodies are associated with protection against *P. falciparum* infection in humans, as shown for individuals from a malaria endemic area. Complement and polymorphonuclear (PMN) cell-dependent mechanisms contribute to the mechanism via which these antibodies prevent the migration of sporozoite from the skin into the liver and inhibit hepatocyte invasion, suppressing the establishment of liver stage of infection. Our findings also reveal that this natural host defense mechanism reduces the rate of disease transmission and provides sterile protection against malaria. Importantly, vaccination against α-gal protects mice against malaria transmission, suggesting that a similar vaccination approach may reduce malaria transmission in humans.

Resumo

A Malária é uma doença infecciosa que afecta humanos e animais, como aves, répteis e mamíferos. Causada por parasitas do género *Plasmodium*, esta doença é transmitida por inoculação de esporozoítos na pele, através de uma picada de um mosquito fêmea, do género *Anopheles*. Apesar de anualmente serem perdidas cerca de 700,000 vidas, em particular crianças de idade inferior a 3-5 anos, devido a infecções por *Plasmodium*, esta infecção muitas vezes mortal, apresenta uma eficiência de transmissão relativamente baixa, o que argumenta em favor de um mecanismo natural de protecção do hospedeiro, que presumivelmente actua durante os primeiros estadios da infecção. Nesta tese de Doutoramento, recorrendo a um modelo de infecção por *Plasmodium* em roedores, foi demonstrado que tal mecanismo é mediado por anticorpos naturais que reconhecem especificamente um epitopo existente em carbohidratos, denominado Galα1-3Galβ1-4GlcNAc-R (α-gal). Este epitopo está presente na estrutura celular do parasita, nas diversas fases do ciclo de vida, mas ausente em células humanas, permitindo assim a produção de elevados níveis de anticorpos anti-α-gal, o que ocorre naturalmente e de forma dependente de células T. Anticorpos anti-α-gal do tipo IgM e IgG, tais como os presentes em indivíduos adultos residentes em áreas endémicas de malária, inibem os esporozoítos de *Plasmodium* na pele, imediatamente após a inoculação por mosquitos *Anopheles*. Estes anticorpos naturais estão também associados à protecção contra a infecção por *Plasmodium falciparum* em humanos, como foi demonstrado em áreas endémicas de malaria. Esta protecção envolve mecanismos que dependem do sistema de complemento e de células polimorfonucleares (PMN), prevenindo a migração de esporozoítos da pele para o fígado, bem como inibindo a invasão de hepatócitos, e consequentemente, suprimindo o estabelecimento do estadio de infecção no fígado. De acordo com esta ideia, as nossas descobertas revelam um mecanismo natural de defesa do hospedeiro em que

anticorpos naturais conferem protecção estéril contra a malária, reduzindo a taxa de transmissão da doença. De salientar que a vacinação contra α-gal protege ratinhos deficientes em *α1,3Gt* contra a malária, sugerindo que estratégias semelhantes de vacinação poderão igualmente reduzir a transmissão de malária em humanos.

Abbreviations and Acronyms

α-gal	Galα1-3Galβ1-4GlcNAc-R
α1,3Gt	UDP-Galactose:β-galactoside-α1-3-galactosyltransferase
ACP	alternative complement pathway
ALUM	aluminum hydroxide Cɣ
BSI-IB_4	lectin from *Bandeiraea simplicifolia*
CFA	complete Freund's adjuvant
CSP	circumsporozoite protein
CT	cell traversal
EEF	exo-erythrocytic form
GF	germ-free
GFP	green fluorescent protein
GI	gastrointestinal
IFA	incomplete Freund's adjuvant
mAb	monoclonal antibodies
NAbs	naturally occurring antibodies
NK	natural killer
ODN	oligodeoxynucleotide
PV	parasitophorous vacuole
PBS	phosphate buffered saline
*Pb*A	*Plasmodium berghei* ANKA
Pf	*Plasmodium falciparum*
Py	*Plasmodium yoelii* 17XNL
PMN	polymorphonuclear cells
RBC	red blood cell
rRBCM	rabbit RBC membrane
SPF	specific-pathogen-free

1

General Introduction

1.1 Malaria: An Ancient Disease

1.1.1 History of the disease

Malaria is one of the most anciently described diseases, reported originally in a Chinese document as early as 2700 BC, in which fever and enlarged spleen were recorded as the major clinical symptoms[1]. Later on, Mesopotamian clay tablets from 2000 BC, Egyptian papyri from 1570 BC and Hindu texts from the 500 BC, provided more medical information about this disease[1,2]. Knowledge related to malaria continued to increase in the early Ancient Greece with Homer (~850 BC), Empedocles of Agrigentum (~550 BC) and Hippocrates (~400 BC) describing its clinical signs (i.e. poor health, intermittent fever and enlarged spleen in people living in marshy places), holding the first clear recordings of malaria infection in ancient times[3]. However, many other studies were required in order to identify the causative agent(s) of the disease, i.e. *Plasmodium*.

The various reports[4] on malaria throughout the history of medicine, spanning more than 4,000 years[5] made it clear that the manifestations and the causes of disease, including fevers and other symptoms were to be considered as miasmas rising from swamps [1] . Modern scientific understanding of malaria however, began only to emerge by the end of the 19th century with the germ theory and the beginning of microbiological studies. The very first understanding of malaria transmission dates back to 1880 with the detection of parasites in the blood of an infected patient, reported by Charles Louis Alphonse Laveran[4]. Meticulous examination of blood samples collected from more than 200 patients revealed that in 150 of those there was a clear detection of "crescentic bodies" that were never detected in healthy individuals. This led Charles Louis Alphonse to conclude that a parasitic protozoan, which he named as *Oscillaria malariae* was the causative agent of the disease called malaria[4]. These observations

[1] The word malaria comes from the Italian mal'aria meaning spoiled air.

made possible the advance of scientific discoveries by Ronald Ross, a British officer of the Indian Medical Service, in 1897, who demonstrated that avian malaria is a disease transmitted via mosquito biting, incriminating for the first time mosquitoes in this vector-borne disease[4]. Ronald Ross described how parasites develop within the midgut of mosquitoes, from where they eventually migrate to the salivary glands[6]. He was able to successfully transmit the disease to healthy birds from an inoculum isolated from infected mosquitoes, thus inferring for the first time that transmission of avian malaria occurred via the bite of an infected mosquito. This was subsequently confirmed in a study carried out with a human parasite by Battista Grassi and colleagues[7]**.** These scientists also identified female *Anopheles* mosquitoes as the main vector of human malaria. In 1890, Grassi and colleagues reported for the first time, that two malaria parasites, named *Plasmodium vivax* and *Plasmodium malariae*, are able to infect humans[4]. This finding was based on a simple experiment in which mosquitoes fed on an infected patient in Rome were sent to London where they were able to transmit the disease to two healthy volunteers[8]. In 1897, William H. Welch identified a third malaria parasite, named *Plasmodium falciparum* and in 1922, John William Watson Stephens, working in West Africa, described yet another human malaria parasite, which resembled *P. vivax* and was named *Plasmodium ovale*[9]. Thirty more years passed until *Plasmodium knowlesi* was identified as another *Plasmodium* parasite able to infect humans[10].

Despite the discovery of several life threatening *Plasmodium* strains, information on the mechanisms by which *Plasmodium* infects and proliferates in humans was still lagging until the beginning of 20th century. In 1902, Friedrich Schaudinn described that *Plasmodium vivax* infective sporozoites contained in the salivary glands of mosquitoes could infect human red blood cells (RBCs)[4]. This was confirmed in 1948 by Cyril Garnham and Henry Shortt, who infected rhesus monkeys using

mosquitoes, which carried *Plasmodium cynomolgi* parasite. The authors demonstrated that when transmitted by mosquitoes, *Plasmodium* sporozoites undergo a first round of multiplication, differentiation and maturation in the liver before being released into the bloodstream[11]**.** These steps represent the first evidence for the occurrence of a 'tissue phase' of *Plasmodium* infection as formally demonstrated in 1948[11]. An American clinician, Wojciech Krotoski showed that in some strains of *Plasmodium vivax*, the liver stage of infection could remain dormant for several months, called as hypnozoites[1]. Seventy years passed until the major human tissues targeted by *Plasmodium* were finally identified (discussed later on in this chapter).

1.1.2 Malaria outcome – current situation

Malaria is a global health problem, affecting more than 100 countries with an estimated 3.4 billion people at risk of developing the disease, i.e. half of the world population. Malaria acts as the 10th leading cause of mortality worldwide[12 13], driven by severe anemia, respiratory distress, multi-organs failure and cerebral malaria. World Health Organization (WHO)[14] reported in 2012 that 219 million individuals were infected with *Plasmodium* parasite (uncertainty range between 135 to 287 million) of which 660 000 succumbed to malaria (uncertainty range between 473 000 to 789 000). In 2013, the WHO Malaria Report showed that ongoing malaria transmission occurs in 97 countries and territories[14]. Moreover, 7 countries in which *Plasmodium* transmission started to be observed again are subjected to preventive measures and this makes to a total of 104 countries to be considered endemic to malaria **(Figure 1.1)**. Another striking fact related to this disease is that 90% of the deaths occur in children and pregnant women. In other words, this deadly parasite steals the life of one African kid, every minute[14].

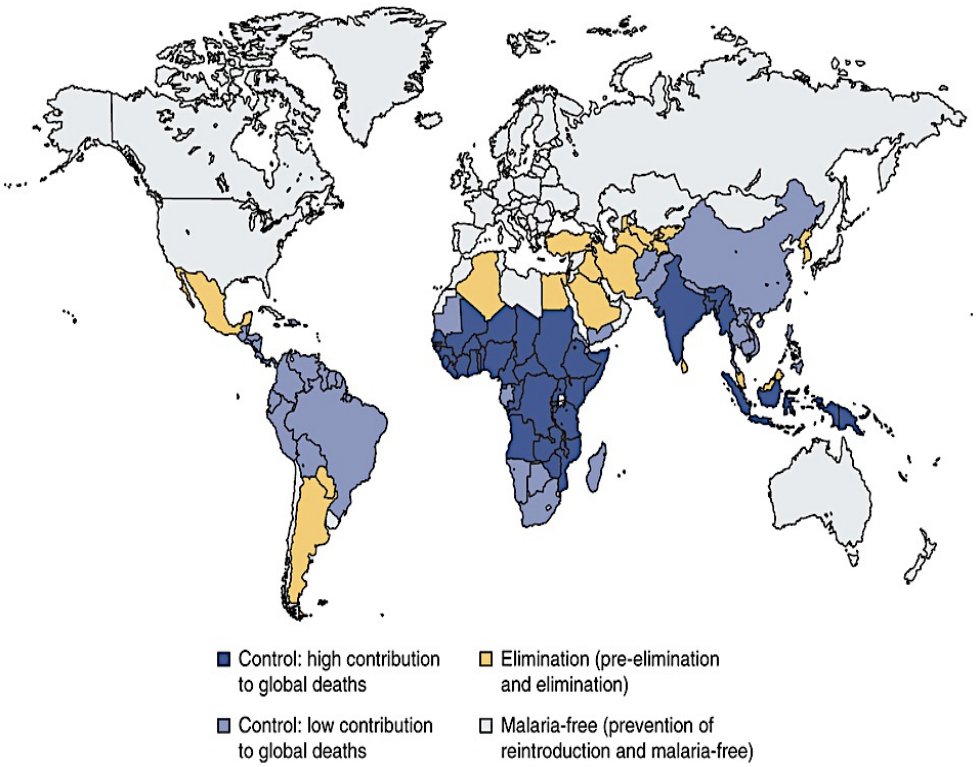

Figure 1.1 Worldwide malaria distribution and burden. Although mortality among infected individuals is "low" (0.3-04%), malaria remains a major health problem and one of the largest scourges in many tropical and subtropical regions. Adapted from[15].

According to the WHO Malaria Report of 2012, the death toll imposed by malaria was reduced by 20-25% from 2000-2010, (a decrease of 33% in Africa), presumably due to the introduction of malaria control programs by the WHO[14]. However, this decrease is not due to lower parasite viability, given the emergence of drug resistance strains of *Plasmodium*. So far, there is no efficient licensed vaccine, which will eventually act as a "game-changer" in the eradication of malaria[14].

1.2 Biology and Life Cycle of *Plasmodium*

1.2.1 *Plasmodium spp.*

Plasmodium is a heteroxenous protozoan parasite, i.e. the completion of its life cycle involves a vertebrate host and an arthropod vector. It belongs to the *Apicomplexa* phylum, the less phylogenetically well-known taxonomic group (only 0.1% of the all species named to date)[16]. The genus *Plasmodium* was first described in 1885 by Ettore Marchiafava and Angelo Celli[4,17] and today, it is known to be infective to a variety of possible hosts, including reptiles, birds and mammals[18]. There are four described human infectious *Plasmodium* species: *P. falciparum*, *vivax*, *malariae,* and *ovale*. In addition, *P. knowlesi*[19], which infects macaques that inhabit the forested areas of Southeast Asia, has recently developed the ability to infect humans and is considered as the fifth causative agent of human malaria. These *Plasmodium* species differ regarding morphology, life cycle and pathologic outcomes imposed to their hosts. Differences include a) blood stage morphology (erythrocytic schizogongy consists of 3-5 rounds), b) characteristics associated with liver stage (a dormant phase called hypnozoite observed in *P. vivax and P. ovale*), c) sequestration of trophozoite- and schizont-infected RBC in microvasculature (exclusive to *P. falciparum*) and clinical manifestations with prolonged pre-patent period for *P. vivax, ovale,* and *malariae* up to several months, d) intensity of febrile attacks or e) duration of clinical symptoms.

P. falciparum is by far the most virulent species to mankind, which accounts for ≈ 85% of all malaria infections, and virtually all malaria-associated morbidity and mortality. The high pathogenicity of this parasite hints that *P. falciparum* may be a recent human parasite transferred from a nonhuman host[20,21].

In 1948, Ignace Vincke and Marcel Lips identified and isolated the first rodent malaria parasite, *P. berghei,* from *Grammomys surdaster* (an African

tree rat) in Central Africa[4]. Since then, three other strains, i.e. *P. yoelii*, *P. vinckei* and *P. chabaudi* were identified, isolated and successfully transferred/adapted to laboratory rodents, thus allowing the establishment of rodent models of the human disease[4,22,23]. The life cycle, physiology and morphologic structure of these parasites resembles in many aspects the human infecting *Plasmodium spp.* and therefore, rodent parasites are considered valuable surrogate models of human malaria[4,22,23]. However, there are reasonable concerns as to what extent the rodent models of malaria mimic disease pathogenesis and immunity in humans. In any case, the spectrum of murine malaria models obtained when using different hosts and parasite strains reflects to a large extent the diversity of human disease with specific parasite-host combinations capturing most if not all the specific aspects of the human disease.

1.2.2 Life-cycle of *Plasmodium* in mammals and mosquitoes

The life-cycle of *Plasmodium* can be extremely complex as it involves different stages occurring in disparate host species such as an arthropod vector and a vertebrate host. Since the original description of the different stages of *Plasmodium* infection, scientists have been trying to understand the life-cycle of *Plasmodium* in further detail. Briefly, the life-cycle in mammals consists of a pre-erythrocytic, erythrocytic and sporogonic phase **(Figure 1.2).** Each of these is explained in detail above. The **pre-erythrocytic stage (Skin and Liver Stage)** begins when a female *Anopheles* mosquito injects sporozoites, i.e. the infectious form of *Plasmodium* parasites, into the skin of a vertebrate host. Parasites spend a certain amount of time in the dermis (from 15 minutes to a couple of hours) before reaching a dermal microvascular blood vessel, through which they are transported via the blood stream, into the liver. At this point, *Plasmodium* sporozoites invade hepatocytes in two minutes, where they mature within 40-48 hours. The **erythrocytic stage (Blood Stage)** of infection begins after the rupture of liver schizonts (mature parasites in the liver), also referred as

exoerythrocytic forms (EEFs), and subsequent release of infectious merozoites into the bloodstream. RBC invasion occurs within 1-2 minutes and then parasites undergo rounds of asexual multiplication leading to RBC disruption and to the clinical outcomes of the disease. In the **sporogonic stage (Mosquito Stage)**, during a blood meal a mosquito ingests, differentiated male and female *Plasmodium* gametocytes from an infected host. Fertilization occurs in the mosquito midgut and the resulting zygotes develop into ookinetes that mature into oocysts, where thousands of sporozoites develop. This final form of the parasites in the mosquito vector migrates to the salivary glands, where it stays until it is injected into another vertebrate host. Each phase of infection is explained in further detail in the next paragraphs.

The **skin stage** of infection is a rapid, clinically silent and apparently immunologically innocuous phase of *Plasmodium* infection. This initial step is critical for the establishment of the infection in the mammalian host[24]. Most of the injected sporozoites, in average 15-123 sporozoites per blood meal, are inoculated into the extravascular matrix of the dermis[25,26] and not directly into the bloodstream as initially thought. This was first demonstrated by Boyd and Kitchen, in 1938, who found the presence of *Plasmodium* sporozoites in human dermal tissue[27], finding as well that removal or heat treatment[28] of the skin area targeted by the mosquito dramatically decreased *Plasmodium* infection[29]. It argues strongly that sporozoites are first deposited into the dermis, while the mosquito probes for a blood vessel and salivates. In further support of this notion, when the mosquito ingests blood it actually re-ingest a proportion of its sporozoites driven by the inward blood pressure, which overrides outwards salivation pressure[30,31]. The development of intravital imaging techniques fully confirmed that most sporozoites are injected into the dermis at low, but still highly variable inoculums.

Mosquito bites are also associated with the ejection of saliva that contains vasodilators like tachykinins and anti-coagulants like thrombin- and F_{xa}-directed molecules, which increase blood flow and inhibit platelet aggregation[32], presumably facilitating blood ingestion[33]. During a mosquito bite, approximately ~1–2.5 sporozoites are released per second through the proboscis. In malaria endemic regions, individuals can be bitten by 1-100 mosquitoes during one single night corresponding to 0-4 infective bites[34]. Considering around 4-5 minutes of mosquito salivation, an *Anopheles* mosquito injects on average about 300 sporozoites per bite in a human host[35,36].

When delivered into the dermis *Plasmodium* sporozoites show significant level of motility before reaching the extracellular matrix of the blood vasculature and contacting with vascular endothelial cells[28,33]. Sporozoites glide in three-dimension with an average velocity of ~1–2 μm per second during the first 30 minutes after injection. While they continue to move for more than one hour, their speed decreases significantly over time. Once *Plasmodium* sporozoites start migrating randomly in the cutaneous tissue, one of four different scenarios will decide their fate. These are dictated by many factors, including blood vessel density at the biting site, saliva components released by the mosquito and the parasite species itself. In any case, it should be noted that out of the ejection of 70-100 *Plasmodium* sporozoites in mice during salivation only 15-25% of those deposited in the skin will manage to successfully establish infection[35]. Under the first scenario, once deposited into the skin sporozoites move at high speed by gliding motility[37] and traverse[38] host cells, piercing host membranes until they find a blood vessel as a way to reach the liver, a process that lasts a couple of minutes[29,39,40]. However, a small proportion of *Plasmodium* sporozoites can accumulate in the skin-draining lymph nodes in the 3 hours that follow the injection[41]. These can reach lymphatic rather than blood vessels, and develop into small exoerythrocytic forms (EEFs), within

the first hours after mosquito bite[40,42]. The development is arrested after a short period of time and small EEFs are cleared from the host. Moreover, this processes can initiate the immune response against *Plasmodium* infection as suggested by the appearance of sporozoite specific cytotoxic T lymphocytes (CTLs) that can accumulate in the skin-draining lymph nodes, as early as two days after the intradermal injection of irradiated sporozoites[42]. The other possible scenario is when the deposited *Plasmodium* sporozoites fail to reach a draining blood or lymphatic micro-vessel in the dermis, as it occurs for approximately 50% of the cases. It is estimated that 10% of these initiate the development of EEFs in the skin hair follicles, which can persist for days without leading to infection[43,44]. The last scenario, as observed by Kebaier and Vanderberg, is when *Plasmodium* sporozoites are re-ingested by mosquitoes[30], with 90% of the mosquitoes re-ingest a highly variable number of sporozoites (1-400 sporozoites) while actively imbibing blood. Among these four scenarios only the first one allows for successful establishment of an infection.

The mechanism via which *Plasmodium* sporozoites manage to proceed with microvascular blood vessel invasion is still not fully understood. Surface phospholipase is important to breach host cell membranes during sporozoite migration and in the absence of this protein, sporozoites' ability to cross through vascular endothelial cells is impaired, with significant reduction of infection[45]. This reveals that transit from the dermis extracellular matrix, where sporozoites are initially deposited, to the blood microcirculation is a tightly regulated process presumably involving several gene products encoded by sporozoites as well as by the host. Transit from the dermis extracellular matrix into blood vessels is associated with decreased *Plasmodium* sporozoite gliding speed, triggered upon contact with endothelial cells, which are then crossed within few minutes[46]. When sporozoites enter blood vessels, they are rapidly transported through the blood circulation and are arrested thereafter in the liver.

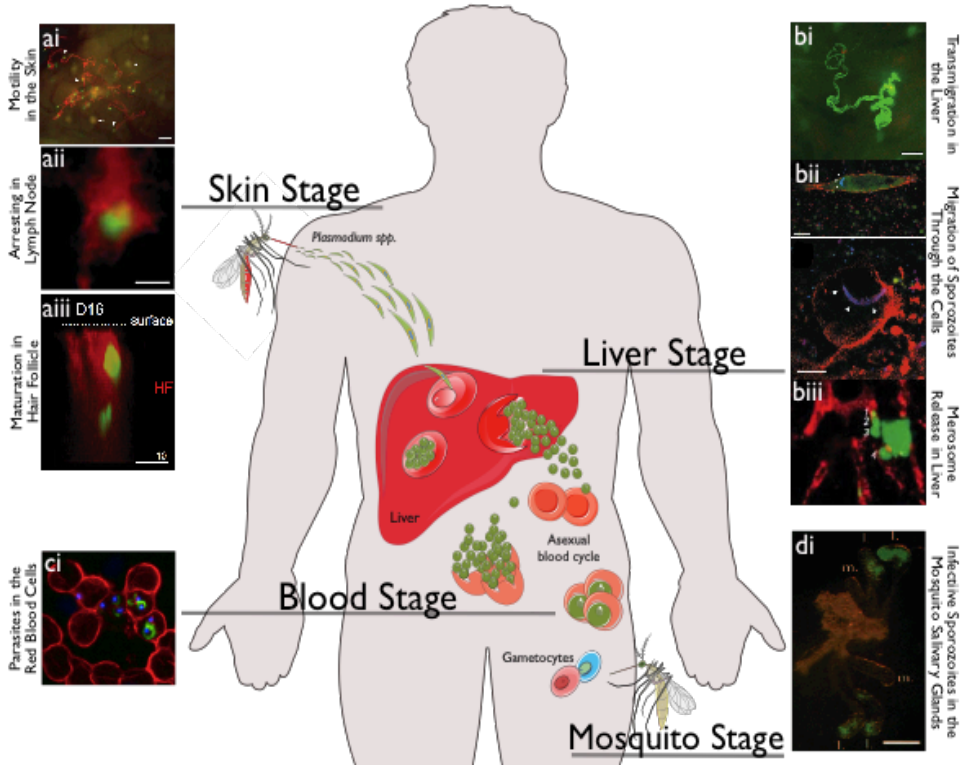

Figure 1.2 The life cycle of *Plasmodium*. A female mosquito transmits a motile *Plasmodium* sporozoite into the skin of a vertebrate, acting as the transmission vector of malaria[40,43]. When sporozoites reach blood vessels, they are arrested in the liver, invading hepatocytes, where thousands of merozoites are produced[38,47]. Upon maturation, merozomes are release into blood circulation, reach the lungs[48] and infect RBC, initiating a series of asexual multiplication cycles. Then, an uninfected mosquito bites an infected host, taking up *Plasmodium* gametocytes along with the blood meal[35]. Fertilization and maturation take place in the mosquito midgut and when fully developed, *Plasmodium* sporozoites migrate to the salivary glands.

Liver stage is the second short-lived and innocuous (asymptomatic) stage of *Plasmodium* infection in vertebrates, characterized by sporozoites migration through the liver sinusoids as to gain access to hepatocytes. During this process that occurs via an unknown mechanism, sporozoites switch from migrating into invasive mode and settle down in a final hepatocyte within two minutes after reaching blood vessels. The tropism of *Plasmodium* sporozoites towards the liver, rather than other organs,

suggests the existence of a selective process between parasite- and host-encoded molecules. One example of a *Plasmodium* encoded-protein involved in this process is the circumsporozoite protein (CSP), a molecule distinctive of the *Plasmodium* genus that accounts for the predominant surface protein covering the entire surface of *Plasmodium* sporozoites, not found in any other *Apicomplexa* parasite[49,50]. Switching to invasive mode correlates with CSP interaction with host heparan sulphate proteoglycans (HSPGs) expressed at the surface of hepatocytes and hepatic stellate cells. These present a significantly higher degree of sulphation when compared to other tissues[51], which may explain the initial tropism of *Plasmodium* sporozoites towards the liver. An early study by Victor Nussenzweig's group showed that CSP binds to the hepatocyte microvilli within the space[2] of Disse[52,53], migrating along fenestrated endothelial cells that allow for direct contact with hepatocytes. Presumably, this allows for sinusoidal barrier crossing and migration into the hepatic parenchyma, where sporozoites traverse several hepatocytes before invading the final one, where they differentiate[47]. During hepatocyte invasion[38], each *Plasmodium* sporozoite forms a parasitophorous vacuole (PV)[47] and resides in it during the liver stage of infection[54].

Survival of sporozoites in the liver requires cell traversal (CT) motility, a wounding and crossing process via which *Plasmodium* parasite passes through host cell plasma membranes and migrates freely in the cytoplasm of host cells, including hepatocytes. During this process, hepatocytes are wounded, releasing so called infection-susceptibility-inducing factors[55,56], e.g. hepatocyte growth factor (HGF)[57], required to promote final hepatocyte infection[38]. In support of this notion CT-deficient sporozoites display highly impaired liver infection *in vivo*, even though normal hepatocyte invasion

[2] Also known as perisinusoidal cells or Ito cells. They are pericytes found in the perisinusoidal space (a small area between the sinusoids and hepatocytes) of the liver - known as the space of Disse.

and development are observed *in vitro*[58,59]. While pre-erythrocytic stage proteins such as the ones essential for cell traversal (SPECT), cell traversal protein for ookinete and sporozoite (CelTOS) or phospholipase (PL) were thought to be essential for cell migration, sporozoites deficient in the genes encoding these proteins can still invade hepatocytes and complete a liver stage development similarly to wild type sporozoites[58,59]. Little is known about the mechanism by which *Plasmodium* sporozoite switches from migration through hepatocytes to invasion of a hepatocyte.

Once inside hepatocytes, sporozoites can develop and replicate within the PV, generating EEFs[60] via asexual multiplication. This culminates in the presence of tens of thousands of infectious merozoites in ~2 days, which ultimately will proceed to the blood stage of infection[61]. However, little is known about the cellular and molecular interactions between parasite and host during this stage of the *Plasmodium* life cycle.

The final important step of *Plasmodium* development in the liver is the exit from the hepatocyte involving the PV lysis and the release of newly formed merozoites contained in vesicles, called merozomes[62]. These bud off from hepatocytes into the sinusoidal lumen, remaining covered by hepatocyte–derived membrane, which is thought to be important initially to afford protection against host innate immune system. Once released into the host circulation, merozomes are ruptured and the hepatic merozoites are free to invade the red blood cells.

The blood stage of infection is associated with all the clinical symptoms of malaria. After the release of merozomes into the blood circulation, shear forces inside the hepatic and other larger veins break down merozomes into smaller units called merozoites. Later, merozomes reach the lung microvasculature, in areas of low macrophage density and reduced shear force presumably enhancing their infection ability[48]. Once merozomes are

ruptured in the lung microvasculature, merozoites are released and upon first contact with RBC membranes invade RBC in a short period of time (27-28s). RBC invasion occurs through several phases **(Figure 1.3)** that involve receptor–ligand interactions involving more than 50 surface and secreted proteins[63]. First, merozoites attach to the RBC surfaces (Phase 1, Pre-Invasion). Then apical reorientation of the parasites occurs, which allows for a tight-junction formation between merozoites and RBC surfaces. This provides an entrance mechanism into the RBC through a movement that propels the merozoites into the host cells (Phase 2, Invasion). A final process allowing for the release of the RBC membrane is associated with potassium and chloride efflux resulting in RBC water loss (Phase 3, Echinocytosis) and the initiation of parasite maturation in RBC begins[64].

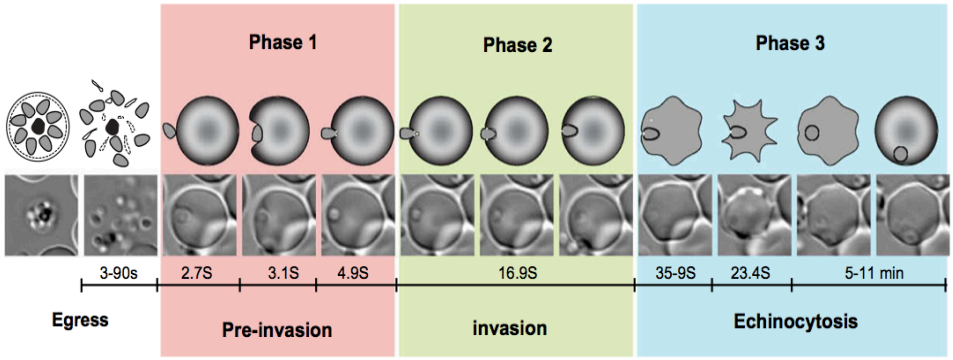

Figure 1.3 Kinetics of RBC invasion. Merozoite achieves infection of RBC in three phases. In Phase 1, merozoite attaches to RBC and causes dramatic RBC deformation and recovery process, afterwards. In Phase 2, merozoite is internalized within the RBC and later on, in Phase 3, dehydration-type morphology occurs in infected RBC (iRBC) and parasite maturation in RBC begins. Adapted from[64].

After RBC invasion, parasites progress through a ring and a mature trophozoite stage, dividing during the subsequent schizont stage and giving rise to 8-32 daughter merozoites contained within a single RBC. Eventually, RBC ruptures and releases the newly formed merozoites[65]. During the successful cycles of invasion and multiplication inside RBCs, the clinical symptoms of the disease begin to appear. However, parasites

are partially hidden from immune recognition inside RBC, which lacks the expression of major histocompatibility complex (MHC) molecule recognized by antigen receptors of the host adaptive immune system. RBC also exposes some proteins at the surface, enabling cyto-adherence to different endothelial receptors and favoring sequestrations in organs while reducing splenic clearance by hemophagocytic monocyte/macrophages (Mø)[66].

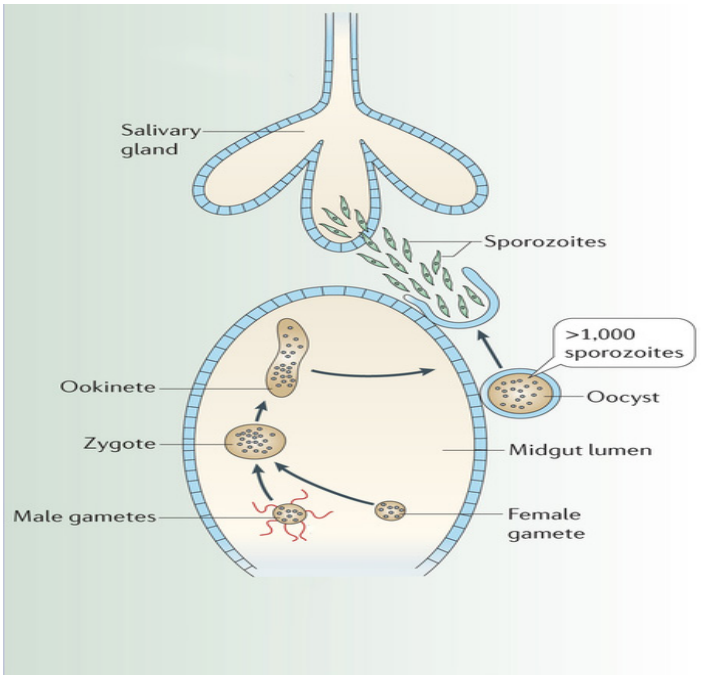

Figure 1.4 Mosquito Stage of *Plasmodium*. In mosquito gut, gametocytes released from burst of iRBC develop further into mature gametes. After the nuclei fusion and fertilization in the mosquito gut, actively moving ookinetes form oocysts. Inside the oocyst, the ookinete produces thousands of sporozoites by cell division, releasing sporozoites that reach the salivary glands. Adapted from[68].

After several asexual cycles inside RBC, a fraction of intraerythrocytic parasites divert from the asexual multiplication pathway towards sexual differentiation, developing highly specialized gametocyte forms (either males or females). These circulate in the bloodstream and are taken up upon the bite of mosquito. This development process in the *Plasmodium*

infected host is called gametocytogenesis and is triggered by genetic and environmental factors[67].

Mosquito stage is the last step of the life cycle of *Plasmodium* infection that begins with the uptake of iRBC from an infected vertebrate. This occurs via the bite of a female mosquito, which ingests both male and female gametocytes that arise during each erythrocytic cycle. Once inside the mosquito midgut, gametocytes undergo fertilization, zygote formation and development into the motile ookinete[69] generating new infectious sporozoites.

Male gametocytes undergo the most drastic transformation while replicating their own genome. They are segregated into eight flagellated male microgametes, whereas female gametocytes transform into macrogametes[69,70]. Exflagellation is a vibratory movement activity that allows the release of male gametes from the gametocytes, enabling them to find female gametes. Subsequently, this process leads to the formation of a zygote, which undergoes meiosis and develops within 24 hours into an ookinete. During the differentiation process and development into a vegetative oocyst, the ookinete rests between the midgut epithelium and the luminal side of the basement membrane of the infected mosquito. Following multiple rounds of nuclear division that occur over 10–14 days, hundreds of sporozoites develop and are released into the mosquito haemolymph[70,71]. From there, sporozoites are carried away to the salivary glands in which they reside until transmission into their next host **(Figure 1.4)**. Even though most sporozoites reside in salivary glands, large numbers are also found in the cavities of secretory cells at the distal end of the glands. These are not ejected during the mosquito blood feeding process. In fact, only a small proportion of sporozoites reach the narrow salivary ducts, and likely also the wide portions of primary ducts. This constitutes a releasable pool of parasites to be transmitted to the mammalian host during

the next blood meal[35]. *Plasmodium* parasites can travel between the distal part of the salivary duct system and the tip of the proboscis in just a few seconds and the speed of ejection can reach approximately 500μm/sec. Surprisingly, the initial period of salivation is extremely important, as many mosquitoes were found to eject sporozoites during this period[26,35].

1.3 The Biology of *Plasmodium* Sporozoite

While *Plasmodium* sporozoites are lower eukaryotes, they have a genetic complexity that is higher than the one found in any bacteria family. This genetic complexity is combined with a considerable number of polymorphic genes in the haploid genome, which generate antigenic diversity[72]. Therefore, *Plasmodium* sporozoites have various and highly optimized adaptation mechanisms, which allow to exploit their hosts in extremely changing situations. This may well explain why the parasite has been so successful in surviving throughout the evolutionary selection process[73]. *Plasmodium* sporozoites also present an active mechanism for cellular motility, which is essential to reach and invade host cells (See *Section 1.3.2*) and also utilize their own locomotion for extracellular migration through different host tissues[31].

1.3.1 Morphology of *Plasmodium* sporozoites

Sporozoites are highly polarized and usually elongated cells (defined by the presence of an apical complex at their anterior pole) of about 10-15 μm in length and 1μm in wide[74]. They have a thin outer membrane and a double inner membrane under which lie the subpelicular microtubules anchored to the apical polar ring elongating underneath the inner membrane complexes (IMC), forming networks of closely apposed flattened vesicles. *Plasmodium* sporozoites have 3 polar rings extending half the length of the body. A morphological hallmark of *Plasmodium* sporozoites is the secretory organelles at the apical tip, called micronemes and rhoptries **(Figure 1.5)**. The contents of both organelles are critical for

recognition and attachment to the host hepatocytes, generation of the non-phagosomal parasitophorous vacuole and remodeling of the host cell following invasion[75]. Sporozoite morphology is established during the development within oocysts, which is dependent on CSP expression[76]. The sporozoite nucleus is divided into several sub-compartments including the nucleolus and the nuclear periphery, presumably involved in transcription control. Mitochondrion, apicoplast and microtubules are linked to the parasite pellicle via long tethering proteins. This defined structure is most likely important to maintain the sporozoite shape[77].

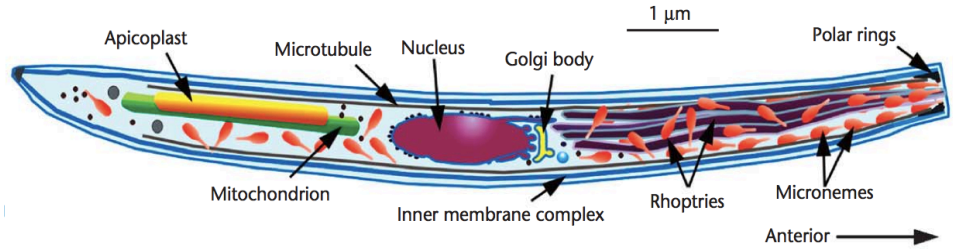

Figure 1.5 Structural illustration of a *Plasmodium* sporozoite. The major compartments such as apicoplast, rhoptries, micronemes and visible structures in a *Plasmodium* sporozoite with its anterior ending towards the right. Adapted from[78].

Plasmodium sporozoites express so called "invasion proteins" such as CSP that localizes mainly on the outer surface and in the micronemes and thrombospondin-related anonymous protein (TRAP), which localizes exclusively in the micronemes and plasma membrane of sporozoites with an irregular distribution. These proteins are often targeted as immunogens for pre-erythrocytic malarial vaccines[74,78,79].

1.3.2 Different modes of sporozoite motility

Single-cellular or multicellular organisms possess distinct features that support cellular locomotion, which are important for reorientation, homing and migration. These provide advantages for development and survival in a variety of complex and stressful environments and are essential to support *Plasmodium* sporozoites transit from the skin into the liver and

from the liver into the blood. They can occur via three modes: gliding, cell traversal and invasion motility, as supported by *in vitro* and *in vivo* studies **(Figure 1.6)**.

Plasmodium sporozoites share with the rest of the *Apicomplexa* phylum a rather unique and mysterious process of locomotion, named gliding motility was first described in *Toxoplasma* and later, in other apicomplexans i.e. *Eimeria*, *Plasmodium* and *Cryptosporidium*[80-82]. Given the apparent absence of specialized locomotive structures like cilia, flagella or pseudopods in *Plasmodium* sporozoites, crawling via gliding activity provides a mode of locomotion[37] at rapid and variable speeds ranging from 1–10 μm/s **(Figure 1.7)**. This mode of locomotion underlies essential processes in the life cycle of *Plasmodium* sporozoites, such as extracellular motility, associated with crawling type movement via a substrate-dependent locomotion on surfaces, as well as intracellular invasion**.**

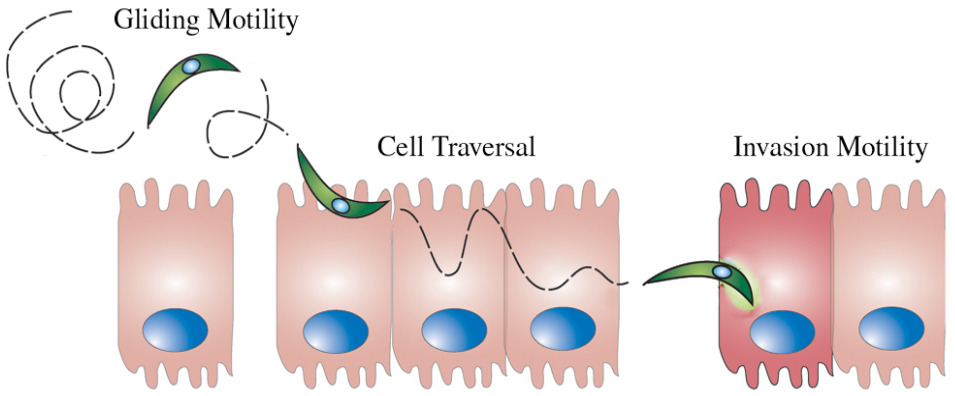

Figure 1.6 Three modes of *Plasmodium* locomotion. Sporozoites deposited into the skin by a female *Anopheles* mosquito exhibit flexing, turning, twisting motions and circular gliding, i.e. gliding motility. *Plasmodium* sporozoites can pass through cells in the skin and enter the bloodstream, reaching the liver and migrating through several hepatocytes before they invade the final one. This wounding movement through hepatocytes is defined as cell traversal and invasion of the last hepatocytes with formation of a parasitophorous vacuole occurs via invasion motility of *Plasmodium* sporozoites. Adapted from[83].

Although, the main components in the core of the machinery regulating gliding motility are known, the exact mechanism by which gliding motility occurs is not fully understood. Gliding motility relies on the activity of an unconventional class of molecules referred to as "neckless" non-muscle myosin (type XIV). These are anchored to the inner membrane complex (IMC) of the pellicle via actin filaments. Pharmacological disruption of microfilaments via inhibition of actin polymerization, using cytochalasins or latrunculins, inhibits gliding motility and host cell invasion, arguing that *Plasmodium* motility requires actin filaments polymerization and depolymerization for infection[84]. Although gliding motility mechanisms are not fully identified, it is likely that the sheer force of polymerizing/depolymerizing actin filaments together with the surface molecules spanning the plasma membrane cluster activate a motor powered by actin-myosin interactions[85].

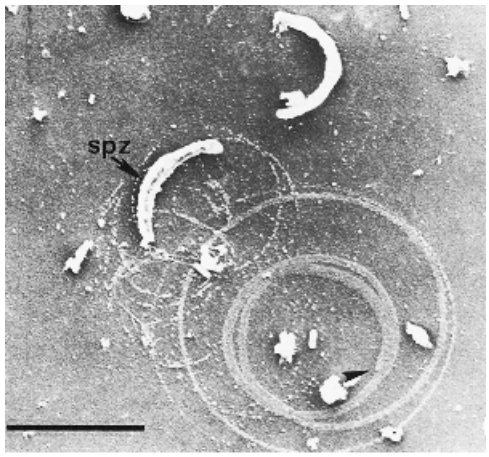

Figure 1.7 Gliding of sporozoites on a glass slide in the presence of albumin. CSP containing trails are deposited by sporozoites *via* on-going secretion from their trailing ends. Adapted from[86].

The very first step towards understanding the mechanisms underlying gliding motility steam from the observation by Dubremetz and Ferreira in 1978, who discovered that cationized ferritin binds the entire surface of *Eimeria* sporozoites and accumulates rapidly at the posterior pole[87]. Based on this basic observation, a model has been proposed for *Plasmodium* gliding motility, which relies on the 'capping process' of membrane components. During this process, capped transmembrane proteins are directed from the anterior to the posterior end of the parasite, by a subcortical actinomyosin complex. It is the backward

movement of this complex that allows the sporozoite to move forward[80,88]. Similar observation was done by C. A. King, who demonstrated that small latex beads are actively transported across the surface of *Eimeria* and *Plasmodium* sporozoites, accumulating at the posterior end from which they are shed[80]. Notably, despite scarce experimental evidence of King's model regarding motor activity required for gliding motility and cell invasion, this model turned out to be essentially correct. In fact, Vanderberg's group was not only able to confirm King's model, but also start elucidating which *Plasmodium* surface membrane components are crucial for gliding motility. He reported that gliding motility relies on a backward redistribution of CSP[89], in which CSP is secreted at the apical end of the parasite and then translocated towards the posterior end, along the sporozoites' surface, by an actin-dependent and cytochalasin-sensitive process[86]. Thus, rearward movement of this complex drives the parasite forward, releasing surface proteins on the substrate, giving rise to the characteristic spiral trails visualized by CSP staining. The gliding activity can also be inhibited by incubation of sporozoites with anti-CSP monoclonal antibodies[90].

Hepatocytes invasion by *Plasmodium* sporozoites is achieved via a process involving **cell traversal motility**. This type of locomotion is defined as the migration of *Plasmodium* sporozoites and ookinetes through the plasma membrane of host cells without forming a PV. This is indispensable for *Plasmodium* to pass through host cellular barriers and reach a hepatocyte as to develop into the next invasive stage. CT activity was first described *in vitro* in 1990 by Vanderberg's group[91], which showed that *Plasmodium* sporozoites can repeatedly enter and exit host monocyte/Mø without being phagocytosed. Migration through host cells is not restricted to Mø and is associated with host cell membrane disruption, with the parasite moving into the cytoplasm and subsequently exiting from the host cells. Afterwards, Maria M. Mota and colleagues (2001) performed the first detailed cell-wounding assay to demonstrate that *Plasmodium* sporozoites

can traverse hepatocytes[38], before it matures in the vicinity of the traversed hepatocytes, but never inside these injured cells. This observation suggests that sporozoites traverse several hepatocytes sequentially before settling in a final one[38]. CT motility is also essential for sporozoites to reach the blood circulation after being deposited in the dermis, thus facilitating access to the blood vessel wall, as demonstrated by Robert Menard and colleagues[58]. Finally, CT motility is also though to play an important role in avoiding sporozoite destruction by Mø as well as by non-professional phagocytes, such as dermal fibroblasts[92] or hair follicles[43].

Invasion motility allows hepatocyte infection. Cell invasion begins with a process that involves tight contact between the apical tip of *Plasmodium* and the hepatocyte cell membrane. Parasite secretes microneme and rhoptry contents, which form junction-like structure, shaped as "bridges" between the host cell cytoskeleton. This allows the parasite motor system to anchor to the host cell[93] forming a ring shape structure, which is associated with the movement of the parasite required to enter the host cell. Intracellular sporozoites form a PV in the hepatocytes cytoplasm connecting the vacuole membrane to the host plasma membrane. The cell membrane of the invaded hepatocyte is not wounded, allowing the parasite to develop into the EEF[94,95].

The mechanism switching CT to invasion motility remains unclear. During the cell invasion process, CSP, which has two conserved 5 amino acid sequence at N-terminus and a cell-adhesive motif repeats, called the type I thrombospondin repeat (TSR) at the C-terminus, is cleaved. Afterwards, the TSR domain is masked by the N-terminus at the skin stage and is unmasked thereafter in the liver stage[96]. This is associated with cell contact-dependent sporozoite activation, turning off CT motility, which is important to avoid lysis of the PV membrane. Sporozoite microneme protein essential for cell traversal genes (*SpectF* and *Spect2F*) deficient

sporozoites that do not have CT activity, readily invade the host cells[92]. While high levels of sulphation of liver HSPGs are likely to contribute to mechanism switching CT to invasion motility[55], cleavage of glycosaminoglycan chains from mouse hepatocytes does not affect sporozoite invasion *in vitro*[97]. Thus, the mechanism switching from CT to invasion requires further investigation to define all the players involved in this process.

1.4 Glycans & Natural Antibodies

1.4.1 The immune system at a glance

All living organisms encounter thought their life cycle disease-causing agents and have developed protective mechanisms against those. This occurs even in single cell organisms such as bacteria, which have dedicated systems of protection against viral infections. These protective mechanisms became more complex and sophisticated as the complexity of organisms increases over evolution. Animals have evolved protective systems in which soluble molecules, cells and tissues have evolved to deal with infections, i.e. the immune system.

Pathogenic microbes can gain systemic access into a potential host at different sites including at epithelial surfaces, e.g. skin, respiratory, gastrointestinal and the genitourinary tract, or via parenteral routes such as those associated with wounds occurring upon injection of pathogens by a vector[98]. The process of microbial invasion, i.e. infection, is countered by resistance mechanisms, mediated by the host immune which exert a negative impact on pathogens. These rely on specialized cellular and soluble molecules that avoid that microorganisms gain systemic access, expelling microorganisms at epithelial surfaces or eventually targeting microorganisms for destruction.

Initially, host can avoid contact with potential pathogens through a crude first line of defense called avoidance[99]. Upon detection of the potential pathogenic organisms in the environment, the putative host can trigger emotional and cognitive responses that prevent the contact with pathogens or with infected individuals[99,100]. This ancestral behavioral defense mechanism relies often on olfactory and gustatory systems, as well as visual signals for some species[99].

Pathogens that escape from host avoidance mechanisms encounter epithelial surfaces that are physical boundaries and protect the host from systemic access. These physical barriers have a significant role in slowing down or blocking pathogenic invasions and are composed of epithelial cells juxtaposed via tight junctions and forming mono or multilayer structures. These barriers have a significant role in slowing down or blocking pathogenic invasions. The physical barriers of the host are composed of epithelial cells, which form mono- or multilayer structures, via tight junctions. Epithelial barriers include the skin and mucosal membranes such as in the digestive, reproductive, respiratory and genitourinary tracts. In the skin, epithelial cells that are held together by tight junctions provide a seal against the invaders. There is also a complex population of normal skin flora, which can also exclude invaders[101]. Additionally, epithelial surfaces can produce microbicidal chemical substances such as lysozymes in tears and saliva that damage bacterial cell walls. The acidity of the stomach is another example, in which host chemical substances inhibit the growth of pathogens outside barrier tissues. Digestive enzymes in the gastrointestinal (GI) tract also create a substantial chemical barrier to infection[102]. Furthermore, resident bacterial flora in most epithelial surfaces including not only the skin but also the intestinal tract can also provide a protective layer of defense against potential invaders via mechanism that control many aspects of host immunity[101]. Moreover, the digestive, reproductive and respiratory tract, as well as sensory organs are

covered by mucous membranes that contain enzymes (lysozymes), antimicrobial peptides, metabolites against invaders and cilia to filter out the substances.

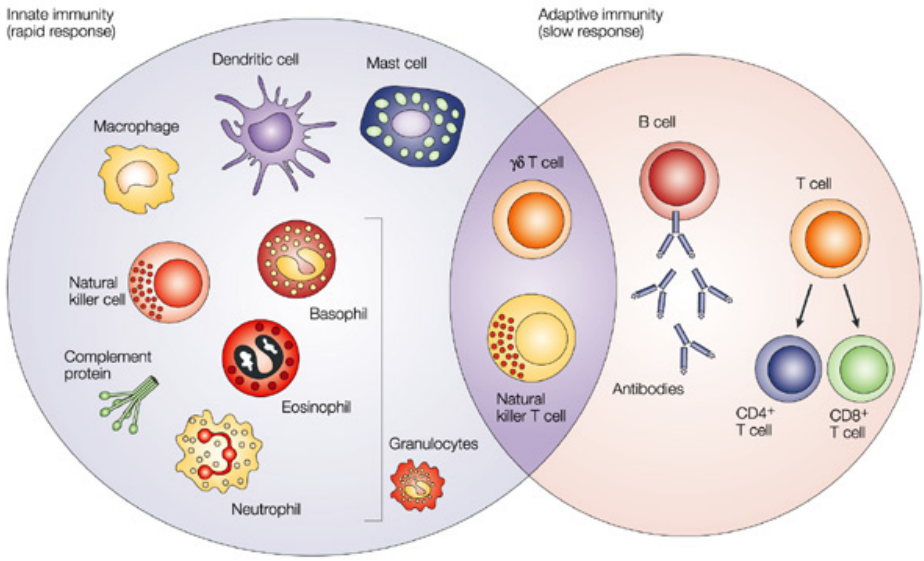

Figure 1.8 Components of immune system. The innate and adaptive immunity are two inter-related defense systems[103]. Innate immunity provides a fast response, which relies on soluble molecules and cell types such as basophils, eosinophils, neutrophils, mast cells, Mø, dendritic cells and natural killer cells. The adaptive immune response provides a slower response but is highly specific and encompasses memory. It is mediated by soluble molecules, e.g. antibodies (Abs), as well B and T lymphocytes. Natural killer T cells and γδT cells are cytotoxic lymphocytes that straddle the interface of innate and adaptive immunity. Adapted from[104].

When pathogens cross epithelial barriers, they are confronted by the host immune system, composed of two inter-related sub-systems **(Figure 1.8)**[103]. The first, referred as the innate immune system, relies on resistance mechanisms activated via a restricted number of germ-line-encoded receptors, called pattern recognition receptors (PRR). These recognize structural components of pathogens called pathogen associated molecular patterns (PAMPs). Innate responses do not have memory, that is, they do not change the amplitude or relative strength of response upon re-exposure

to the same challenge, i.e. microorganisms, although this notion has been put into question more recently[105]. The second layer of the immune system, referred as the adaptive immune system, provides a more specific and robust defense mechanism activated via antigen receptors, which trigger clonal expansion of antigen-specific effector cells. Contrary to PRRs, antigen receptors can refine and increase their specificities and affinities towards antigens via a complex process involving gene recombination and allowing for affinity maturation[102]. These two lines of defense serve the same purpose - to recognize and eliminate or expel pathogens.

As microorganisms breach epithelial barriers, they are sensed by a restricted number of PRRs[106,107] that include Toll-like receptors (TLRs), soluble receptors (i.e. lipopolysaccharide binding protein and soluble CD14 receptor, mannan binding lectin, C-reactive protein), scavenger receptors (i.e. macrophage scavenger receptor, dectin-1, mannose receptor), complement/Fc receptors and intracellular receptor (i.e. NOD-like receptor 2, protein kinase R and oligoadenylate synthetases). It is estimated that the innate immune system can recognize about 10^3 PAMPs[108].

PRRs do not undergo affinity maturation via gene recombination, in clear distinction with antigen receptors of adaptive immunity. Engagement of PRRs on DCs, monocyte/Mø, polymorphonuclear (PMN) cells, e.g. neutrophils, eosinophils, as well as natural killer (NK) cells and lymphokine-activated killer cells, triggers innate resistance mechanisms that expel or destroy pathogens[109]. Innate resistance mechanisms include microbial opsonization and production of intracellular anti-microbial molecules[110] as well as granuloma formation[103]. Other key component of innate immunity are soluble anti-microbial peptides[111], including defensins as well as the complement system that trigger the lysis of microbial cell membranes via a proteolytic cascade that forms membrane pores while promoting the effector function of innate and adaptive immune cells[112,113].

In addition, innate immune cells express intracellular enzymes such as lysozyme that initiate the digestion of bacterial cell walls. Production of free radicals via the NADPH oxidase (NOX) family of reactive oxygen species (ROS) generating enzymes is another common resistance mechanism used by innate immune cells. This cytotoxic mechanisms can be further enhanced by PRR-driven nitric oxidase production, which occurs via the induction of the inducible form of nitric oxide synthase (iNOS/NOS2) as well as by mechanisms regulation intracellular iron metabolism, which impact on the production of free radicals[114,115]. PRR are also expressed on cells of epithelial barriers where they trigger the production of anti-microbial defense mechanisms while maintaining the functional integrity of tight junctions underlying barrier function integrity.

The inflammatory response triggered by soluble and cellular components of the innate immune system must be tightly regulated so that it targets microorganisms as soon as these gain systemic access. One of the constraints is that soluble and cellular components of innate immunity must migrate towards the exact site of infection[109]. This occurs via the expression of a variety of so-called pro-inflammatory genes encoding cytokines as well as other small proteins involved in cell-cell communication such as chemokines[116]. This immediate response encompasses local increase of microvascular permeability, increased expression of adhesion molecules by microvascular endothelial cells, which promote leukocytes recruitment at the site of infection. The adhesive and chemotactic gradient generated towards the site of infection recruits phagocytic cells, i.e. Mø and PMN cells that uptake and destroy extracellular pathogens. Cytokines and chemokines also alert other components of the adaptive immune system for the occurrence of infection.

Pathogens can evolve strategies to evade resistance mechanisms, such as the infection of central cellular components of innate immunity including

Mø or PMN cells. These intracellular pathogens can be sensed by cytosolic PRRs, expressed in Mø and other innate immune cells such as PMN cells. PRR signaling is critical to trigger cell-autonomous immunity underlying host resistance to such intracellular pathogens. These intracellular PRRs include Nod-like receptors family members governing transcriptional responses (NOD1 and NOD2) and the activation of inflammasomes (NLRP3, NLRC4, NAIP, NLRP6 and NLRP12) among others. The activation of cytosolic PRRs triggers that cell-autonomous immune response that cell-autonomous immune response restricts intracellular pathogen replication and promotes pathogen clearance. This is assisted by non-cell autonomous responses involving NK cells activated in response to proinflammatory cytokine i.e. IFN-γ and macrophage-derived cytokines to promote cytolytic and proinflammatory mechanisms[102,108]. Activated NK cells release cytotoxic granules such as perforin that forms a pore on cytosolic membranes and proteases known as granzymes resulting in programmed cell death of infected cells.

When pathogens are not eliminated via innate immune defense mechanisms, they can still be detected and eliminated by resistance mechanisms mediated by adaptive immunity, encompassing so called immunological memory that allows rapid and swift responses upon re-infection[102,117]. This second layer of the immune system evolved approximately 500 million years ago in early vertebrates[118] and affords a more robust and specific defense mechanism that neutralizes and thereafter removes pathogens. Adaptive immunity is based on antigen recognition, that is, the recognition of proteins or macromolecules that elicit an immune response. This occurs via antigen receptors expressed on B cells and/or T cells, known as B cell receptors (BCRs) and T cell receptor (TCRs), respectively. Upon recognition, antigens can elicit an immune response in which B and/or T cells are activated. In contrast to PRRs that can recognize a fixed structural motif and do not undergo rearrangement, B cell and T cell

receptors are generated through random somatic chromosomal rearrangements and can bind a huge variety of antigens. However, PRRs play an important role in shaping adaptive immunity since the capacity of a given antigen to elicit an immune response relies strictly on antigen presentation by called innate antigen presenting cells that are activated via the engagement of PRR, upon the recognition of PAMPs[103,119] **(Figure 1.9)**. This is achieved essentially, but not exclusively, by DCs as well as Mø. They sample the environment for the presence of pathogens and recognize, engulf and digest antigenic peptides expressed by those pathogens. These are subsequently loaded into newly synthesized major histocompatibility complex (MHC) molecules to be presented to T cells. The engagement of PRRs on DCs and other antigen presenting cells is essential to induce the activation of a genetic program underlying the activation of antigen presenting cell (APC). This process is required so that APC become immunogenic, that is, are capable of triggering an immune response against specific antigens expressed by pathogens and loaded into the MHC class I and II molecules. This process that links innate and adaptive immunity allows for an integrated response of the host immune system, which provides protection against infection[119].

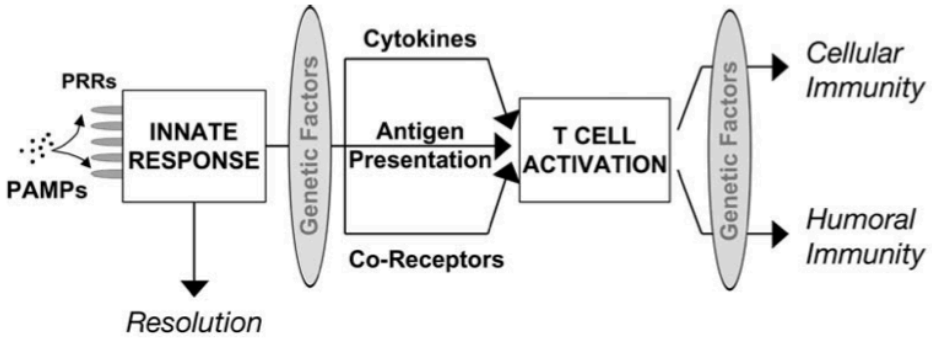

Figure 1.9 Interaction between innate immunity and adaptive immunity. Innate immune components and genetic factors focus the specific adaptive immune response against antigenic targets.

There are two main components of the adaptive immune system. One drives cellular immune response mediated by T cells and the other humoral immune response mediated by soluble antibodies (Abs) produced by B cells **(Figure 1.9)**. Major determinants of adaptive immune activation are dependent on whether the pathogen resides on cytosol, intracellular endosomes or extracellular environment[102]. Main components of cell-mediated immune system include cytotoxic T cells ($CD8^+$) that recognize antigens expressed by intracellular pathogens loaded into MHC class I. T helper cells ($CD4^+$) recognize antigens expressed by extracellular pathogens, loaded into MHC class II molecules. When sensed by specialized tissue resident APCs, pathogens are taken up and digested by the phagolysosome system[102]. This process achieves the destruction of microbial organisms while processing and loading antigens onto MHC class I or II molecules. Activated, tissue resident APC migrate to secondary lymphoid organism, such as lymph nodes and the spleen, in which they interact with antigen-specific naive T cells[102]. Antigen recognition in the context of MHC class I and II by TCR is essential for T cell activation and differentiation into specific effector functions.

Peptide structures derived from extracellular bacteria and toxins are presented to $CD4^+$ T cells via MHC class II molecules and can trigger the differentiation of naïve T_H cells into different effector functions that include T_H1 and T_H2 cells. T_H1 cells produce the cytokine IFN-γ whereas IL-4, IL-5 and IL-10 are the signature cytokines of T_H2. There is also a tight relationship between the T_H cell activation and T cell dependent Ab responses by B cells. Activation of T_H cells by DCs as well as by B cells, towards specific effector functions, such as T_H1 or T_H2, can drive the production of different classes of Abs via cytokine dependent mechanisms regulating Ab class-switch recombination. The key transcription factors in T_H1 differentiation are signal transducer and activator of transcription 4 (STAT4) and transcription factor T-bet. T_H1 cells are effective against

intracellular bacteria infections as well as protozoan infections via a mechanism involving the secretion of IL-2, IL-12 and IFN-γ. T_H1 cells induce microbicidal activities of phagocytes and via help of IFN-γ stimulation, opsonizing and complement-fixing IgG Abs, which promote the phagocytosis of infectious agents[102,120]. Moreover, IFN-γ induces the production of NO, H_2O_2 and superoxide, thus contributing to pathogen clearance. The key transcription factors in T_H2 differentiation are trans-acting T-cell-specific transcription factor GATA-3 and signal transducer and activator of transcription 6 (STAT6). T_H2 cells are effective against extracellular parasites and allergens upon triggering IL-4 and IL-5. T_H2 cells promote IgE- and eosinophil/mast cell mediated immune activity and also activate naïve B cells to secrete IgM and other neutralizing isotype Abs afterwards[102,120]. Although T_H2 cells are related with helminth infections, the roles of IL-4 and IL-5 in protective immunity remain unclear. The third subset of $CD4^+$ T cells is T_H17 cells that are protective against extracellular bacterial and fungal infection. These secrete IL-17 and IL-22 and are distinct from other T_H cells in their gene expression/regulation profile and also as it relates to their biological functions. Orphan nuclear receptor RORγt and STAT3 are the key transcription factors in T_H17 cells differentiation. The main role of this T cell subset is to provide anti-microbial immunity at epithelial/mucosal barriers. However, T_H17 can promote inflammation and tissue injury in autoimmune disease (i.e. multiple sclerosis)[102,120].

Microbial peptide digested from intracellular pathogens are presented to naïve $CD8^+$ T cells upon loading into MHC class I molecules. When naïve $CD8^+$ T cells are activated they differentiated into functional cytotoxic T cells (CTLs) that deliver cytotoxic proteins (i.e. granzymes, perforin and serglycin) that kill infected target cells. These cells can decide whether host cell is infected or not, signal for self-destruction in which pathogen, namely virus, can be eliminated during the process before pathogen has a chance to replicate again. In some cases, they signal for the activation of Mø to

destroy phagocytosed microbes or secrete cytokines to attract immune cells to the site of the infection[102].

Memory T cells are derived from $CD4^+$ or $CD8^+$ and persist for years, even a lifetime. Upon re-exposure to the pathogen, memory T cells can mount a faster and stronger immune response, as compared to the first infection. Memory T cells are further divided into two subsets, namely, central memory T cells (home to lymph node and function against antigen by proliferation and generation of effector cells) and effector memory T cells (home to mucosal sites and function against antigen by secreting the cytokines). As pathogens are eliminated, effector cells undergo apoptosis, while memory cells persist in the circulation by the action of cytokines such as IL-7 and IL-15 without the requirement of peptide antigen or MHC engagement for homeostatic proliferation.

In contrast to cell-mediated immune system, humoral responses of the adaptive immune system are driven by B cells, which develop from progenitors in the bone marrow. The BCR is made of immunoglobulins (Ig)s. These are referred to as Abs because they can recognize antigens through their variable region, recognizing up to 10^{12} specific epitopes, that is, the molecular pattern recognized by an Ab on an antigen[102,121]. Primary B cell responses are generated upon engagement of the BCR and clonal expansion and differentiation of naïve B cells that give rise to short-lived plasma cells, which produce Abs. A fraction of B cells migrate to the B-cell follicle, seed a germinal center, and can persist as dormant memory cells that survive in the body for a long term and are called memory B cells[122]. Memory B cells can respond faster and more effectively against re-infection[123]. They can produce Abs with higher affinities than primary immune response Abs[102 124]. Re-infection with the same pathogen will trigger the response of memory B cell clones to increase generation a polyclonal response. Therefore, higher titers of more diverse Ab molecules

towards an antigen are produced in the secondary immune response. Memory B cells produce soluble high affinity Abs[125].

B cell activation occurs through engagement of the BCR in peripheral mature B cells, mostly in lymphoid organs as well as in the spleen. This can occur with or without subsequent interaction of B cells with T_H cells recognizing antigenic peptides loaded in the MHC class II of activated B cells. Once activated, B cells proliferate extensively and differentiate into memory B cells or Ab-secreting cells.

Several genetic mechanisms evolved in vertebrates to generate the enormous diversity of the BCR and the soluble Ab-secreting cells. These are also relevant to the generation of TCR diversity. These mechanisms include somatic recombination, also known as V(D)J recombination. Briefly, in the case of the BCR the heavy chain of the Ig variable region contains variable (V), joining (J) segment and an additional diversity (D) segment region in the light chain. Immature B cells in the bone marrow express surface Ig encoded by a combination of one V, D and J gene segment (plus one V and J segment for the light chain) as generated through random DNA recombination. Approximately, 10^9 distinct Ab molecules can be generated via V(D)J recombination, thus contributing significantly to Ab diversity. This is further enhanced by somatic hypermutation, an antigen dependent-mechanism involving the enzyme activation-induced deaminase (AID) and driven by deamination of cytosine to uracil in the variable region of the BCR[126]. Upon activation B cells can undergo a process of BCR affinity maturation in which AID driven mutation/repair modifies one nucleotide in the Ig V segment per cell division, resulting in increase affinity of BCR for cognate antigen recognition in germinal centers of secondary lymphoid organs[126], i.e. spleen, lymph nodes and Payer's patches. This process is assisted by cognate interactions with T_H cells as well as follicular DCs. Somatic hypermutation and clonal selection are the processes underlying

affinity maturation of the BCR in which somatic hypermutation generates a spectrum of BCR affinities and clonal selection eliminates B cells carrying BCR with lower affinities while rescuing those carrying BCR with the highest affinities. This process also insures through the generation of memory B cells, which provide a rapid and high affinity Ab response, contributing to host resistance to re-infection with the same pathogen expressing similar Ags[102,121].

Table 1.1 Ig classes and their functions Adapted from[127].

Isotype	Heavy chain	Serum concentration*	Main function	Complement fixation†	Placental passage	Reaction with Fc receptors‡
IgM	μ	0.5–2.0	Neutralization and opsonization	+++	–	L
IgG_1	γ_1	5.0–12.0	Opsonization	+++	++	M, N, P, L, E
IgG_2	γ_2	2.0–6.0		+	±	P, L
IgG_3	γ_3	0.5–1.0	Opsonization	+++	++	M, N, P, L, E
IgG_4	γ_4	0.1–1.0		–	+	N, L, P
IgA_1	α_1	0.5–3.0	Neutralization at mucosal surfaces	–	–	M, N
IgA_2	α_2	0.0–0.2		–	–	–
IgD	δ	Trace	Lymphocyte membrane receptor	–	–	–
IgE	ε	Trace	Mast cell attachment	–	–	B, E, L

*Normal adult range in g/l.
†Classical pathway.
‡Fc receptors on: basophils/mast cells, B; on eosinophils, E; on lymphocytes, L; on macrophages, M; on neutrophils, N; on platelets, P.

B cells also undergo Ig class switch, a process assisted by T_H cells in primary foci as well as in the germinal centers, which consists in switching the production of Abs from IgM (μ) to other Ig classes. This occurs DNA rearrangements in the gene segments encoding different Ig heavy chains and defining different isotypes, namely IgM (μ), IgD (δ), IgA (α), IgE (ε) and IgG (γ). These differ in size, charge, and determine to a large extent the effector functions of different classes of Abs **(Table 1.1)**. During the early stages of B cell development, immature B cell expresses intracellular μ heavy chains that are expressed at the cell surface combined with one κ or λ light chain. Primary B cell responses are often characterized by the production of secreted IgM without class switching. Activated T_H cells can

engage several con-stimulatory molecules in activated B cells, e.g. CD40 via the CD40 ligand (CD40L) expressed on activated T cells, which favor class switch[128]. There are also subclasses of IgA, e.g. IgAl, IgA2 and IgG, e.g. IgGl, IgG2, IgG3, and IgG4 in humans and IgGl, IgG2a, IgG2b, IgG2c and IgG3 in mice. Different Ig isotypes (classes) and subclasses have different effector functions in host defense[108] driven by the binding of heavy chain C regions to complement and/or Fc receptors expressed on different immune cells[102] **(Table 1.1)**.

The effector function of Ab relies often on their cognate interaction with different Fc receptors (FcRs) on the surface of immune cells including B cells, follicular DCs, NK cells, Mø, neutrophils, eosinophils, basophils and mast cells, providing an essential link between humoral and cellular immunity. In general, Fc receptors can activate different responses such endocytosis, phagocytosis, transcytosis, exocytosis, superoxide generation, Ab-dependent cell-mediated cytotoxicity (ADCC) and cytokine release. FcRs can interact with all Ig classes and the name of each Fc receptor is derived from its binding to a specific class of Ig. IgA/IgM **receptor (FcμR)**[129,130] is a high affinity receptor expressed mainly on lymphoid cells, including B and T cells, enhancing B-cell survival following BCR cross-linking. When expressed on T cells FcμR can interact with the IgM BCR or with soluble IgM/antigen complexes as to facilitate T and B cell interactions and enhance B cell activation and IgM production. Moreover, FcμR might also activate cytotoxic T cells in IgM ADCC. There are at least four types of IgG receptor **(Fcγ)**[131]. The FcγRI/CD64 is a high-affinity IgG receptor expressed on Mø and neutrophils that promotes phagocytosis. The FcγRII/CD32 is a low-affinity IgG receptor also expressed on Mø and neutrophils that enhances phagocytosis and inhibits B cell activation. The FcγRIII/CD16 is a low affinity IgG receptor expressed on NK cells, neutrophils and monocytes and involved in ADCC. The FcRn is a variable

affinity receptor for IgG expressed in placenta and promoting IgG mother to fetus transcytosis. Different FcγR are also important for endocytosis of soluble proteins. There are two types of **Fcε receptors**[127] **(**IgE receptor). The FcεRI is a high affinity IgE receptor expressed on Langerhans cells, eosinophils, mast cells and basophils and involved in the control of allergic responses, triggering cellular degranulation involved in immunity to parasites such as worms, e.g. *S. mansoni, T. spiralis, F. hepatica*[102]. The FcεRII/CD23 is a low affinity IgE receptor expressed on B cells, eosinophils, Langerhans cells and involved in IgE transport across the intestinal epithelium while also enhancing allergic sensitization and expulsion of large sized pathogens. There are at least two **Fc*α* receptor**[132] (IgA receptor). The FcRα/CD89 is a low affinity IgA receptor expressed on eosinophils, monocytes/Mø , neutrophils, interstitial DCs and Kupffer cells and promoting phagocytosis, superoxide generation, release of inflammatory mediators and eventually ADCC. FcRα expression is critical to prevent pathogen attachment and invasion of epithelial cells. The Fcα/μR is the other IgA receptor expressed on B cells, mesangial cells, Mø and promoting endocytosis.

Mice have FcγRI, FcγRIIB, FcγRIII and FcγRIV which are conserved between different mammals, however in humans, have FcγRI gene family (which includes *Fcgria*, *Fcgrib* and *Fcgric*) and a FcγRII gene family (which includes *Fcgriia* and *Fcgriic*) and several allelic FcγR variants[131]. There are similarities and differences between mouse and human FcR. Based on genomic localization and sequence similarities, mouse FcγRIV is the orthologue of human FcγRIIIA, and mouse FcγRIII is most closely related to human FcγRIIA[131]. Moreover, both species have two classes of FcRs, which can be distinguished functionally as activating and inhibitory receptors. However, the intracellular domains such as human FcγRIIA contain immunoreceptor tyrosine-based activation motif (ITAM) is not found in mouse FcγRIII[131] or

the affinity of the mouse FcγRs for the different IgG subclasses is higher than human FcγRs. Moreover, mice do not have FcαRI/CD89 and presumably have alternative receptors, such as Fcα/μR[133].

Interactions of different Ig classes and subclasses with specific Fc receptors in different cells types can trigger different effector mechanisms such as phagocytosis, degranulation and cytokine releases that promote the destruction of pathogens[102]. However, some viruses such as flaviviruses can use Fc receptors of cells to infect them via a mechanism called Ab-dependent enhancement of infection.

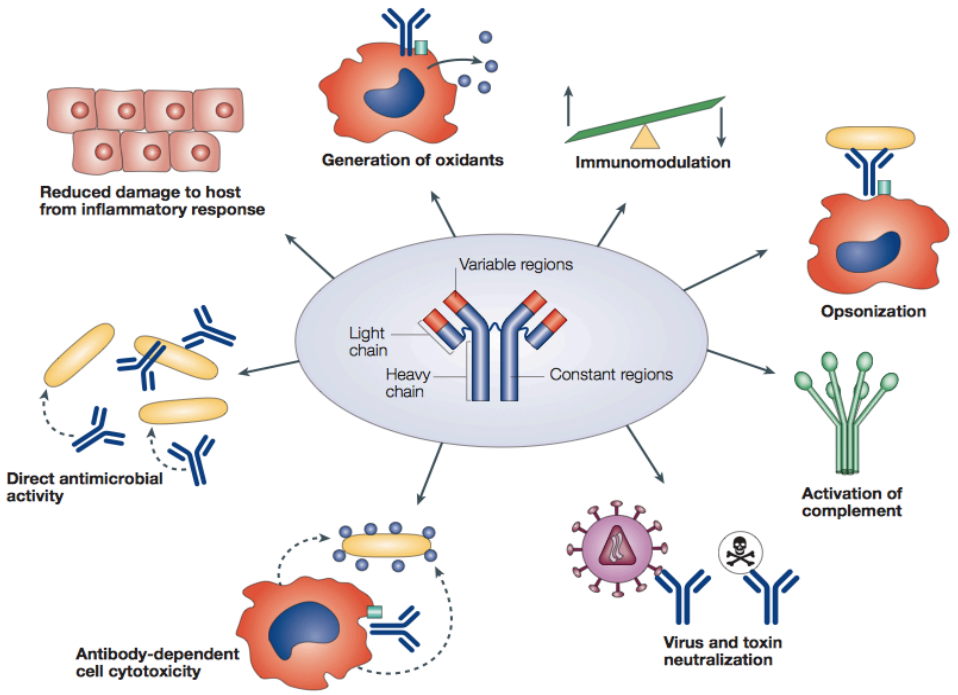

Figure 1.10 Ab effector functions. Abs exist as membrane-bound BCR expressed on B cell surface or are secreted in large quantities. Abs can neutralize toxins and viruses, activate the complement system and act as direct antimicrobial agent independently of other components of the host immune system. However, Ab-dependent cellular cytotoxicity and opsonization depend on the expression of Fc receptors on other host cells such as T cells and Mø. Individual roles of each Ab are summarized in Table 1.1 for humans and depicted in here. Adapted from[134].

Abs act in different ways to confer host protection against pathogens **(Figure 1.10)**. Briefly, membrane-bound Abs act as BCR whereas secreted forms neutralize or mark pathogens for the elimination by other effector mechanisms by effector cells since Abs alone are not able to kill the pathogens. Abs can block the binding of microbes and toxins to cellular receptors in host, a mechanism defined as neutralization effect of Abs. IgM and IgA Abs are particularly good at this. For instance, envelope hemagglutinin of influenza virus or pili of bacteria that help to attach and infect host cells can be neutralized by Abs[108]. IgG Abs can help to opsonize microbes by innate immune cells such as Mø, PMN, mast cells or NK cells and promote phagocytosis[108], via a mechanism involving the expression of different Fc receptors in the effector cells[108]. The phagocytosis is facilitated upon binding of Fab portion of the Ab to an antigen and Fc portion of the Ab to an Fc receptor on the phagocyte. In this process, an antigen becomes coated with primarily IgG Abs to be engulfed later[108]. Moreover, Abs can activate the classical pathway of complement and generate C3b attaches to microbial cell surfaces making pathogens susceptible to Mø and neutrophils phagocytosis via a mechanism involving the expression of iC3b receptor, which are very efficient in promoting phagocytosis. Byproducts of complement activation such as C3b and C4b are deposited on the surface of the pathogens and contribute to the destruction of pathogen via complement system. Pathogen opsonization by soluble Abs can also trigger ADCC via IgG and sometimes IgE, whereby an effector cell actively lyses a target cell. This process can lead an inflammation to surrounding tissues and cause damage to healthy cells. Furthermore, IgM also mediates agglutination reactions in which Abs cause cells to clump together. The Abs bind multiple particles and join them to create a large complex that is attacked and engulfed later by other cells such as Mø for destruction. Lastly, Abs can activate complement system to promote bacterial lysis/accelerated phagocytic uptake upon Ab binding onto an antigen (discussed in Chapter 5).

1.4.2 Natural Abs

In 1900, Landsteiner and colleagues demonstrated that humans that were not immunized specifically against a given antigen had circulating Abs reacting against that specific antigen, as illustrated for blood group antigens[135]. Later on, in 1955, Niels Jerne postulated that the immune system generates natural Abs (NAbs) that can recognize antigen without prior immunization and revived the NAbs concept by introducing "natural selection" theory of Ab formation[136]. In this context, NAbs were defined as those Abs present in the circulation of physiologically healthy individuals without traceable immunization against the antigen recognized[137,138]. These are in most cases multi-reactive and low affinity IgM Abs, as detected in the circulation of healthy vertebrates, including chickens, rabbits, mice, rats, and humans. Growing body of experimental evidence also suggests that NAb are produced to a large extent via exposure, i.e. immunization, to components of the microbiota. This notion is supported by the observation that gut microbiota colonization triggers the development of CD5+ B-1 lymphocytes, responsible for NAb secretion[139]. However, germ-free (GF) mice that lack microbiota can produce IgM NAbs even when fed with a diet free of foreign antigens. This suggests that other factors are involved in the clonal selection and development of B-1 cells producing polyreactive IgM Abs[140]. This process can be influenced by microbiota, as illustrated by the observation that GF mice mono-colonized with either *Morganella morganii* or segmented filamentous bacteria, produce B1-derived IgM NAbs and subsequently stimulates B2 cells to produce IgM NAbs[141]. This suggests that host response to gut flora components can contribute to the production of NAbs[139,142]. These NAbs also display broad reactivity towards a variety of self-antigens recognized with low affinity but high avidity[3].

[3] Avidity refers to several antigen-binding sites that simultaneously interact with the antigen epitope

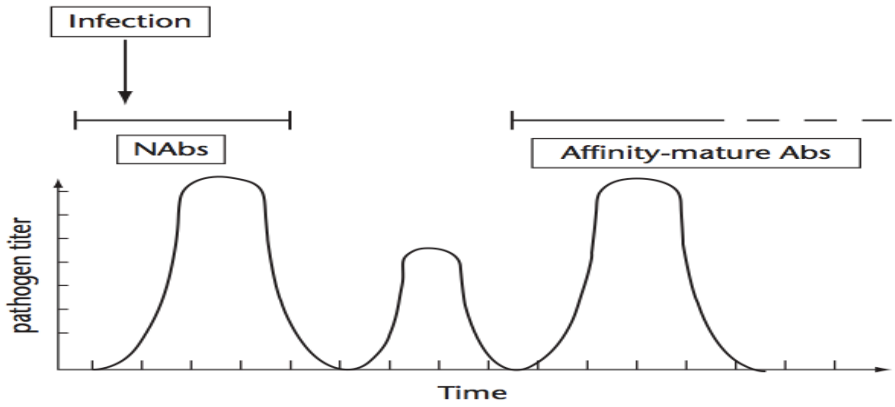

Figure 1.11 Role of NAbs in infection. Upon an infection, NAbs contribute to the to initial recognition and elimination of pathogens. With time, affinity-matured, somatically selected Abs are generated and potent adaptive defense mechanism against pathogen is enhanced. Adapted from[137].

NAbs are thought to provide an efficient first-line of defense against pathogens, thus preventing the initial spread of pathogens into vital organs[143]. The physiological roles of NAbs can ascribed to three categories[137]. The first is protection against infectious agents, serving as a supplementary or alternative host recognition and defense mechanism, preventing the initial spread of pathogens into vital organs[143] **(Figure 1.11)**. Second, NAbs provide homeostatic balance as supported by indirect evidence suggesting that NAbs can present self-antigens and tolerize T cells hence minimizing auto-reactive T cell driven pathology. Since NAbs are present at high titers in the circulation, they can bind and present self-antigens to naïve T cells, possibly without activating co-stimulatory molecules required to support T cell activation and proliferation[144]. In addition, NAbs can interact with the inhibitor receptor FcγRIIb to regulate B-cell activation/functions. Moreover, NAbs can also contribute to the clearance of apoptotic and altered cells through complement-dependent mechanisms, inhibiting inflammation and immunogenicity against self antigens[145]. Another possible effect of NAbs is that these might also play a pathologic role in that polyreactivity can act directly or indirectly in a

pathogenic manner when recognizing self-antigens. For instance, during hepatitis C virus infection, IgM NAbs react with the virus specific Abs and form pathogenic Ab complexes resulting in systemic vasculitis[146,147].

NAbs are produced mainly by a population of long living B1 cells ($CD5^+$ in mice and $CD20^+CD27^+CD43^+$ $CD70^-$ in humans) comprising 20-35% of total B-cells population[148]. In general, NAbs can be categorized as "conservative" (same in all healthy donors), "allo-Abs" (specific to blood group antigens) and "plastic Abs" (concentration of these Abs changes during diseases and some temporary conditions)[148]. A wide variety of NAbs, which are not only conservative within a species, but also between species, are directed to glycans[148]. In humans, relatively high levels of circulating poly-specific NAbs recognize glycans expressed by microorganisms, including pathogens[149].

1.4.3 The α-gal glycan as a target of NAbs

1.4.3.1 Glycans

Glycans consist of 2–20 monosaccharide residues linked via glycosidic bonds[150] and in generic terms, glycans refer to any sugar, an array of covalently attached sugars (monosaccharides) or sugar chains (oligosaccharides), in a free form or an attached to another molecules. Glycans coat all cellular organisms[151] and are found on the outer surfaces of cellular and secreted macromolecules in multicellular organisms. They contribute to several fundamental biologic activities including cell/cell recognition and many physiologic mechanisms, i.e., sperm/egg interactions as well as host-pathogen interactions and their associated pathophysiologic outcomes[150]. Glycans have surprisingly diverse structures, biochemical and regulatory properties and hence, characterization of their biologic functions created a new scientific field, i.e. glycobiology, in which traditional disciplines of carbohydrate chemistry and biochemistry came together to provide understanding of biology of

glycans[152]. During last 10–15 years, important advances have been made in terms of our understanding of glycan structures with separation and isolation of individual structures probing their functional properties within glycoconjugates.

Glycans[4] can be conjugated to biological molecules through an enzymatic process termed glycosylation. When conjugated to lipids or proteins, they give rise to glycolipids and glycoproteins, respectively. When heavily glycosylated, glycoproteins are referred to as proteoglycans. These are the most abundant glycoconjugates in mammals, being expressed predominantly on outer cell walls and secreted fluids[153,154]. Glycosyltransferases utilize specific sugar nucleotide as donor substrates[154] and catalyze a site-specific modification to generate N-linked glycans in the ER, or O-linked glycans in the Golgi as well as O-GlcNAc modifications in the cytoplasm or nucleus[150].

Cell–specific glycan expression patterns are generated via regulated expression of specific enzymes that generate glycans, i.e. include glycosyltransferases, glycosylhydrolases as well as enzymes that degrade glycans, such as glycosidases, exoglycosidases or endoglycosidases. These are encoded by up to 2% of the mammalian genome, arguing further for the biologic importance of these processes[150,156]. In keeping with this notion specific deletion of genes encoding glycosyltransferases is often lethal in mice, arguing that the expression of the corresponding glycans is critical for the survival, often at a early stage of development in mice[157].

[4] Any form of mono-, oligo-, or polysaccharides that are either free or covalently attached to another molecules. We used glycan and saccharides interchangeably.

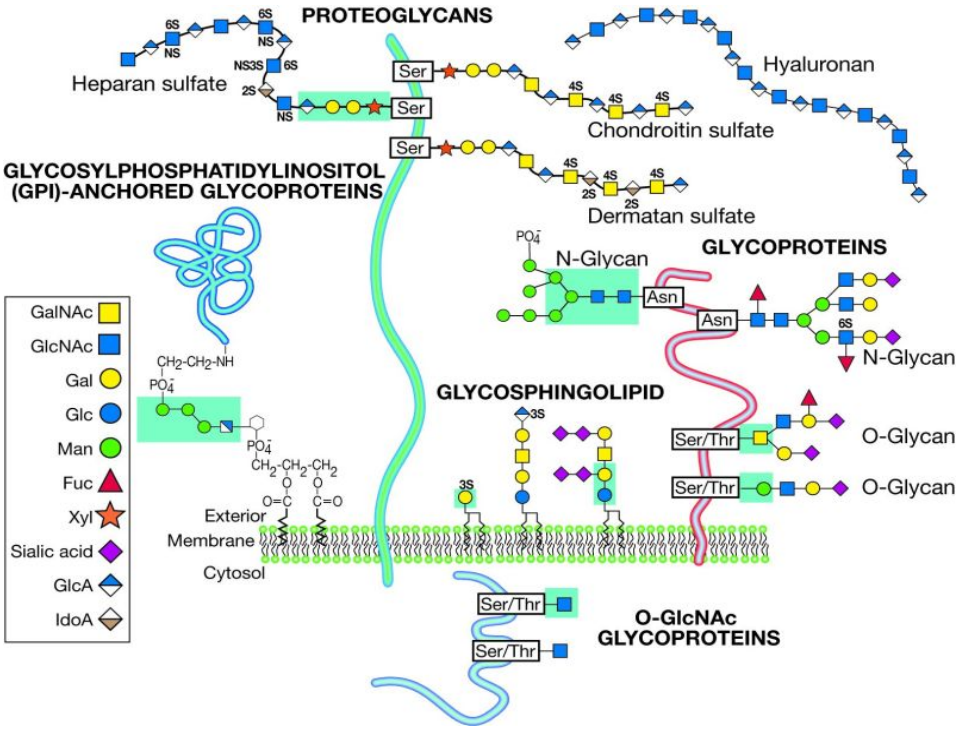

Figure 1.12 Glycan families. The common glycans expressed by eukaryotic cells are categorized according to their linkage to protein or lipid. Glycans serve important functions in the cells such as proper protein folding, protein stability and cell-cell adhesion. Adapted from[150,155].

Glycans abundantly expressed by eukaryotic cells fall into 5 classes **(Figure 1.12)**[150]. **(1)** Glycans that are either *N-linked (nitrogen atom)* or *O-linked (oxygen atom)* to proteins. N-linked glycans are covalently bound to an asparagine residue in a polypeptide chain. This occurs via a N-glycosidic bond, involving N-acetyl-D-glucosamine (GlcNAc) and the Asn-X-Ser/Thr peptide sequence. Until now, N-linked glycan attached to secreted proteins are the best described. N-linked glycans are generated by glycosyltransferases and glycosidases in the Golgi apparatus and provide structural components of extracellular matrix and cell wall, increasing protein stability and solubility, maintaining growth factor and cytokine receptors at the cell surfaces, as well as regulating protein trafficking and cell-cell interactions[158]. In contrast to N-glycans, O-linked glycans are

attached via a N-acetylgalactosamine (GalNAc) to the hydroxyl group of Ser or Thr in the polypeptide chain of glycoproteins, as found in mucin-type glycans. O-linked glycans are important in processes supporting gut colonization by microbiota, via bacteria binding specific mucins. Other biological functions involving O-linked glycans include cellular signaling (i.e. insulin signaling and RNA transcription regulation), sperm reception by eggs, hematopoiesis and inflammatory response mechanisms[150]. Generation of O-linked glycans is controlled by glycosyltransferases analogous to the ones generating N-linked glycans, but their organization is slightly different. **(2)** *O-linked GlcNAc* glycans are abundant within glycoproteins expressed in the nucleus and cytoplasm but they can be found in almost all cellular compartments. O-GlcNAcylated proteins are linked to O-linked GlcNAc glycans via Ser or Thr through a reaction catalyzed by O-N-acetyl-D-glucosaminetransferase. O-linked GlcNAc glycans have several important functions that include regulation of transcription and translation, protein trafficking, capping phosphorylation sites as well as in stress responses associated with increased glycosylation[150]. **(3)** *Proteoglycans* (heparan sulphate and chondroitin sulphate) have core proteins covalently attached to one or more glycosaminoglycan (GAG) chains that are linear polysaccharides composed of amino sugar, uronic acid and galactose[155]. Attachment of the glycans occurs via a xylose residue linked to the hydroxyl group of a serine residue[150]. Proteoglycans are produced and secreted into the extracellular matrix in all mammals, but can also be integrated in the plasma membrane or made available in secretory granules[159]. They are critical in maintaining tissue structure, porosity, and integrity as well as in defining cell specification during development and epithelial cell migration, proliferation, and differentiation[150]. **(4)** *Glycophosphatidylinositol (GPI)-anchored glycoprotein* bridges the phosphatidylinositol and a phosphoethanolamine at the carboxyl terminus of a protein[160]. GPI anchors show some level of diversity depending on the organism and proteins involved. Occasionally, GPI

anchors can also be found in protein free form in mammalian cell surfaces, but their functions are unknown. GPI anchors support essential physiologic processes such as membrane protein transportation, cell adhesion, cell wall synthesis or cell surface protection[160]. **(5)** *Glycosphingolipid* glycoconjugates can be neutral or anionic. They can have glucose or galactose glycan attached to terminal primary hydroxyl group of a lipid and can be neutral or anionic. These glycans are found in all cell membranes and are the main glycans (80% of glycoconjugates) in vertebrates[150]. Their physiological functions include the regulation of cell–cell interactions, signal transduction, protein activity, etc.

Broadly, glycans have direct effects on the regulation of cytosolic/nuclear functions, immune surveillance, auto-immunity, inflammation, hormone action and tumor progression[150,155].

1.4.3.2 Evolution of glycans

There are some shared and unique features in glycan structures across different kingdoms and taxa. N- and O-linked glycans are more complex in recently evolved taxa and present high level of variation intra and interspecies[150,154]. Presumably, glycans with unique structures generated by corresponding glycosyltransferases or other glycan-modifying enzymes have more specific biological roles. Genes encoding glycosyltransferases or other glycan-modifying enzymes are under natural selective pressure and as such the corresponding glycans generated by these enzymes can evolve rapidly. One of the reasons for this appears to be the involvement of glycan in the establishment of host-microbe interaction at different levels. As such modification of glycan structures impacts a major driving force in evolution[154].

Like many biological molecules, glycans are prone to undergo rapid evolutionary changes due to several selective pressure processes.

Divergence of evolutionary lineages is one of the reasons existing glycan evolution. Independent mutations on genes responsible glycan synthesis and modification shaped the glycan repertoires of different lineages[161]. For instance, the existence of cellulose in plants but not in metazoan is a result of divergence. Moreover, due to the divergence, different glycans can be recruited over loss one. In contrast, convergence is the opposite process to generate diversity[161]. This can occurs in distantly related lineages gain similar subclasses of glycan repertoires. For example, Lewis A antigen in catarrhines and plants can be the existence of convergence mechanism. Co-evolutionary process is the other selective mechanism in glycan evolution where organisms from different lineages are constantly in interactions that affect their mutual glycome evolution[161]. Glycans such as sialic acids and glycosaminoglycans found in multicellular hosts and their pathogens are one of the examples to this class of glycan evolution. Lastly, natural selection is one of the most important processes affecting the glycan evolution[161]. This mechanism can maintain the particular glycan or reduce the survival of organisms expressing a certain glycan. Disruption of N-glycans that have lethal consequences to all eukaryotes or negative selection of specific glycans could occur when a glycan is exploited by highly virulent pathogens. Therefore, there are several major contributors for the functionally inactivation of enzymes responsible in the production of specific glycan. However, negative selection occurring through natural selective pressure is importantly effective in dealing with host-microbe interaction. These types of interactions are probably major driving forces in the rapid evolution of glycans since many pathogens use glycan-glycan interactions as primary or secondary targets to recognize and invade host cells. Depending on the pathogen virulence, mutations in the host genome that reduce the expression of these glycans should reduce pathogenicity and as such may be naturally selected so that the host can evade infection[154].

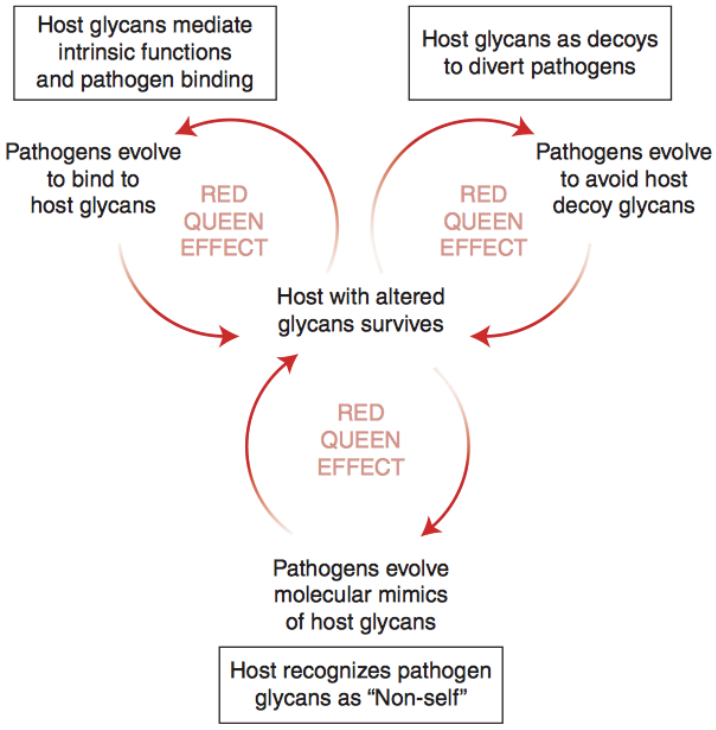

Figure 1.13 Red Queen Effect on glycan alteration. An infected host must constantly escape the negative impact imposed by pathogens, which is achieved in some case by altering its glycan composition. This can occur via natural selection of mutations that have a direct impact on the function of genes encoding enzymes that catalyze the generation of specific glycans. Examples include genes encoding enzymes responsible for the production of soluble glycans such as mucin that act as decoy to keep pathogen away from epithelial cell surfaces or can recognize pathogen glycan as non-self. However, pathogen can also adjust their glycan profiles, via natural selection of genes encoding glycans, interfering with these host defense mechanisms. This type of interaction between host and pathogen exert the red queen effect in which host constantly tries to escape from the pathogen that evolve rapidly. Adapted from[162].

On the other hand, microbes can evolve a thousand fold faster that their mammalian hosts leading to a "harms race" in which the pathogen is likely to win[154]. Therefore, "Red Queen Effects" drive the changes of glycans on complex multicellular organisms, in which multicellular organisms evolve rapidly to survive against pathogens that can replicate and evolve faster **(Figure 1.13)**. Evolutionary forces potentially and simultaneously generate

the diversification of glycan expression in organisms. Therefore, negative natural selection on glycan has an active role to limit the pathogen interaction with host and consequently, possible infection. For instance, sudden elimination of a glycan in an entire evolutionary lineage such as α-gal led the production anti-α-gal Abs[163] that are effective against the enveloped viruses that can infect New World monkeys but not Old World monkey (α-gal glycan and anti-α-gal Abs will be discussed later in this chapter). It is also known that many infectious organisms such as parasites and microbes have gained numerous specialized glycans to be effective on host cells under the evolutionary selective pressure.

Glycosylation processes generate much of the glycan density, complexity, and diversity on cell surfaces. Considering changes occurring in glycans structures found cellular surfaces, expression patterns of glycans may show a compromise between an evading pathogen and its host. Host can show an effort to preserve the specific glycans as much as possible due to their important intrinsic functions for the host i.e., serving as an attractive molecule for the essential symbionts in GI tract[150]. However, pathogens also try to adapt to the changes in the host organism via generation their own glycan structures. Likewise, there are still some common terminal glycan structures on different core glycans that are preserved among some species by regulated glycosylation. Nevertheless, there are many important questions about glycan evolution and functions that remain to be answered.

1.4.3.3 Glycan patterns in protozoan parasites

Protozoan parasites express O-linked and N-linked glycans with unique moieties on several glycoproteins as well as uncommon glycolipid structures and polysaccharides **(Table 1.1)**. The core structures of glycans expressed by many protozoan parasites are similar. The surface structures are often decorated by a glycocalyx, which promotes interactions with

mammalian host cells. Additionally, surface structures can also be coated by host glycans, often used by parasites to escape immune recognition[164].

Glycans can dominate the antigenic profile of parasites and are readily recognized by host Abs. The diversity of glycans and the range of their functions is outstanding. The diversity and similarities of glycan among protozoan parasites gives insights about their evolutionary relationship. *Leishmania spp*. and *Trypanosoma (T.) cruzi* or *T. brucei* (the diseases caused by these parasites are explained in Section 1.5) have common GPI glycolipids that bind to the C-terminus of proteins during post-translational modification[165]. Survival of these parasites in their mammalian host is strictly dependent on the expression of these surface glycoconjugates. *T. brucei* trypomastigote surface is covered with highly glycosylated variable surface glycoprotein[166] carrying at least one N-linked glycosylation that is switched into alternative structures upon interaction with the host immune system. This allows *T.* parasites to escape complement-mediated lysis. Four classes (I-IV) of variable surface glycoproteins exist in *T. brucei* and most of the parasites are class I or II[165]. Class I has one N-glycosylation site and mannose structures close to its C-terminus ($Man_{5-9}GlcNAc_2$). Class II has high mannose structures or polylactosamine rich structures at C-terminal site, and the inner site consists of smaller oligosaccharides whereas Class II has three putative N-glycosylation sites modified with either high mannose or bi-antennary structures. GPI anchored variable surface glycoproteins monomers[167] can be glycosylated with the α-gal glycans (described later), i.e. 3-6 in class I and II has, respectively. Additionally, Class II variable surface glycoproteins possess α-gal and β-gal glycan structures[165]. Moreover, the surface coat of the procyclic form of *T. brucei* contains acidic glycoproteins called procyclic acidic repetitive proteins[165]. EP-procyclic acidic repetitive proteins that have glutamate-proline repeats and GPEET-procyclic acidic repetitive proteins that have glycine-proline-glutamate-glutamate-

threonine repeat sequences are the main families of these proteins. These procyclic acidic repetitive proteins can be expressed in a cell cycle–specific manner and thus, it is thought that oligosaccharide chains may serve as lectin binding ligands in fly midgut[165].

In contrast to *T. brucei* that has N-linked glycosylated sites, *T.cruzi* expresses a range of conserved, O-linked glycosylated, small family of mucins and glycosylinositolphospholipids (GIPLs)[168]. The O-linkages are generally O-GlcNAc, not O-GalNAc and the overall composition consists of GlcNAc and Gal residues[169]. Moreover, *Trypanosomes* do not synthesize sialic acids and thus, they sialylate their Gal-rich mucin (as an acceptor) by capturing host sialic acid (as a substrate) and transfer this sialic acid to β-Gal residues of the mucin[170].

Table 1.1 Glycans in parasites. Adapted from[165].

Parasite	Glycoconjugate
Trypanosoma brucei	Variant surface glycoprotein (VSG)
	Procyclic acidic repetitive protein (PARP)
Trypanosoma cruzi	Mucins
	Glycosylinositolphospholipids (GIPLs)
	Lipopeptidophosphoglycan (LPPG)
Leishmania	Lipophosphoglycan (LPG)
	GIPLs
	GP63
	Secreted acid phosphatase (sAP)
	Proteophosphoglycan (PPG)
	Phosphoglycan
Plasmodia	*N*-glycosylation
	O-glycosylation

In *Leishmania*, the building blocks for glycoconjugates are quite similar to African trypanosomes. *Leishmania* has a dense cell surface glycoconjugates

including lipophosphoglycan, GP63 (cell surface glycoprotein), glycosylinositolphospholipids and secreted glycoconjugates, proteophosphoglycan and secreted acid phosphatase[152,165,169]. Although different *Leishmania* strains have different glycan structures and antigenicity, the surface of all strains is uniquely coated with lipophosphoglycan that shares a similar structure to GPI tail, and is localized over the entire parasite surface including its flagellum. These structures which have conserved lipid anchor, the glycan core, and the Gal(β1,4)Man(α1)-PO_4 backbone of repeat units have variations only in the carbohydrate chains that divide the main backbone and in the cap structures[152,158,165]. Depending on the strains, they can have a repeated unit of β-Gal or β-Glc in side chains. Species-specific differences have biologically important roles such as β-1,3-Gal substitutions in core repeat carries of *L. major* that helps parasite to attach to midgut of sand-fly or addition of an Ara residue in α-1,2-linkage that helps parasite to detach for invasion[169]. Moreover, glycosylinositolphospholipids are the major glycolipids in *Leishmania*. These structures contain Gal-Man-PO_4 repeats and resemble LPG without the linker or cap saccharides[169]. Although the function of glycosylinositolphospholipids is clearly yet identified in *Leishmania*, it is thought that they play a role in macrophage invasion. The other important structure in *Leishmania* is GP63, which is the major cell surface glycoprotein (1% of all cellular proteins) and found in the flagellar pocket and attached to surface via a myristic acid containing GPI anchor[165,171]. It contains N-linked glycans with three potential glycosylation sites[171]. Although the importance of this glycoprotein is not well known, it is believed that it has a role of degrading host macromolecules, a ligand for the macrophage receptor via complement components.

Compared to the trypanosomatids, the level of glycosylation in *Plasmodium* proteins is much lower. There are a few examples of N- or O-glycosylation

in *Plasmodium*[172]. GPI anchor glycans are the most prominent and are quite similar to other protozoan GPIs. It has been argued that GPIs are recognized by mammalian host PRR[173] but whether this has an impact on host resistance to *Plasmodium* infection is not clear. The asexual stages of *P. falciparum* and some proteins such as merozoite surface proteins (MSP1 and MSP2), a heat shock protein 72 (HSP72), an RBC binding antigen (EBA-175), merozoite rhoptry antigen and transferrin receptor were identified as glycosylated expressing N- and O-glycans. However, the exact roles of glycosylation on these proteins are unknown. In contrast, lack of N- and O-linked glycans on merozoite surface proteins-1 and -2 was documented and proposed that GPI anchors are the major players for glycosylation processes *Plasmodium*[174,175]. Additionally, *Plasmodium* parasites can use host glycans to avoid detection by the host immune system. Other critical processes in the life cycle of *Plasmodium* are also dependent on glycosylation processes, as illustrated for RBC invasion, which relies on the interactions of *Plasmodium* with sialylated glycans expressed on RBC glycophorin A in mammalian host while the attachment of *Plasmodium* to midgut of its mosquito host is depend on the interaction with complex oligosaccharides[176,177].

1.4.3.4 The α-gal glycan

There is an additional layer of complexity in which regulated glycosylation processes can add branching residues and terminal sugars to core glycans via a process regulated by glycosyltransferases. Terminal glycosylation of core glycan structures falls into **Type-1 and Type-2 glycan units**. Type 1 units are generated by β1–3 linkage of galactose to GlcNAc in N-glycans, O-glycans and glycolipids**. Type-2 glycan units** are generated by β1–4 linkage of galactose to Galβ1–4GlcNAc, also called *N*-acetyllactosamine. Many of these glycosylation processes occur during embryogenesis and post-natal period but function of generated natural oligosaccharide structures is yet to be fully characterized[150].

Glycans carrying Gal and GalNAc residues are mutual receptors found on several microbial infections such as gonorrhea, sleeping sickness, meningitis, diarrhea, pneumonia and influenza[178]. The involvement of anomerity and α- or β- linkage of Gal and GalNAc in various organisms generate different glycan structures. Generation of the α-gal glycans, namely, Gal1-α-3Gal-R or Gal1-α-4Gal-R, falls into Type-2 unit synthesis in which β1–4 linkage occurs both on glycolipids and glycoproteins **(Figure 1.14)**[179] of many mammals including mouse, sheep, pig, rabbit, cow and rat[180,181], prosimians and New World monkey. The generation of this glycan structure is strictly dependent on an enzyme called UDP-Gal:β-galactosyl-α1–3-galactosyltransferase (α1,3GT) that is not functional in Old World monkey, apes and humans due to the inactivation of the α1,3-galactosyltransferase gene around 20-28 million years ago (explained in details in Section 1.4.4). Therefore, the α-gal glycan is not expressed on Old World monkey, apes and humans.

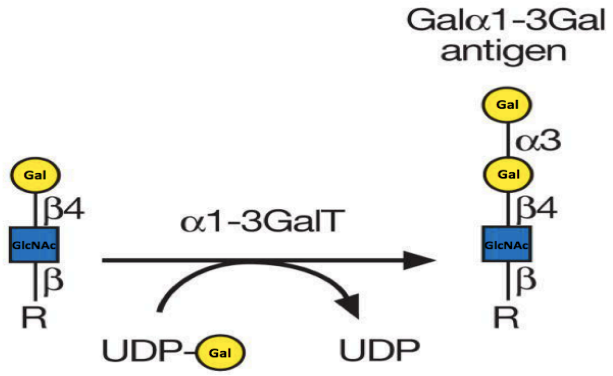

Figure 1.14 Synthesis of α-gal carbohydrate. The synthesis of α-gal is catalyzed by α1,3-galactosyltransferase enzyme (shown as α1–3GalT), which uses type-2 glycan units on glycoproteins or glycolipids and forms α-gal epitope. Adapted from[150].

In 1968, Yamakawa and co-workers described for the first time a glycolipid (ceramide pentahexoside) expressing the α-gal epitope[182]. Galα1-3Gal-R and Galα1-4Gal-R structures were detected in carbohydrate chains of the

two major glycolipids in rabbit RBC membranes (rRBC): ceramide trihexoside and ceramide pentahexoside, further characterized by Hakomori and coworkers in 1972[183]. Later on, it was shown that RRBC contains a wide range of glycolipids of different lengths that terminate with a α-gal glycan[184,185]. These glycolipids are probably multi-branched, containing 35 and 40 carbohydrates per glycolipid[185]. Moreover, α-gal conjugation to neutral glycolipids and gangliosides [5] lipids was also reported on bovine RBCs were reported[186,187].

In parallel to the discovery of anti-α-gal NAbs, the presence of α-gal glycan on different organs of animals, including sheep, pig, rabbit, cow and rat[180] and as well as in the thymus tissue of sheep, pig and rabbit[181] was identified. Expression of the α-gal was also found linked to protein structures, as demonstrated originally by Spiro and Bhoyroo for thyroglobulin[188]. Vliegenthart and coworkers showed that α-gal is expressed on N-linked glycans from mouse, bovine and porcine cells[189]. Detailed analysis of N-linked glycans extracted from pig kidney tissue showed that Galα1–3Galβ1–4GlcNAc-R terminal are found on a variety of complex bi-, tri- and tetra-antennary N-glycans[190]. Later, it was also demonstrated that renal proximal convoluted tubules, respiratory epithelium, pancreatic ducts, epidermis and vascular endothelium of pig contains Galα1–3Galβ1–4GlcNAc-R expressing glycans[191].

1.4.4 Anti-α-gal Abs

Anti-α-gal Abs account for ~1-5% of the total circulating IgM and IgG in healthy humans and are produced by corresponding 1% of human B cell

[5] A ganglioside is composed of one or more sialic acid linked to glycosphingolipid (ceramide and oligosaccharide)

repertoire[192]. In 1983, during his years at Hadassah Hospital in Jerusalem, Galili worked on the potential destructive effect of Abs on RBCs from b-thalassemic patients. He and co-workers discovered that thalassemic RBCs carry several hundred IgG molecules that could be eluted at 37°C using galactose and galactose-like compounds. Later, it was shown that this was also the case for RBC from sickle cell anemia patients[193,194]. They used α-galactosyl coupled to Sepharose column to identify the reactivity of these RBC-bound Abs. Surprisingly, 1% of human serum IgG, corresponding to 30-100 μg/mL, was found to bind α-gal avidly [163]. Then, Galili and Macher performed immunostaining of rRBC glycolipids by thin layer chromatography and showed that NAbs bound to rRBC[195]. They demonstrated as well that these are anti-α-gal Abs, which recognize predominantly non-reducing terminal Galα1–3Galβ1–4GlcNAc-R structures on glycosphingolipids. They first called this Ab "anti-α-galactosyl Ab" and later on defined it as "anti-α-gal (Anti-Gal) Ab." They further identified bacteria from the normal human gastrointestinal flora that is recognized by anti-α-gal Abs (discussed later) and hypothesized that these Abs are produced throughout life as a consequence of a continuous stimulus provided by α-gal expression in the gut microbiota[196,197].

Table 1.2 Human blood groups and α-gal. Adapted from[198].

Blood Group	Antigenic Epitope on RBC	Anti-blood Antigen	Antigens interacting with Anti-α-gal Abs
A	GalNAcα1-3(Fucα1-2)Gal	Anti-B	Galα1-3Gal
			Galα1-3(Fucα1-2)Gal
B	Galα1-3(Fucα1-2)Gal	Anti-A	Galα1-3Gal
AB	Galα1-3(Fucα1-2)Gal	None	Galα1-3Gal
	GalNAcα1-3(Fucα1-2)Gal		
O (H)	Fucα1-2Gal	Anti-A	Galα1-3Gal
		Anti-B	Galα1-3(Fucα1-2)Gal

Galili also demonstrated the unique binding of anti-α-gal NAbs to a series of Galα1–3Galβ1–4GlcNAc-R glycosphingolipids isolated from rRBC, but not to glycosphingolipids with Galα1–4Galβ1–4GlcNAc-R structures. This demonstrated the fine specificity of the anti-α-gal Abs. It was concluded that anti-α-gal Abs detect glycan linkages of the terminal galactosyl residues that consist of same carbohydrate sequence, but with different carbon configuration[195]. Further studies revealed differences in the fine specificity of natural anti-α-gal Abs in individuals of various blood types. Non-reducing terminal GalNAcα1–3GalNAc disaccharide (Forssman Antigen) or A blood group structure GalNAcαl–3(Fucαl–2)Gal-R are not detected by anti-α-gal Abs. However, these Abs can detect blood group B antigen and approximately 85% of purified anti-B-antigen Abs are also anti-α-gal Abs[198]. In contrast, purified anti-α-gal Abs from human sera of blood groups B or AB can bind to the α-gal, but not to blood group B antigen **(Table 1.2)**[198]. Moreover, human sera from blood group A and O has a variety of anti-α-gal Abs that bind to the canonical α-gal epitope as well as to α-gal epitopes in which a Fuc is linked α-1,2 to the penultimate galactose **(Table 1.2)**[198]. All these fine specificities of anti-α-gal Abs in individuals with various blood types imply that a slight different angle in its 3-dimensional form of the α-gal glycan can be detected by these Abs.

1.4.5 Evolutionary inactivation of α-gal expression and emergence of NAbs recognizing α-gal

The discovery of the α-gal glycan led scientists to identify the distribution pattern of this glycan and anti-α-gal Abs in mammals. Analysis of primates and New World Monkeys from the San Francisco Zoo in USA and São Paulo in Brazil, respectively, revealed that New World monkeys and lemurs express the α-gal glycan whereas primates, including humans, apes

and Old World monkeys do not. The conclusion was that the production of anti-α-gal Abs emerged in the complete absence of α-gal glycan in anthropoid monkeys, including humans[198].

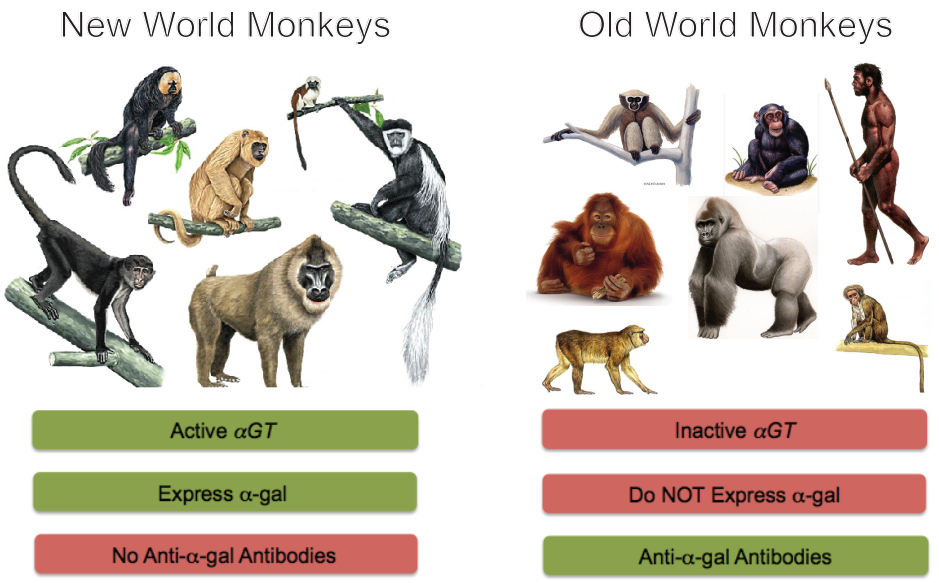

Figure 1.15 Distribution of the α-gal glycan *vs.* α1,3GT activity and anti-α-gal Abs production. New World monkeys, including lemurs, encode the active form of α1,3GT and express α-gal as a self-glycan. As such, these fail to produce anti-α-gal Abs. In contrast, Old World monkeys and humans encode an inactive form of α1,3GT and can produce anti-α-gal Abs. Adapted from[199,200].

The α1,3GT enzyme catalyzes the synthesis of α-gal glycan on lipids and/or proteins. It utilizes as UDP-Gal (nucleotide sugar donor) and either a glycosphingolipid or glycoprotein carrying Galβ1–4GlcNAc-R or Galβ1–3GlcNAc-R (acceptor substrate) as substrates[201]. α1,3GT is a membrane bound type 2 protein around 370 amino acids (a.a.) expressed in the Golgi apparatus, where it competes with sialyltransferase for N-acetyllactosamine non-reducing terminal residues on glycoconjugates[202]. Although the N-terminal region (amino acids 1–99) of α1,3GT varies among species, the remaining sequence until the C-terminus, which is critical for enzyme activity[203], presents high degree of homology. α1,3GT

activity is detected in murine, bovine and New World monkey cells, but not in human cells, with a parallel expression of α-gal glycans[199] **(Figure 1.15)**. Galili and colleagues hypothesized that the evolutionary elimination of the α-gal glycan could be directly related to the inactivation of *α1,3GT* gene (also called GGTA1) since human cells have both UDP-Gal and N-acetyllactosamine acceptors[199].

Identification of *α1,3GT* gene in human genome was only possible after the murine and bovine counterpart were cloned[204,205]. Later, the human *α1,3GT* gene have been sequenced and it was found out that it contains several frame-shift mutations and internal stop codons. Lowe and his group identified the first α1,3GT pseudogene on human chromosome 9, containing intronic sequences, and one exonic sequence corresponding to the largest part of the catalytic domain of the α1,3GT enzyme and the same exon/intron organization as found in mice[206]. Two point mutations that cause a frame-shift and premature stop codon were detected in the *α1,3GT* pseudogene in bases 820-824 and 902-906 rendering the *α1,3GT* pseudogene nonfunctional[207]. Later on, an additional frame-shift mutation was identified in exons 7 and 8 of the *α1,3GT* pseudogene, suggesting that structural mutations such as deletions in the coding regions of the gene were the main reasons for the evolutionary inactivation of this gene[208]. Similar observations were made in the chimpanzee genome while only the first frame-shift mutation was demonstrated in the gorilla and orangutan genomes[209]. There is a second *α1,3GT* gene in the human genome located on chromosome 12, which does not have intronic sequences[210]. This intronless pseudogene contains several deletions in exon 4 and in a fragment encodes last 230 amino acids of the carboxyl-terminal. It is likely that *α1,3GT* cDNA was inserted into chromosome 12[210].

Although humans and chimpanzees present similar *α1,3GT* mutations, these differ from other Old World monkeys, which carry common mutations shared by humans and chimpanzees, suggesting that the *α1,3GT* gene was first inactivated in ancestral primates presumably after the divergence of apes and monkeys[209]. Natural selection of mutations leading to the inactivation in the *α1,3GT* gene was probably driven by a highly virulent pathogen associated or with a major catastrophic epidemiological event or endemic to the Old World, but in either case should be correlated with the almost complete extinction of the hominoid lineage. In keeping with this notion, some highly virulent pathogens express the α-gal glycan (discuss later in this chapter) and the production of anti-α-gal Abs in ancestral primates might have provided immune resistance to these pathogens. However, New World monkeys from the American continent, which were separated from the African continent almost 35 million years ago as well as lemurs, which are found in the Madagascar, an island isolated from the African continent 60 million years ago did not undergo this selective pressure. This is most probably because they were isolated from the Old World continents along distinct geographical boundaries such as oceanic barriers[179,211].

The existing theories on the evolutionary inactivation of *α1,3GT* gene that results in the suppression of α-gal expression in mammals of the Old World can be divided into two categories. The first is based on production of anti-α-gal Abs upon elimination of immune tolerance to α-gal glycan and consequently, protection against pathogen(s) expressing α-gal[212-215]. Production of large amounts of anti-α-gal Abs should provide immune protection against pathogens endemic to the Old World continents, which were detrimental to primates expressing α-gal epitopes. The second theory proposes that loss of α-gal is associated with the loss of host

receptors/ligands required to support infection by virulent pathogens that exploit host cell surface glycans for infection. In support of this hypothesis α-gal expression can render cells resistant to some pathogens but sensitive to others as demonstrated for *Clostridium difficile* infection. In this context the enterotoxin (toxin A) produced by *C. difficile*, a non-invasive Gram positive toxigenic bacterium, can bind α-gal on host cells, also the preferred binding sites for viruses and cause cytotoxicity[216,217] on the intestinal cells of mammalian host[218]. When α-gal expression is removed enzymatically from epithelial cells, toxin A binding is significantly reduced and therefore its cytotoxic effect is prevented[218]. Assuming that this might be the case for toxins produced by other bacterial strains, it would suggest that loss of α-gal expression had a strong selective pressure. In accordance, Old World primates that lack α-gal are not susceptible to toxin effect.

Regardless of the event that led to the inactivation of the *α1,3GT* gene in ancestral Old World monkeys and apes, it is safe to state that this was one of the major evolutionary events of primates towards humans.

1.5 Anti-α-gal Abs and Infection

Bacteria. In 1951, it was argued by Wiener that NAbs (i.e. blood group hemagglutinins) are produced in response to microbial agents. Later, it was shown that glycans similar to those detected by anti-blood group Abs are also found in bacteria[219]. Given that humans produce high titers of anti-α-gal NAbs throughout adult life this raises an important question about the immunogenic stimuli driving the continuous synthesis of these NAbs[163]. Anti-α-gal NAbs recognize α-galactosyl or α-galactosyl-like structures on bacterial lipopolysaccharides (LPS) from a variety of *Escherichia*, *Klebsiella*, *Serratia* and *Salmonella*, *Clostridia* isolates from normal stool or from the blood of sepsis patient[196,197]. It is possible therefore that anti-α-gal Abs

would provide resistance to such pathogens. Although these Abs can recognize pathogens proliferating in the human body, those found specifically in the blood circulation are supporting the idea of that pathogens are able to develop protective defense mechanisms against the detrimental effects of NAbs[191,192]. Moreover, anti-α-gal Abs may also play a role in some autoimmune phenomena, as suggested by the high titer of these Abs in sera of patients with autoimmune thyroiditis, IgA nephropathy, and Henoch-Shoenlein purpura, rheumatoid arthritis, glomerulonephritis, and Chagas' disease, as compared to normal human sera[196].

In 1988, Galili and colleagues described that there is a group of bacteria, i.e. *Klebsiella* strains 18022 and 18033, *S. minnesota* 1127, *E. coli* 15293 and K92 and *S. marcescens* 18021, which are recognized by human anti-α-gal Abs[196]. These bacteria express the α-gal glycan on their cell wall, specifically on the LPS structure. In contrast, *E. coli* O86 expresses α-gal glycan on the capsule or the glycoprotein portion of the bacterial wall, rather than on the LPS portion. Hamadeh and colleagues in 1992 provided the first example of binding of human anti-α-gal Abs to pathogens[197] demonstrating that binding of anti-α-gal Abs to blood bacterial isolates was higher in sepsis patients, as compared to healthy individuals, suggesting that anti-α-gal NAbs may confer a survival advantage against systemic infections. In keeping with this notion, Hamadeh and colleagues also showed that anti-α-gal NAbs can recognize up to 66% of bacterial isolates obtained from blood samples of patients undergoing gram-negative sepsis, as compared to 26% of the entire isolates collected from the stools of healthy laboratory volunteers. In principle, the recognition of α-gal expressing bacteria by anti-α-gal Abs should trigger bacterial lysis, presumably through complement activation. This is however, not straightforward as illustrated

for a *Serratia marcescens* strain isolated from sepsis patients. While anti-α-gal Abs can binds the LPS portion of *S. marcescens*, the bacteria manages to escape complement-mediated killing, despite the activation of the classical pathway of complement and the formation of lytic membrane attack complexes (MAC). Complement-mediated lysis is avoided presumably because MAC is "relocated" on the surface of bacteria to a LPS portion that is not lytic to the bacteria. In that context, anti-α-gal NAbs may promote bacterial survival by blocking alternative complement pathway-mediated lysis when bound to this decoy α-gal epitope on LPS.

Trypanosoma. Anti-α-gal NAbs can also interact with other classes of pathogens, including *T. cruzi*, a protozoan parasite named by the Brazilian physician Carlos Chagas in honor of his mentor, Oswaldo Cruz[220]. *T. cruzi* is the causative agent of zoonotic Chagas' disease, commonly transmitted to humans and other mammals by blood-sucking triatomine bugs (also called kissing bugs or conenose bugs)[220]. This disease is characterized by dilated cardiomyopathy, heart failure, ventricular arrhythmias, heart blocks, and sudden death[221]. The acute phase of disease can last up to 1-2 months and is characterized by high blood parasitemia detected in fresh blood sample. After this stage, a life-long chronic phase begins, which correlates with a scarce subpatent parasitemia that can only be revealed by haemoculture or xenodiagnostic. Individuals infected with *T. cruzi* produce Abs against parasite proteins that cross-react with blood vessels, endocardium, striated muscle, and peripheral nerves, which are thought to be involved in the development of degenerative changes in various organs[222]. In 1990, the structure of the *N*-linked oligosaccharide of 85-kDa surface glycoprotein, named Tc-85, expressed by the trypomastigote form of *T. cruzi* was shown[223]. Presumably, this explains why human and experimental animal models infected by *T. cruzi* produced 10-30 fold higher levels of anti-α-gal Abs, when compared to uninfected individuals[224].

Anti-α-gal NAbs kill the parasite via complement-mediated lysis as well as cell-mediated lysis *in vitro*, suggesting that anti-α-gal Abs contributes to protection against *T. cruzi* infections. However, this protective mechanism has never been show *in vivo*[225].

Although *Trypanosoma* parasites express α-gal glycan on their membrane surface, they can escape the cytotoxic action of anti-α-gal Abs using several strategies including invasion of host cells. Presumably, this can explain why intracellular *Trypanosoma* parasites are protected from anti-α-gal Ab-mediated lysis[226,227]. Moreover, they produce and release glycoinositolphospholipids and lipophosphoglycans expressing α-gal[227], immunizing the infected host chronically against this glycan[224]. This chronic Ab response may contribute to trigger the "autoimmune-like" inflammatory reaction associated with acute and chronic Chagas' disease[228,229]. In keeping with this notion, a study carried out in 1988 showed that blood group A and O patients with Chagas' disease display significantly higher titers of anti-α-gal Abs, probably explaining the higher incidence of severe forms of disease in Chagatic patients of blood groups AB and B. Taken together, these studies argue that anti-α-gal Abs might provide some level of resistance to *Trypanosoma* while promoting morbidity in Chagatic patients [230,231].

Leishmania. Anti-α-gal Abs may also confer resistance to Leishmaniasis, the disease caused by the protozoan parasite *Leishmania*, transmitted by the bite of Phlebotomine sand flies. It was named in 1903 after the discovery of Scottish pathologist William Boog Leishman[1]. *L chagasi* and *L. mexicana* species are responsible for human visceral leishmaniasis and localized cutaneous leishmaniasis or diffuse cutaneous leishmaniasis, respectively while *L. braziliensis* is the main cause of localized cutaneous leishmaniasis and mucocutaneous leishmaniasis[213]. The lipid composition of

promastigotes cultures from pathogenic and nonpathogenic *Leishmania* strains revealed that 5-10% of the total lipids are composed of glycolipids containing mannose and galactose[232]. Glycoinositolphospholipids of *Leishmania* contain glucosamine (GIcN) and variable amounts of galactose, mannose, glucose and phosphate[233]. The first correlation between anti-α-gal Abs and *Leishmania* parasites was found in 1987, in that sera from patients with American cutaneous leishmaniasis bind strongly to the α-gal glycan[222]. Moreover, titers of anti-α-gal Abs are elevated in patients with cutaneous leishmaniasis[222,234] and the α-gal glycan is expressed by *Leishmania*[224].

***Plasmodium*.** Impact of α-gal glycan and anti-α-gal Abs in malaria are the main focuses of this thesis and are addressed in detail, in *Chapter 2*.

Viruses. Expression of α-gal and concomitant production of anti-α-gal Abs may also have an impact on human viral infections. Virions that are produced in cells from species that express α-gal, express the α-gal glycan on glycoproteins in the enveloping cellular membrane. This was first demonstrated in 1984 for the Friend leukemia virus that contains N-acetyllactosamine repeating units and in some cases replaced by α-gal[235]. In 1994, it was shown that eastern equine encephalitis virus can also express α-gal glycan and be neutralized *in vitro* by anti-α-gal Abs[215]. Expression of this glycan on this virus is dependent on the expression of α-gal by the cells producing the virions[215], which reflects on the ability of anti-α-gal NAbs to neutralize these viruses. This is relevant for influenza virus, for which the major envelope glycoproteins consist of hemagglutinin molecules that provide recognition of host sialic acids. When produced in species that express α-gal, i.e. chicken, pig, and influenza virus expresses α-gal and as such can be neutralized by anti-α-gal NAbs[236]. This suggests that human infection by influenza virus derived from animals that express α-gal may

be suppressed initially by the immediate responses provided by anti-α-gal Nabs. However, this defense mechanism becomes inefficient once the virus is transmitted from human to human, based on the lack of α-gal expression. Because, virus can manage to find another way to infect human host without using α-gal glycan. A similar situation should occur for other viruses such as demonstrated for the murine retrovirus of New World Monkeys, which can be neutralized by anti-α-gal Abs when grown in cells that express α-gal but not in cells that do not express α-gal expression could[237].

1.6 Aim of This Study: Objectives and Outline

Mutation in human *α1,3GT* might have been naturally selected throughout evolution to allow for the production of anti-α-gal Abs affording protection against pathogens that express α-gal glycan. Serum titers of anti-α-gal Abs increase steadily during the first years of life, suggesting that exposure to this immunogenic glycan occurs immediately after birth[238]. Presumably, this occurs via recognition of α-gal glycan expressed by specific components of the gut microbiota[196]. Under the assumption that *P. falciparum* can express the α-gal glycan[239] and anti-α-gal Abs would confer resistance to *Plasmodium* infection. We reasoned that the relative lack of anti-gal Abs in children under the age of 3-5 years old may explain their higher susceptibility to malaria[14,240,241]. If proven correct, this raises a second hypothesis, namely that gut bacteria might control adaptive immunity against *Plasmodium* infection, through the activation of anti-α-gal B cells. The aim of this study was to establish whether anti-α-gal Abs provide resistance to *Plasmodium* infection and whether this protective effect was driven by components of the gut microbiota. To test this hypothesis, we used α1,3GT deficient (*α1,3Gt*$^{-/-}$) mice, which in a similar to humans can produce high titers of anti-α-gal Abs when colonized by components of the

gut microbiota expressing α-gal[214]. We then assessed whether anti-α-gal Abs confer protection against *Plasmodium* infection in mice. The specific aims of this study were:

Specific Aim #1: To establish whether *Plasmodium spp.* express α-gal.

Specific Aim #2: To establish whether anti-α-gal Abs afford protection against *Plasmodium* infection.

Specific Aim #3: To define the immunological components involved in the protective mechanism via which anti-α-gal Abs confer protection against *Plasmodium* infection.

Specific Aim #4: To establish whether component of the gut microbiota that elicit the production of anti-α-gal Abs afford protection against *Plasmodium* infection in mice.

References

1. Cox, F.E. History of human parasitology. *Clinical microbiology reviews* **15**, 595-612 (2002).
2. Bryan, C.P. & Joachim, H. *The Papyrus Ebers*, (G. Bles, London,, 1930).
3. Retief, F. & Cilliers, L. Periodic pyrexia and malaria in antiquity. *South African medical journal = Suid-Afrikaanse tydskrif vir geneeskunde* **96**, 684, 686-688 (2006).
4. Cox, F.E. History of the discovery of the malaria parasites and their vectors. *Parasites & vectors* **3**, 5 (2010).
5. Carter, R. & Mendis, K.N. Evolutionary and historical aspects of the burden of malaria. *Clinical microbiology reviews* **15**, 564-594 (2002).

6. Ross, R. On some Peculiar Pigmented Cells Found in Two Mosquitos Fed on Malarial Blood. *British medical journal* **2**, 1786-1788 (1897).
7. Capanna, E. Grassi versus Ross: who solved the riddle of malaria? *International microbiology : the official journal of the Spanish Society for Microbiology* **9**, 69-74 (2006).
8. Grassi, B. Studi di uno Zoologo Sulla Malaria. *Roma : R. Accademia dei lincei* (1901).
9. Stephens, J. A New Malaria Parasite of Man. *Proceedings of the Royal Society of London, Series B* **87**, 375 - 377 (1922).
10. Chin, W., Contacos, P.G., Coatney, G.R. & Kimball, H.R. A Naturally Acquired Quotidian-Type Malaria in Man Transferable to Monkeys. *Science* **149**(1965).
11. Shortt, H.E., Garnham, P. C. C. & Malamos, B. The first demonstration that sporozoites of Plasmodium spp. which infect mammals transform in the liver. *Br. Med. J.* **1**, 192–194 (1948).
12. WHO, W.H.O. World Health Statistic. *WHO Press* (2014).
13. WHO, W.H.O. World Malaria Report. 284 (2013).
14. WHO, W.H.O. Global Malaria Programme (2012). *World malaria report 2012*. (2012).
15. Alonso, P. & Tanner, M. Public health challenges and prospects for malaria control and elimination. *Nature medicine* **19**, 150-155 (2013).
16. Morrison, D.A. Evolution of the Apicomplexa: where are we now? *Trends in parasitology* **25**, 375-382 (2009).
17. White, N.J., Turner, G.D., Day, N.P. & Dondorp, A.M. Lethal malaria: Marchiafava and Bignami were right. *The Journal of infectious diseases* **208**, 192-198 (2013).
18. Martinsen, E.S., Perkins, S.L. & Schall, J.J. A three-genome phylogeny of malaria parasites (Plasmodium and closely related genera): evolution of life-history traits and host switches. *Molecular phylogenetics and evolution* **47**, 261-273 (2008).

19. Singh, B., *et al.* A large focus of naturally acquired Plasmodium knowlesi infections in human beings. *Lancet* **363**, 1017-1024 (2004).
20. Rich, S.M., *et al.* The origin of malignant malaria. *Proceedings of the National Academy of Sciences of the United States of America* **106**, 14902-14907 (2009).
21. Waters, A.P., Higgins, D.G. & McCutchan, T.F. Plasmodium falciparum appears to have arisen as a result of lateral transfer between avian and human hosts. *Proceedings of the National Academy of Sciences of the United States of America* **88**, 3140-3144 (1991).
22. Landau, I., Boulard, Y. *Rodent Malaria*, (Academic Press In, London, 1978).
23. Yoeli, M. & Hargreaves, B.J. Brain capillary blockage produced by a virulent strain of rodent malaria. *Science* **184**, 572-573 (1974).
24. Sinnis, P. & Zavala, F. The skin stage of malaria infection: biology and relevance to the malaria vaccine effort. *Future microbiology* **3**, 275-278 (2008).
25. Medica, D.L. & Sinnis, P. Quantitative dynamics of Plasmodium yoelii sporozoite transmission by infected anopheline mosquitoes. *Infection and immunity* **73**, 4363-4369 (2005).
26. Rosenberg, R., Wirtz, R.A., Schneider, I. & Burge, R. An estimation of the number of malaria sporozoites ejected by a feeding mosquito. *Transactions of the Royal Society of Tropical Medicine and Hygiene* **84**, 209-212 (1990).
27. Boyd, M.K.S. The Demonstration of Sporozoites in Human Tissues. *J Am Mosq Control Assoc* **8**, 404 - 408 (1938).
28. Matsuoka, H., Yoshida, S., Hirai, M. & Ishii, A. A rodent malaria, Plasmodium berghei, is experimentally transmitted to mice by merely probing of infective mosquito, Anopheles stephensi. *Parasitology international* **51**, 17-23 (2002).

29. Sidjanski, S. & Vanderberg, J.P. Delayed migration of Plasmodium sporozoites from the mosquito bite site to the blood. *The American journal of tropical medicine and hygiene* **57**, 426-429 (1997).
30. Kebaier, C. & Vanderberg, J.P. Re-ingestion of Plasmodium berghei sporozoites after delivery into the host by mosquitoes. *The American journal of tropical medicine and hygiene* **75**, 1200-1204 (2006).
31. Vanderberg, J.P. Imaging mosquito transmission of Plasmodium sporozoites into the mammalian host: Immunological implications. *Parasitology international* (2013).
32. Dhar, R.K., N. Role of mosquito salivary glands. *Current Science* **85**, 1308 - 1313 (2003).
33. Vanderberg, J.P. & Frevert, U. Intravital microscopy demonstrating antibody-mediated immobilisation of Plasmodium berghei sporozoites injected into skin by mosquitoes. *International journal for parasitology* **34**, 991-996 (2004).
34. Combes, C. *Parasitism: The Ecology and Evolution of Intimate Interactions*, (University of Chicago Press, USA, 2001).
35. Frischknecht, F., *et al.* Imaging movement of malaria parasites during transmission by Anopheles mosquitoes. *Cellular microbiology* **6**, 687-694 (2004).
36. Jin, Y., Kebaier, C. & Vanderberg, J. Direct microscopic quantification of dynamics of Plasmodium berghei sporozoite transmission from mosquitoes to mice. *Infection and immunity* **75**, 5532-5539 (2007).
37. Vanderberg, J.P. Studies on the motility of Plasmodium sporozoites. *The Journal of protozoology* **21**, 527-537 (1974).
38. Mota, M.M., *et al.* Migration of Plasmodium sporozoites through cells before infection. *Science* **291**, 141-144 (2001).
39. Shortt, H.E. & Garnham, P.C. Pre-erythrocytic stage in mammalian malaria parasites. *Nature* **161**, 126 (1948).
40. Amino, R., *et al.* Quantitative imaging of Plasmodium transmission from mosquito to mammal. *Nature medicine* **12**, 220-224 (2006).

41. Yamauchi, L.M., Coppi, A., Snounou, G. & Sinnis, P. Plasmodium sporozoites trickle out of the injection site. *Cellular microbiology* **9**, 1215-1222 (2007).
42. Chakravarty, S., *et al.* CD8+ T lymphocytes protective against malaria liver stages are primed in skin-draining lymph nodes. *Nature medicine* **13**, 1035-1041 (2007).
43. Gueirard, P., *et al.* Development of the malaria parasite in the skin of the mammalian host. *Proceedings of the National Academy of Sciences of the United States of America* **107**, 18640-18645 (2010).
44. Voza, T., Miller, J.L., Kappe, S.H. & Sinnis, P. Extrahepatic exoerythrocytic forms of rodent malaria parasites at the site of inoculation: clearance after immunization, susceptibility to primaquine, and contribution to blood-stage infection. *Infection and immunity* **80**, 2158-2164 (2012).
45. Bhanot, P., Schauer, K., Coppens, I. & Nussenzweig, V. A surface phospholipase is involved in the migration of plasmodium sporozoites through cells. *The Journal of biological chemistry* **280**, 6752-6760 (2005).
46. Thiberge, S., *et al.* In vivo imaging of malaria parasites in the murine liver. *Nature protocols* **2**, 1811-1818 (2007).
47. Frevert, U., *et al.* Intravital observation of Plasmodium berghei sporozoite infection of the liver. *PLoS biology* **3**, e192 (2005).
48. Baer, K., Klotz, C., Kappe, S.H., Schnieder, T. & Frevert, U. Release of hepatic Plasmodium yoelii merozoites into the pulmonary microvasculature. *PLoS pathogens* **3**, e171 (2007).
49. Nussenzweig, V. & Nussenzweig, R.S. Rationale for the development of an engineered sporozoite malaria vaccine. *Advances in immunology* **45**, 283-334 (1989).
50. Nussenzweig, V. & Nussenzweig, R.S. Circumsporozoite proteins of malaria parasites. *Bulletin et memoires de l'Academie royale de medecine de Belgique* **144**, 493-504 (1989).

51. Pradel, G., Garapaty, S. & Frevert, U. Proteoglycans mediate malaria sporozoite targeting to the liver. *Molecular microbiology* **45**, 637-651 (2002).
52. Frevert, U., *et al.* Malaria circumsporozoite protein binds to heparan sulfate proteoglycans associated with the surface membrane of hepatocytes. *The Journal of experimental medicine* **177**, 1287-1298 (1993).
53. Lyon, M., Deakin, J.A. & Gallagher, J.T. Liver heparan sulfate structure. A novel molecular design. *The Journal of biological chemistry* **269**, 11208-11215 (1994).
54. Lindner, S.E., Miller, J.L. & Kappe, S.H. Malaria parasite pre-erythrocytic infection: preparation meets opportunity. *Cellular microbiology* **14**, 316-324 (2012).
55. Coppi, A., *et al.* Heparan sulfate proteoglycans provide a signal to Plasmodium sporozoites to stop migrating and productively invade host cells. *Cell host & microbe* **2**, 316-327 (2007).
56. Mota, M.M., Hafalla, J.C. & Rodriguez, A. Migration through host cells activates Plasmodium sporozoites for infection. *Nature medicine* **8**, 1318-1322 (2002).
57. Carrolo, M., *et al.* Hepatocyte growth factor and its receptor are required for malaria infection. *Nature medicine* **9**, 1363-1369 (2003).
58. Ishino, T., Yano, K., Chinzei, Y. & Yuda, M. Cell-passage activity is required for the malarial parasite to cross the liver sinusoidal cell layer. *PLoS biology* **2**, E4 (2004).
59. Ishino, T., Chinzei, Y. & Yuda, M. A Plasmodium sporozoite protein with a membrane attack complex domain is required for breaching the liver sinusoidal cell layer prior to hepatocyte infection. *Cellular microbiology* **7**, 199-208 (2005).
60. Shin, S.C., Vanderberg, J.P. & Terzakis, J.A. Direct infection of hepatocytes by sporozoites of Plasmodium berghei. *The Journal of protozoology* **29**, 448-454 (1982).

61. Khan, Z.M. & Vanderberg, J.P. Role of host cellular response in differential susceptibility of nonimmunized BALB/c mice to Plasmodium berghei and Plasmodium yoelii sporozoites. *Infection and immunity* **59**, 2529-2534 (1991).
62. Sturm, A. & Heussler, V. Live and let die: manipulation of host hepatocytes by exoerythrocytic Plasmodium parasites. *Medical microbiology and immunology* **196**, 127-133 (2007).
63. Maier, A.G., Cooke, B.M., Cowman, A.F. & Tilley, L. Malaria parasite proteins that remodel the host erythrocyte. *Nature reviews. Microbiology* **7**, 341-354 (2009).
64. Gilson, P.R. & Crabb, B.S. Morphology and kinetics of the three distinct phases of red blood cell invasion by Plasmodium falciparum merozoites. *International journal for parasitology* **39**, 91-96 (2009).
65. Bannister, L.H., Hopkins, J.M., Fowler, R.E., Krishna, S. & Mitchell, G.H. A brief illustrated guide to the ultrastructure of Plasmodium falciparum asexual blood stages. *Parasitol Today* **16**, 427-433 (2000).
66. Richards, J.S. & Beeson, J.G. The future for blood-stage vaccines against malaria. *Immunology and cell biology* **87**, 377-390 (2009).
67. Tilley, L., Dixon, M.W. & Kirk, K. The Plasmodium falciparum-infected red blood cell. *The international journal of biochemistry & cell biology* **43**, 839-842 (2011).
68. Menard, R., *et al.* Looking under the skin: the first steps in malarial infection and immunity. *Nature reviews. Microbiology* **11**, 701-712 (2013).
69. Billker, O., Shaw, M.K., Margos, G. & Sinden, R.E. The roles of temperature, pH and mosquito factors as triggers of male and female gametogenesis of Plasmodium berghei in vitro. *Parasitology* **115 (Pt 1)**, 1-7 (1997).
70. Angrisano, F., Tan, Y.H., Sturm, A., McFadden, G.I. & Baum, J. Malaria parasite colonisation of the mosquito midgut--placing the Plasmodium ookinete centre stage. *International journal for parasitology* **42**, 519-527 (2012).

71. Aly, A.S., Vaughan, A.M. & Kappe, S.H. Malaria parasite development in the mosquito and infection of the mammalian host. *Annual review of microbiology* **63**, 195-221 (2009).
72. Day, K.P. & Marsh, K. Naturally acquired immunity to Plasmodium falciparum. *Immunology today* **12**, A68-71 (1991).
73. Aravind, L., Iyer, L.M., Wellems, T.E. & Miller, L.H. Plasmodium biology: genomic gleanings. *Cell* **115**, 771-785 (2003).
74. Kappe, S.H., Kaiser, K. & Matuschewski, K. The Plasmodium sporozoite journey: a rite of passage. *Trends in parasitology* **19**, 135-143 (2003).
75. Plattner, F. & Soldati-Favre, D. Hijacking of host cellular functions by the Apicomplexa. *Annual review of microbiology* **62**, 471-487 (2008).
76. Thathy, V., *et al.* Levels of circumsporozoite protein in the Plasmodium oocyst determine sporozoite morphology. *The EMBO journal* **21**, 1586-1596 (2002).
77. Kudryashev, M., *et al.* Positioning of large organelles by a membrane-associated cytoskeleton in Plasmodium sporozoites. *Cellular microbiology* **12**, 362-371 (2010).
78. Bannister, L.H. & Sherman, I.W. Plasmodium. *eLS* (2009).
79. Menard, R., *et al.* Circumsporozoite protein is required for development of malaria sporozoites in mosquitoes. *Nature* **385**, 336-340 (1997).
80. King, C.A. Cell motility of sporozoan protozoa. *Parasitol Today* **4**, 315-319 (1988).
81. Menard, R. Gliding motility and cell invasion by Apicomplexa: insights from the Plasmodium sporozoite. *Cellular microbiology* **3**, 63-73 (2001).
82. Opitz, C. & Soldati, D. 'The glideosome': a dynamic complex powering gliding motion and host cell invasion by Toxoplasma gondii. *Molecular microbiology* **45**, 597-604 (2002).

83. Rennenberg, A., *et al.* Exoerythrocytic Plasmodium parasites secrete a cysteine protease inhibitor involved in sporozoite invasion and capable of blocking cell death of host hepatocytes. *PLoS pathogens* **6**, e1000825 (2010).
84. Sibley, L.D., Hakansson, S. & Carruthers, V.B. Gliding motility: an efficient mechanism for cell penetration. *Current biology : CB* **8**, R12-14 (1998).
85. Sultan, A.A. Molecular mechanisms of malaria sporozoite motility and invasion of host cells. *International microbiology : the official journal of the Spanish Society for Microbiology* **2**, 155-160 (1999).
86. Stewart, M.J. & Vanderberg, J.P. Malaria sporozoites leave behind trails of circumsporozoite protein during gliding motility. *The Journal of protozoology* **35**, 389-393 (1988).
87. Dubremetz, J.F. & Torpier, G. Freeze fracture study of the pellicle of an eimerian sporozoite (Protozoa, Coccidia). *Journal of ultrastructure research* **62**, 94-109 (1978).
88. Russell, D.G. Host cell invasion by Apicomplexa: an expression of the parasite's contractile system? *Parasitology* **87 (Pt 2)**, 199-209 (1983).
89. Stewart, M.J. & Vanderberg, J.P. Malaria sporozoites release circumsporozoite protein from their apical end and translocate it along their surface. *The Journal of protozoology* **38**, 411-421 (1991).
90. Mota, M.M. & Rodriguez, A. Invasion of mammalian host cells by Plasmodium sporozoites. *BioEssays : news and reviews in molecular, cellular and developmental biology* **24**, 149-156 (2002).
91. Vanderberg, J.P., Chew, S. & Stewart, M.J. Plasmodium sporozoite interactions with macrophages in vitro: a videomicroscopic analysis. *The Journal of protozoology* **37**, 528-536 (1990).
92. Amino, R., *et al.* Host cell traversal is important for progression of the malaria parasite through the dermis to the liver. *Cell host & microbe* **3**, 88-96 (2008).

93. Gonzalez, V., *et al.* Host cell entry by apicomplexa parasites requires actin polymerization in the host cell. *Cell host & microbe* **5**, 259-272 (2009).
94. Aikawa, M., Miller, L.H., Johnson, J. & Rabbege, J. Erythrocyte entry by malarial parasites. A moving junction between erythrocyte and parasite. *The Journal of cell biology* **77**, 72-82 (1978).
95. Ward, G.E., Miller, L.H. & Dvorak, J.A. The origin of parasitophorous vacuole membrane lipids in malaria-infected erythrocytes. *Journal of cell science* **106 (Pt 1)**, 237-248 (1993).
96. Coppi, A., *et al.* The malaria circumsporozoite protein has two functional domains, each with distinct roles as sporozoites journey from mosquito to mammalian host. *The Journal of experimental medicine* **208**, 341-356 (2011).
97. Frevert, U., Sinnis, P., Esko, J.D. & Nussenzweig, V. Cell surface glycosaminoglycans are not obligatory for Plasmodium berghei sporozoite invasion in vitro. *Molecular and biochemical parasitology* **76**, 257-266 (1996).
98. Strelkauskas, A. & Strelkauskas, J. *Microbiology - A Clinical Approach*, (Garland Science, 2009).
99. Schaller, M. & Park, J.H. The Behavioral Immune System (and Why It Matters). *Current Directions in Psychological Science* **20**(2011).
100. Medzhitov, R., Schneider, D.S. & Soares, M.P. Disease tolerance as a defense strategy. *Science* **335**, 936-941 (2012).
101. Belkaid, Y. & Naik, S. Compartmentalized and systemic control of tissue immunity by commensals. *Nature immunology* **14**, 646-653 (2013).
102. Janeway, C.A., Jr., Travers, P., Walport, M. & Shlomchik, M.J. *Immunobiology, 5th edition - The Immune System in Health and Disease*, (Garland Science, New York, 2001).
103. Dempsey, P.W., Vaidya, S.A. & Cheng, G. The art of war: Innate and adaptive immune responses. *Cellular and molecular life sciences : CMLS* **60**, 2604-2621 (2003).

104. Dranoff, G. Cytokines in cancer pathogenesis and cancer therapy. *Nature reviews. Cancer* **4**, 11-22 (2004).
105. Netea, M.G., Quintin, J. & van der Meer, J.W. Trained immunity: a memory for innate host defense. *Cell host & microbe* **9**, 355-361 (2011).
106. Medzhitov, R. & Janeway, C. Decoding the patterns of self and nonself by the innate immune system. *Science (New York, N.Y.)* **296**, 298-300 (2002).
107. Medzhitov, R. & Janeway, C.A., Jr. Innate immunity: the virtues of a nonclonal system of recognition. *Cell* **91**, 295-298 (1997).
108. Abbas, A.L., A.H.; Pillai, S. *Cellular and Molecular Immunology*, (Elsevier Health Sciences, 2009).
109. Iwasaki, A. & Medzhitov, R. Regulation of adaptive immunity by the innate immune system. *Science* **327**, 291-295 (2010).
110. Thallinger, B., Prasetyo, E.N., Nyanhongo, G.S. & Guebitz, G.M. Antimicrobial enzymes: an emerging strategy to fight microbes and microbial biofilms. *Biotechnology journal* **8**, 97-109 (2013).
111. Jenssen, H., Hamill, P. & Hancock, R.E. Peptide antimicrobial agents. *Clinical microbiology reviews* **19**, 491-511 (2006).
112. Walport, M.J. Complement. First of two parts. *The New England journal of medicine* **344**, 1058-1066 (2001).
113. Walport, M.J. Complement. Second of two parts. *The New England journal of medicine* **344**, 1140-1144 (2001).
114. Gozzelino, R. & Soares, M.P. Coupling Heme and Iron Metabolism via Ferritin H Chain. *Antioxid Redox Signal* (2013).
115. Nairz, M., Schroll, A., Sonnweber, T. & Weiss, G. The struggle for iron - a metal at the host-pathogen interface. *Cell Microbiol* **12**, 1691-1702 (2010).
116. Mogensen, T.H. Pathogen recognition and inflammatory signaling in innate immune defenses. *Clinical microbiology reviews* **22**, 240-273, Table of Contents (2009).

117. Pancer, Z. & Cooper, M.D. The evolution of adaptive immunity. *Annual review of immunology* **24**, 497-518 (2006).
118. Kato, L.M., Kawamoto, S., Maruya, M. & Fagarasan, S. The role of the adaptive immune system in regulation of gut microbiota. *Immunological reviews* **260**, 67-75 (2014).
119. Palm, N.W. & Medzhitov, R. Pattern recognition receptors and control of adaptive immunity. *Immunological reviews* **227**, 221-233 (2009).
120. Parker, D.C. T cell-dependent B cell activation. *Annual review of immunology* **11**, 331-360 (1993).
121. Paul, W.E. Bridging innate and adaptive immunity. *Cell* **147**, 1212-1215 (2011).
122. Tangye, S.G. & Tarlinton, D.M. Memory B cells: effectors of long-lived immune responses. *Eur J Immunol* **39**, 2065-2075 (2009).
123. Gatto, D. & Brink, R. The germinal center reaction. *The Journal of allergy and clinical immunology* **126**, 898-907; quiz 908-899 (2010).
124. Kalia, V., Sarkar, S., Gourley, T.S., Rouse, B.T. & Ahmed, R. Differentiation of memory B and T cells. *Current opinion in immunology* **18**, 255-264 (2006).
125. Vitetta, E.S., *et al.* Memory B and T cells. *Annual review of immunology* **9**, 193-217 (1991).
126. Teng, G. & Papavasiliou, F.N. Immunoglobulin somatic hypermutation. *Annual review of genetics* **41**, 107-120 (2007).
127. Chapel, H., Haeney, M., Misbah, S. & Snowden, N. *Essential Clinical Immunology*, (Wiley Blackwell, 2014).
128. Brekke, O.H. & Sandlie, I. Therapeutic antibodies for human diseases at the dawn of the twenty-first century. *Nature reviews. Drug discovery* **2**, 52-62 (2003).
129. Ouchida, R., *et al.* Critical role of the IgM Fc receptor in IgM homeostasis, B-cell survival, and humoral immune responses. *Proceedings of the National Academy of Sciences of the United States of America* **109**, E2699-2706 (2012).

130. Kubagawa, H., *et al.* Identity of the elusive IgM Fc receptor (FcmuR) in humans. *The Journal of experimental medicine* **206**, 2779-2793 (2009).
131. Nimmerjahn, F. & Ravetch, J.V. Fcgamma receptors as regulators of immune responses. *Nat Rev Immunol* **8**, 34-47 (2008).
132. Monteiro, R.C. & Van De Winkel, J.G. IgA Fc receptors. *Annual review of immunology* **21**, 177-204 (2003).
133. Mestas, J. & Hughes, C.C. Of mice and not men: differences between mouse and human immunology. *J Immunol* **172**, 2731-2738 (2004).
134. Casadevall, A., Dadachova, E. & Pirofski, L.A. Passive antibody therapy for infectious diseases. *Nature reviews. Microbiology* **2**, 695-703 (2004).
135. Landsteiner, K. The Specificity of Serological Reactions. *Courier Dover Publications* **27**, 357 - 371 (1900).
136. Jerne, N.K. The Natural-Selection Theory of Antibody Formation. *Proceedings of the National Academy of Sciences of the United States of America* **41**, 849-857 (1955).
137. Zouali, M. Natural Antibodies. *eLS*, 1-9 (2009).
138. Boyden, S.V. Natural antibodies and the immune response. *Advances in immunology* **5**, 1-28 (1966).
139. Berg, R.D. Immunity: Stimulation by Indigenous Gastrointestinal Microflora. *ENCYCLOPEDIA OF LIFE SCIENCES*, 1-7 (2001).
140. Bos, N.A., *et al.* Serum immunoglobulin levels and naturally occurring antibodies against carbohydrate antigens in germ-free BALB/c mice fed chemically defined ultrafiltered diet. *Eur J Immunol* **19**, 2335-2339 (1989).
141. Thurnheer, M.C., Zuercher, A.W., Cebra, J.J. & Bos, N.A. B1 cells contribute to serum IgM, but not to intestinal IgA, production in gnotobiotic Ig allotype chimeric mice. *J Immunol* **170**, 4564-4571 (2003).
142. Coutinho, A., Kazatchkine, M.D. & Avrameas, S. Natural autoantibodies. *Current opinion in immunology* **7**, 812-818 (1995).

143. Ochsenbein, A.F., *et al.* Control of early viral and bacterial distribution and disease by natural antibodies. *Science* **286**, 2156-2159 (1999).
144. Zouali, M. Immunological Tolerance: Mechanisms. *eLS*, 1-13 (2014).
145. Kaveri, S.V., Silverman, G.J. & Bayry, J. Natural IgM in immune equilibrium and harnessing their therapeutic potential. *J Immunol* **188**, 939-945 (2012).
146. Fehr, T., *et al.* Role of repetitive antigen patterns for induction of antibodies against antibodies. *The Journal of experimental medicine* **185**, 1785-1792 (1997).
147. Posnett, D.N. & Edinger, J. When do microbes stimulate rheumatoid factor? *The Journal of experimental medicine* **185**, 1721-1723 (1997).
148. Bovin, N.V. Natural antibodies to glycans. *Biochemistry. Biokhimiia* **78**, 786-797 (2013).
149. Oyelaran, O., McShane, L.M., Dodd, L. & Gildersleeve, J.C. Profiling human serum antibodies with a carbohydrate antigen microarray. *Journal of proteome research* **8**, 4301-4310 (2009).
150. Varki A, C.R., Esko JD,Hudson H Freeze, Pamela Stanley, Carolyn R Bertozzi, Gerald W Hart, and Marilynn E Etzler. *Essentials of Glycobiology, 2nd edition*, (Cold Spring Harbor Laboratory Press, Cold Spring Harbor (NY), 2009).
151. Springer, S.A. & Gagneux, P. Glycan evolution in response to collaboration, conflict, and constraint. *The Journal of biological chemistry* **288**, 6904-6911 (2013).
152. Rademacher, T.W., Parekh, R.B. & Dwek, R.A. Glycobiology. *Annual review of biochemistry* **57**, 785-838 (1988).
153. Axford, J. Glycobiology and medicine: an introduction. *Journal of the Royal Society of Medicine* **90**, 260-264 (1997).
154. Varki, A. Nothing in glycobiology makes sense, except in the light of evolution. *Cell* **126**, 841-845 (2006).
155. Fuster, M.M. & Esko, J.D. The sweet and sour of cancer: glycans as novel therapeutic targets. *Nature reviews. Cancer* **5**, 526-542 (2005).

156. Dwek, R.A. Glycobiology: Toward Understanding the Function of Sugars. *Chemical reviews* **96**, 683-720 (1996).
157. Taniguchi, N., Honke, K. & Fukuda, M. *Handbook of glycosyltransferases and related gene*, (Springer Japan, Japan, 2002).
158. Drickamer, K. & Taylor, M.E. *Introduction to Glycobiology*, (Oxford University Press, USA, 2006).
159. Kolset, S.O., Prydz, K. & Pejler, G. Intracellular proteoglycans. *The Biochemical journal* **379**, 217-227 (2004).
160. Taylor, D.R. & Hooper, N.M. GPI-Anchored Proteins in Health and Disease. in *Post-Translational Modifications in Health and Disease, Protein Reviews* Vol. 13 39-55 (Springer Science+Business Media, 2011).
161. Bishop, J.R. & Gagneux, P. Evolution of carbohydrate antigens--microbial forces shaping host glycomes? *Glycobiology* **17**, 23R-34R (2007).
162. Varki, A. Evolutionary forces shaping the Golgi glycosylation machinery: why cell surface glycans are universal to living cells. *Cold Spring Harbor perspectives in biology* **3**(2011).
163. Galili, U., Rachmilewitz, E.A., Peleg, A. & Flechner, I. A unique natural human IgG antibody with anti-alpha-galactosyl specificity. *The Journal of experimental medicine* **160**, 1519-1531 (1984).
164. van Die, I. & Cummings, R.D. Glycan gimmickry by parasitic helminths: a strategy for modulating the host immune response? *Glycobiology* **20**, 2-12 (2010).
165. Guha-Niyogi, A., Sullivan, D.R. & Turco, S.J. Glycoconjugate structures of parasitic protozoa. *Glycobiology* **11**, 45R-59R (2001).
166. Borst, P. & Rudenko, G. Antigenic variation in African trypanosomes. *Science* **264**, 1872-1873 (1994).
167. Ferguson, M.A., Homans, S.W., Dwek, R.A. & Rademacher, T.W. Glycosyl-phosphatidylinositol moiety that anchors Trypanosoma brucei variant surface glycoprotein to the membrane. *Science* **239**, 753-759 (1988).

168. de Lederkremer, R.M., *et al.* Complete structure of the glycan of lipopeptidophosphoglycan from Trypanosoma cruzi Epimastigotes. *The Journal of biological chemistry* **266**, 23670-23675 (1991).
169. Maizels, R.M. & Hewitson, J.P. Immune Recognition of Parasite Glycans. in *'Anticarbohydrate Antibodies – From Molecular Basis to Clinical Application'* (eds. P., K. & Müller-Loennies, S.) (Springer, 2012).
170. Todeschini, A.R., *et al.* Alpha-N-acetylglucosamine-linked O-glycans of sialoglycoproteins (Tc-mucins) from Trypanosoma cruzi Colombiana strain. *Memorias do Instituto Oswaldo Cruz* **104 Suppl 1**, 270-274 (2009).
171. Button, L.L. & McMaster, W.R. Molecular cloning of the major surface antigen of leishmania. *The Journal of experimental medicine* **167**, 724-729 (1988).
172. Macedo, C.S., Schwarz, R.T., Todeschini, A.R., Previato, J.O. & Mendonca-Previato, L. Overlooked post-translational modifications of proteins in Plasmodium falciparum: N- and O-glycosylation -- a review. *Memorias do Instituto Oswaldo Cruz* **105**, 949-956 (2010).
173. Tachado, S.D., Mazhari-Tabrizi, R. & Schofield, L. Specificity in signal transduction among glycosylphosphatidylinositols of Plasmodium falciparum, Trypanosoma brucei, Trypanosoma cruzi and Leishmania spp. *Parasite immunology* **21**, 609-617 (1999).
174. Berhe, S., Gerold, P., Kedees, M.H., Holder, A.A. & Schwarz, R.T. Plasmodium falciparum: merozoite surface proteins 1 and 2 are not posttranslationally modified by classical N- or O-glycans. *Exp Parasitol* **94**, 194-197 (2000).
175. Gowda, D.C., Gupta, P. & Davidson, E.A. Glycosylphosphatidylinositol anchors represent the major carbohydrate modification in proteins of intraerythrocytic stage Plasmodium falciparum. *The Journal of biological chemistry* **272**, 6428-6439 (1997).
176. Dinglasan, R.R., *et al.* Plasmodium falciparum ookinetes require mosquito midgut chondroitin sulfate proteoglycans for cell invasion.

Proceedings of the National Academy of Sciences of the United States of America **104**, 15882-15887 (2007).

177. Dinglasan, R.R., Fields, I., Shahabuddin, M., Azad, A.F. & Sacci, J.B., Jr. Monoclonal antibody MG96 completely blocks Plasmodium yoelii development in Anopheles stephensi. *Infection and immunity* **71**, 6995-7001 (2003).
178. Hussain, M.R.M., Hassan, M., Afzala, I. & Afzal, A. Role of Gal and GalNAc containing glycans in various physiological processes. *Egyptian Journal of Medical Human Genetics* **13**, 1-9 (2012).
179. Macher, B.A. & Galili, U. The Galalpha1,3Galbeta1,4GlcNAc-R (alpha-Gal) epitope: a carbohydrate of unique evolution and clinical relevance. *Biochimica et biophysica acta* **1780**, 75-88 (2008).
180. Hendricks, S.P., He, P., Stults, C.L. & Macher, B.A. Regulation of the expression of Gal alpha 1-3Gal beta 1-4GlcNAc glycosphingolipids in kidney. *The Journal of biological chemistry* **265**, 17621-17626 (1990).
181. He, P., Hu, J. & Macher, B.A. Glycosphingolipids of rabbit, sheep, and pig thymus. *Archives of biochemistry and biophysics* **305**, 350-361 (1993).
182. Eto, T., Ichikawa, Y., Nishimura, K., Ando, S. & Yamakawa, T. Chemistry of lipid of the posthemyolytic residue or stroma of erythrocytes. XVI. Occurrence of ceramide pentasaccharide in the membrane of erythrocytes and reticulocytes of rabbit. *Journal of biochemistry* **64**, 205-213 (1968).
183. Stellner, K., Saito, H. & Hakomori, S.I. Determination of aminosugar linkages in glycolipids by methylation. Aminosugar linkages of ceramide pentasaccharides of rabbit erythrocytes and of Forssman antigen. *Archives of biochemistry and biophysics* **155**, 464-472 (1973).
184. Dabrowski, U., Hanfland, P., Egge, H., Kuhn, S. & Dabrowski, J. Immunochemistry of I/i-active oligo- and polyglycosylceramides from rabbit erythrocyte membranes. Determination of branching patterns of a ceramide pentadecasaccharide by 1H nuclear magnetic resonance. *The Journal of biological chemistry* **259**, 7648-7651 (1984).

185. Hanfland, P., *et al.* Structure elucidation of blood group B-like and I-active ceramide eicosa- and pentacosasaccharides from rabbit erythrocyte membranes by combined gas chromatography-mass spectrometry; electron-impact and fast-atom-bombardment mass spectrometry; and two-dimensional correlated, relayed-coherence transfer, and nuclear Overhauser effect 500-MHz 1H-n.m.r. spectroscopy. *Carbohydrate research* **178**, 1-21 (1988).
186. Uemura, K., Yuzawa, M. & Taketomi, T. Characterization of major glycolipids in bovine erythrocyte membrane. *Journal of biochemistry* **83**, 463-471 (1978).
187. Watanabe, K., Hakomori, S.I., Childs, R.A. & Feizi, T. Characterization of a blood group I-active ganglioside. Structural requirements for I and i specificities. *The Journal of biological chemistry* **254**, 3221-3228 (1979).
188. Spiro, R.G. & Bhoyroo, V.D. Occurrence of alpha-D-galactosyl residues in the thyroglobulins from several species. Localization in the saccharide chains of the complex carbohydrate units. *The Journal of biological chemistry* **259**, 9858-9866 (1984).
189. Dorland, L., van Halbeek, H. & Vliegenthart, J.F. The identification of terminal alpha (1----3)-linked galactose in N-acetyllactosamine type of glycopeptides by means of 500-MHz 1H-NMR spectroscopy. *Biochemical and biophysical research communications* **122**, 859-866 (1984).
190. Kim, Y.G., *et al.* The identification and characterization of xenoantigenic nonhuman carbohydrate sequences in membrane proteins from porcine kidney. *Proteomics* **6**, 1133-1142 (2006).
191. Oriol, R., Ye, Y., Koren, E. & Cooper, D.K. Carbohydrate antigens of pig tissues reacting with human natural antibodies as potential targets for hyperacute vascular rejection in pig-to-man organ xenotransplantation. *Transplantation* **56**, 1433-1442 (1993).
192. Galili, U., Anaraki, F., Thall, A., Hill-Black, C. & Radic, M. One percent of human circulating B lymphocytes are capable of producing the natural anti-Gal antibody. *Blood* **82**, 2485-2493 (1993).

193. Galili, U., Korkesh, A., Kahane, I. & Rachmilewitz, E.A. Demonstration of a natural antigalactosyl IgG antibody on thalassemic red blood cells. *Blood* **61**, 1258-1264 (1983).
194. Galili, U., Clark, M.R. & Shohet, S.B. Excessive binding of natural anti-alpha-galactosyl immunoglobin G to sickle erythrocytes may contribute to extravascular cell destruction. *The Journal of clinical investigation* **77**, 27-33 (1986).
195. Galili, U., Macher, B.A., Buehler, J. & Shohet, S.B. Human natural anti-alpha-galactosyl IgG. II. The specific recognition of alpha (1----3)-linked galactose residues. *The Journal of experimental medicine* **162**, 573-582 (1985).
196. Galili, U., Mandrell, R.E., Hamadeh, R.M., Shohet, S.B. & Griffiss, J.M. Interaction between human natural anti-alpha-galactosyl immunoglobulin G and bacteria of the human flora. *Infection and immunity* **56**, 1730-1737 (1988).
197. Hamadeh, R.M., *et al.* Human natural anti-Gal IgG regulates alternative complement pathway activation on bacterial surfaces. *The Journal of clinical investigation* **89**, 1223-1235 (1992).
198. Galili, U., Buehler, J., Shohet, S.B. & Macher, B.A. The human natural anti-Gal IgG. III. The subtlety of immune tolerance in man as demonstrated by crossreactivity between natural anti-Gal and anti-B antibodies. *The Journal of experimental medicine* **165**, 693-704 (1987).
199. Galili, U., Shohet, S.B., Kobrin, E., Stults, C.L. & Macher, B.A. Man, apes, and Old World monkeys differ from other mammals in the expression of alpha-galactosyl epitopes on nucleated cells. *The Journal of biological chemistry* **263**, 17755-17762 (1988).
200. Thall, A., Etienne-Decerf, J., Winand, R.J. & Galili, U. The alpha-galactosyl epitope on mammalian thyroid cells. *Acta endocrinologica* **124**, 692-699 (1991).

201. Basu, M. & Basu, S. Enzymatic synthesis of a blood group B-related pentaglycosylceramide by an alpha-galactosyltransferase from rabbit bone marrow. *The Journal of biological chemistry* **248**, 1700-1706 (1973).
202. Smith, D.F., Larsen, R.D., Mattox, S., Lowe, J.B. & Cummings, R.D. Transfer and expression of a murine UDP-Gal:beta-D-Gal-alpha 1,3-galactosyltransferase gene in transfected Chinese hamster ovary cells. Competition reactions between the alpha 1,3-galactosyltransferase and the endogenous alpha 2,3-sialyltransferase. *The Journal of biological chemistry* **265**, 6225-6234 (1990).
203. Shetterly, S., *et al.* Alpha 1,3 galactosyltransferase: new sequences and characterization of conserved cysteine residues. *Glycobiology* **11**, 645-653 (2001).
204. Joziasse, D.H., Shaper, J.H., Van den Eijnden, D.H., Van Tunen, A.J. & Shaper, N.L. Bovine alpha 1----3-galactosyltransferase: isolation and characterization of a cDNA clone. Identification of homologous sequences in human genomic DNA. *The Journal of biological chemistry* **264**, 14290-14297 (1989).
205. Larsen, R.D., *et al.* Isolation of a cDNA encoding a murine UDPgalactose:beta-D-galactosyl- 1,4-N-acetyl-D-glucosaminide alpha-1,3-galactosyltransferase: expression cloning by gene transfer. *Proceedings of the National Academy of Sciences of the United States of America* **86**, 8227-8231 (1989).
206. Larsen, R.D., Rivera-Marrero, C.A., Ernst, L.K., Cummings, R.D. & Lowe, J.B. Frameshift and nonsense mutations in a human genomic sequence homologous to a murine UDP-Gal:beta-D-Gal(1,4)-D-GlcNAc alpha(1,3)-galactosyltransferase cDNA. *The Journal of biological chemistry* **265**, 7055-7061 (1990).
207. Lanteri, M., Giordanengo, V., Vidal, F., Gaudray, P. & Lefebvre, J.C. A complete alpha1,3-galactosyltransferase gene is present in the human genome and partially transcribed. *Glycobiology* **12**, 785-792 (2002).

208. Koike, C., *et al.* Molecular basis of evolutionary loss of the alpha 1,3-galactosyltransferase gene in higher primates. *The Journal of biological chemistry* **277**, 10114-10120 (2002).
209. Galili, U. & Swanson, K. Gene sequences suggest inactivation of alpha-1,3-galactosyltransferase in catarrhines after the divergence of apes from monkeys. *Proceedings of the National Academy of Sciences of the United States of America* **88**, 7401-7404 (1991).
210. Joziasse, D.H., Shaper, J.H., Jabs, E.W. & Shaper, N.L. Characterization of an alpha 1----3-galactosyltransferase homologue on human chromosome 12 that is organized as a processed pseudogene. *The Journal of biological chemistry* **266**, 6991-6998 (1991).
211. Galili, U., Clark, M.R., Shohet, S.B., Buehler, J. & Macher, B.A. Evolutionary relationship between the natural anti-Gal antibody and the Gal alpha 1----3Gal epitope in primates. *Proceedings of the National Academy of Sciences of the United States of America* **84**, 1369-1373 (1987).
212. Almeida, I.C., Milani, S.R., Gorin, P.A. & Travassos, L.R. Complement-mediated lysis of Trypanosoma cruzi trypomastigotes by human anti-alpha-galactosyl antibodies. *J Immunol* **146**, 2394-2400 (1991).
213. Avila, J.L. & Rojas, M. A galactosyl(alpha 1-3)mannose epitope on phospholipids of Leishmania mexicana and L. braziliensis is recognized by trypanosomatid-infected human sera. *Journal of clinical microbiology* **28**, 1530-1537 (1990).
214. Posekany, K.J., Pittman, H.K., Bradfield, J.F., Haisch, C.E. & Verbanac, K.M. Induction of cytolytic anti-Gal antibodies in alpha-1,3-galactosyltransferase gene knockout mice by oral inoculation with Escherichia coli O86:B7 bacteria. *Infection and immunity* **70**, 6215-6222 (2002).
215. Repik, P.M., Strizki, J.M. & Galili, U. Differential host-dependent expression of alpha-galactosyl epitopes on viral glycoproteins: a study of eastern equine encephalitis virus as a model. *The Journal of general virology* **75 (Pt 5)**, 1177-1181 (1994).

216. Teneberg, S., *et al.* Molecular mimicry in the recognition of glycosphingolipids by Gal alpha 3 Gal beta 4 GlcNAc beta-binding Clostridium difficile toxin A, human natural anti alpha-galactosyl IgG and the monoclonal antibody Gal-13: characterization of a binding-active human glycosphingolipid, non-identical with the animal receptor. *Glycobiology* **6**, 599-609 (1996).
217. Rodriguez, I.A. & Welsh, R.M. Possible role of a cell surface carbohydrate in evolution of resistance to viral infections in old world primates. *Journal of virology* **87**, 8317-8326 (2013).
218. Krivan, H.C., Clark, G.F., Smith, D.F. & Wilkins, T.D. Cell surface binding site for Clostridium difficile enterotoxin: evidence for a glycoconjugate containing the sequence Gal alpha 1-3Gal beta 1-4GlcNAc. *Infection and immunity* **53**, 573-581 (1986).
219. Springer, G.F. Blood-group and Forssman antigenic determinants shared between microbes and mammalian cells. *Progress in allergy* **15**, 9-77 (1971).
220. Chagas, C. Nova tripanozomiaze humana. Estudos sobre a morfolojia e o ciclo evolutivo do Schizotrypanum cruzi n.gen. n.sp., ajente etiolojico de nova entidade morbida do homem. . *Memorias do Instituto Oswaldo Cruz*, 11 - 62 (1909).
221. Ribeiro, A.L., Nunes, M.P., Teixeira, M.M. & Rocha, M.O. Diagnosis and management of Chagas disease and cardiomyopathy. *Nature reviews. Cardiology* **9**, 576-589 (2012).
222. Towbin, H., *et al.* Circulating antibodies to mouse laminin in Chagas disease, American cutaneous leishmaniasis, and normal individuals recognize terminal galactosyl(alpha 1-3)-galactose epitopes. *The Journal of experimental medicine* **166**, 419-432 (1987).
223. Couto, A.S., Goncalves, M.F., Colli, W. & de Lederkremer, R.M. The N-linked carbohydrate chain of the 85-kilodalton glycoprotein from Trypanosoma cruzi trypomastigotes contains sialyl, fucosyl and

galactosyl (alpha 1-3)galactose units. *Molecular and biochemical parasitology* **39**, 101-107 (1990).

224. Avila, J.L., Rojas, M. & Galili, U. Immunogenic Gal alpha 1----3Gal carbohydrate epitopes are present on pathogenic American Trypanosoma and Leishmania. *J Immunol* **142**, 2828-2834 (1989).
225. Abrahamsohn, I.A. & Silva, W.D. Antibody dependent cell-mediated cytotoxicity against Trypanosoma cruzi. *Parasitology* **75**, 317-323 (1977).
226. Gazzinelli, R.T., Pereira, M.E., Romanha, A., Gazzinelli, G. & Brener, Z. Direct lysis of Trypanosoma cruzi: a novel effector mechanism of protection mediated by human anti-gal antibodies. *Parasite immunology* **13**, 345-356 (1991).
227. Souto-Padron, T., Almeida, I.C., de Souza, W. & Travassos, L.R. Distribution of alpha-galactosyl-containing epitopes on Trypanosoma cruzi trypomastigote and amastigote forms from infected Vero cells detected by Chagasic antibodies. *The Journal of eukaryotic microbiology* **41**, 47-54 (1994).
228. Avila, J.L. alpha-Galactosyl-bearing epitopes as potent immunogens in Chagas' disease and leishmaniasis. *Sub-cellular biochemistry* **32**, 173-213 (1999).
229. Travassos, L.R. & Almeida, I.C. Carbohydrate immunity in American trypanosomiasis. *Springer seminars in immunopathology* **15**, 183-204 (1993).
230. Gazzinelli, R.T., *et al.* Anti-Trypanosoma cruzi and anti-laminin antibodies in chagasic patients after specific treatment. *Journal of clinical microbiology* **26**, 1795-1800 (1988).
231. Vicente de Paula Antunes Teixeira, E.M., Hipolito de Oliveira Almeida, Sheila Soares, Hélio Moraes de Souza e César Augusto de Morais. Sistema ABO e formas anatomoclínicas da doença de Chagas crônica. *Revista da Sociedade Brasileira de Medicina Tropical* **20**, 163-167 (1987).

232. Wassef, M.K., Fioretti, T.B. & Dwyer, D.M. Lipid analyses of isolated surface membranes of Leishmania donovani promastigotes. *Lipids* **20**, 108-115 (1985).
233. McConville, M.J. & Bacic, A. A family of glycoinositol phospholipids from Leishmania major. Isolation, characterization, and antigenicity. *The Journal of biological chemistry* **264**, 757-766 (1989).
234. Avila, J.L., Rojas, M. & Towbin, H. Serological activity against galactosyl-alpha(1-3)galactose in sera from patients with several kinetoplastida infections. *Journal of clinical microbiology* **26**, 126-132 (1988).
235. Geyer, R., *et al.* Major oligosaccharides in the glycoprotein of Friend murine leukemia virus: structure elucidation by one- and two-dimensional proton nuclear magnetic resonance and methylation analysis. *Biochemistry* **23**, 5628-5637 (1984).
236. Galili, U., *et al.* Enhancement of antigen presentation of influenza virus hemagglutinin by the natural human anti-Gal antibody. *Vaccine* **14**, 321-328 (1996).
237. Takeuchi, Y., *et al.* Sensitization of cells and retroviruses to human serum by (alpha 1-3) galactosyltransferase. *Nature* **379**, 85-88 (1996).
238. Doenz, U., Nydegger, U.E., Kueng, A., Carrel, T. & Mohacsi, P. Anti-Galalpha1-3Gal IgM/IgG antibody levels in infants: do they have a clinical relevance in pediatric xenotransplantation? *J Heart Lung Transplant* **19**, 1108-1113 (2000).
239. Ramasamy, R. & Reese, R.T. Terminal galactose residues and the antigenicity of Plasmodium falciparum glycoproteins. *Molecular and biochemical parasitology* **19**, 91-101 (1986).
240. Nahlen, B.L., Korenromp, E.L., Miller, J.M. & Shibuya, K. Malaria risk: estimating clinical episodes of malaria. *Nature* **437**, E3; discussion E4-5 (2005).

241. WHO, W.H.O. Severe falciparum malaria. World Health Organization, Communicable Diseases Cluster. *Transactions of the Royal Society of Tropical Medicine and Hygiene* **94 Suppl 1**, S1-90 (2000).

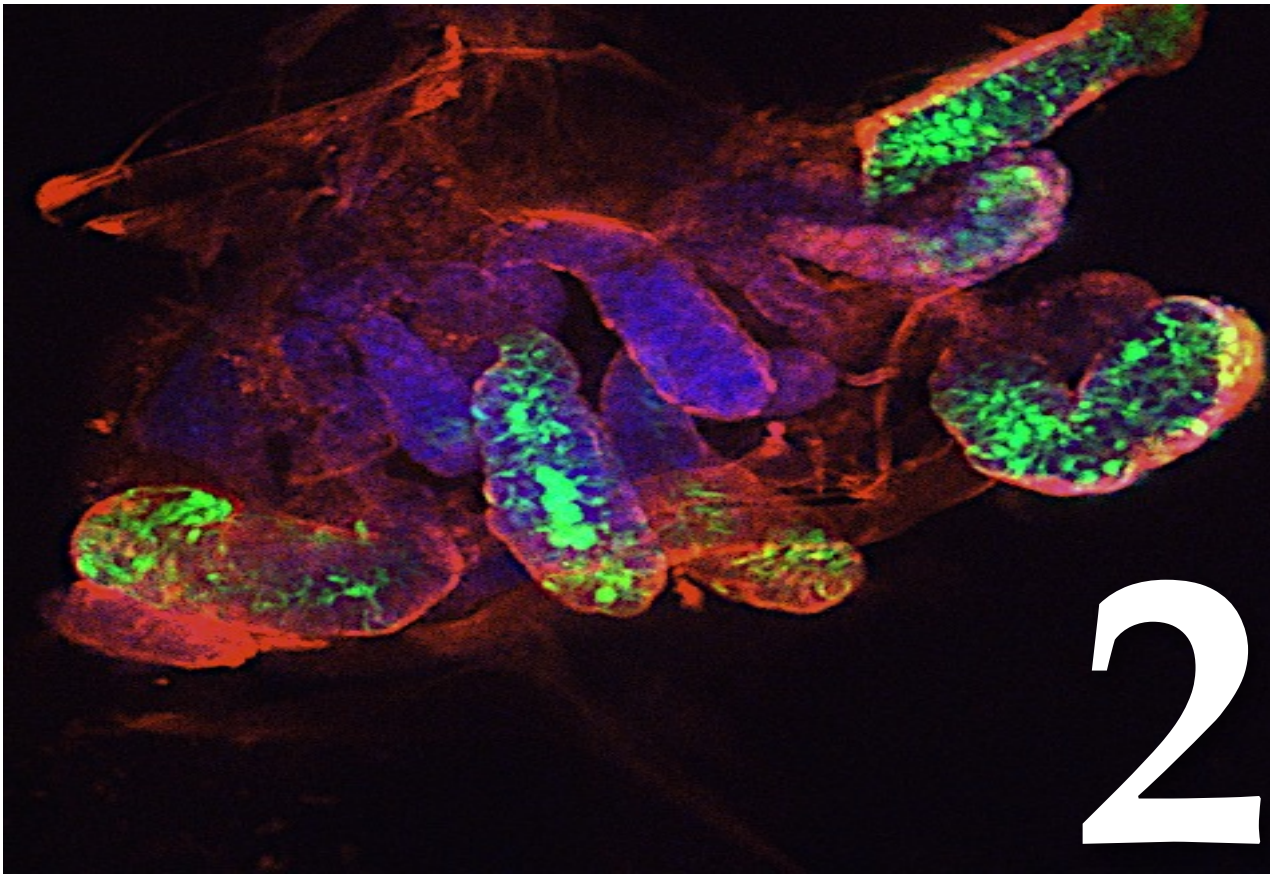

2

α-gal Glycan & *Plasmodium*

.

Abstract

There is a significant interest in developing effective vaccines against life-threatening infectious diseases, specifically against *Plasmodium* infection. Major progress has been made on the characterization of potential antigens associated with surface proteins expressed by blood stage merozoites or parasitized erythrocytes that can be used as immunogens for an effective vaccine. Glycans expressed by different stages of *Plasmodium* infection have not been considered as antigenic determinants for the generation of vaccines. Here, we demonstrate that *Plasmodium* sporozoites express α-gal, a glycan also expressed during the exo-erythrocytic and erythrocytic stages of infection. The association of α-gal glycan to *Plasmodium* proteins was demonstrated by Western blot technique. Removal of α-gal from the surface of *Plasmodium* suggests that this glycan is bound to surface GPI-anchored proteins. Detection of α-gal glycan in the salivary glands of uninfected female *Anopheles* mosquitoes suggests for an unknown mechanism that incorporates α-gal at the *Plasmodium* surface.

2.1 Introduction

Although *Plasmodium* proteins and lipids can be glycosylated, it is believed that the overall glycosylation profile of *Plasmodium* is somehow lower when compared to other protozoan parasites such as trypanosomatid[1]. It is well established that *Plasmodium* relies on recognition/binding of host glycans, expressed by *Anopheles* mosquitoes and humans, for the progression through its life-cycle. This notion is supported by the finding that *Plasmodium* ookinete-to-oocyst transition is inhibited when glycoconjugate antigens are targeted by monoclonal Abs (mAbs)[2-4]. Moreover, *Plasmodium* sporozoites can interact with oligosaccharides such as GlcNAc and GalNAc present on mosquito proteins, such as laminin, which confers ookinetes the ability to traverse the mosquito midgut and allows sporozoites to avoid immune recognition by the mosquito immune system[2-4]. Additionally, *Plasmodium* merozoites rely on the recognition of sialylated glycans, associated to the RBC glycophorin A, for invasion of RBC in their human host[5]. Moreover, GPI-anchors account for the most prominent glycan expressed in *Plasmodium* and can act as putative PAMPs recognized by PRRs expressed in mammalian hosts[6]. It is also known that this glycan triggers the inflammatory response that underlies some of the clinical symptoms of malaria, including cytokine production (i.e., tumor necrosis factor α (TNF-α) and interleukin-1α (IL-1α)), as well as fever and hypoglycaemia[7]. These pathogenic effects can be inhibited by anti-GPI Abs[8].

Although glycosylation processes in *Plasmodium* have not been fully characterized, experimental evidence shows that *Plasmodium* parasites can synthesize UDP-GlcnAc and GDP-Man[9]. However, the intermediate glycan produced through the classical *N*-glycosylation pathway appears to be absent, arguing for presence of an unusual type of N-linked oligosaccharide in *Plasmodium*[9]. However, *Plasmodium* expresses N-linked

glycans, indicating that α-gal can be detected in the asexual blood stages of infection in its mammalian host[10,11].

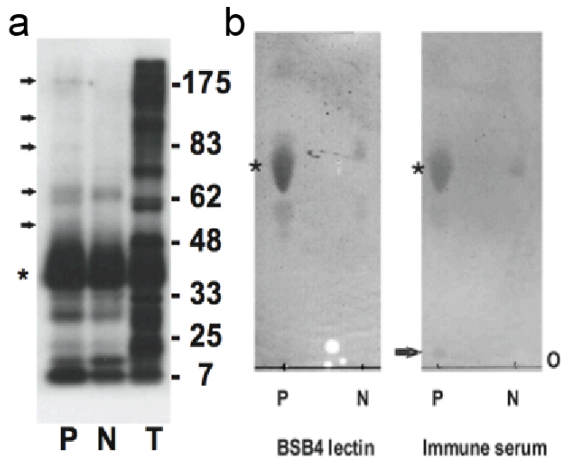

Figure 2.1 Detection of α-gal epitope on parasites. a) Biotin-BSI-IB_4 lectin blot of protein samples from *P. falciparum* late blood stages (P), *T.brucei* trypomastigotes (T), and control, non-infected (N) RBC proteins binding to BSB_4-Sepharose. The asterisk indicates the migration position of eluted BSI-IB_4 that also reacts with biotin-BSI-IB_4. **b)** Blot of lipids prepared from *P. falciparum* late asexual stages (P), and control, non-infected RBC lipids (N), reacting with BSI-IB_4 lectin (*left panel*) and pooled immune malaria sera (*right panel*), obtained from a malaria endemic area in Uganda. The asterisks show the major lipid species of the parasites that also reacted with streptavidin-peroxidase alone or with non-immune human serum after treatment with peroxidase-conjugated anti-human immunoglobulin. Adapted from[12].

Several studies by Ravindran and co-workers also argued for the expression of α-gal glycan in *Plasmodium* as well as for a putative role of anti-α-gal Abs in host protection against *Plasmodium* infection in individuals from malaria endemic areas[13]. The data supporting this notion was however, largely circumstantial. The levels of anti-α-gal Abs in individuals developing a severe form of malaria know as cerebral malaria were found to be lower, as compared to infected individuals that did not develop this severe form of disease. This suggested that anti-α-gal Abs might act in a protective manner against erythrocytic stages of infection, preventing the onset of cerebral malaria. In keeping with this notion, the α-gal glycan was found on the surface *P. falciparum* infected RBCs[13]. More

than a decade later, a study by the same group suggested the presence of α-gal in a wide range of *T. brucei* bloodstream trypomastigote glycoproteins and glycolipids. By comparison, there were relatively low or almost no α-gal in *P. falciparum* asexual blood stage glycoconjugates **(Figure 2.1)**[12]. Nonetheless, a hydrophilic lipid moiety specific to *P. falciparum* was found to react with immune human sera[12].

Despite these studies, it was still unclear whether *Plasmodium* expresses α-gal or not. Here, we showed unequivocally that *Plasmodium spp.* present α-gal during their exo-erythrocytic and erythrocytic stages. Moreover, we demonstrated that female *Anopheles* mosquitoes also express α-gal glycan; raising the possibility that this glycan from the mosquito might bind and be incorporated to glycoconjugates in *Plasmodium* sporozoites.

2.2 Materials and Methods

2.2.1 Parasites maintenance and mosquitoes rearing

Transgenic *P. berghei* ANKA strains expressing green fluorescent protein (GFP) under the EEF1α promoter, i.e. *Pb*A$^{EEF1a\text{-}GFP}$ (259cl1; MR4; MRA-865)[14] or under the *hsp70* promoter[15] i.e. *PbA*$^{Hsp70\text{-}GFP}$ (kindly provided by Robert Menard, Institut Pasteur, France), transgenic *P. yoelii* 17XNL strain expressing GFP under the *PbA* EEF1 promoter (MR4; MRA-817; kindly provided by Robert Menard, Institut Pasteur, France)[16] were used.

Female *A. stephensi* mosquitoes (28°C; 70–80% humidity under 12h/12h light/dark cycle) were reared[17] at the Center of the Instituto de Higiene e Medicina Tropical (IHMT), Universidade Nova de Lisboa, Portugal, and maintained using 10% sucrose (or glucose) and infected 3-5 days after emergence.

For sporozoite production, *P. berghei* ANKA infected RBC ($1x10^6$) were

administered i.p. to BALB/c mice and the presence of gametocyte-stage parasites capable of exflagellation was monitored in fresh blood preparations. Infected BALB/c mice were used to feed 3 to 4-day-old female *A.* mosquitoes (~1h), which were used 18-25 days post-infection for subsequent infections. When infected with *P. berghei* ANKA mosquitoes were maintained at 26°C (Center of the Instituto de Higiene e Medicina Tropical (IHMT)) whereas mosquitoes infected with *P. yoelii* 17XNL-GFP[18] were maintained at 24-25°C (Centre for Production and Infection of *Anopheles*; CEPIA, Pasteur Institute, France). Alternatively, *P. yoelii* 17XNL (MR4; MRA-593)[16] infected mosquitoes were purchased from Radboud University Nijmegen Medical Centre (Nijmegen, Netherlands). *P. falciparum* 3D7 sporozoites were kindly provided by Robert Menard, (Institut Pasteur, France)[19].

2.2.2 Anti-α-gal monoclonal Abs

Anti-α-gal hybridomas were cultured in RPMI 1640 (Invitrogen Life Technologies) supplemented with 0.1 mM Sodium Pyruvate, 0.01 M HEPES, 0.05 mM β-mercaptoethanol and 2% FBS (IgG depleted). The anti-α-gal IgG2a, IgG2b and IgG3 hybridomas were derived by sub-cloning of the original IgG1 (GT6-27) hybridoma and as such have similar affinities for α-gal, as described before[20,21]. Antibodies were purified by affinity chromatography using HiTrap Protein G columns (GE Healthcare Life Sciences). Anti-α-gal IgG3 purification was carried out by a non-chromatographic method taking advantage of its euglobulin properties as described[22]. Purified mAbs were extensively dialyzed against PBS. Protein concentration was determined using NanoDrop ND-1000 (λ=280nm; Thermo Scientific) and purity confirmed by SDS-PAGE analysis. When indicated, mAbs were labeled with Alexa Fluor® 647 Protein Labeling Kit (A20173), as per manufacturer recommendations (Molecular Probes®,

Invitrogen). Anti-mouse IgM total-A647 (Clone: R33.24.12) was used to reveal anti-α-gal IgM mAb in immunofluorescence assay.

2.2.3 Specificity of anti-α-gal Abs

96-well plates (PolySorp; Nunc) were coated with α-gal (α-gal-BSA; 50μL; 10μg/mL in 0.5M carbonate bicarbonate buffer; pH 9.5; 2h at 37°C or overnight at 4°C), blocked with BSA (100μL; 1% w/v in PBS; 1h; RT) and washed (5X; PBS/0.05% Tween-20). Plates were incubated (1h; RT) with serum serial dilutions in PBS, 1% BSA and washed (5X; PBS/0.05% Tween-20). Anti-α-gal antibodies were detected using HRP-conjugated anti-mouse IgM, total IgG, IgG1, IgG2a, IgG2b or IgG3 (50μL, 1:1-2000 dilution, 1h, RT) and washed (5X; PBS/0.05% Tween-20). Purified anti-α-gal IgM[23], IgG1 (GT6-27), IgG2a and IgG2b and IgG3 (GT4-31) mAb[20,21] were used as standards. 3,3,5,5-Tetramethylbenzidine (TMB) Substrate Reagent Set (BD Biosciences) was used to reveal peroxidase activity (15-30min; RT) and reaction was stopped using 2N sulfuric acid. Optical densities (OD) were reported at λ=450nm and normalized by subtracting background OD values (λ=600nm; Victor 3; PerkinElmer). Concentration of each anti-α-gal IgG subclass determined, as described[24].

2.2.4 Isolation of sporozoites from salivary glands

Mosquitoes were narcotized (-20°C; 3-5min), washed in 70% ethanol (1X; 10-20sec) and PBS (3X; 10-20sec; Ambion). Salivary glands were obtained by dissection under a zoom stereomicroscope (3X magnification; Nikon SMZ800, Japan) and preserved in RPMI 1640 medium (Gibco BRL) or PBS. Salivary glands were smashed using Pellet pestles cordless motor (10-15sec; Sigma) to release sporozoites and centrifuged (100g; 5min) in LoBind microfuge tubes (Eppendorf). Supernatant was filtered (100μm cell strainers; BD Falcon™) to exclude debris. Sporozoites were counted using KOVA Glasstic Slide 10, with a quantitative grid (Fisher Scientific GMBH).

2.2.5 Detection of α-gal in *Plasmodium* sporozoites

*Pb*A$^{EEF1a\text{-}GFP}$, *Pb*A$^{Hsp70\text{-}GFP}$, *P. falciparum* 3D7 or *P. yoelii* 17XNL-GFP sporozoites, isolated from the salivary glands of *A. stephensi* or *A. gambiae* mosquitoes, 18-25 days post-infection were allowed to attach to Teflon printed (10 wells, 8mm; no-adherent surface; Immuno-Cell Int.) or to diagnostic glass slides. Sporozoites were fixed (20-50μL; 4% PFA; 20-30min; RT or 37°C) and washed gently (1X; PBS). Sporozoites were stained with Alexa Fluor® 647 conjugated BSI-IB_4 (100μL; 200μg/mL; 2h, RT), Alexa Fluor® 647 conjugated anti-α-gal IgG1, IgG2a, IgG2b, IgG3 mAb (100μL; 50μg/mL; overnight; 4°C) or with non-conjugated anti-α-gal IgM (M86) mAb (100μL; 50μg/mL; overnight; 4°C) and washed (1X; PBS). Non-conjugated IgM antibodies were detected using Alexa Fluor® 647 conjugated goat anti-mouse IgM (100μL; 10μg/mL; overnight, 4°C) (Molecular Probes®, Invitrogen). After washing (1X; PBS), slides were incubated with 4',6-diamidino-2-phenylindole (DAPI) (100μL; 10μg/mL; 10min; RT) (Molecular Probes®, washed (1X; PBS) and dried in dark room without covering with coverslip (RT). Images of *Pb*A sporozoites were obtained by DeltaVision Core immunofluorescence microscopy (Applied Precision/Olympus) or Spinning Disk Confocal microscopy Revolution xD (Andor Technology) at 100X magnification. Actin was detected using Alexa Fluor® 568 Phalloidin (Molecular Probes®; 100μL; 3units/mL; 1h; RT) in *P. falciparum* 3D7 and *P. yoelii* 17XNL-GFP sporozoites to which was added ProLong® Gold Antifade Reagent (Invitrogen) and wells were covered with coverslips. Slides were visualized with Axiovert II fluorescence microscope (Zeiss). Images were analyzed using bicubic interpolation and rescaling with ImageJ software (NIH).

For detection of α-gal by flow cytometry, *Pb*A$^{Hsp70\text{-}GFP}$ sporozoites were isolated from the salivary glands of *A. stephensi* mosquitoes 19-25 days post-infection (10^5; 30-40ul; PBS; ice cold; 30min), fixed (30-40μL; 4% PFA in

PBS; 20-30min; 37°C) and washed (1X; PBS; 9300g; 2min). Staining was performed with Alexa Fluor® 647 conjugated BSI-IB_4 (100μg/mL; 1h; 37°C). Sporozoites were washed (1X; PBS; 9300g; 2min) and Alexa Fluor® 647 BSI-IB_4 signal was detected in CyAn™ ADP flow cytometry (Beckman Coulter; USA) with the Summit Software (v4.3; Beckman Coulter), gating on FITC (for sporozoite detection) and APC (for α-gal detection).

For detection of α-gal by Western blotting, *Pb*A$^{Hsp70\text{-}GFP}$, *P. falciparum* 3D7 and *P. yoelii* 17XNL-GFP sporozoites were isolated from the salivary glands of 40-70 mosquitoes, 21-25 days after infection. Briefly, salivary glands were collected into LoBind microfuge tubes (PBS; on ice), smashed using pellet pestles cordless motor (10-15sec; 2X) and a short spin was applied to pellet the debris. Supernatant (30-50μL; 1-2.5x10^5 sporozoites) was transferred into LoBind microfuge tube and aliquots were stored at -80°C until used. Number of *Plasmodium* sporozoites (equivalent to 10^5 per sample) was normalized to corresponding number of salivary glands from non-infected mosquitoes. Samples were lysed (50mM Tris/HCl pH 7.5, 150mM NaCl, 1% TritonX-100, Roche complete EDTA-free protease inhibitor cocktail; 1h; on ice) and centrifuged (16.000g; 10min; 4°C). Samples (supernatant) were denatured with Laemmli buffer (1% β-mercaptoethanol; 2%SDS; 95ºC; 2min) and separated in a SDS-PAGE gradient gel (12% acrylamide/bisacrylamide gel, 29:1; 100V; 2h). Proteins were transferred into a PVDF membrane (90min; 12V), blocked (3% BSA) and incubated overnight with anti-α-gal IgG2b mAb (1μg/mL; 50mL). Membrane was washed with 20mM Tris/HCl pH 7.5, 150mM NaCl and 0.1% Tween-20 buffer (TBST, 3X; 5min; RT) and incubated with HRP-conjugated goat anti-mouse IgG2b-HRP (SouthernBiotech; 50ng/mL; 1h; 50mL; RT). Membrane was washed (TBST; 1h; RT) and developed (SuperSignal Chemiluminescent detection kit; West Pico, Thermo Scientific).

In some experiments, enzyme treatments were processed as described in *Section 2.2.8* of this chapter.

2.2.6 Detection of α-gal during the erythrocytic stage of *Plasmodium* infection

P. falciparum 3D7 (kindly provided by Fatima Nogueira (IHMT, Lisbon, Portugal) was expanded in human RBCs *in vitro* (10-12% parasitemia). *Pb*A, *P. yoelii* 17XL and *P. chabaudi chabaudi* AS were expanded *in vivo* using $\alpha 1,3Gt^{+/+}$ or $\alpha 1,3Gt^{-/-}$ mice (10-25% parasitemias)[25,26]. Blood smears of RBC infected with *Plasmodium spp.* were fixed (2% PFA in PBS; 20-30min; RT), washed (1X; PBS) and stained for DNA (DAPI; 10-20μg/mL; 100μL; 10min; RT). The α-gal epitope was stained using FITC-conjugated BSI-IB_4 (100μL; 100μg/mL; 2h; RT) and actin was stained using Alexa Fluor® 568 Phalloidin (Molecular Probes®; 100μL; 3units/mL; 1h; RT). Images for *P. falciparum, P. berghei* ANKA and *P. yoelii* 17XL were obtained by using fluorescent microscopy DeltaVision Core immunofluorescence microscopy (Applied Precision). Images for *P. chabaudi chabaudi* AS were obtained by using Andor Spinning Disk Confocal microscopy Revolution xD (Andor Technology). Images were analyzed using ImageJ software (NIH). All images were analyzed and processed with the ImageJ (NIH), software containing the LOCI plugin.

2.2.7 Whole-mount *Anopheles* mosquito salivary gland staining

Pb$A^{Hsp70\text{-}GFP}$ infected and non-infected female *Anopheles* mosquitoes were dissected and salivary glands were collected into an ibiTreat, tissue culture treated, sterile μ-Slide 8 well (PBS; on ice; Ibidi). Salivary glands were fixed (300μl; 4% PFA; 30min; 37°C) and washed (1X; PBS), incubated with BSI-IB_4-Alexa Fluor® 647 (100μl; 200μg/ml; 2h; RT) and washed (2X; PBS). Slides were dried in a dark chamber without coverslip (20-30 min; RT) and salivary glands were visualized using Spinning Disk Confocal microscopy

(Andor) with 10-60x objectives. Images were processed using ImageJ (NIH) software.

2.2.8 Enzymatic removal of α-gal

Removal of α-gal was performed using green coffee bean α-galactosidase (50-200μL; 5U/mL; 60-90min; 25°C; Sigma), which hydrolyzes specifically the terminal α-gal moieties from glycolipids and glycoproteins[27]. The α-gal glycan was stained thereafter, as described in previous sections.

2.2.9 Removal of GPI anchor from *Plasmodium* sporozoites

*Pb*A$^{Hsp70\text{-}GFP}$ sporozoites were isolated from the salivary glands of *A. stephensi* mosquitoes 19-25 days post-infection (5x10^5; PBS; ice cold), fixed (4% PFA in PBS; 20-30min; 37°C) and washed (1X; PBS; 9300g; 2min). Sporozoites were treated with phosphatidylinositol-specific phospholipase C from *Bacillus cereus* (5U/ml; 14-16h; 37°C) to cleave GPI-anchors at the sporozoite surface. Detection of α-gal was performed as described above and CSP was detected using an anti-CSP mAb (3D11) conjugated to Alexa Fluor® 647 in CyAn^{TM} ADP Analyzer (Beckman Coulter).

2.3 Results

2.3.1 Detection of α-gal in *Plasmodium spp.*

The α-gal glycan was detected by immunofluorescence at the surface of *Plasmodium spp*. sporozoites, including the human pathogen *P. falciparum* 3D7, as well the transgenic green fluorescent protein (GFP) expressing strains of the rodent pathogens *Pb*A or *P. yoelii* 17XNL. The α-gal was detected using an anti-α-gal IgM (M86) mAb[23] **(Figure 2.2a)** or BSI-B$_4$[28,29] **(Figure 2.2b)**. Relative binding to α-gal was similar for all anti-α-gal IgG mAbs, as assessed by ELISA using α-gal-BSA as a solid phase antigen

(Figure 2.3a) or by immunofluorescence using *Pb*A sporozoites **(Figure 2.3b)**.

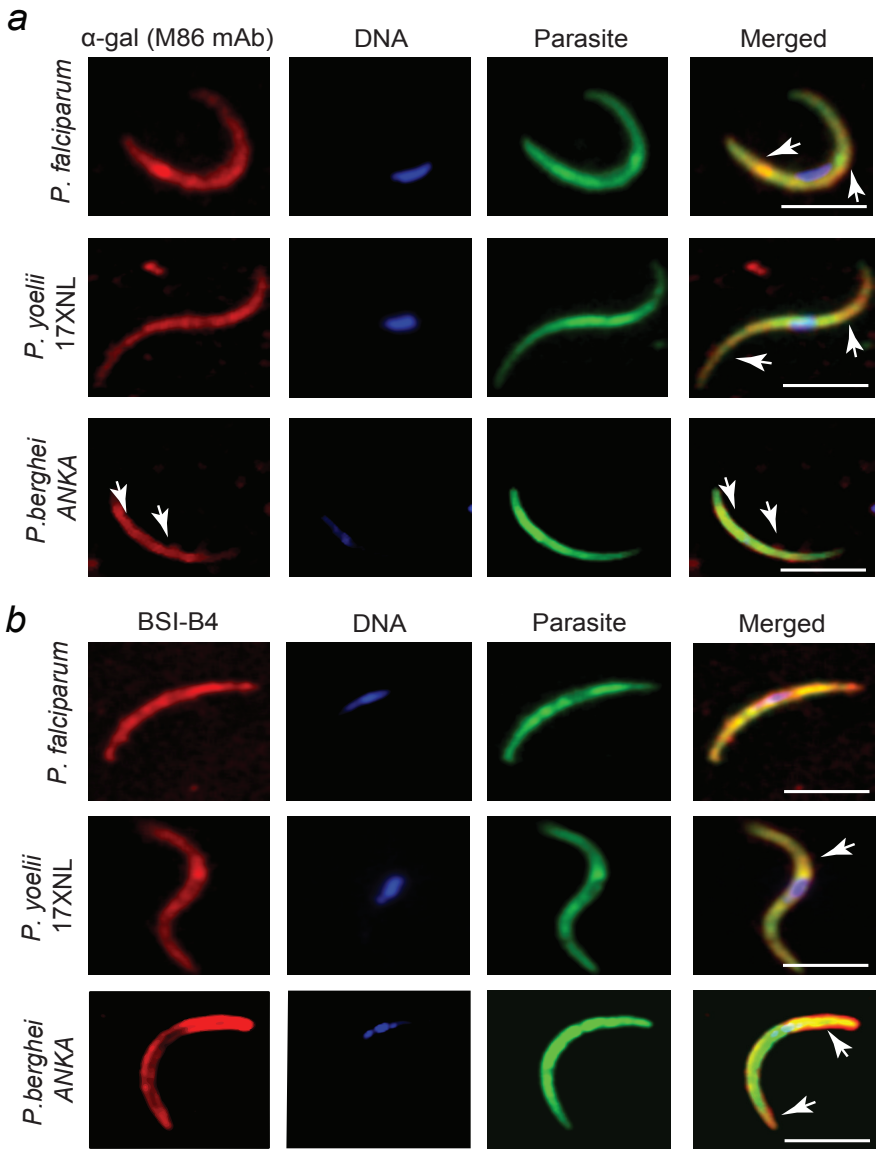

Figure 2.2 Recognition of α-gal in *Plasmodium* sporozoites. α-gal (red) staining of *Plasmodium* strains using **a)** an anti-α-gal mAb (M86) or **b)** BSI-B_4. DNA was stained with DAPI (blue). Green staining corresponds to the actin staining in *P. falciparum* 3D7 and *P. yoelii* 17XNL sporozoites and GFP expression in *Pb*A$^{EEF1a\text{-}GFP}$ sporozoites. Images are at 100X magnification and are representative of two-three independent experiments. Scale bar: 5μm.

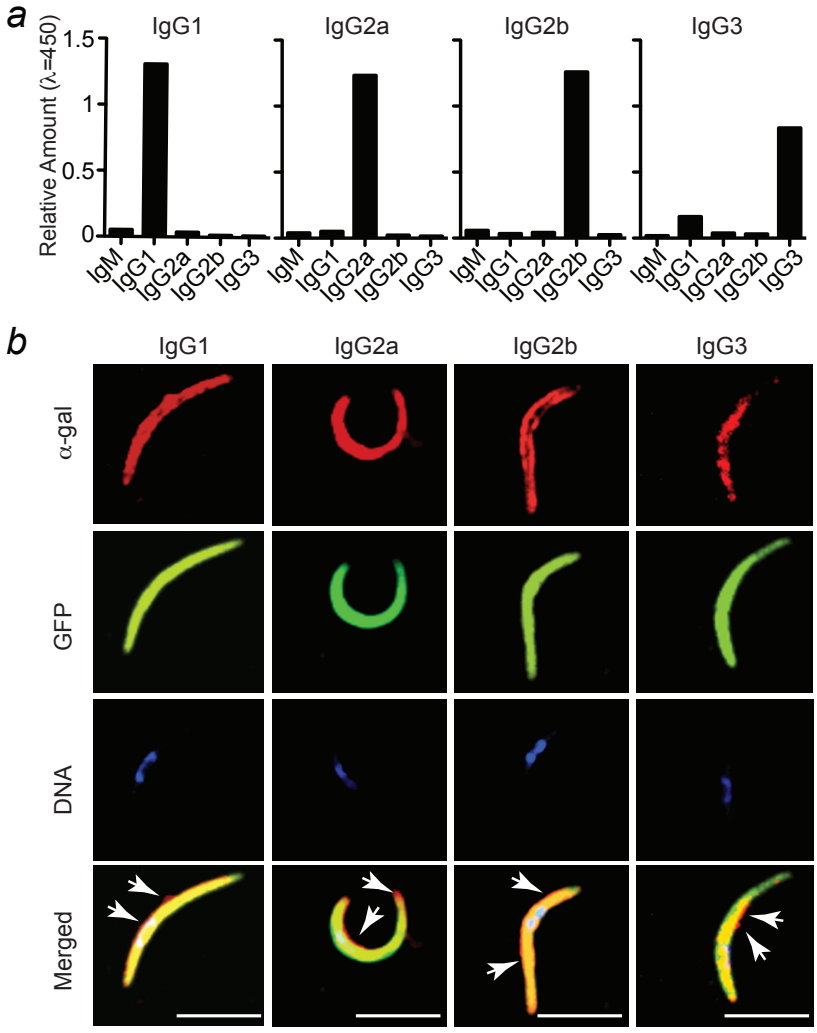

Figure 2.3 Recognition of α-gal on *Pb*A sporozoites using anti-α-gal IgG mAbs. **a)** Specificity of mAbs detecting the respective Ig subclass was determined by ELISA. **b)** α-gal staining of *Pb*A$^{EEF1a\text{-}GFP}$ using anti-α-gal IgG mAbs (red). DNA was stained with DAPI (blue). Green staining corresponds to GFP expression in *Pb*A$^{EEF1a\text{-}GFP}$ sporozoites. Images were obtained at 100X magnification and are representative of two-three independent experiments. Scale bar: 5μm.

Specificity of BSI-B_4 for pathogen *P. falciparum* 3D7 and the rodent *Pb*A sporozoites **(Figure 2.4a)** and anti-α-gal mAbs binding to *Pb*A sporozoites **(Figure 2.4b)** were assessed by enzymatic removal of α-gal, confirming that these mAbs recognize specifically and only α-gal on the surface of

Plasmodium sporozoites. IgG2a, IgG2b and IgG3 mAbs are class switched mutants derived from the original anti-α-gal IgG1 clone and as such have similar affinities for α-gal[20].

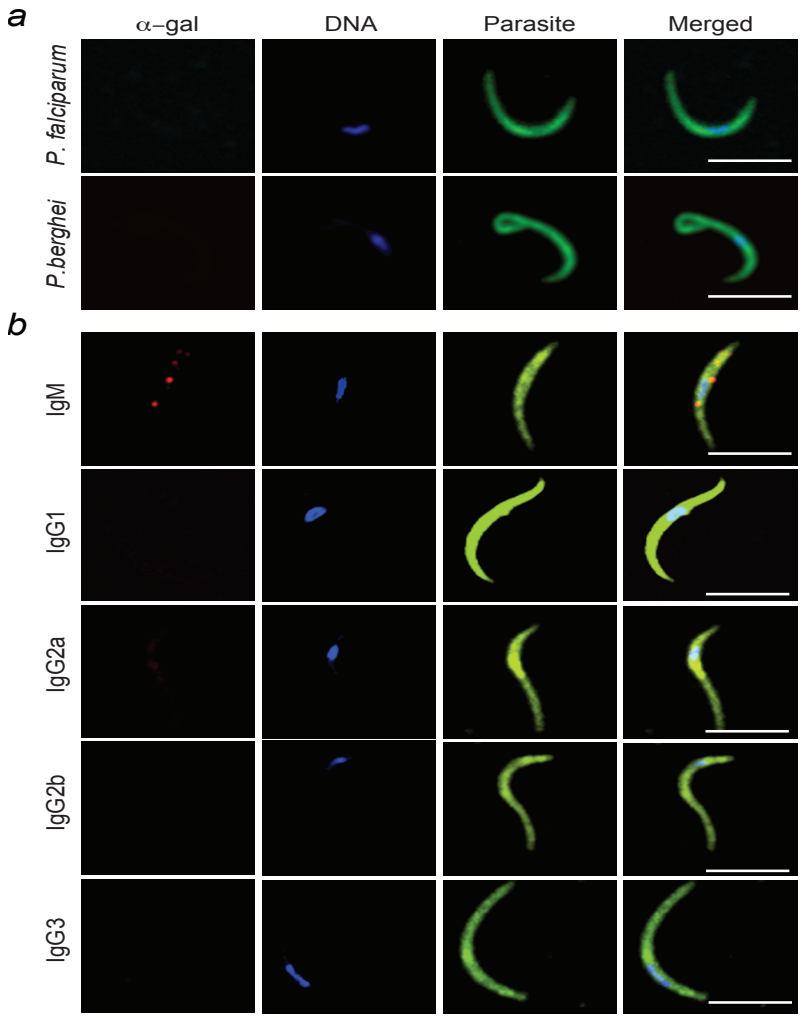

Figure 2.4 Specificity of α-gal detection was confirmed by its enzymatic removal. *Pb*A$^{EEF1a\text{-}GFP}$ and *P. falciparum* 3D7 sporozoites treated with α-galactosidase and were stained using **a)** BSI-B_4 and **b)** anti-α-gal mAbs to detect α-gal (red). DNA was stained with DAPI (blue). Green staining in *P. falciparum* corresponds to actin staining using phalloidin (green) and to GFP expression in *Pb*A sporozoites. Detection with anti-α-gal mAbs in b) only applied for *PbA* sporozoites. Images in (a) and (b) represent composite staining, at 100X magnification and are representative of two independent experiments. Scale bar: 5μm.

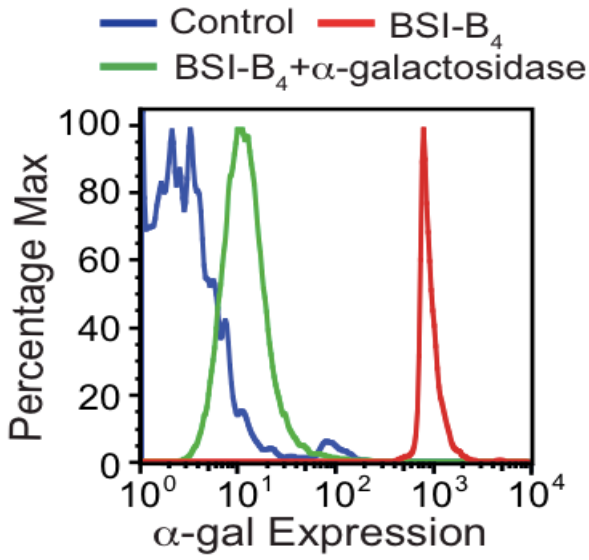

Figure 2.5 Detection of α-gal glycan on *Plasmodium* by flow cytometry. BSI-B_4 was used to detect *Pb*A$^{Hsp70\text{-}GFP}$ sporozoites α-gal (red), which expression was confirmed by its enzymatic removal with α-galactosidase (green). Non-stained sporozoites were used as reference point and labeled as control (blue histogram). Histograms are representative of three experiments.

Expression of α-gal glycan on the surface of *Pb*A sporozoites isolated from the salivary glands of *A. stephensi* mosquitoes was confirmed using flow cytometry technique **(Figure 2.5)**. Removal of the α-gal glycan from *Pb*A$^{Hsp70\text{-}GFP}$ sporozoites, using α-galactosidase enzyme, significantly reduced the expression of α-gal detected by BSI-B_4. Similar results were initially obtained by immunofluorescence technique **(Figure 2.2b and 2.4a)**. Additionally, the erythrocytic stage of different *Plasmodium* strains was also associated with α-gal expression, as assessed for *P. falciparum* 3D7, *Pb*A, *P. yoelii* 17XNL and *P. chabaudi chabaudi* AS using BSI-B_4-FITC **(Figure 2.6)**.

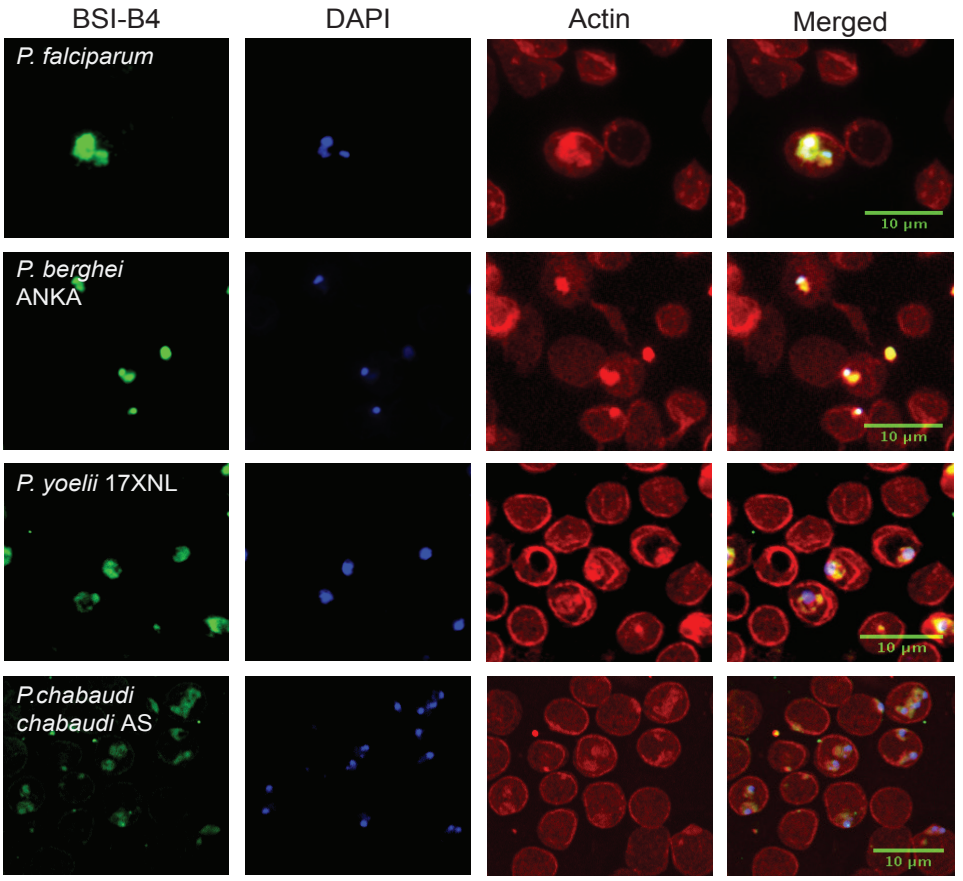

Figure 2.6 Detection of α-gal during the erythrocytic stage of *Plasmodium* infection. *P. falciparum* 3D7 was expanded *in vitro* in human RBCs (10-12% parasitemia). *Pb*A, *P. yoelii* 17XNL and *P. chabaudi chabaudi* AS were expanded *in vivo* (10-25% parasitemia). DNA was stained with DAPI (blue). Red corresponds to the actin staining phalloidin and green to α-gal. Images are at 100X magnification and are representative of two independent experiments. Scale bar: 10μm.

2.3.2 Detection of α-gal in *Plasmodium spp.* proteins

The α-gal glycan in *Plasmodium* sporozoites was associated with proteins, as assessed by Western blot using whole cell extracts isolated from mosquito salivary glands infected with *P. falciparum* 3D7, *Pb*A$^{Hsp70\text{-}GFP}$ or *P. yoelii* 17XNL **(Figure 2.7)** and confirmed by enzymatic removal of α-gal using α-galactosidase (E). The pattern of α-gal expression compared to

non-treated samples or non-infected salivary glands (NI). Enzymatic treatment successfully removed most of α-gal conjugated to proteins. Moreover, residual levels of α-gal expression were detected in the salivary glands of non-infected mosquito salivary glands suggesting that the α-gal may be generated at least partially by *Anopheles* mosquitoes **(Figure 2.7)**. Histone 3 (Hist3) and GFP detecting antibodies were used as loading control to show similar amount of antibodies were analyzed.

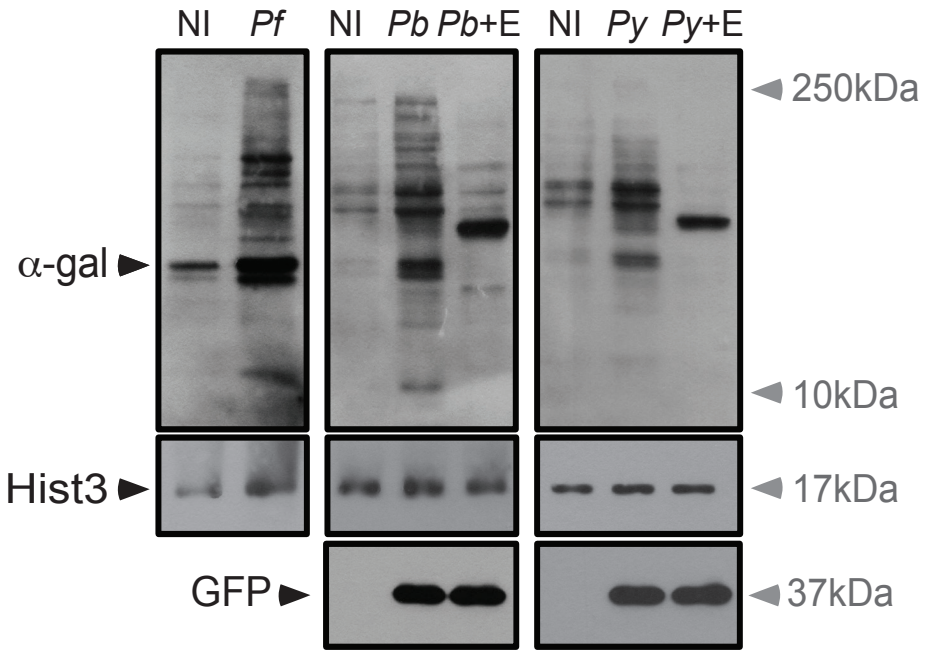

Figure 2.7 Detection of α-gal was also associated with proteins. α-gal was detected in proteins extracted from *P. falciparum* 3D7 (*Pf*), *Pb*A$^{Hsp70\text{-}GFP}$ (*Pb*) and *P. yoelii* 17XNL (*Py*) infected or non-infected salivary glands (NI) using anti-α-gal IgG2b mAbs. Detection of Histone H3 (Hist3) with a specific mAb was used as a loading control. GFP protein was detected in *Pb* and *Py* using the GFP (3H9) mAb. When indicated, α-gal was removed using α-galactosidase (E).

Then, we asked if the α-gal epitope is bound to GPI-anchors or proteins that are GPI-anchored. Expression of α-gal by *Pb*A$^{Hsp70\text{-}GFP}$ sporozoites was reduced by ~4-fold when the GPI-anchor was cleaved by phospholipase C

(PLC), as assessed by flow cytometry **(Figure 2.8a)**. In contrast, GPI cleavage failed to reduce the expression of circumsporozoite protein (CSP) **(Figure 2.8b)**. This suggests that α-gal is bound to GPI-anchored surface proteins, including or not CSP which, despite being GPI-anchored[30] is resistant to PLC cleavage[31].

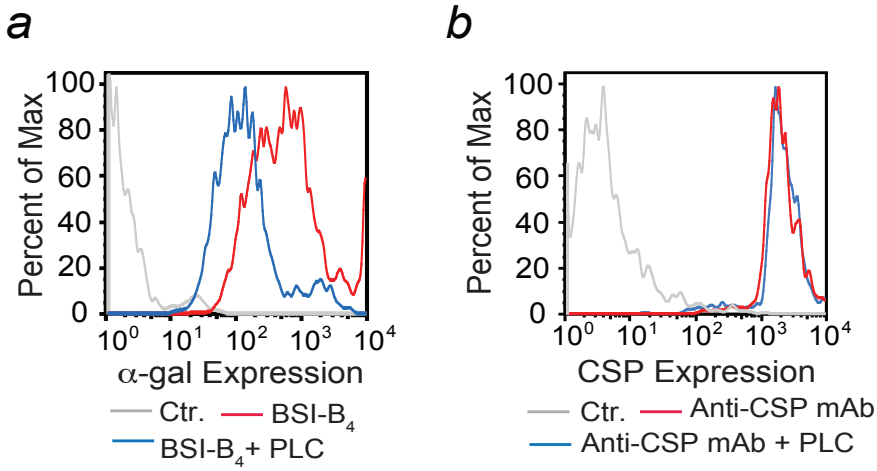

Figure 2.8 GPI-bound α-gal in *Plasmodium*. a) Expression of α-gal detected by BSI-B_4 and quantified by flow cytometry in *Pb*A$^{Hsp70\text{-}GFP}$ sporozoites treated with phospholipase C (PLC) or not. Notice reduction of α-gal expression upon GPI cleavage by phospholipase C (PLC) digestion. Histograms are representative of 4 experiments. **b)** Expression of CSP detected by anti-CSP mAb and analyzed by flow cytometry in *Pb*A$^{Hsp70\text{-}GFP}$ sporozoites treated with phospholipase C (PLC) or not. Notice that there is no reduction of CSP expression upon GPI cleavage by phospholipase C (PLC) digestion. Representative of two experiments.

2.3.3 Detection of α-gal in salivary glands of *Anopheles* mosquitoes

Bioinformatic analyzes failed to identify putative genes that utilize UDP-Gal to produce α-gal in *Plasmodium*. This led us to ask if the α-gal glycan is expressed in the mosquito salivary glands, which could act as the source of α-gal detected as *Plasmodium* glycoconjugates. Expression of α-gal was detected at the surface of *Pb*A$^{Hsp70\text{-}GFP}$ in the salivary glands of *Anopheles stephensi* mosquitoes and although to a lower extent in the salivary glands of non-infected *A. stephensi* mosquitoes **(Figure 2.9)**.

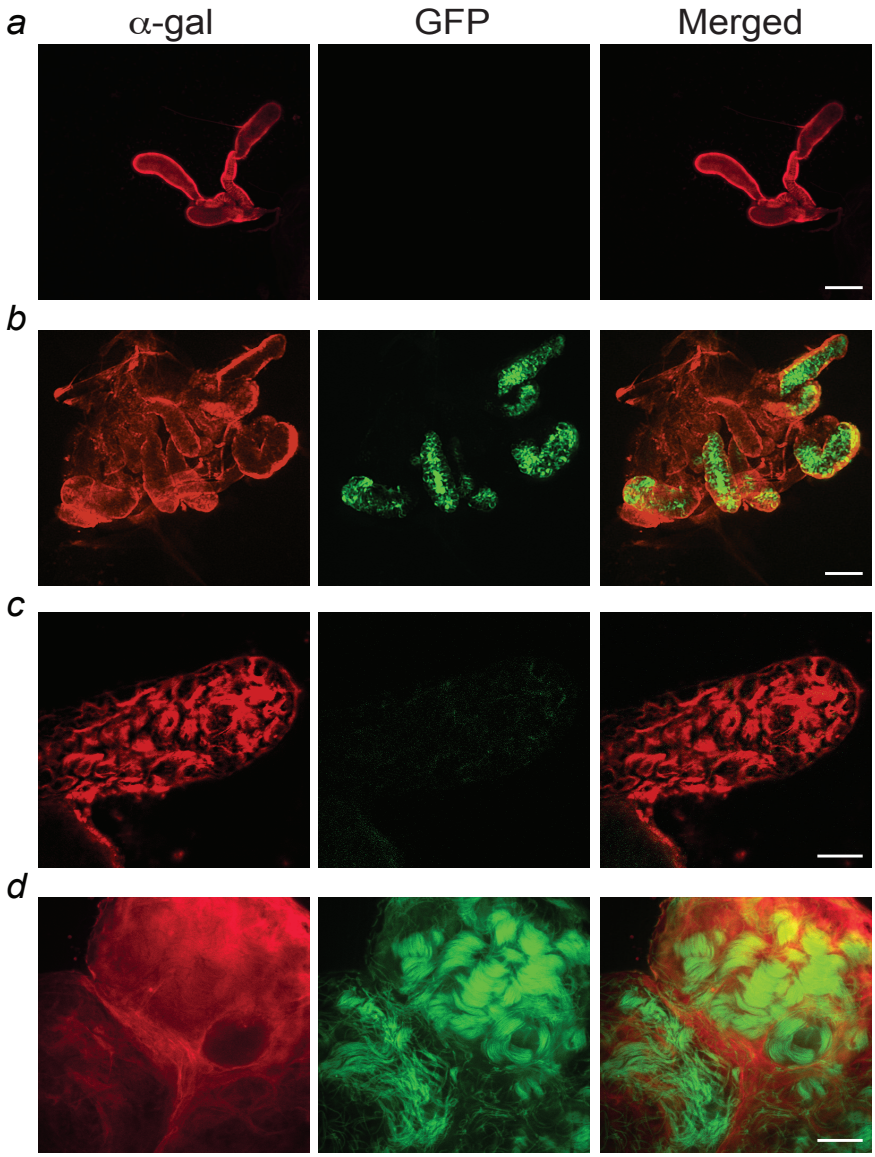

Figure 2.9 Detection of α-gal in salivary glands of *A. stephensi* mosquitoes. Non-infected and infected salivary glands of mosquitoes were stained for α-gal using BSI-IB_4 (red). *Pb*$A^{Hsp70\text{-}GFP}$ sporozoites in infected salivary glands were detected with GFP (green). Images in (a) and (c) are representative of non-infected female mosquito salivary glands and images in (b) and (d) are representative of infected female mosquito salivary glands. Images in (a and b) and in (c and d) are merged, i.e. red and green at 10X and at 60X magnification, respectively and are representative of two independent experiments. Scale bars: 100μm in (a) and 20μm in (b).

The signal intensity of α-gal expression in non-infected salivary glands was lower, as compared to *Plasmodium* infected salivary glands. In addition, when analyzed at higher magnification co-localization pattern between α-gal and sporozoites was clearly noticed. This confirmed that the salivary glands of female *A. stephensi* mosquitoes express residual levels of α-gal, as detected by Western blot technique **(Figure 2.7)**. It suggests therefore that α-gal may be generated, at least partially, by *Anopheles* mosquitoes and presumably bound to *Plasmodium* proteins.

2.4 Chapter Discussions and Conclusion

The presence of α-gal was initially studied in mammals. It was shown that it is abundantly expressed on glycoconjugates of non-primate mammals, prosimians and New World monkeys and is absent on Old World monkeys, including apes and humans. These studies were later extended for pathobiont bacteria in which detection of α-gal glycan was shown[32]. However, expression of this glycan on parasite is still not very clear and highly debatable. Our interest, in this part of the study, was to demonstrate the presence of terminal α-gal residues in *Plasmodium spp*.

We demonstrated that the α-gal is expressed during the blood stages of *Plasmodium spp*., including the human pathogen *P. falciparum* as well as the rodent pathogens *Pb*A, *P. yoelii* 17XNL and *P. chabaudi chabaudi* AS **(Figure 2.6)**. Lectin BSI-B_4 shows high specificity for α-gal and its binding to mature asexual blood stages and merozoites suggested the presence of α-gal-containing glycoconjugates in the parasites **(Figure 2.6)**, consistent with previous observations using the asexual blood stages of *P. falciparum*[11,33]. The expression pattern suggests that α-gal is located mostly away from the infected RBC membrane, specifically on *Plasmodium* parasites or around PV membrane. More importantly, α-gal glycan can also be detected on

Plasmodium sporozoites isolated from salivary glands of *A. stephensi* mosquitoes, as assessed by immunofluorescence assay **(Figure 2.2)** and flow cytometry **(Figure 2.5)** using BSI-IB_4 lectin or anti-α-gal mAbs **(Figure 2.3)**. It is noteworthy that the expression of α-gal on sporozoites was never been shown before. These results allowed to conclude that not only erythrocytic stage of *Plasmodium* infection but also exo-erythrocytic stage of *Plasmodium* is associated with α-gal expression.

It was previously demonstrated that human anti-α-gal Abs in the sera of individuals from malaria endemic-areas react with a relatively hydrophilic lipid present in parasitized as well as with non-infected RBCs. However, when compared to glycoproteins, parasite-specific glycolipids seem to react weakly, if at all, with BSI-IB_4, which prompted us to assess the presence of α-gal in parasite proteins, rather than in lipids[12]. This was achieved by detecting α-gal glycan by Western blots technique **(Figure 2.7)**. The results obtained here demonstrate that *Plasmodium* sporozoites, as well as non-infected female mosquito salivary glands, express α-gal attached to proteins. The presence of α-gal conjugated to lipids cannot be excluded from our study. This needs to be further characterized. We also confirmed using immunofluorescence assays that salivary glands from non-infected mosquitoes express α-gal glycan **(Figure 2.9)**. Whether the α-gal detected on the surface of *Plasmodium* sporozoites is produced by the sporozoites and/or by the mosquito and to what extent the mosquito may control the expression of α-gal on *Plasmodium* sporozoites and vice versa requires further investigation.

We observed a significant reduction in the expression of α-gal by *Plasmodium* sporozoites in which GPI was cleaved by enzymatic treatment using phospholipase C **(Figure 2.8a)**. This suggests that α-gal glycan is

associated GPI anchored proteins. In contrast, GPI cleavage with phospholipase C failed to reduce CSP expression **(Figure 2.8b)**. This suggests that α-gal is bound to GPI-anchored surface proteins, that might include CSP or not which, despite being GPI-anchored[30], is resistant to phospholipase C cleavage.

Bioinformatical analysis of *Plasmodium* genome showed no direct evidence of candidate gene(s) for generating an enzyme that can transfer α-gal to protein or lipid structures. However, *Plasmodium* may have some unclassified glycosyltransferases genes that can serve for production of α-gal glycan on its surface[34]. Even though the presence of N- and O-linked glycans in *Plasmodium* has been controversial, it is known that N-glycosylation sites are present in the primary amino acid sequences of *Plasmodium* and there is a little information O-glycosylation in *Plasmodium*, if it occurs at all. GPI anchor linked synthesis may be the only glycosylation form of *Plasmodium*[1]. However, the source of these glycosylations in *Plasmodium* sporozoites was not addressed[34]. Our results directed us to ask whether α-gal glycan can be obtained from *Anopheles* mosquitoes since no candidate gene was found in *Plasmodium*. Non-infected female *Anopheles* mosquitoes express the α-gal glycan in the salivary glands **(Figure 2.9)**. However, bioinformatics analysis also filed to identify *α1,3GT* in mosquitoes. It is known that mosquitoes have enzymes that support glycosylation in the midgut such as galactosyltransferase-I and II, *N*-acetylgalactosaminyltransferase-I and *N*-acetylglucosaminyltransferase-I, all of which belong to the glycosyltransferase family of enzymes. In a similar manner to α1,3GT enzyme, these mosquito glycosyltransferases produce linear heteropolysaccharides, in this case of repeating glucoronic acid (GlcA) and *N*-acetylgalactosamine (GalNAc) disaccharide units[35]. This shows that *Anopheles* mosquitoes express oligosaccharides on their midgut proteins, which are heavily glycosylated with *N*-linked GlcNAc- and

GalNAc-terminal oligosaccharides[4]. Moreover, carbohydrates are the main elements supporting the interaction of *Plasmodium* parasites with their host vector. This is illustrated for the interaction of *P. gallinaceum* ookinetes with a specific type of *N*-linked glycan expressed in midgut epithelium of *A. aegypti*[36]. It is possible therefore that *Plasmodium* sporozoites as they traverse the midgut and migrate into the salivary glands may become coated with mosquito carbohydrates, as suggested for laminin protein and the proteoglycan chondroitin sulphate. We speculate that this type of interaction retains the α-gal glycan on surface of *Plasmodium* sporozoites, protecting sporozoites from the mosquito immune system.

In conclusion, our data suggests that different *Plasmodium spp.* may have a yet unidentified homologue of the *α1,3GT* gene encoding an α-gal producing enzyme, suggesting that *Plasmodium* sporozoites use an alternative mechanism, that differs from that in mammals, to utilize UDP-Gal. Moreover, *Plasmodium* may have a mechanism that retains the α-gal glycan from its mosquito vector while traversing the midgut into salivary gland. Nonetheless, our data shows that this sugar epitope can be found on several stages of *Plasmodium spp.* life cycle including human parasite and that it can be recognized by anti-α-gal Abs *in vitro*.

Contributions

The author of this dissertation performed all experiments described in this chapter of the thesis except the detection of α-gal glycoproteins in *Plasmodium spp*. Raffaella Gozzelino performed the Western blots for the detection of α-gal glycan on *Plasmodium* sporozoites. Susana Ramos assisted on the detection of α-gal glycan on *Plasmodium* sporozoites by flow cytometry.

Acknowledgements

Thanks to Raffaella Gozzelino and Susana Ramos for comments on this chapter, Pedro Almada and Nuno Pimpão Martins (Imaging Facility, IGC) for technical support, Joana Tavares, Rogerio Amino and Robert Ménard (Institute Pasteur, France) for *Plasmodium* strains used, Ana Ferreira teaching on how to infect mice with *Plasmodium*, Fatima Nogueira (IHMT, Lisbon, Portugal) for *P. falciparum* 3D7 culture, Susana Ramos flow cytometry, Ana Regelado (Antibody Service, IGC) for producing anti-α-gal mAbs from hybridomas provided by Anita Chong (University of Chicago, IL, USA), Dr. Uri Galili (University of Massachusetts Medical School, Worcester, MA, USA) for the M86 anti-α-gal IgM mAb, Joana Gomes and Henrique Silveira (IHMT, Lisbon, Portugal) for the establishment and maintenance of *Plasmodium* infected *A. stephensi* mosquitoes.

References

1. Macedo, C.S., Schwarz, R.T., Todeschini, A.R., Previato, J.O. & Mendonca-Previato, L. Overlooked post-translational modifications of proteins in *Plasmodium falciparum*: N- and O-glycosylation -- a review. *Memorias do Instituto Oswaldo Cruz* **105**, 949-956 (2010).
2. Dinglasan, R.R., Fields, I., Shahabuddin, M., Azad, A.F. & Sacci, J.B., Jr. Monoclonal antibody MG96 completely blocks *Plasmodium yoelii* development in *Anopheles stephensi*. *Infection and immunity* **71**, 6995-7001 (2003).
3. Nacer, A., Walker, K. & Hurd, H. Localisation of laminin within Plasmodium berghei oocysts and the midgut epithelial cells of Anopheles stephensi. *Parasites & vectors* **1**, 33 (2008).
4. Wilkins, S. & Billingsley, P.F. Mosquito cell line glycoproteins: an unsuitable model system for the Plasmodium ookinete-mosquito midgut interaction? *Parasites & vectors* **3**, 22 (2010).

5. Salinas, N.D., Paing, M.M. & Tolia, N.H. Critical glycosylated residues in exon three of erythrocyte glycophorin a engage *Plasmodium falciparum* EBA-175 and define receptor specificity. *mBio* **5**, e01606-01614 (2014).
6. Boutlis, C.S., Riley, E.M., Anstey, N.M. & de Souza, J.B. Glycosylphosphatidylinositols in malaria pathogenesis and immunity: potential for therapeutic inhibition and vaccination. *Current topics in microbiology and immunology* **297**, 145-185 (2005).
7. Schofield, L. & Hackett, F. Signal transduction in host cells by a glycosylphosphatidylinositol toxin of malaria parasites. *The Journal of experimental medicine* **177**, 145-153 (1993).
8. Maizels, R.M. & Hewitson, J.P. Immune Recognition of Parasite Glycans. in *Anti-Carbohydrate Antibodies - From Molecular Basis to Clinical Application* (eds. Kosma, P. & Müller-Loennies, S.) (Springer, Wien, 2012).
9. Ramasamy, R. Studies on glycoproteins in the human malaria parasite *Plasmodium falciparum*--lectin binding properties and the possible carbohydrate-protein linkage. *Immunology and cell biology* **65 (Pt 2)**, 147-152 (1987).
10. Ramasamy, R. & Reese, R.T. A role for carbohydrate moieties in the immune response to malaria. *J Immunol* **134**, 1952-1955 (1985).
11. Ramasamy, R. & Reese, R.T. Terminal galactose residues and the antigenicity of *Plasmodium falciparum* glycoproteins. *Molecular and biochemical parasitology* **19**, 91-101 (1986).
12. Ramasamy, R. & Field, M.C. Terminal galactosylation of glycoconjugates in *Plasmodium falciparum* asexual blood stages and *Trypanosoma brucei* bloodstream trypomastigotes. *Exp Parasitol* **130**, 314-320 (2012).
13. Ravindran, B., Satapathy, A.K. & Das, M.K. Naturally-occurring anti-alpha-galactosyl antibodies in human *Plasmodium falciparum* infections-

-a possible role for autoantibodies in malaria. *Immunology letters* **19**, 137-141 (1988).

14. Franke-Fayard, B., *et al.* A *Plasmodium berghei* reference line that constitutively expresses GFP at a high level throughout the complete life cycle. *Mol Biochem Parasitol* **137**, 23-33 (2004).
15. Ishino, T., Orito, Y., Chinzei, Y. & Yuda, M. A calcium-dependent protein kinase regulates *Plasmodium* ookinete access to the midgut epithelial cell. *Molecular microbiology* **59**, 1175-1184 (2006).
16. Weiss, W.R., Good, M.F., Hollingdale, M.R., Miller, L.H. & Berzofsky, J.A. Genetic control of immunity to *Plasmodium yoelii* sporozoites. *J Immunol* **143**, 4263-4266 (1989).
17. Das, S., Garver, L. & Dimopoulos, G. Protocol for mosquito rearing (A. gambiae). *Journal of visualized experiments : JoVE*, 221 (2007).
18. Ono, T., Tadakuma, T. & Rodriguez, A. *Plasmodium yoelii yoelii* 17XNL constitutively expressing GFP throughout the life cycle. *Exp Parasitol* **115**, 310-313 (2007).
19. Walliker, D., *et al.* Genetic analysis of the human malaria parasite *Plasmodium falciparum*. *Science* **236**, 1661-1666 (1987).
20. Ding, J.W., *et al.* Hyperacute rejection by anti-Gal IgG1, IgG2a, and IgG2b is dependent on complement and Fc-gamma receptors. *J Immunol* **180**, 261-268 (2008).
21. Yin, D., *et al.* Cutting Edge: NK cells mediate IgG1-dependent hyperacute rejection of xenografts. *J Immunol* **172**, 7235-7238 (2004).
22. Garcia-Gonzalez, M., *et al.* Purification of murine IgG3 and IgM monoclonal antibodies by euglobulin precipitation. *Journal of immunological methods* **111**, 17-23 (1988).
23. Galili, U., LaTemple, D.C. & Radic, M.Z. A sensitive assay for measuring alpha-Gal epitope expression on cells by a monoclonal anti-Gal antibody. *Transplantation* **65**, 1129-1132 (1998).

24. Spalter, S.H., *et al.* Normal human serum contains natural antibodies reactive with autologous ABO blood group antigens. *Blood* **93**, 4418-4424 (1999).
25. Biswas, S., Saxena, Q.B., Roy, A. & Sharma, V.P. Isolation of different erythrocytic stages of *Plasmodium falciparum* and synchronization in culture. *Indian journal of malariology* **25**, 7-10 (1988).
26. Lambros, C. & Vanderberg, J.P. Synchronization of *Plasmodium falciparum* erythrocytic stages in culture. *The Journal of parasitology* **65**, 418-420 (1979).
27. Luo, Y., Wen, J., Luo, C., Cummings, R.D. & Cooper, D.K. Pig xenogeneic antigen modification with green coffee bean alpha-galactosidase. *Xenotransplantation* **6**, 238-248 (1999).
28. Galili, U., Macher, B.A., Buehler, J. & Shohet, S.B. Human natural anti-alpha-galactosyl IgG. II. The specific recognition of alpha (1----3)-linked galactose residues. *The Journal of experimental medicine* **162**, 573-582 (1985).
29. Kisailus, E.C. & Kabat, E.A. A study of the specificity of *Bandeiraea simplicifolia* lectin I by competitive-binding assay with blood-group substances and with blood-group A and B active and other oligosaccharides. *Carbohydrate research* **67**, 243-255 (1978).
30. Moran, P. & Caras, I.W. Requirements for glycosylphosphatidylinositol attachment are similar but not identical in mammalian cells and parasitic protozoa. *The Journal of cell biology* **125**, 333-343 (1994).
31. Kimmel, J., *et al.* Glycosylphosphatidyl-inositols in murine malaria: Plasmodium yoelii yoelii. *Biochimie* **85**, 473-481 (2003).
32. Galili, U., Mandrell, R.E., Hamadeh, R.M., Shohet, S.B. & Griffiss, J.M. Interaction between human natural anti-alpha-galactosyl immunoglobulin G and bacteria of the human flora. *Infection and immunity* **56**, 1730-1737 (1988).
33. Jakobsen, P.H., Theander, T.G., Jensen, J.B., Molbak, K. & Jepsen, S. Soluble *Plasmodium falciparum* antigens contain carbohydrate moieties

important for immune reactivity. *Journal of clinical microbiology* **25**, 2075-2079 (1987).

34. Varki A, C.R., Esko JD,Hudson H Freeze, Pamela Stanley, Carolyn R Bertozzi, Gerald W Hart, and Marilynn E Etzler. *Essentials of Glycobiology, 2nd edition*, (Cold Spring Harbor Laboratory Press, Cold Spring Harbor (NY), 2009).
35. Dinglasan, R.R.*, et al*. *Plasmodium falciparum* ookinetes require mosquito midgut chondroitin sulfate proteoglycans for cell invasion. *Proceedings of the National Academy of Sciences of the United States of America* **104**, 15882-15887 (2007).
36. Zieler, H., Nawrocki, J.P. & Shahabuddin, M. *Plasmodium gallinaceum* ookinetes adhere specifically to the midgut epithelium of *Aedes aegypti* by interaction with a carbohydrate ligand. *The Journal of experimental biology* **202**, 485-495 (1999).

3

Naturally Occurring Anti-α-gal Abs Confer Protection Against *Plasmodium* Infection

Abstract

Malaria is transmitted to humans via the inoculation of *Plasmodium* sporozoites into the skin through the bite of female *Anopheles* mosquitoes. Relatively low efficiency of *Plasmodium* infection argues for a natural protective mechanism of host, presumably acting at an early stage of infection. Here, we tested whether inactivation of the *α1,3GT* gene in ancestral anthropoid primates, which allows for the production of anti-α-gal Abs, increases resistance to *Plasmodium* infection, a major driving force in human evolution. Under this chapter, we demonstrate that circulating anti-α-gal Abs are associated with protection against malaria transmission in humans as well as in *α1,3Gt* deficient mice, which like humans do not express α-gal and can produce anti-α-gal Abs. We also show that immunization against α-gal enhances this protective effect. The data obtained provides new insight for a natural protective mechanism against *Plasmodium* infection and additionally, suggests that vaccination against α-gal glycan may reduce malaria transmission and incidence in humans.

3.1 Introduction

Natural anti-glycan Abs generated in the absence of known specific immunization play a major role in enhancing anti-microbial immunity[1]. Paradoxically, these NAbs are also thought to be involved in several pathologies such as allergy[2], diabetes[2], multiple sclerosis[3], atherosclerosis[2] and other forms of autoimmunity[4]. These NAbs are predominately of IgM isotype, polyreactive with low affinity, encoded by variable genes in germline configuration and often produced by B-1 cells ($CD5^+$ in mice and $CD20^+CD27^+CD43^+CD70^-$ in humans), which are not subjected to somatic hypermutation or affinity maturation[5]. B-1 cells are one of two main populations of B-lymphocytes and mature earlier than B-2 cells, in the following weeks after birth. These cells produce IgM NAbs constitutively as well as low amount of IgG and IgA while B-2 cells are activated, proliferate and differentiate into Ig producing plasma cells upon immunization with protein antigens[6]. Production of NAbs can occur in either T-cell independent (immediate response) or T-cell dependent (slower response but high-affinity Abs) manner[7].

A significant proportion of NAbs recognizes glycans such as α-gal[8]. High levels of maternal driven anti-α-gal IgG Abs are present at birth, decreasing during the first few months of post-natal life and increasing thereafter to reach a steady state within the first 3-5 years while anti-α-gal IgM NAbs are absent after birth but increase considerably with age[9-11]. NAbs are most probably produced in children as a result of exposure to components of the gut microbiota expressing glycans, such as the α-gal carbohydrate. Anti-α-gal NAbs are also present in serum and secretory fluids, such as colostrum and saliva. These NAbs can orchestrate a robust and immediate cytotoxic response against α-gal expressing cells, tissues or organs[12]. This cytotoxic response relies on the activation of the classical pathway of complement[13,14] as well as on ADCC[14].

The generation of *α1,3Gt*$^{-/-}$ deficient mice has provided an experimental model system to investigate the role of anti-α-gal Abs in the context of infection since α-gal is a xeno-glycan for *α1,3Gt*$^{-/-}$ deficient mice, acting as a highly immunogenic epitope[15]. Ig knock-in *α1,3Gt*$^{-/-}$ mice have been generated to overcome the fact that the frequency of B cells producing anti-α-gal NAbs in naive *α1,3Gt*$^{-/-}$ mice is extremely low[16]. These mice produce sufficient amount of anti-α-gal IgM NAbs spontaneously from B cells resident in the spleen, bone marrow, and lymph nodes, but not in the peritoneum. sIgM^{high} IgD^{low} and CD21^{high} marginal zone B cells in the spleen bind the α-gal glycan and hence, anti-α-gal Abs are thought to be produced mainly by MZ marginal zone B cells[16].

Interestingly, somatic mutations in Ig VH genes were observed in hybridomas producing anti-α-gal Abs, suggesting that the production of these NAbs may occur in a T cell dependent manner. Studies performed using αβ T cell receptor deficient *α1,3Gt*$^{-/-}$ mice (*α1,3Gt*$^{-/-}$ *Tcrβ*$^{-/-}$) showed that the majority of the anti-α-gal Abs are T cell dependent[17]. Moreover, interaction of CD40, a B-cell surface molecule essential for the activation of resting B cells by CD4^{+} T_H cells, and CD154, a co-stimulatory ligand expressed on activated T cells (CD40L), are required for the production of anti-α-gal Ab *in vivo*[17]. This suggests again that for the T_H cell dependent antibody responses, the production of anti-α-gal NAbs requires the cognate interaction of B cells with T cells that leads to B cell activation, proliferation and/or differentiation, as shown **(Figure 3.1)**.

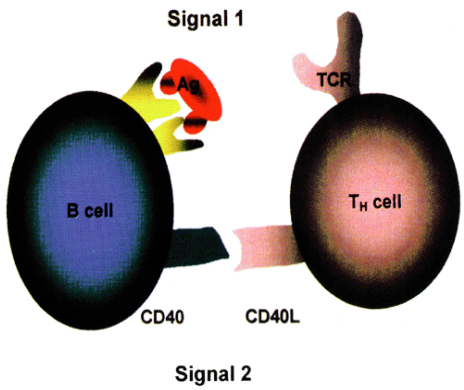

Figure 3.1 The interaction between B and T cell for the activation of B cell. An antigen is recognized B cells and generates the first signal. CD40 ligand (CD40L) on $CD4^+$ T cell engages with CD40 receptor on B cell and generates the second signal. These two signals lead to B cell activation, proliferation and differentiation. Adapted from[18].

The reason why humans have high levels of circulating anti-α-gal NAbs was argued to related resistance to pathogens expressing α-gal. In keeping with this notion, these Abs can be highly cytotoxic *in vitro* towards α-gal expressing pathogens, as demonstrated for bacteria[19], protozoan parasites[20] and viruses enveloped by xenogeneic α-gal expressing cell membranes[21]. Whether anti-α-gal Abs confers resistance to infection by pathogens, including *Plasmodium*, has not, to the best of our knowledge, been established. In this chapter of the thesis, we tested whether when present at the time of infection, anti-α-gal Abs could orchestrate a protective effect against murine *Plasmodium*[22-24]. We demonstrated that preformed anti-α-gal Abs can target *Plasmodium* sporozoites immediately after inoculation and contribute critically to reduce malaria transmission.

3.2 Materials and Methods

3.2.1 Subjects and clinical samples

The Ethics Committee of the Faculty of Medicine, Pharmacy and Dentistry at the University of Sciences, Technique and Technology of Bamako, and the Institutional Review Board of the National Institute of Allergy and Infectious Diseases, National Institutes of Health approved the cohort study. Written, informed consent was obtained from adult participants and from the parents or guardians of participating children. In May 2011, just before the 6-month malaria season, 695 individuals aged 3 months to 25

years were enrolled in a cohort study in the rural village of Kalifabougou, Mali. Individuals were invited to participate after random selection from an age-stratified census of the entire village population (n=4394). Enrollment exclusion criteria were hemoglobin level <7 g/dL, axillary temperature ≥37.5°C, acute systemic illness, use of anti-malarial or immunosuppressive medications in the past 30 days, and pregnancy. After enrollment, individuals were followed during the malaria season for 7 months. Clinical malaria was detected prospectively by self-referral and weekly active clinical surveillance. All individuals with signs and symptoms of malaria and any level of *Plasmodium* parasitemia detected by light microscopy were treated according to the National guidelines in Mali. The research definition of malaria was parasitemia ≥2500 parasites/μL, temperature ≥37.5°C and no other cause of fever discernible by physical exam. During scheduled clinic visits, blood was collected by finger prick every two weeks on filter paper. Detection of asymptomatic *Plasmodium* infection by PCR was done retrospectively at the end of the surveillance period. For each participant, PCR was performed on blood samples in chronological order from enrollment onwards until the first *P. falciparum* infection was detected. Detailed methods for *P. falciparum* PCR detection have been described before[25]. α-gal-specific IgM and IgG Ab levels were determined by ELISA on plasma collected at enrollment from the subset of individuals who were confirmed to be negative for *Plasmodium* infection by PCR. Statistical analyses were described in *Section 3.2.15*.

3.2.2 Mice

Mice were bred and maintained under specific pathogen-free (SPF) conditions, according to protocols approved by the Instituto Gulbenkian de Ciencia (IGC) and by the Portuguese National Entity (DGAV - Direção Geral de Alimentação e Veterinária. All murine experiments followed the Portuguese (Decreto-Lei nº 113/2013) and European (Directive 2010/63/EU) legislations, concerning housing, husbandry and animal

welfare. C57BL/6 $\alpha 1,3Gt^{-/-}$deficient mice[15,26] were provided originally by Prof. Peter Cowan (Immunology Research Centre, St. Vincent's Hospital, Department of Medicine, University of Melbourne, Victoria, Australia).

$\alpha 1,3Gt^{-/-}$	Sequence 5' --> 3'
NeoF	5′-TCTTGACGAGTTCTTCTGAG-3′
E9F-5	5′-TCAGCATGATGCGCATGAAGA-3′
E9R	5′-GCCAGAGGCCACTTGTGTAG-3′

$J_HT^{-/-}$	Sequence 5' --> 3'
JHT1	5′-CAGTGAATGACAGATGGACCTCC-3′
JHT2	5′-GCAGAAGCCACAACCATACATTC-3′
JHT3	5′-ACAGTAACTCGTTCTTCTCTGC-3′

$Aid^{-/-}$	Sequence 5' --> 3'
FR310	5′-GGCCAGCTCATTCCTCCACT-3′
FR311	5′-CACTGAGCGCACCTGTAGCC-3′
FR312	5′-CCTAGTGGCCAAGGTGCAGT-3′
FR313	5′-TCAGGCTGAGGTTAGGGTTCC-3′

$Tcr\beta^{-/-}$	Sequence 5' --> 3'
oIMR1781	5′-TGTCTGAAGGGCAATGACTG-3′
oIMR1782	5′-GCTGATCCGTGGCATCTATT-3′
oIMR6916	5′-CTTGGGTGGAGAGGCTATTC-3′
oIMR6917	5′-AGGTGAGATGACAGGAGATC-3′

C57BL/6 $J_HT^{-/-}$[27], $Aid^{-/-}$[28], $\mu S^{-/-}$[29] and $Tcr\beta^{-/-}$[30] were crossed with $\alpha 1,3Gt^{-/-}$ mice to generate $\alpha 1,3Gt^{-/-}$ mice lacking circulating Ig ($\alpha 1,3Gt^{-/-}J_Ht^{-/-}$), IgM $\alpha 1,3Gt^{-/-}\mu S^{-/-}$), IgA, IgG and IgE ($\alpha 1,3Gt^{-/-}Aid^{-/-}$) and T cells ($\alpha 1,3Gt^{-/-}Tcr\beta^{-/-}$). Mice were genotyped by PCR using tail genomic DNA and primers above.

3.2.3 Mice genotyping

Total genomic DNA was isolated from the tail using a standard protocol. Briefly, tails (0,5 to 1 cm) were obtained and submerged into DirectPCR Lysis Reagent (200-300µL; Viagen Biotech, Inc.) containing Proteinase K (100µg/mL) and incubated (overnight; 55°C) under vigorous agitation. Next day, samples were centrifuged (16000g; 5-10 sec; RT) and supernatant

(1μL) was amplified by PCR: 95°C (15min), 30 cycles of 94°C (45sec), 60°C (90sec) (except *Aid*$^{-/-}$ genotyping; 63°C), 72°C (90sec) and 72°C (15min). Visualizations of PCR results were done on 1.5-2% agarose gel (80-100V; 1-2h). $\mu S^{-/-}$ mice were phenotyped by ELISA, as described[29].

3.2.4 Anti-α-gal mAb production *See Section 2.2.2*

3.2.5 Immunization protocol

rRBCM expressing high levels of α-gal[31] were prepared from lyzed RBC (50mM sodium phosphate buffer pH 8), washed (5-7X; sodium phosphate buffer; 10,000g; 20min; 4°C) until supernatant was hemoglobin-free, essentially as described [32]. Membranes were collected by centrifugation (20,000g; 20min; 4°C), re-suspended in PBS and stored (-80°C) until used. Eight to ten weeks old mice received 3x10^8 RBC equivalents (100μL; PBS; i.p.). When indicated rRBCM were emulsified in Incomplete Freund's Adjuvant (IFA) or Complete Freund's Adjuvant (CFA; IFA plus *Mycobacterium tuberculosis* H37 RA; 4mg/mL; DIFCO) or CFA+CpG (50μg/mouse; ODN M362; Invivogen) and administered subcutaneously (s.c.). Alternatively, rRBCM were emulsified in Aluminum hydroxide Cγ (Alu-Gel-S; SERVA Electrophoresis GmbH) and administered i.p. Emulsions were prepared at 1:1 (v/v) and administered at 200μL per mouse, 3x at two weeks intervals. When indicated, mice were immunized (s.c.) with α-gal-BSA (75μg/mouse) emulsified in CFA with two subsequent immunizations, 2 and 4 weeks, thereafter with α-gal-BSA emulsified in IFA.

3.2.6 Passive immunization with anti-α-gal mAbs

α1,3Gt$^{-/-}$ mice received anti-α-gal IgG1, IgG2a, IgG2b or IgG3 mAbs via a single i.v. injection (150μg; 100μL per mouse), 24h prior to mosquito

exposure. Passive anti-α-gal IgM transfer was performed using polyclonal IgM. Briefly, eight to ten weeks old *α1,3Gt*$^{-/-}$*Aid*$^{-/-}$ mice received 3x10^8 RBC equivalents of rRBCM in PBS (100μL; i.p.). Serum was collected two weeks after the last immunization and concentration of anti-α-gal IgM was determined by ELISA[11,33]. Serum collected from naïve *α1,3Gt*$^{-/-}$*Aid*$^{-/-}$ mice was used as control. *α1,3Gt*$^{-/-}$ mice received the polyclonal IgM via a single i.v. (150μg; 300-400μL per mouse), 24h prior to mosquito exposure.

3.2.7 Anti-α-gal ELISA

Mouse serum was collected two weeks after immunization and circulating anti-α-gal antibodies were quantified by ELISA, as described[11,33]. Briefly, 96-well plates (PolySorp; Nunc) were coated with α-gal (α-gal-HSA or α-gal-BSA; 50μL; 10μg/mL in 0.5M carbonate bicarbonate buffer; pH 9.5; 2h at 37°C or overnight at 4°C), blocked with BSA (100μL; 1% w/v in PBS; 1h; RT) and washed (5X; PBS/0.05% Tween-20). Plates were incubated (1h; RT) with serum serial dilutions in PBS, 1% BSA and washed (5x; PBS/0.05% Tween-20). Anti-α-gal antibodies were detected using HRP-conjugated anti-mouse IgM, total IgG, IgG1, IgG2a, IgG2b or IgG3 (50μL, 1:1-2000 dilution, 1h, RT) and washed (5X; PBS/0.05% Tween-20). Purified anti-α-gal IgM[33], IgG1 (GT6-27), IgG2a and IgG2b and IgG3 (GT4-31) mAb[14,34] were used as standards. TMB Substrate Reagent Set (BD Biosciences) was used to reveal peroxidase activity (15-30min; RT) and reaction was stopped using 2N sulfuric acid. Optical densities (OD) were reported at λ=450nm and normalized by subtracting background OD values (λ=600nm) (Victor 3; PerkinElmer). Concentration of each anti-α-gal IgG subclass determined, as described[35]. Concentration of anti-α-gal antibodies in human plasma was analyzed using a similar assay and a standard curve to transform absorbance into immunoglobulin concentration was obtained by coating 8 duplicate wells in every plate with purified human IgG and IgM (500 to 1.5

ng/mL) and performing the protocol described above in the absence of diluted serum.

3.2.8 Parasites maintenance and mosquitoes rearing *See Section 2.2.1*

3.2.9 *Plasmodium* transmission

Anopheles mosquitoes (18–25 days after the infectious blood meal) were deprived of 10% glucose for 3-6 hours before *in vivo* experiments to increase the rate of mosquito bite. *A. stephensi* or *gambiae* mosquitoes were allowed to feed on anesthetized mice (ketamine; i.p.; 125 mg/kg, Imalgene 1000, Merial; Xylazine, i.p., 12.5mg/kg, Rompun 2%; Bayer) placed on a warming tray. Two mosquitoes were allowed to probe and feed independently (90-100 sec) on a restricted edge of the mouse ear (10-12/3-4 mm) and dissected thereafter for confirmation of sporozoites in salivary glands. If negative, infection was repeated.

3.2.10 Disease assessment

Mice were monitored daily for clinical symptoms of development of blood stage of infection verified by measuring parasitemia (%) in flow cytometry (FacScan analyzer; BD Biosciences) and was analyzed with FlowJo software (Tree Star Inc.) or blood smear using Giemsa staining, as described[36,37]. The day of mosquito exposure was considered as day 0. Blood stage of infection was considered positive when parasitemia, i.e. percentage of infected RBC, was higher than 1%.

3.2.11 Isolation of sporozoites from salivary glands *See Section 2.2.4*

3.2.12 Sporozoites inoculation

*Pb*A$^{EEF1a\text{-}GFP}$ sporozoites were inoculated i.d. in the ear pinna (750 sporozoites in 20-30µL; 1% BSA in PBS) or i.v. (retro-orbital; 150 sporozoites

in 50µL; 1% BSA in PBS) using a microsyringe (NanofilTM 100µL; 33G beveled needle; World Precision Instruments).

3.2.13 Relative gene expression of parasite in ear and liver

For relative quantification of sporozoites at the site of inoculation, the mouse ear was excised immediately after mosquito feeding and frozen in liquid nitrogen. For quantification of sporozoites in the liver, the whole liver was harvested 40h after mosquito feeding. In both cases, tissues were homogenized in TRIzol® (Life Technologies), total RNA was isolated according to the manufacturer's instructions (RNeasy Mini kit; Qiagen). cDNA was synthesized using random primers and oligod(T) with SuperScript® II Reverse Transcriptase (Invitrogen). Briefly, RNA (2μg; 10μL) was mixed with random primers (1μL) and dNTPs (10mM; 1μL), incubated (65°C; 5min), placed on ice and incubated in PCR Buffer (0.1M DTT; 40units/μL RNaseOUT™; 2min; 42°C;). Superscript RT (SSIIRT) was added (1μL; 42°C; 50min) and samples were heated to finalize synthesis (15min; 70°C). qRT-PCR was performed using the following primers:

18S rRNA	Sequence 5' --> 3'
Forward	5'AAGCATTAAATAAAGCGAATACATCCTTAC-3'
Reverse	5'-TCAGCATGATGCGCATGAAGA-3'

Arbp0	Sequence 5' --> 3'
Forward	5'-CTTTGGGCATCACCACGAA-3'
Reverse	5'-GCAGAAGCCACAACCATACATTC-3'

Applied Biosystems' Power SYBR Green PCR Master Mix was used as per manufacturer's instructions (ABI Prism 7000 system; Applied Biosystems). Data is presented as relative expression of *Pb*A 18S rRNA normalized to mouse *Arbp0* mRNA.

3.2.14 Passive transfer of RBCs of mice exposed to mosquito biting

α1,3Gt$^{-/-}$ mice immunized with rRBCM and age matched naïve *α1,3Gt*$^{-/-}$ mice were exposed to *Pb*A$^{EEF1a\text{-}GFP}$ infected mosquitoes, as described above. Parasitemia was monitored by flow cytometry in FacScan analyzer (BD Biosciences). Nine days post- mosquito feeding, blood was collected and injected i.p. (100-200μL) to naive *α1,3Gt*$^{-/-}$ mice. Infection was monitored daily for parasitemia and clinical symptoms, starting from day 3-4 post-infection RBC administration.

3.2.15 Statistical analysis

All tests (except human cohort studies) were performed using the GraphPad Prism v6.0 (GraphPad Software). Human analyses were performed in R version 3.0.2 (*http://www.R-project.org*). Ab levels between groups were compared with the Kruskal-Wallis test. The relationship between Ab levels and time to *P. falciparum* infection and febrile malaria was determined by Kaplan-Meier survival analysis and the log-rank test. Age dependent differences in anti-α-gal IgM and IgG antibody concentrations in human serum were determined using non-parametric Mann-Whitney test. Differences in anti-α-gal antibody concentration in mouse serum were determined using non-parametric Kruskal-Wallis test with Dunn's multiple comparison post-test. Incidence of infection was compared using log rank (Mantel-Cox) test. Survival curves were plotted using Kaplan-Meier plot and significant differences among experimental groups were determined using the Log-Rank (Mantel-Cox) test. Data corresponding to relative amount of *Plasmodium* in the skin and liver obtained from qRT-PCR was analyzed using non-parametric Mann–Whitney test. A p value equal to or below 0.05 was considered statistically significant.

3.3 Results

3.3.1 Human anti-α-gal IgM Abs confer protection against *P. falciparum* infection in endemic area

We initially investigated the potential implications of α-gal expression on *Plasmodium* in a cohort study in Mali where the 6-month malaria season is predictable and intense[38]. We examined the relationship between plasma levels of anti-α-gal NAbs measured in healthy uninfected children and adults before the malaria season (n=229 for IgM; n=330 for IgG) and the subsequent risk of *P. falciparum* infection (determined by bi-weekly PCR analysis of fingerprick blood samples) and febrile malaria (determined by weekly physical examination) during the ensuing 6-month malaria season. In children <2 years the average level of anti-α-gal IgM Abs was 33.4 μg/mL [95% CI: 18.4-48.3 μg/mL] **(Figure 3.2a)** similar to that reported in children with no history of malaria exposure[8,10,39,40]. However, anti-α-gal IgM Abs increased with age (surrogate for malaria exposure), reaching an average of 123.03 μg/mL [95% CI: 79.3-166.7 μg/mL] in adults **(Figure 3.2a)** —more than twice the level reported in adults with no malaria exposure, i.e. 51.6 μg/mL [95% CI: 14.9-88.3 μg/mL] **(Figure 3.2a)**[8,10,39,40]. The average level of anti-α-gal IgG Abs in children under 2 years was 1.46 μg/mL [95% CI: 0.22-0.69 μg/mL], and increased in adults to 3.66 μg/mL [95% CI: 3.04-4.28 μg/mL] **(Figure 3.2c)**. In contrast to IgM, levels of circulating anti-α-gal IgG were similar between malaria-exposed and non-exposed adults suggesting that *P. falciparum* infection fails to drive an IgG response directed against the α-gal glycan[8,10,39,40]. Time-to-event analysis did not show a correlation between anti-α-gal IgM and IgG Abs levels before the malaria season and the subsequent risk of *P. falciparum* infection (p=0.76 and p=0.08, respectively) or febrile malaria (p=0.35 and p=0.18, respectively). However, the average level of anti-α-gal IgM Abs in children >4 years of age who had no *P. falciparum* infections detected during the 6-

month malaria season (n=13) was higher than those who became infected (n=141) **(Figure 3.2b)**, suggesting that anti-α-gal IgM Abs plays a role in protecting against *P. falciparum* infection. Levels of circulating anti-α-gal IgG Abs in individuals from a malaria endemic area are on average 33-fold lower than levels of IgM anti-α-gal NAbs and we could not find any correlation between non-infected children and anti-α-gal IgG Abs **(Figure 3.2d)**.

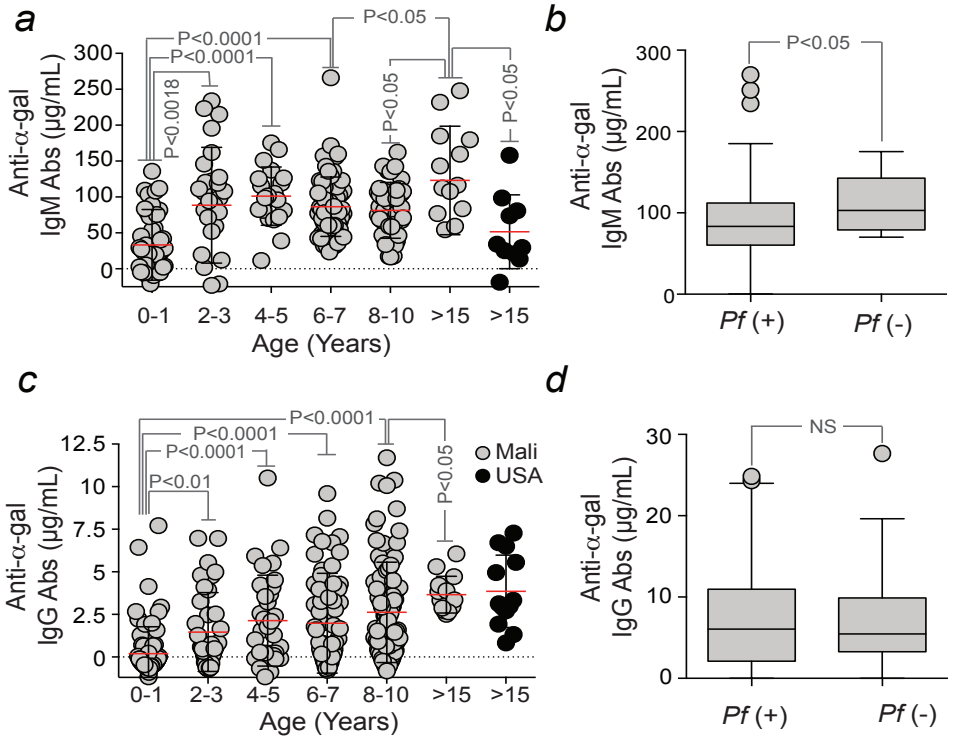

Figure 3.2. Anti-α-gal IgM and IgG Abs in circulation increase with age. a) Anti-α-gal IgM Abs in individuals (dots) from an endemic area of malaria in Mali or from the USA. Mean (red bars) and STD. **b)** Levels of anti-α-gal IgM Abs in *P. falciparum* infected individuals (*Pf+*) *vs.* non-infected individuals (*Pf-*), same population as (a). **c)** Anti-α-gal IgG Abs in individuals (dots) from an endemic area of malaria in Mali or from the USA. Mean (red bars) and STD. **d)** Levels of anti-α-gal IgG Abs in *P. falciparum* infected individuals (*Pf+*) *vs.* non-infected individuals (*Pf-*), same population as (c). Serum samples from Mali were shown with grey circles whereas serum samples from USA were shown with black circles. Ab levels between groups in humans were compared with the Kruskal-Wallis test.

3.3.2 Immunization against α-gal confers sterile protection against malaria

To test the protective role of anti-α-gal NAbs experimentally, we took advantage of "human-like" *α1,3Gt* deficient mice that can generate anti-α-gal Abs. Unlike humans, mice express a functional *α1,3Gt* gene that produces α-gal. As such anti-α-gal-reactive B cells are deleted from the peripheral B cell repertoire of mice, which fail to produce anti-α-gal Abs[41]. Deletion of the *α1,3Gt* gene in mice (*α1,3Gt*$^{-/-}$)[15,26] is sufficient to allow the generation of robust antibody responses against α-gal[15]. Consistent with previous studies[42]. However, under specific pathogen free conditions *α1,3Gt*$^{-/-}$ mice produce residual levels of circulating anti-α-gal IgM Abs, below 0.1-1μg/mL **(Figure 3.3b)**. This is not the case for anti-α-gal IgG Abs. In contrast; *α1,3Gt*$^{+/+}$ mice do not produce circulating anti-α-gal IgM and IgG Abs **(Figure 3.3b)**. Circulating anti-α-gal IgM Abs but not IgG were detected in *α1,3Gt*$^{-/-}$ mice maintained under germ-free conditions, revealing that a fraction of anti-α-gal IgM Abs are NAbs (*See Chapter 5*).

Immunization of *α1,3Gt*$^{-/-}$ mice against α-gal, using rabbit RBC membranes (rRBCM) expressing high levels of α-gal or synthetic α-gal conjugated to bovine serum albumin (α-gal-BSA), elicited the production of circulating anti-α-gal IgM and IgG Abs **(Figure 3.3b)**. As expected, control *α1,3Gt*$^{+/+}$ mice failed to produce anti-α-gal NAbs **(Figure 3.3a)**[15,41,42]. Circulating anti-α-gal IgA and IgE Abs were undetectable in control or immunized *α1,3Gt*$^{-/-}$ and *α1,3Gt*$^{+/+}$ mice *(data not shown).* Levels of circulating IgM Abs in immunized *α1,3Gt*$^{-/-}$ mice was in the range of adult individuals from an endemic area of malaria **(Figure 3.2a)** while the range of concentrations of anti-α-gal IgG Abs in immunized *α1,3Gt*$^{-/-}$ mice was higher to that found in

of adult individuals from an endemic area of malaria range **(Figure 3.2b)**. IgG anti-α-gal Abs in immunized *α1,3Gt*$^{-/-}$ mice were present at higher concentration, predominantly from the IgG1, IgG2b and IgG3 subclasses, with little or no anti-α-gal IgG2a **(Figure 3.3b)** or IgG2c *(data not shown)*.

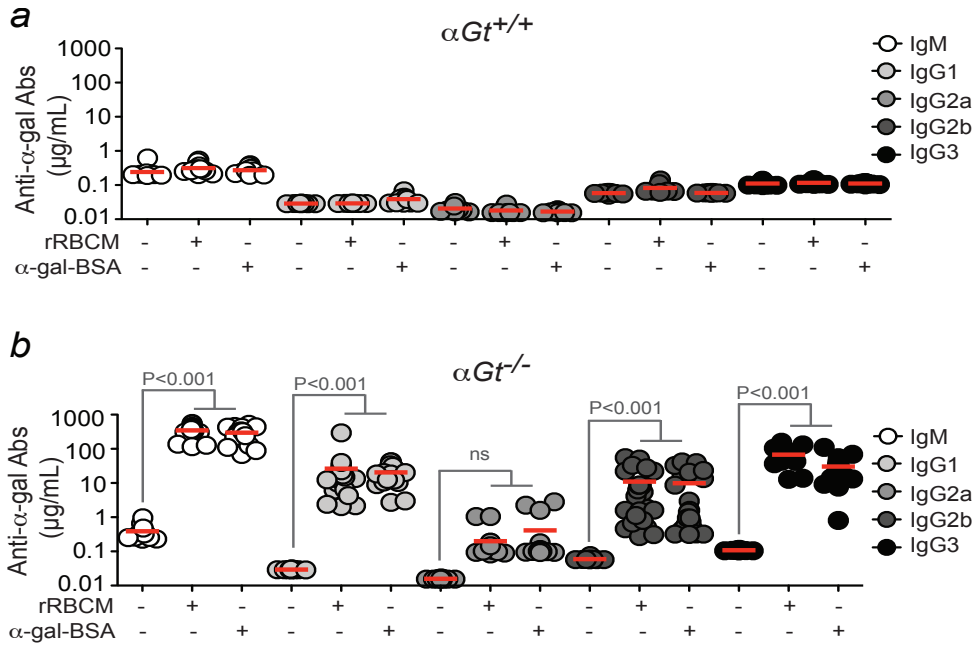

Figure 3.3 Concentration of anti-α-gal Abs in mice. Concentration of anti-α-gal Abs in the serum of **a)** *α1,3Gt*$^{+/+}$ and **b)** *α1,3Gt*$^{-/-}$ mice immunized with rRBCM (+) or with α-gal-BSA (+) *vs.* control naïve (-) *α1,3Gt*$^{-/-}$ mice. Dots represent individual mice (n=12-29 mice per group) pooled from 2-3 independent experiments. Red bars represent mean values. Statistically significant correlations among the groups were determined by Kruskal-Wallis test with Dunn's multiple comparison post-test.

Immunization against α-gal protected *α1,3Gt*$^{-/-}$ mice from *Pb*A infection transmitted *A. stephensi* mosquitoes, as compared to control non-immunized *α1,3Gt*$^{-/-}$ mice **(Figure 3.4a)**. Protection was not observed in immunized control *α1,3Gt*$^{+/+}$ mice, as compared to non-immunized *α1,3Gt*$^{+/+}$ mice **(Figure 3.4a)**. Immunized *α1,3Gt*$^{-/-}$ mice were also protected from infection by other *Plasmodium* strains, as illustrated for *P. yoelli* 17XNL

infection, as compared to non-immunized $\alpha 1,3Gt^{-/-}$ mice as well as to immunized or non-immunized $\alpha 1,3Gt^{+/+}$ mice **(Figure 3.4b)**.

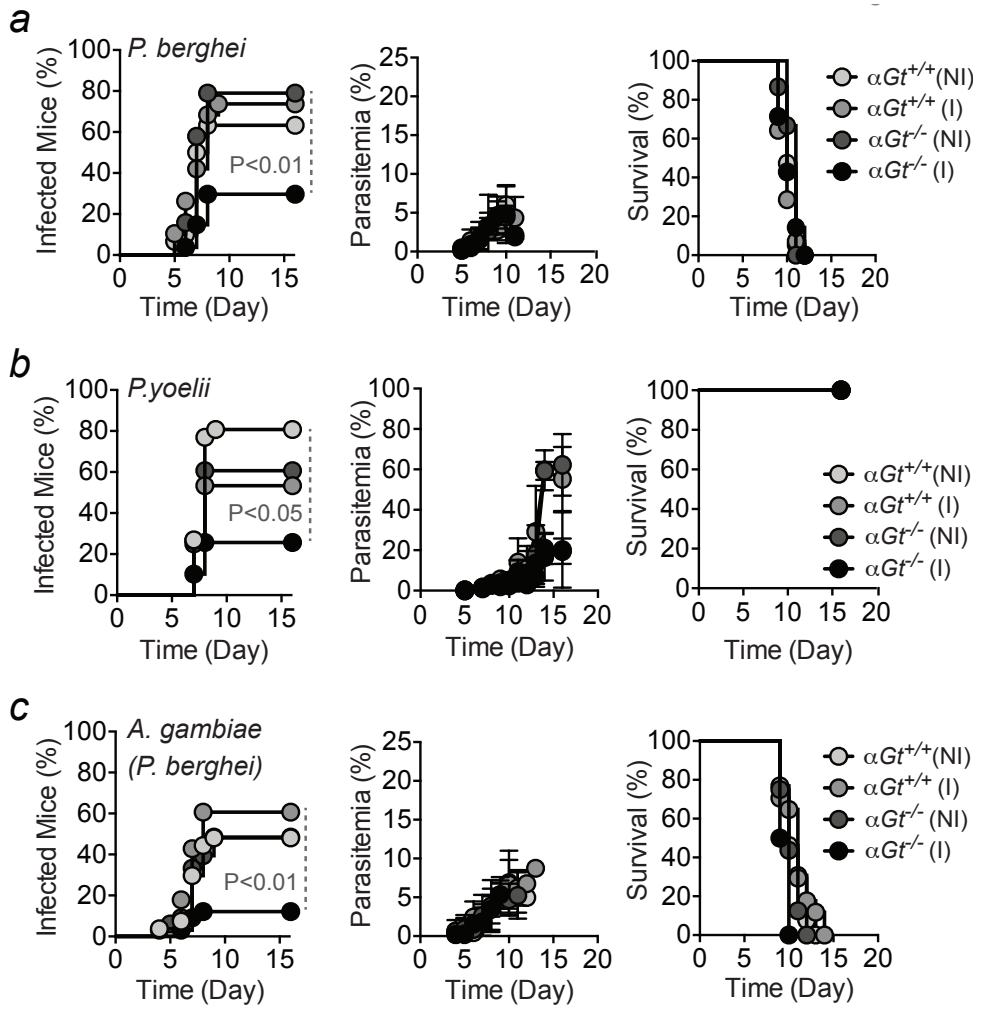

Figure 3.4 Immunization against α-gal confers protection against *Plasmodium* infection in mice, irrespectively of *Plasmodium* strains or vector species. Incidence of blood stage (%) infection with respective parasitemia (%) and survival (%) of **a)** *Pb*A$^{EEF1a\text{-}GFP}$, **b)** *P. yoelii* 17XNL infection transmitted by *A. stephensi* mosquitoes and **c)** *Pb*A$^{EEF1a\text{-}GFP}$ transmitted by *A. gambiae* mosquitoes to $\alpha 1,3Gt^{-/-}$ mice immunized (I) with rRBCM *vs.* non-immunized (NI) $\alpha 1,3Gt^{-/-}$ mice or control immunized (I) or non-immunized (NI) $\alpha 1,3Gt^{+/+}$ mice. Data shown is from 3-5 independent experiments with similar trend, (n=15-34 mice per group). Statistical significance between groups in incidence of infection was determined by log rank (Mantel-Cox) test.

Immunization also protected *α1,3Gt*$^{-/-}$ mice against *Pb*A infection by other mosquito strains, as illustrated for *Anopheles gambiae*, as compared to non-immunized *α1,3Gt*$^{-/-}$ mice as well as to immunized or non-immunized *α1,3Gt*$^{+/+}$ mice **(Figure 3.4c)**. Altogether, this shows that anti-α-gal Abs confer protection against *Plasmodium* infection irrespective of *Plasmodium* strains or vector species.

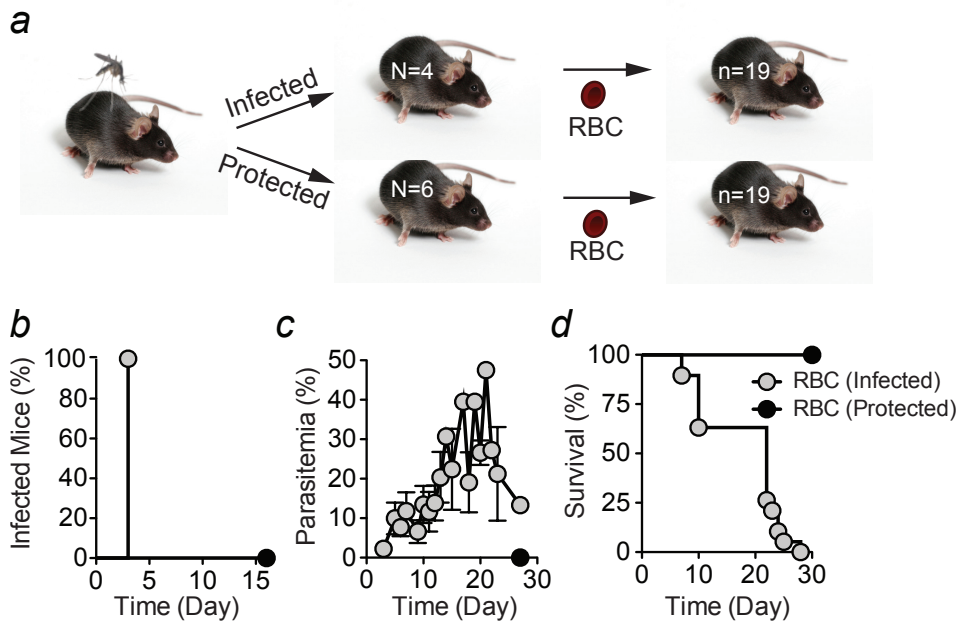

Figure 3.5 Immunization against α-gal confers sterile protection against *Plasmodium* transmission. a) Schematic representation of infection protocol and **b)** incidence of blood stage of infection (%) in *α1,3Gt*$^{-/-}$ mice transferred with RBC from *α1,3Gt*$^{-/-}$ mice infected *Pb*A$^{EEF1a\text{-}GFP}$ or protected from transmission of *Pb*A$^{EEF1a\text{-}GFP}$ infection by *A. stephensi* mosquitoes (2 experiments; n=19 mice per group). Parasitemia (%) and survival (%) are in **c)** and **d)**, respectively.

We then asked whether α-gal immunization provides sterile protection against malaria. To test this hypothesis, RBC from immunized *α1,3Gt*$^{-/-}$ mice protected from transmission of *Pb*A infection by *Anopheles* mosquitoes were passively transferred to naive *α1,3Gt*$^{-/-}$ mice and disease transmission was followed. Schematic view of infection procedure was shown in **Figure**

3.5a. Passive transfer of RBCs failed to transmit infection or disease to naïve *α1,3Gt*$^{-/-}$ mice **(Figure 3.5b-d)**. In contrast, passive transfer of RBC from immunized *α1,3Gt*$^{-/-}$ mice not protected from *Pb*A transmission by *Anopheles* mosquitoes, readily transmitted infection and disease to naïve *α1,3Gt*$^{-/-}$ mice **(Figure 3.5b-d)**. This demonstrates that immunization against α-gal confers sterile protection against malaria.

3.3.3 *Plasmodium* sporozoites are arrested in the skin

The percentage of infected RBC, i.e. parasitemia, was similar in immunized *α1,3Gt*$^{-/-}$ mice not protected from *Pb*A infection *vs.* control non-immunized *α1,3Gt*$^{-/-}$ mice as well as control non-immunized or immunized *α1,3Gt*$^{+/+}$ mice and when infected, all mice succumbed to experimental cerebral malaria **(Figure 3.4)**. This suggests that while protective against malaria transmission, α-gal immunization is not protective against the development of disease. In keeping with this notion, when inoculated with *Pb*A infected RBC, immunized *α1,3Gt*$^{-/-}$ mice developed similar levels of parasitemia *vs.* control non-immunized *α1,3Gt*$^{-/-}$ mice as well as to control non-immunized or immunized *α1,3Gt*$^{+/+}$ mice **(Figure 3.6a)**. These results also suggest that protective effect against *Plasmodium* occurs before the erythrocytic stage established. In keeping with this notion, we tested this hypothesis via injection of *Pb*A intravenously (i.v.) or intradermally (i.d.). Immunized *α1,3Gt*$^{-/-}$ mice were protected from artificial transmission of *Pb*A sporozoites via intradermal inoculation *vs.* control non-immunized *α1,3Gt*$^{-/-}$ mice or control immunized or non-immunized *α1,3Gt*$^{+/+}$ mice **(Figure 3.6c)**. Protection was no longer observed when sporozoites were artificially inoculated intravenously **(Figure 3.6b)** suggesting that the protective effect of α-gal immunization acts in the skin via a mechanism that is no longer operational in blood.

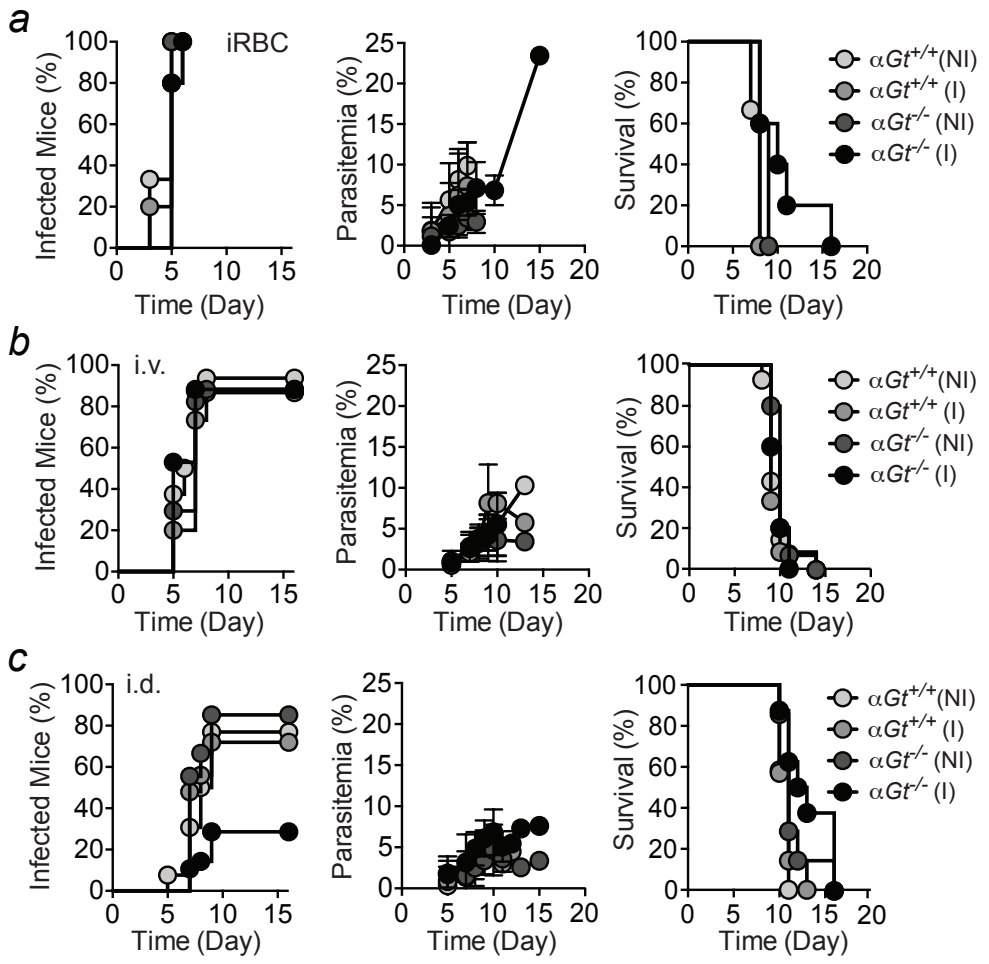

Figure 3.6 Immunization against α-gal confers protection against *Plasmodium* infection at pre-erythrocytic stage. Incidence of blood stage infection (%), parasitemia (%) and survival of *α1,3Gt*$^{-/-}$ mice immunized (I) with rRBCM *vs.* control non-immunized (NI) *α1,3Gt*$^{-/-}$ mice or control immunized (I) or non-immunized (NI) *α1,3Gt*$^{+/+}$ mice inoculated with **a)** *Pb*A$^{EEF1a\text{-}GFP}$ iRBC intraperitoneally (i.p.), **b)** *Pb*A$^{EEF1a\text{-}GFP}$ sporozoites (i.d.) or **c)** *Pb*A$^{EEF1a\text{-}GFP}$ sporozoites (i.v.). Data shown in (a) is from 1 experiment (n=4-6 mice per group) and (b-c) is from 3-5 independent experiments with similar trend (n=15-34 mice per group). Statistical significance among groups in the incidence of infection was determined by log rank (Mantel-Cox) test.

Transmission of *Pb*A was associated with *Plasmodium* 18S rRNA accumulation at the site of inoculation, as quantified in the ear pinna by

qRT-PCR **(Figure 3.7a)**. The relative amount of *Plasmodium* 18S rRNA was similar in immunized *vs.* control non-immunized *α1,3Gt*$^{+}$ mice or control immunized or non-immunized *α1,3Gt*$^{+/+}$ mice **(Figure 3.7a)**. Immunized *α1,3Gt*$^{-/-}$ mice did not accumulate *Plasmodium* 18S rRNA in the liver *vs.* control non-immunized *α1,3Gt*$^{-/-}$ mice or non-immunized or immunized *α1,3Gt*$^{+/+}$ mice **(Figure 3.7b)**. This suggests that α-gal immunization does not interfere with sporozoite inoculation by *Anopheles* mosquitoes, but rather arrests sporozoite migration from the skin into the liver.

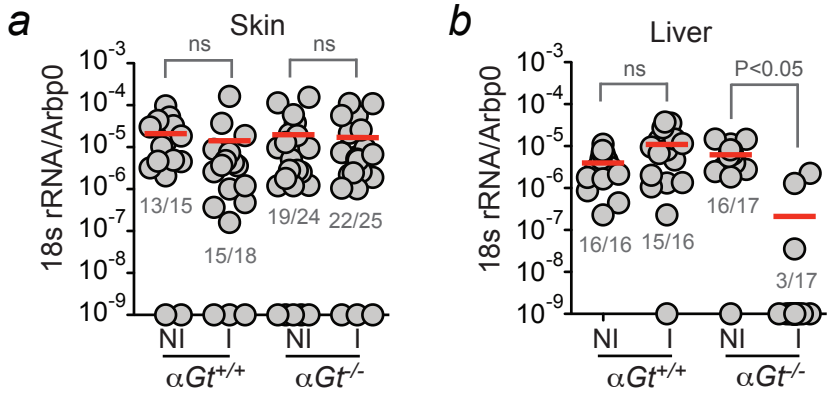

Figure 3.7 Parasite burden is reduced in immunized *α1,3Gt*$^{+}$ livers. *Plasmodium* 18s rRNA/ mouse *Arbp0* mRNA in **a)** skin and **b)** liver non-immunized (Control) *vs.* immunized (rRBCM) *α1,3Gt*$^{-/-}$ mice exposed to *Pb*A$^{EEF1a\text{-}GFP}$ infected *A. stephensi* mosquitoes (3-5 experiments). Infected/total mice (grey dot represents individual mouse). Data was pooled from 3-5 experiments and bars represent mean values. Significance of expression difference among the groups was determined with non-parametric Mann–Whitney test.

3.3.4 Anti-α-gal Abs are protective against *Plasmodium* infection

To establish whether the protective effect of α-gal immunization is mediated by anti-α-gal Abs, incidence of blood stage of *Plasmodium* infection was compared in *α1,3Gt*$^{-/-}$ mice lacking specific components of humoral and cellular adaptive immunity **(Figure 3.8)**.

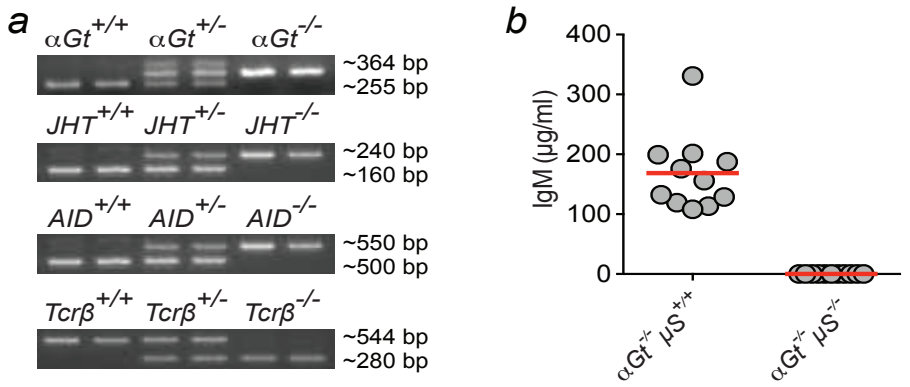

Figure 3.8 Generation of double-knockout mice. *α1,3Gt*$^{-/-}$ mice were crossed with *J*$_H$*t*$^{-/-}$, *Aid*$^{-/-}$, *µ*$_s$$^{-/-}$ and *Tcrβ*$^{-/-}$ to generate double-knockout mice. Representative band size of WT mice (+/+), Het (+/-) and KO mice (-/-) were displayed from each genotypes were determined with **a)** PCR by using genomic DNA from tail clips except **b)** *µ*$_s$$^{-/-}$ mice that was analyzed with ELISA by using mouse serum.

To establish whether the protective effect of α-gal immunization is mediated by anti-α-gal NAbs, *PbA* transmission was compared in immunized *α1,3Gt*$^{-/-}$ *vs. α1,3Gt*$^{-/-}$*J*$_H$*T*$^{-/-}$ mice, lacking B cells[27]. Immunized *α1,3Gt*$^{-/-}$*J*$_H$*T*$^{-/-}$ mice failed to produce anti-α-gal IgM or IgG Abs *vs.* naïve *α1,3Gt*$^{-/-}$*J*$_H$*T*$^{-/-}$ mice or to immunized *α1,3Gt*$^{-/-}$mice **(Figure 3.9)**. Moreover, immunized *α1,3Gt*$^{-/-}$*J*$_H$*T*$^{-/-}$ mice were not protected against *Pb*A transmission by *Anopheles* mosquitoes *vs.* control non-immunized *α1,3Gt*$^{-/-}$*J*$_H$*T*$^{-/-}$ mice **(Figure 3.10a)**. This shows that the protective effect of α-gal immunization is mediated via a B cell-dependent mechanism.

Immunization of *α1,3Gt*$^{-/-}$*Aid*$^{-/-}$ mice, that cannot undergo Ig class switch recombination[28], failed to induce the production of anti-α-gal IgG but not IgM Abs *vs.* naïve *α1,3Gt*$^{-/-}$*Aid*$^{-/-}$ or immunized *α1,3Gt*$^{-/-}$ mice **(Figure 3.9)**. Immunized *α1,3Gt*$^{-/-}$*Aid*$^{-/-}$mice were nevertheless protected against *Pb*A transmission *vs.* non-immunized *α1,3Gt*$^{-/-}$*Aid*$^{-/-}$ mice **(Figure 3.10b)**. This

confirms **(Figure 3.2b)** that anti-α-gal IgM Abs confer protection against malaria transmission.

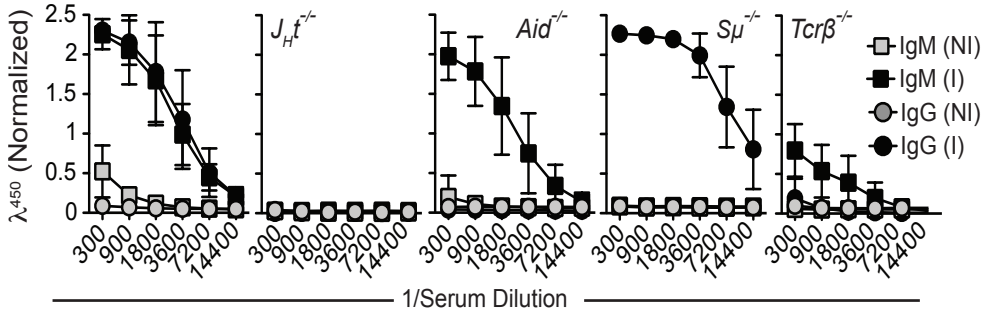

Figure 3.9 Anti-α-gal Abs in double knockout mice. Relative levels of circulating anti-α-gal IgM and total IgG Abs, as detected by ELISA in non-immunized (NI) or rRBCM immunized (I) *α1,3Gt*$^{-/-}$, *α1,3Gt*$^{-/-}$*J*$_H$*t*$^{-/-}$, *α1,3Gt*$^{-/-}$*Aid*$^{-/-}$, *α1,3Gt*$^{-/-}$*μS*$^{-/-}$ and *α1,3Gt*$^{-/-}$*Tcrβ*$^{-/-}$ mice. Square and circle marker show anti-α-gal IgM and total IgG Abs, respectively. Data is shown as mean ± standard deviation (n=10 mice per group), pooled from individual mice in 2-3 independent experiments.

Immunization of *α1,3Gt*$^{-/-}$*μS*$^{-/-}$ mice, which lack circulating IgM[43], failed to induce anti-α-gal IgM Abs, without interfering with anti-α-gal IgG Ab response *vs.* naïve *α1,3Gt*$^{-/-}$*μS*$^{-/-}$ mice or immunized *α1,3Gt*$^{-/-}$ mice **(Figure 3.9)**. Immunized *α1,3Gt*$^{-/-}$*μS*$^{-/-}$ mice were protected from *Pb*A transmission *vs.* control naïve *α1,3Gt*$^{-/-}$*μS*$^{-/-}$ mice **(Figure 3.10c)**. It should be noted here that immunized *α1,3Gt*$^{-/-}$ mice do not produce circulating IgA or IgE anti-α-gal Abs (*data not shown*) and therefore a putative protective effect for these Ig isotypes can be excluded.

Immunization of *α1,3Gt*$^{-/-}$*Tcrβ*$^{-/-}$ mice lacking mature αβ T cells[30] compromised the anti-α-gal IgM and IgG response *vs.* control immunized *α1,3Gt*$^{-/-}$ mice **(Figure 3.9)**. Immunized *α1,3Gt*$^{-/-}$*Tcrβ*$^{-/-}$ mice were not protected from *Pb*A transmission *vs.* control naïve *α1,3Gt*$^{-/-}$*Tcrβ*$^{-/-}$ mice **(Figure 3.10d)**. This confirms that anti-α-gal Abs are produced in a T cell-

dependent manner[16,17] and demonstrates that the protective effect of these Abs against *Plasmodium* infection occurs in a T cell-dependent manner.

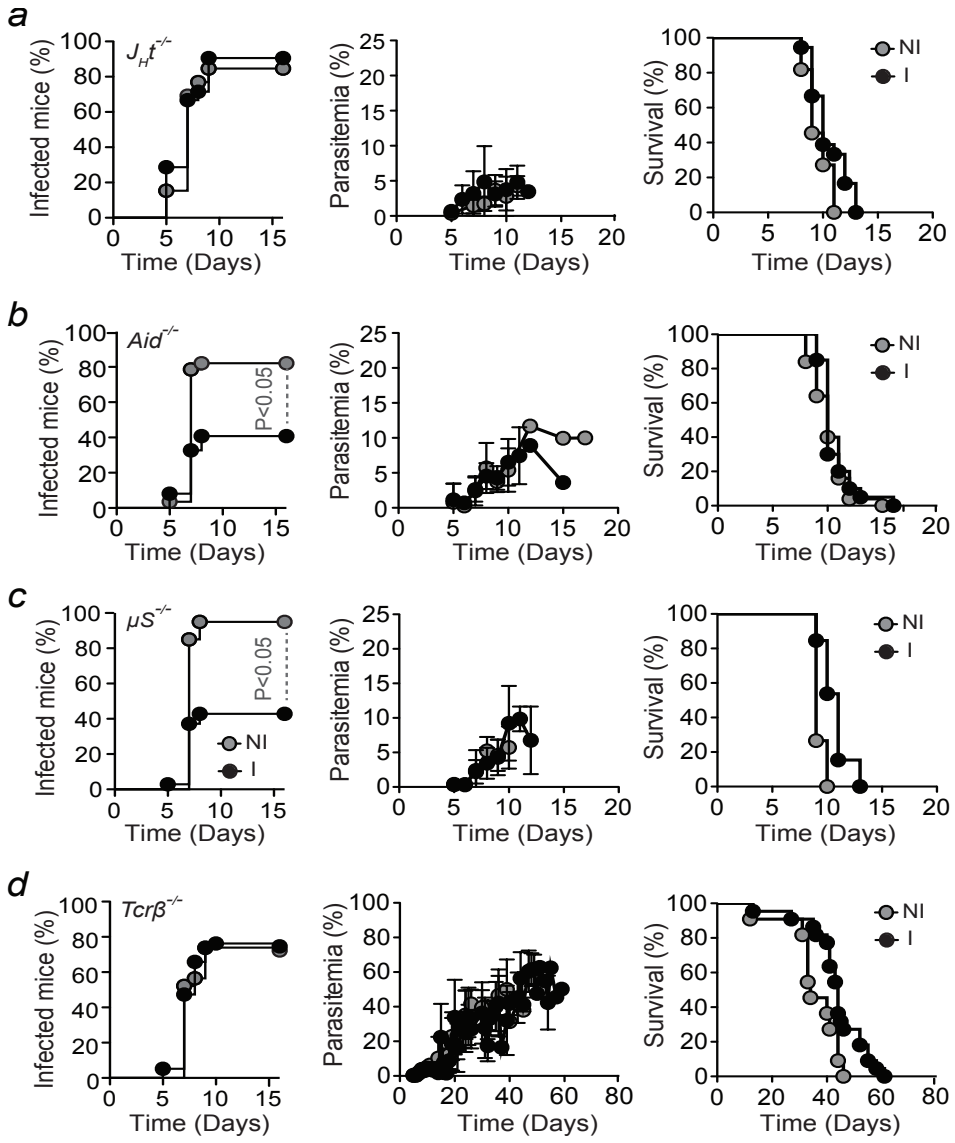

Figure 3.10 Protective effect against *Pb*A transmission is mediated by anti-α-gal Abs. Incidence of blood stage infection (%) with respective parasitemia (%) and survival (%) were determined in non-immunized (NI) or rRBCM immunized (I) **a)** *α1,3Gt*$^{-/-}$*J*$_{H}$*t*$^{-/-}$, **b)** *α1,3Gt*$^{-/-}$*Aid*$^{-/-}$ **c)** *α1,3Gt*$^{-/-}$*μS*$^{-/-}$, and **d)** *α1,3Gt*$^{-/-}$*Tcrβ*$^{-/-}$ mice after exposing to *Pb*A infected mosquitoes. Data in **(a-d)** was pooled from 3-7 independent experiments (n=13-41 mice per group). Statistical significance among groups in the incidence of infection was determined by log rank (Mantel-Cox) test.

Non-immunized as well as immunized *α1,3Gt*$^{-/-}$*J*$_H$*T*$^{-/-}$, *α1,3Gt*$^{-/-}$*Aid*$^{-/-}$ and *α1,3Gt*$^{-/-}$*μS*$^{-/-}$ mice, not protected from *Pb*A transmission, developed similar levels of parasitemia and succumbed to experimental cerebral malaria **(Figure 3.10)**. This was not the case for *α1,3Gt*$^{-/-}$*Tcrβ*$^{-/-}$ mice **(Figure 3.10)**, consistent with the involvement of T cells in the pathogenesis of experimental cerebral malaria[44].

We then asked whether passively transferred anti-α-gal Abs are sufficient *per se* to prevent *Plasmodium* infection. Passive transfer of anti-α-gal IgM to naïve *α1,3Gt*$^{-/-}$ mice conferred protection against *Pb*A transmission **(Figure 3.11a)**. This was also the case for passive transfer of anti-α-gal IgG Abs from specific subclasses, including IgG2b or IgG3 but not IgG1 or IgG2a **(Figure 3.11b-d)** mAb. Relative binding of different mAbs to α-gal was similar, as assessed by ELISA using α-gal conjugated to BSA **(Figure 2.3a)** or by immunofluorescence using *Pb*A sporozoites **(Figure 2.3b)**. Moreover, the specificity of these mAbs binding to *Pb*A sporozoites was shown before by removal of α-gal glycan by α-galactosidase, revealing that anti-α-gal IgM and IgG mAb recognize specifically and only α-gal glycan on the surface of *Plasmodium* sporozoites **(Figure 2.4b)**. It is worth noticing that the IgG2a, IgG2b and IgG3 mAbs are class switched mutants of the anti-α-gal IgG1 clone and as such have similar affinities for α-gal[14]. This confirms that anti-α-gal IgM NAbs are sufficient *per se* to confer protection against malaria transmission and shows that specific anti-α-gal IgG Ab subclasses can enhance this protective effect.

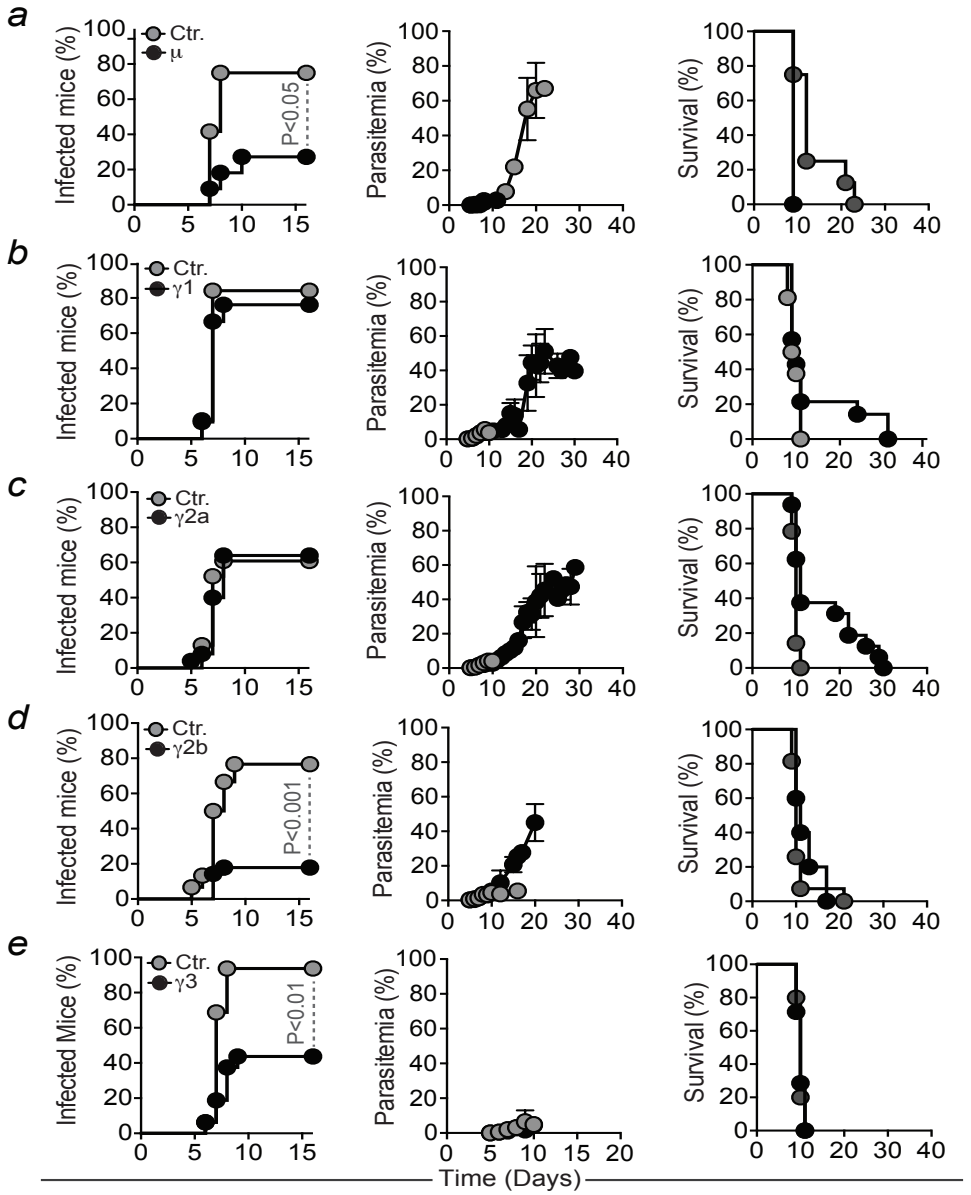

Figure 3.11 Passive transfer of anti-α-gal IgM, IgG2b and IgG3 to naïve *α1,3Gt*$^{-/-}$ mice conferred protection against *Pb*A transmission by *A.* mosquitoes. Incidence of blood stage of infection (%) with respective parasitemia (%) and survival (%) in *α1,3Gt*$^{-/-}$ mice receiving polyclonal anti-α-gal IgM Abs or monoclonal anti-α-gal IgG Abs (150μg/mL) *vs.* controls (Ctr.) exposed to *Pb*A$^{EEF1a\text{-}GFP}$ infected mosquitoes. Data was pooled from 4-7 independent experiments (n=19-32 mice per group). Statistical significance among groups in the incidence of infection was determined by log rank (Mantel-Cox) test.

3.3.5 Protective effect of anti-α-gal Abs against *Plasmodium* infection can be enhanced with CpG oligodeoxynucleotide

We asked whether immunization against α-gal that confers protection against *Plasmodium* infection by *Anopheles* mosquitoes could be enhanced different regimes of immunization. Immunization against α-gal using rRBCM was associated with 61% reduction of *Pb*A transmission by *A. stephensi* mosquitoes upon immunization without adjuvant [95% CI: 0.209-0.726] as compared to control naïve $\alpha 1,3Gt^{-/-}$ or $\alpha 1,3Gt^{+/+}$ mice or to immunized $\alpha 1,3Gt^{+/+}$ mice **(Figure 3.4)**. Immunization with rRBCM emulsified in either incomplete Freud's adjuvant (IFA), complete Freud's adjuvant (CFA) or Alum provided similar levels of protection against *Pb*A infected mosquitoes in $\alpha 1,3Gt^{-/-}$ mice, as compared to immunization without adjuvant **(Figure 3.12 and 3.13)**. These immunizations also enhanced the anti-α-gal IgG Ab response **(Figure 3.12a-c)**. But this was not associated with increased protection against transmission of *Pb*A infection *vs.* immunization without adjuvant **(Figure 3.3a)**. Moreover, we tested immunization with α-gal-BSA emulsified in CFA against *Plasmodium* infection **(Figure 3.13d)** that conferred the same level of protection against *Pb*A infection. This excludes the presence of any other antigen in rRBCM favoring the protective mechanism against *Plasmodium* infection. Collectively, these immunization protocols show that immunization against α-gal can confer sterile protection against *Plasmodium* infection with the same rate.

We then asked whether introducing a PAMP with potent immunostimulatory properties could also be useful as an adjuvant against *Plasmodium* infection. CpG-ODN, toll like receptor 9 agonist, can induce production of IL-12, which enhances IFN-γ production, antibody production, and cytotoxicity of NK cells and CD8+ T cells[45-47].

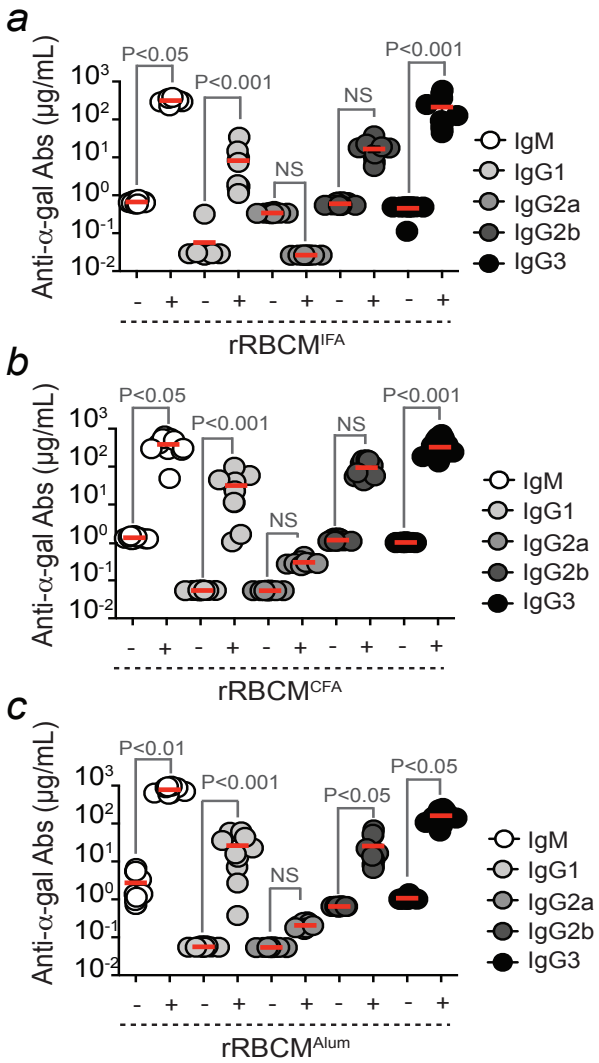

Figure 3.12 Immunization against α-gal using different adjuvants. Anti-α-gal Abs in control *α1,3Gt*$^{-/-}$ mice non-immunized (-) *vs.* immunized (+) with rRBCM emulsified in **a)** IFA (rRBCM^{IFA}), **b)** CFA (rRBCM^{CFA}) or **c)** Alum (rRBCM^{Alum}) Dots represent individual mice (n=12-29 mice per group) pooled from 2-3 independent experiments. Bars represent mean values. Statistically significant correlations among the groups were determined by Kruskal-Wallis test with Dunn's multiple comparison post-test.

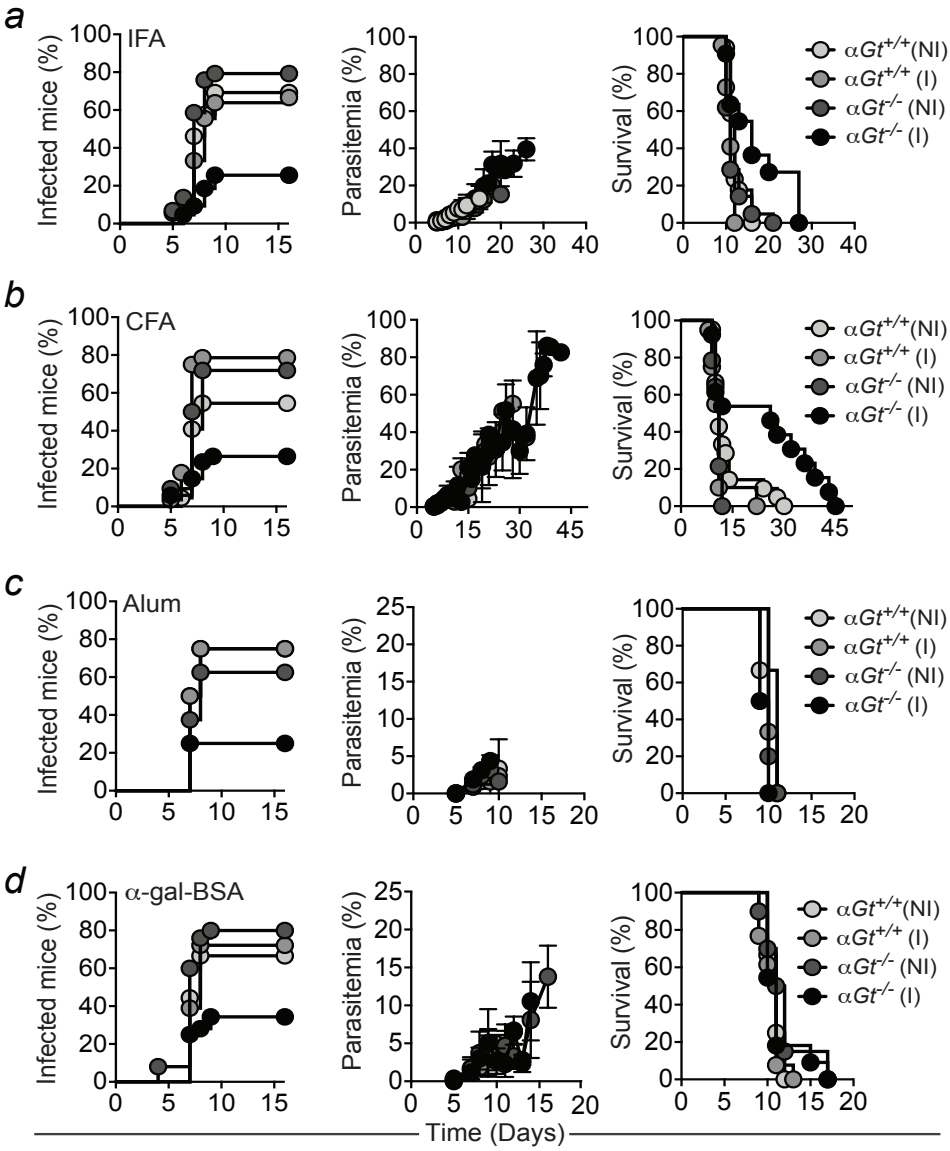

Figure 3.13 Protective effect of anti-α-gal immunization using different adjuvants formulation. Incidence of blood stage infection (%) with respective parasitemia (%) and survival (%) in *α1,3Gt*$^{-/-}$ mice immunized (I) with **a)** IFA + rRBCM, **b)** CFA + rRBCM (two booster immunizations with IFA + rRBCM), **c)** Alum + rRBCM or **d)** CFA + α-gal-BSA (two booster immunizations with IFA + α-gal-BSA) *vs.* non-immunized (NI) *α1,3Gt*$^{-/-}$ mice or control immunized (I) or non-immunized (NI) *α1,3Gt*$^{+/+}$ mice. Incidence of infection significance among groups was determined by log rank (Mantel-Cox) test. A p value equal to or below 0.05 was considered statistically significant.

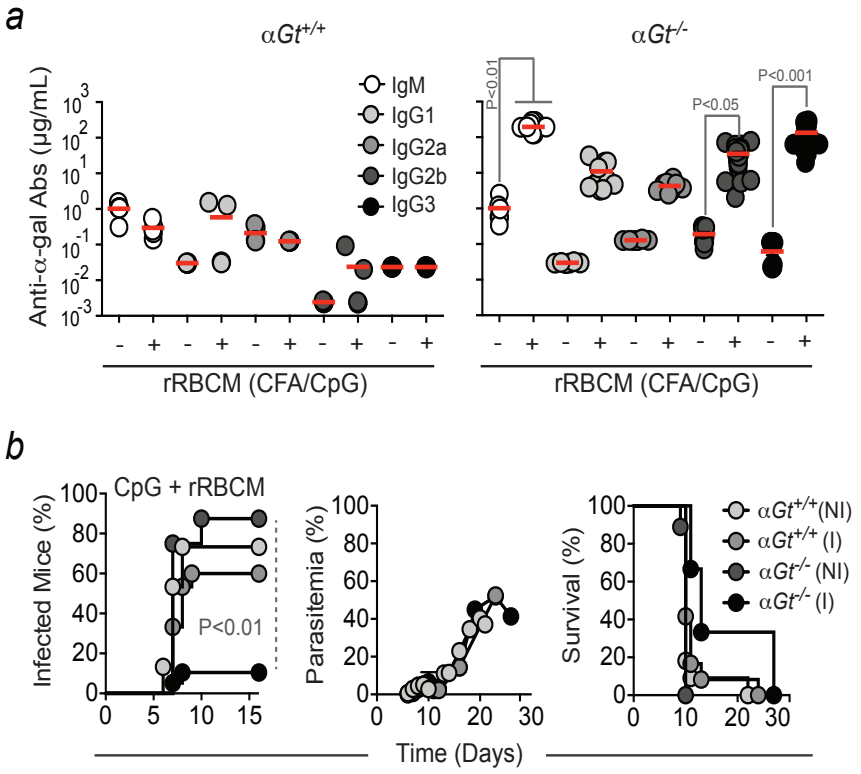

Figure 3.14 Protective effect of anti-α-gal immunization using CpG as an adjuvant. Concentration of anti-α-gal Abs **a)** in the serum of *α1,3Gt*$^{-/-}$ mice immunized (I) with rRBCM emulsified in CFA and supplemented with CpG *vs.* non-immunized (NI) *α1,3Gt*$^{-/-}$ mice or control immunized (I) or non-immunized (NI) *α1,3Gt*$^{+/+}$ mice. **b)** Incidence of blood stage infection (%) with respective parasitemia (%) and survival (%) mice in (a). Dots in (a) represent individual mice (n=6-22 mice per group) pooled from 2 independent experiments. Bars represent mean values. Statistically correlations among the groups were determined with Kruskal-Wallis with Dunn's multiple comparison post-test. Data in (b) show is from 3 independent experiments (n=16-19 mice per group). Incidence of infection significance among groups was determined by log rank (Mantel-Cox) test.

Immunization of *α1,3Gt*$^{-/-}$ mice with rRBCM emulsified in complete Freund´s adjuvant (CFA) supplemented with toll like receptor 9 agonist CpG, enhanced the anti-α-gal IgG2b and IgG3 Ab response 2-3 fold **(Figure 3.14a)** *vs.* immunization without adjuvant. This was associated with 88% reduction **(Figure 3.14b)** in the relative risk of infection [95% CI: 0.032-

0.452] *vs.* 61% reduction upon immunization without adjuvant [95% CI: 0.209-0.726]. This was not observed in control *α1,3Gt*$^{+/+}$ mice. This suggests that the protective effect of α-gal immunization is enhanced by specific adjuvants, e.g. CpG, that favor the production of anti-α-gal Abs from specific IgG subclasses, i.e. IgG2b and IgG3.

3.5 Chapter Discussions and Conclusion

When inoculated into the human dermis, *Plasmodium spp*. sporozoites are confronted with high levels of cytotoxic anti-α-gal IgM Abs recognizing the α-gal glycan **(Figure 3.2a)** that prevent malaria transmission, as demonstrated in individuals from malaria endemic area. Briefly, those who showed evidence of decreased *P. falciparum* infection risk have higher levels of circulating anti-α-gal IgM Abs, compared to individuals who are susceptible to *P. falciparum* infection. Levels of circulating anti-α-gal IgG Abs in individuals from a malaria endemic area are on average significantly lower than levels of anti-α-gal IgM Abs **(Figure 3.2c)**. This may help explain why anti-α-gal IgG Abs are not associated with decreased risk of *P. falciparum* infection in this study **(Figure 3.1d)**. This also suggests that infection by *P. falciparum* in malaria endemic regions fails to induce class switch to anti-α-gal IgG Abs. The reason for this is not clear but the observation that immunization with rRBCM or with synthetic α-gal-BSA can induce class switch to anti-α-gal IgG Abs in mice suggests that *P. falciparum* may actively repress this phenomenon. However, when present above a certain threshold level as it was shown in murine model **(Figure 3.3b)**, anti-α-gal IgG Abs are protective against malaria transmission **(Figure 3.10 and 3.11)**.

Anti-α-gal Abs exert a negative impact on the initial phase of *Plasmodium* infection in the dermis **(Figure 3.6 and 3.7)**. This notion is supported by the

observation that human-like *α1,3Gt*$^{-/-}$ mice immunized with rRBCM carrying circulating anti-α-gal IgM Abs **(Figure 3.3b)** at similar levels to those of adult individuals from an endemic area of malaria **(Figure 3.2a)** are protected against transmission of *Plasmodium* infection by *Anopheles* mosquitoes **(Figure 3.10b and 3.11a)**. This protective effect in *α1,3Gt*$^{-/-}$ mice is not complete, consistent with malaria transmission in endemic areas of malaria, despite the likely protective effect of these Abs in adult humans **(Figure 3.2b)**.

The protective effect exerted by anti-α-gal IgM Abs may be relevant to understand the higher rates of malaria incidence in young children, as compared to adults. Newborns and children under the age of 2-3 years have only residual levels of anti-α-gal IgM Abs, as compared to adults from the same endemic area of malaria **(Figure 3.2a)**. The observation that anti-α-gal IgM Abs are protective against malaria transmission in human **(Figure 3.2b)** and human-like *α1,3Gt*$^{-/-}$ mice **(Figure 3.10b and 3.11a)** suggests that anti-α-gal IgM should be over certain threshold. Lack of these Abs in newborns and young infants contributes to their higher risk of malaria transmission. The ability of anti-α-gal NAbs to reduce very significantly transmission of *Plasmodium* infection via *Anopheles* mosquitoes bites might also contribute to explain why malaria transmission is a rather inefficient process even when performed under controlled experimental conditions in adult humans[48-50].

We also asked whether the protective of these Abs in murine model is vector or parasite strain dependent. *Plasmodium* infection in mice was tested with *P. yoelii* 17XNL strain in addition to *Pb*A strain. Since there is no identified gene that favors the production of α-gal sugar epitope by *Plasmodium*, one can argue that *Plasmodium* sporozoites might uptake α-gal

from mosquitoes. This would make the protective effect against *Pb*A infected *A. stephensi* possibly vector-dependent. Therefore, we performed additional experiments using *Pb*A infected *A. gambiae* and showed that anti-α-gal Abs conferred protection against infection, as transmitted by *A. gambiae* mosquitoes. Together, these results demonstrate that anti-α-gal Abs confer protection against *Plasmodium* infection irrespectively of *Plasmodium* strain or vector species **(Figure 3.4)**.

While anti-α-gal Abs can provide sterile protection against malaria in mouse model **(Figure 3.5)**, this is not commonly observed in malaria endemic areas, possibly because the levels of circulating anti-α-gal Abs are below a certain threshold level required to provide sterile protection. This also suggests that immunization against this carbohydrate may be useful not only in terms of preventing individual infection but also disease transmission to whole populations in endemic areas of malaria. However, this natural mechanism of protection against malaria transmission can be enhanced *via* immunization against α-gal emulsifying in adjuvants **(Figure 3.14a)** that favor the production of T cell-dependent complement fixing anti-α-gal IgG Abs. Moreover, if coupled to other *Plasmodium* antigens (such as CSP that is the antigen of RTS,S vaccine), this approach could enhance the immunogenicity[51] and hence the protective efficacy of candidate malaria vaccines[52], preventing individual infections as well as disease transmission. The therapeutic efficiency of this type of approach in which anti-α-gal Abs and parasite protein specific Abs specifically can be enhanced will be critically dependent on the capacity of the immunization protocol to induce T cell-dependent complement fixing anti-α-gal IgG responses that will be able to arrest *Plasmodium* sporozoites in the skin immediately after inoculation by *Anopheles* mosquitoes.

Contributions

All experiments in this chapter performed by the author of this dissertation except ELISA of human plasma samples were performed by Silvia Portugal and were analyzed Tuan Tran and Peter Crompton.

Acknowledgements

Thanks to Raffaella Gozzelino, Susana Ramos and Sumnima Singh for comments on this chapter of the thesis, Joana Tavares, Rogerio Amino and Robert Ménard (Institute Pasteur, France) for providing *P.yoelii* 17XNL-GFP infected mosquito to perform biting experiments, Virginia de Oliveira Marques for teaching me to analyze mouse serum samples by ELISA, Andreia Cunha and Ivo Marguti for immunization protocols, Silvia Cardoso and Sofia Rebelo for initially helping me out to learn mouse breeding and genotyping, Lígia Antunes Gonçalves for providing us 18S rRNA primers and enduring all my naïve questions about *Plasmodium* infection. We are indebted to Ana Regelado (Antibody Service, IGC) for producing anti-α-gal mAbs from anti-α-gal hybridomas, which were a generous gift from Dr. Anita Chong (University of Chicago, IL, USA). We are also thankful to Dr. Uri Galili (University of Massachusetts Medical School, Worcester, MA, USA) for providing us M86 mAbs. Finally, I'd like to thank to Joana Gomes and Henrique Silveira (IHMT, Lisbon, Portugal) for the establishment and maintenance of *Plasmodium* infected *A. stephensi* and *A. gambiae* mosquitoes.

References

1. Bovin, N.V. Natural antibodies to glycans. *Biochemistry. Biokhimiia* **78**, 786-797 (2013).
2. Lutz, H.U. *Naturally Occurring Antibodies (NAbs)*, (Landes Bioscience and Springer Science, USA, 2012).

3. Bovin, N., *et al.* Repertoire of human natural anti-glycan immunoglobulins. Do we have auto-antibodies? *Biochimica et biophysica acta* **1820**, 1373-1382 (2012).
4. Bendelac, A., Bonneville, M. & Kearney, J.F. Autoreactivity by design: innate B and T lymphocytes. *Nat Rev Immunol* **1**, 177-186 (2001).
5. Lalor, P.A. & Morahan, G. The Peritoneal Ly-1 (Cd5) B-Cell Repertoire Is Unique among Murine B-Cell Repertoires. *Eur J Immunol* **20**, 485-492 (1990).
6. Montecino-Rodriguez, E. & Dorshkind, K. B-1 B cell development in the fetus and adult. *Immunity* **36**, 13-21 (2012).
7. Christiansen, D., *et al.* Antibody responses to glycolipid-borne carbohydrates require CD4+ T cells but not CD1 or NKT cells. *Immunology and cell biology* **89**, 502-510 (2011).
8. Galili, U., Rachmilewitz, E.A., Peleg, A. & Flechner, I. A unique natural human IgG antibody with anti-alpha-galactosyl specificity. *The Journal of experimental medicine* **160**, 1519-1531 (1984).
9. Avila, J.L. & Rojas, M. A galactosyl(alpha 1-3)mannose epitope on phospholipids of *Leishmania mexicana* and *L. braziliensis* is recognized by trypanosomatid-infected human sera. *Journal of clinical microbiology* **28**, 1530-1537 (1990).
10. Doenz, U., Nydegger, U.E., Kueng, A., Carrel, T. & Mohacsi, P. Anti-Galalpha1-3Gal IgM/IgG antibody levels in infants: do they have a clinical relevance in pediatric xenotransplantation? *J Heart Lung Transplant* **19**, 1108-1113 (2000).
11. LaTemple, D.C. & Galili, U. Adult and neonatal anti-Gal response in knock-out mice for alpha1,3galactosyltransferase. *Xenotransplantation* **5**, 191-196 (1998).
12. Cascalho, M. & Platt, J.L. Xenotransplantation and other means of organ replacement. *Nat Rev Immunol* **1**, 154-160 (2001).
13. Yu, P.B., Holzknecht, Z.E., Bruno, D., Parker, W. & Platt, J.L. Modulation of natural IgM binding and complement activation by

natural IgG antibodies: a role for IgG anti-Gal alpha1-3Gal antibodies. *Journal of Immunology* **157**, 5163-5168 (1996).

14. Ding, J.W., *et al.* Hyperacute rejection by anti-Gal IgG1, IgG2a, and IgG2b is dependent on complement and Fc-gamma receptors. *J Immunol* **180**, 261-268 (2008).
15. Tearle, R.G., *et al.* The alpha-1,3-galactosyltransferase knockout mouse. Implications for xenotransplantation. *Transplantation* **61**, 13-19 (1996).
16. Benatuil, L., *et al.* Ig knock-in mice producing anti-carbohydrate antibodies: breakthrough of B cells producing low affinity anti-self antibodies. *J Immunol* **180**, 3839-3848 (2008).
17. Cretin, N., Bracy, J., Hanson, K. & Iacomini, J. The role of T cell help in the production of antibodies specific for Gal alpha 1-3Gal. *J Immunol* **168**, 1479-1483 (2002).
18. Donjerkovic, D. & Scott, D.W. Activation-induced cell death in B lymphocytes. *Cell research* **10**, 179-192 (2000).
19. Galili, U., Mandrell, R.E., Hamadeh, R.M., Shohet, S.B. & Griffiss, J.M. Interaction between human natural anti-alpha-galactosyl immunoglobulin G and bacteria of the human flora. *Infection and immunity* **56**, 1730-1737 (1988).
20. Avila, J.L., Rojas, M. & Galili, U. Immunogenic Gal alpha 1----3Gal carbohydrate epitopes are present on pathogenic American *Trypanosoma* and *Leishmania*. *J Immunol* **142**, 2828-2834 (1989).
21. Takeuchi, Y., *et al.* Sensitization of cells and retroviruses to human serum by (alpha 1-3) galactosyltransferase. *Nature* **379**, 85-88 (1996).
22. Ramasamy, R. & Field, M.C. Terminal galactosylation of glycoconjugates in *Plasmodium falciparum* asexual blood stages and Trypanosoma brucei bloodstream trypomastigotes. *Exp Parasitol* **130**, 314-320 (2012).
23. Ramasamy, R. & Reese, R.T. Terminal galactose residues and the antigenicity of *Plasmodium falciparum* glycoproteins. *Molecular and biochemical parasitology* **19**, 91-101 (1986).

24. Ramasamy, R., Ramasamy, M. & Yasawardena, S. Antibodies and *Plasmodium falciparum* merozoites. *Trends in parasitology* **17**, 194-197 (2001).
25. Tran, T.M., *et al.* An intensive longitudinal cohort study of Malian children and adults reveals no evidence of acquired immunity to Plasmodium falciparum infection. *Clinical infectious diseases : an official publication of the Infectious Diseases Society of America* **57**, 40-47 (2013).
26. Shinkel, T.A., *et al.* Changes in cell surface glycosylation in alpha1,3-galactosyltransferase knockout and alpha1,2-fucosyltransferase transgenic mice. *Transplantation* **64**, 197-204 (1997).
27. Gu, H., Zou, Y.R. & Rajewsky, K. Independent control of immunoglobulin switch recombination at individual switch regions evidenced through Cre-loxP-mediated gene targeting. *Cell* **73**, 1155-1164 (1993).
28. Muramatsu, M., *et al.* Class switch recombination and hypermutation require activation-induced cytidine deaminase (AID), a potential RNA editing enzyme. *Cell* **102**, 553-563 (2000).
29. Ehrenstein, M.R., O'Keefe, T.L., Davies, S.L. & Neuberger, M.S. Targeted gene disruption reveals a role for natural secretory IgM in the maturation of the primary immune response. *Proceedings of the National Academy of Sciences of the United States of America* **95**, 10089-10093 (1998).
30. Mombaerts, P., *et al.* Mutations in T-cell antigen receptor genes alpha and beta block thymocyte development at different stages. *Nature* **360**, 225-231 (1992).
31. Eto, T., Ichikawa, Y., Nishimura, K., Ando, S. & Yamakawa, T. Chemistry of lipid of the posthemyolytic residue or stroma of erythrocytes. XVI. Occurrence of ceramide pentasaccharide in the membrane of erythrocytes and reticulocytes of rabbit. *J Biochem* **64**, 205-213 (1968).

32. Matsuzawa, T. & Ikarashi, Y. Haemolysis of various mammalian erythrocytes in sodium chloride, glucose and phosphate-buffer solutions. *Laboratory animals* **13**, 329-331 (1979).
33. Galili, U., LaTemple, D.C. & Radic, M.Z. A sensitive assay for measuring alpha-Gal epitope expression on cells by a monoclonal anti-Gal antibody. *Transplantation* **65**, 1129-1132 (1998).
34. Yin, D., *et al.* Cutting Edge: NK cells mediate IgG1-dependent hyperacute rejection of xenografts. *J Immunol* **172**, 7235-7238 (2004).
35. Spalter, S.H., *et al.* Normal human serum contains natural antibodies reactive with autologous ABO blood group antigens. *Blood* **93**, 4418-4424 (1999).
36. Ferreira, A., *et al.* Sickle Hemoglobin Confers Tolerance to *Plasmodium* Infection. *Cell* **145**, 398–409 (2011).
37. Giemsa, G. Eine Vereinfachung und Vervollkommnung meiner Methylenazur- Methylenblau-Eosin-Färbemethode zur Erzielung der Romanowsky-Nochtschen Chromatinfärbung. *Centralblatt für Bakteriologie* **37**, 308–311 (1904).
38. Tran, T.M., *et al.* Naturally acquired antibodies specific for *Plasmodium falciparum* reticulocyte-binding protein homologue 5 inhibit parasite growth and predict protection from malaria. *The Journal of infectious diseases* **209**, 789-798 (2014).
39. Avila, J.L., Rojas, M. & Velazquez-Avila, G. Characterization of a natural human antibody with anti-galactosyl(alpha 1-2)galactose specificity that is present at high titers in chronic *Trypanosoma cruzi* infection. *The American journal of tropical medicine and hygiene* **47**, 413-421 (1992).
40. Parker, W., *et al.* Naturally occurring anti-alpha-galactosyl antibodies: relationship to xenoreactive anti-alpha-galactosyl antibodies. *Glycobiology* **9**, 865-873 (1999).

41. Yang, Y.G., *et al.* Tolerization of Anti-Gal-Alpha-1-3gal Natural Antibody-Forming B Cells By Induction of Mixed Chimerism. *Journal of Experimental Medicine* **187**, 1335-1342 (1998).
42. Chiang, T.R., *et al.* Anti-Gal antibodies in humans and 1,3alpha-galactosyltransferase knock-out mice. *Transplantation* **69**, 2593-2600 (2000).
43. Boes, M., *et al.* Accelerated development of IgG autoantibodies and autoimmune disease in the absence of secreted IgM. *Proceedings of the National Academy of Sciences of the United States of America* **97**, 1184-1189 (2000).
44. Belnoue, E., *et al.* On the pathogenic role of brain-sequestered alphabeta CD8+ T cells in experimental cerebral malaria. *J Immunol* **169**, 6369-6375 (2002).
45. Brazolot Millan, C.L., Weeratna, R., Krieg, A.M., Siegrist, C.A. & Davis, H.L. CpG DNA can induce strong Th1 humoral and cell-mediated immune responses against hepatitis B surface antigen in young mice. *Proceedings of the National Academy of Sciences of the United States of America* **95**, 15553-15558 (1998).
46. Davis, H.L., *et al.* CpG DNA is a potent enhancer of specific immunity in mice immunized with recombinant hepatitis B surface antigen. *J Immunol* **160**, 870-876 (1998).
47. Zhang, X., He, P., Hu, Z., Wang, X. & Liang, Z. Enhanced specific immune responses by CpG DNA in mice immunized with recombinant hepatitis B surface antigen and HB vaccine. *Virology journal* **8**, 78 (2011).
48. Verhage, D.F., *et al.* Clinical outcome of experimental human malaria induced by *Plasmodium falciparum*-infected mosquitoes. *Neth J Med* **63**, 52-58 (2005).
49. Sauerwein, R.W., Roestenberg, M. & Moorthy, V.S. Experimental human challenge infections can accelerate clinical malaria vaccine development. *Nat Rev Immunol* **11**, 57-64 (2011).

50. Rickman, L.S., *et al.* *Plasmodium falciparum*-infected Anopheles stephensi inconsistently transmit malaria to humans. *The American journal of tropical medicine and hygiene* **43**, 441-445 (1990).
51. Benatuil, L., *et al.* The influence of natural antibody specificity on antigen immunogenicity. *Eur J Immunol* **35**, 2638-2647 (2005).
52. Olotu, A., *et al.* Four-year efficacy of RTS,S/AS01E and its interaction with malaria exposure. *N Engl J Med* **368**, 1111-1120 (2013).

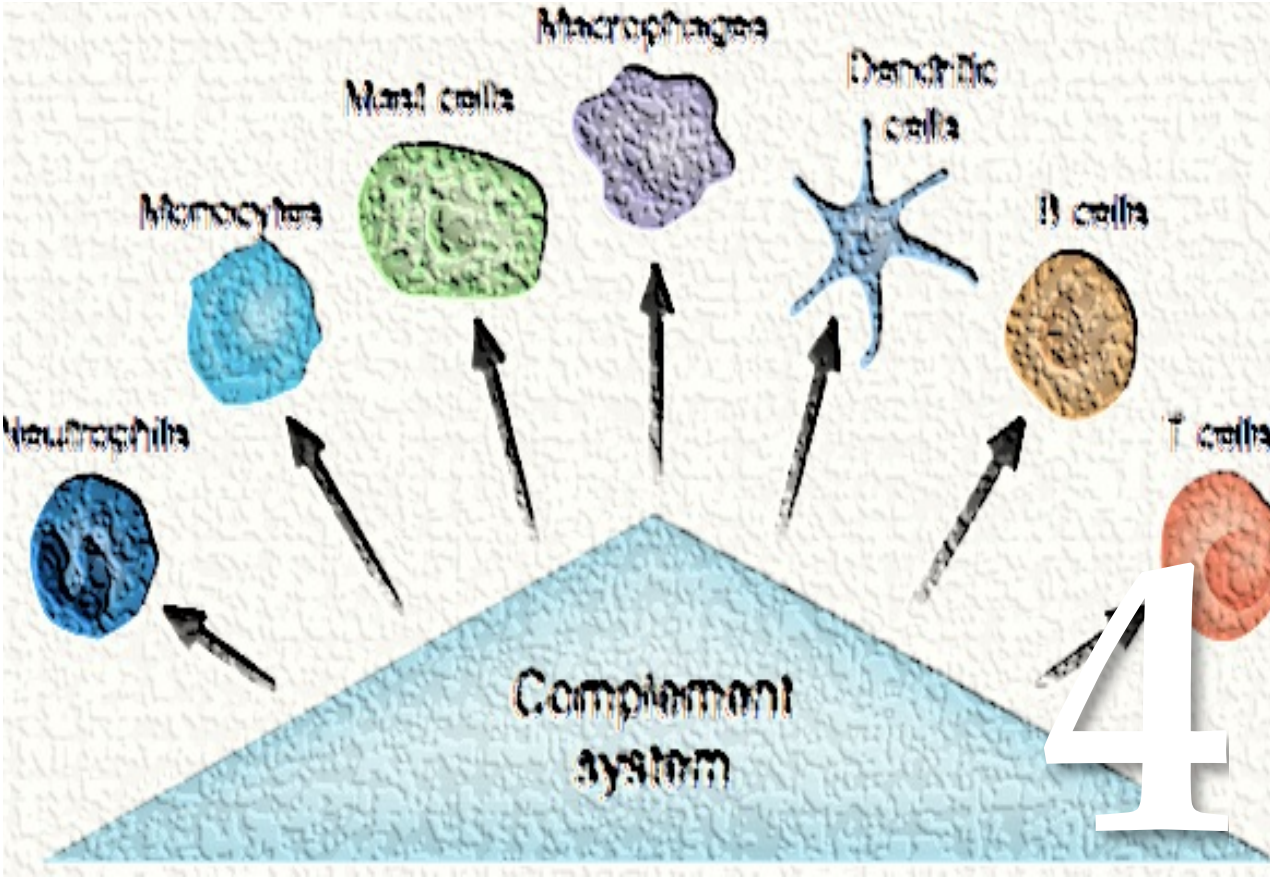

Interface Elements of Innate and Adaptive Immunity Play an Active Role on Protective Mechanism against *Plasmodium* Infection

Abstract

Anti-α-gal Abs are natural defense mechanism against malaria transmission, targeting *Plasmodium* sporozoites in the skin immediately after inoculation by *Anopheles* mosquitoes (*Chapter 3*). Here, we addressed mechanistically, how anti-α-gal Abs target *Plasmodium* sporozoites and inhibit the progression of infection. We demonstrate that preformed anti-α-gal Abs target *Plasmodium* sporozoites for complement-mediated cytotoxicity. Complement activation by anti-α-gal Abs is cytotoxic to sporozoites and thus is sufficient per se to prevent sporozoite migration to the liver and to inhibit hepatocyte invasion, suppressing the establishment of liver stage infection. Collectively, these observations reveal that the protective effect exerted by anti-α-gal Abs is strictly dependent on complement activation.

4.1 Introduction

The innate immune system of vertebrates has the ability to recognize evolutionarily conserved molecular patterns that are unique to microorganisms[1]. PAMPs that form molecular signatures of microbial invaders are detected PRRs expressed on the cell surfaces, in intracellular compartments or secreted extracellularly[2,3] (*see Section 1.4.1*). This recognition process results in the activation of innate immune responses and subsequent induction of the effector functions conferring host resistance to pathogens. The complement system acts as one of such components of innate immunity that targets pathogens for cytotoxicity.

The complement system was named by Belgian immunologist and microbiologist, Jules Bordet in 1896. An experiment on blood serum components led him to discover that the lytic effect of Abs is significantly increased by the presence of innate serum components referred to as complements. The complement mechanism has the ability to 'complement' the antibacterial properties of the Abs by a heat-stable fraction of serum, enhancing bacteria opsonization and subsequently killing. This now well-characterized system consists of a complex network of plasma and membrane-associated proteins that provide a highly efficient defense response against bacteria, viruses or protozoan parasites[4].

The complement system can be activated on the surface of a pathogen in the early phases of an infection through three different pathways which are **classical**, **alternative** and **lectin pathways (Figure 4.1)**[4-6].

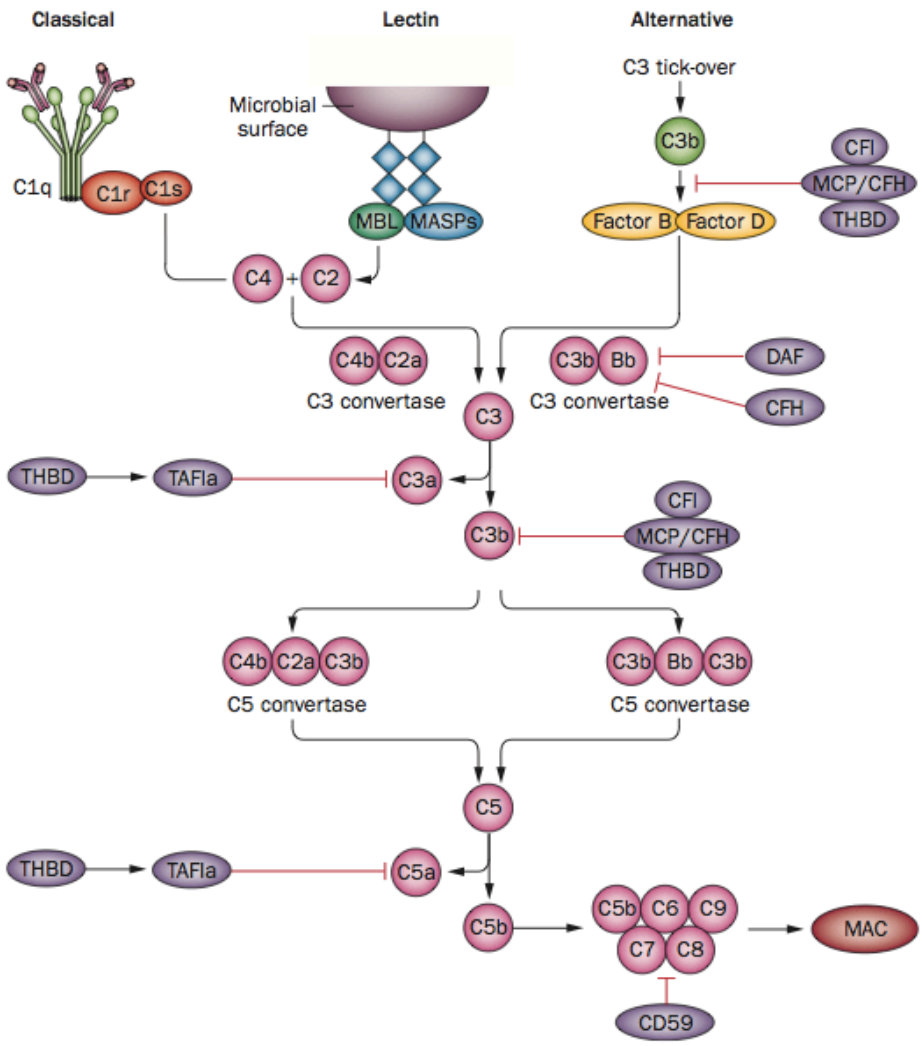

Figure 4.1 Overview of complement activation. The complement system consists of three pathways leading to activation of the complement cascade. These pathways converge at the cleavage/activation of membrane bound C3, leading to generation of C3a and C5a that promotes opsonization of pathogens as well as the membrane attack complex (C5b-9) that disrupts the membrane integrity of pathogens and promotes their killing and clearance. Adapted from[7].

Activation of the classical and lectin pathways depends on the recognition of pathogens by antibodies (pentraxins and C1q that binds to an antibody attached to antigen in the classical pathway) and pattern recognition molecules (lectins and ficolins for the lectin pathway), respectively[8]. In the

classical pathway, complement activation is triggered upon the binding of the C1 complex, which consists of one molecule of C1q, two serine protease proenzymes C1r and C1s, to an Ab bound to a microbial organism[9]. Activation of C1s cleaves C4 that binds covalently to the infectious agent surface, cleaving C2. The lectin pathway can be activated by binding of a serum protein called mannan-binding lectin to carbohydrates containing mannose on bacteria or viruses[10]. This activates the Mannose Binding Ligand-associated serine proteases (MASPs) and leads to the cleavage of C4 and C2 [11]. These two pathways meet at the level of C4b/C2a (C3-convertase enzyme) leading to C3 proteolysis and the generation of C3a and C3b. The alternative pathway, that is mechanistically distinct from these two pathways, is initiated spontaneously when a complement component binds to the surface of a pathogen, relying on spontaneous low-level formation of C3b (C3 tick-over)[7]. All three pathways generate a protease called a C3 convertase through proteolytical activation, binding covalently C3b to C4bC2a and forming the C5 convertase (C4bC2aC3b complex) while in the alternative pathways, Factors B and D are the key players that lead to spontaneous C3 hydrolysis and eventual formation of C3 (C3bBb) and C5 (C3bBbC3b) convertases. The alternative pathway stabilized and facilitated by properdin. The formation of convertases also generates anaphylatoxins (C4a/C3a/C5a) that act as potent inflammatory soluble molecules while forming the membrane attack complex (MAC), which creates a highly cytotoxic pore in the cell membranes of pathogens. Of note, opsonins (C3b) mark pathogens for phagocyte opsonization via the engagement of receptors [complement receptors 1-4 (CR1-4) and CRIg] for C3b[4,12].

4.1.1 Positive feedback loop between complement system and neutrophils

Neutrophils are the most abundant (50-75%) type of circulating white blood cells in humans. Together with the complement system, neutrophils are a major player in the process of innate cell-mediated immunity.

However, neutrophils often fail to provide host defense against pathogens in the absence of opsonins. Neutrophils are abundant in viral, bacterial and fungal induced lesions where they bind opsonized pathogens as well as viral infected cells via an oxidative burst often triggered via the engagement of Ab (Fc) and complement (iC3b) receptors[13].

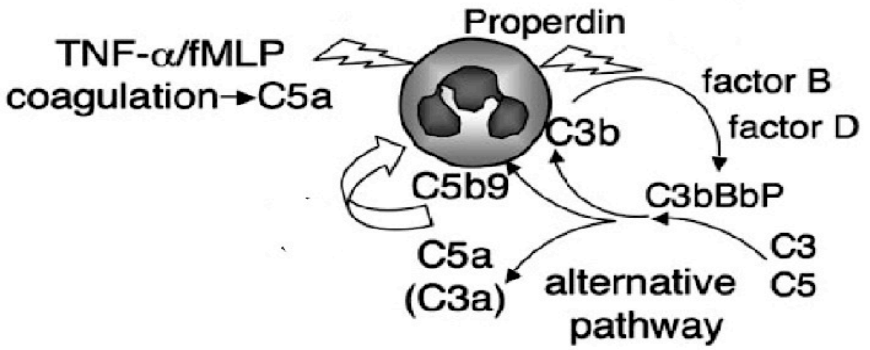

Figure 4.2 An amplification loop between complement and neutrophil. Engagement of PRR activates neutrophils, triggering the complement alternative pathway. Activation of the alternative pathway increases neutrophil and cellular responses. Adapted from[14].

Complement-neutrophil interactions are mediated via C3a, C4a, and C5a and their respective receptors[15,16]. Neutrophil proteases and oxidants can activate complement in fluid phase and activated neutrophils can also release unknown complement activating factors. Moreover, complement activation can be triggered by the expression of molecules on the surface of apoptotic or necrotic cells. Recently, Camous and colleagues **(Figure 4.2)** have shown that suboptimal levels of cytokine or coagulation-derived factors serve as initial stimulus to activate neutrophils and later on, to secrete properdin that triggers complement activation through the alternative pathway. This positive feedback loop enhances the activity of neutrophils and cell responses, such as degranulation and oxidative burst[14,17,18].

4.1.2 Anti-α-gal Abs and complement mediated cytotoxicity

Activation of complement by anti-α-gal Abs is particularly well documented in the context of the xenograft rejection in which anti-α-gal Abs recognize α-gal expressed in the transplanted organ and activate complement via the classical pathway. This leads to endothelial cell damage, platelet aggregation, occlusion of small blood vessels and collapse of the vascular bed, resulting in graft rejection within minutes to hours. Anti-α-gal IgM Abs trigger the activation of the classical pathway of complement as well as the activation of MBL/MASP2 **(Figure 4.1)**[19] suggesting that the lectin pathway may be activated by anti-α-gal IgM Abs[20]. Mouse anti-α-gal IgG2a, IgG2b and IgG3 are also potent activators of complement and can mediate the xenograft rejection[21-24]. By comparison, anti-α-gal IgG1 mAb activates complement poorly[22] although it can act in a cytotoxic manner via the activation of Fc-γ receptors expressed on several cell types, including NK cells[23]. Anti-α-gal IgG subclasses vary on their ability to engage Fc-γ receptors, i.e. IgG1>IgG2b >>IgG2a =IgG3[24].

In this chapter, we asked whether complement activation contributes to the protective effect exerted by anti-α-gal Abs against *Plasmodium* infection. We determined the subclass(es) of anti-α-gal IgG that confer protection against *Plasmodium* infection and asked whether neutrophils have a role on this protective mechanism driven by anti-α-gal Abs.

4.2 Materials and Methods

4.2.1 Mice *See also Section 3.2.2*

To generate *α1,3Gt*$^{-/-}$*C3*$^{-/-}$ double knockout mice, C57BL/6 *α1,3Gt*$^{-/-}$ mice were crossed with homozygous C57BL/6 complement 3 deficient (*C3*$^{-/-}$;

line B6.129S4-C3tm1Crr/*J*) mice[25]. Animals were genotyped by PCR using the following primers:

Primer	Sequence 5' --> 3'	Primer Type
oIMR1325	5′-ATCTTGAGTGCACCAAGCC-3′	Common
oIMR1326	5′-GGTTGCAGCAGTCTATGAAGG-3′	Wild type Reverse
oIMR7415	5′-GCCAGAGGCCACTTGTGTAG-3′	Mutant Reverse

In addition, mouse complement factor 3 in serum was determined using highly sensitive two-site enzyme linked immunosorbent (ELISA), as described in the manufacturer's instructions (GenWay Biotech, Inc., USA).

4.2.2 Passive immunization with anti-α-gal mAbs

α1,3Gt$^{-/-}$*C3*$^{-/-}$ mice received anti-α-gal IgM, IgG2b and IgG3 Abs (150*μ*g; 100*μ*l per mouse) via a single intravenous injection, 24h prior to mosquito exposure. See *Section 2.2.2 and Section 3.2.6* for more details.

4.2.3 *In vivo* PMN depletion

Anti-Gr1 mAb (Clone: RB6-8C5; RB6-8C5 hybridoma) was produced at the Instituto Gulbenkian de Ciência under serum-free conditions using a CELLine (Integra, Switzerland)[26]. Neutrophils were depleted in *α1,3Gt*$^{-/-}$ mouse by a single intravenous anti-Gr1 mAb injection (250*μ*g), 48h prior to mosquito biting. PMN depletion was confirmed by staining for CD11b-FITC (Integrin α[M] chain, Mac-1α chain, CR3, BD Pharmingen™) and Anti-Gr1-PE (1A8, BD Pharmingen™) and analyzed in flow cytometry[27] (CyAn™ ADP Analyzer, Beckman Coulter).

4.2.4 Parasites maintenance and mosquitoes rearing *See Section 2.2.1*

4.2.5 *Plasmodium* transmission *See Section 3.2.9*

4.2.6 Disease assessment *See Section 3.2.10*

4.2.7 Isolation of sporozoites from salivary glands *See Section 2.2.4*

4.2.8 C3b deposition on *Plasmodium*

*Pb*A$^{Hsp70\text{-}GFP}$ sporozoites were exposed to anti-α-gal mAbs (150μg/mL; in 50μL DMEM; 60min; 4°C) and subsequently to naive C57BL/6 mouse plasma (1:5 in 0.1% gelatin in Veronal Buffer (VB)++; 50μL; 60min; 37°C) (Lonza), used as a source of complement. Samples were washed (1X; PBS) and mouse C3 deposition was detected using APC labeled anti-C3/C3b/iC3b (Clone: 6C9; 1:100; 50μL; 45min; 4°C) and analyzed in CyAnTM ADP Analyzer (Beckman Coulter).

4.2.9 Complement mediated cytotoxicity in *Plasmodium*

*Pb*A$^{Hsp70\text{-}GFP}$ sporozoites (10-50x10^3) were incubated with anti-α-gal or isotype matched anti-DNP mAbs (150*μ*g/mL mAb in 10*μ*L DMEM GlutaMAXTM; 60min; 4°C). Naive C57BL/6 mouse plasma (1:5) or baby rabbit complement (1:10; Cedarlane Laboratories) was added (0.1% gelatin in VB++) as a source of complement (60min; 37°C). Cytotoxicity was quantified according to GFP expression of *Plasmodium* sporozoites in Andor Spinning Disk Confocal Microscopy (Andor Technology).

4.2.10 Invasion/Wounding Assay (Cell Traversal)

Human hepatoma cells (HepG2; kindly provided from Robert Menard, Institut Pasteur, France) were cultured (4x10^4/well; 200μL in 96-well plates) in DMEM (GlutaMAXTM, 10% FBS, 100U/mL penicillin/streptomycin; Life Technologies) (37°C; 5%CO_2; 2 days). *Pb*A$^{Hsp70\text{-}GFP}$ sporozoites (19-25 days post-infection) were pre-incubated with anti-a-gal or isotype matched control anti-DNP mAbs (150μg/mL in 20-50μL; 60min; 4°C). Plasma from C57BL/6 mice (1:5 in 20-50μL 0.1% gelatin in VB++ buffer; Lonza) was added (60min; 37°C) as a source of complement and sporozoites were immediately transferred onto HepG2 cells at a 1:4 parasite/cell ratio. Co-

cultures were incubated (120min; 37°C) with Tetramethylrhodamine-Dextran (10,000MW, 1:1; 2mg/mL; Molecular Probes®), washed (2X; PBS) and trypsinized (30-50µL; 0.05% Trypsin-EDTA, Phenol Red (Gibco®). Wounded (%) and parasite-invaded (%) cells was determined by flow cytometry analysis (FACScan, BD Biosciences), gating on FL1 (GFP; invasion) and FL2 (Dextran-Red; wounding). Sporozoite maturation was determined by quantifying the number of EEFs per field and EEF area after 40h co-culture in 15 µ-Slide 8 well (ibiTreat; IBIDI; Germany) using fluorescence microscopy (Screening Microscopy; Nikon Eclipse TE2000-S). Images were obtained at 20X magnification. Pictures were analyzed using Image J software (NIH).

4.2.11 Statistical analysis

All tests were performed using the GraphPad software V6.0 (Prism) and statistical significance was determined by repeated measures one-way ANOVA, when data assumed Gaussian distribution after *arcsin* transformation, and followed by Tukey's multiple comparison post-test. Survival curves were plotted using Kaplan-Meier plot, and significant differences between groups were determined with the Log-Rank (Mantel-Cox) test. A p value equal to or below 0.05 was considered statistically significant.

4.3 Results

4.3.1 Generation of *α1,3Gt*$^{-/-}$*C3*$^{-/-}$ mice

α1,3Gt$^{-/-}$ mice were crossed with mice lacking complement C3 (*C3*$^{-/-}$ mice) and C3 gene deletion was confirmed by PCR **(Figure 4.3a)**. *α1,3Gt*$^{-/-}$*C3*$^{-/-}$ mice are viable and fertile. Depletion of soluble C3 was confirmed by ELISA in mouse plasma samples **(Figure 4.3b)**. Complement C3 in normal mouse plasma ranges from 0.18-1.26 mg/mL with an average concentration of 1 mg/mL[28] that is comparable with *α1,3Gt*$^{-/-}$ mice **(Figure**

4.3b). In *α1,3Gt*$^{-/-}$*C3*$^{-/-}$ mice complement C3 concentration was reduced to zero, as expected. Anti-α-gal IgM titers after immunization with rRBCM are equal in *α1,3Gt*$^{-/-}$ and *α1,3Gt*$^{-/-}$*C3*$^{-/-}$ mice **(Figure 4.3c)**. However, anti-α-gal IgG Abs in *α1,3Gt*$^{-/-}$*C3*$^{-/-}$ mice were relatively but not significantly lower than in *α1,3Gt*$^{-/-}$ mice and showed bigger variation among the serum samples **(Figure 4.3c)**.

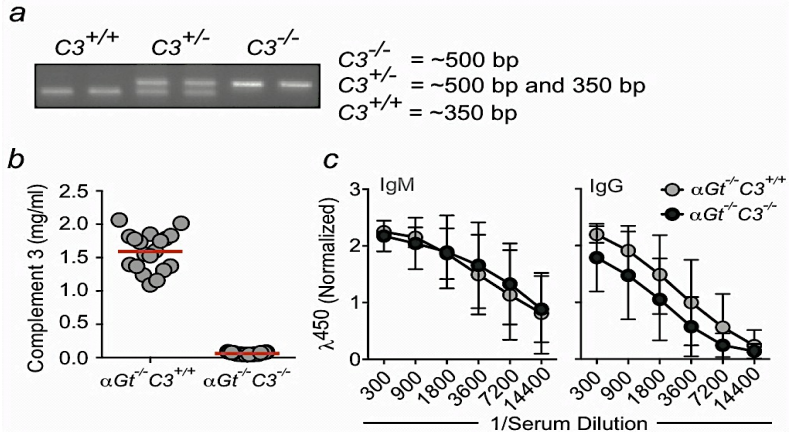

Figure 4.3 C3 concentration and anti-α-gal antibodies levels in *α1,3Gt*$^{-/-}$*C3*$^{+/+}$ and *α1,3Gt*$^{-/-}$*C3*$^{-/-}$ mice. a) Complement C3 gene deletion was determined by PCR detecting the absence of the WT C3 allele PCR product (lower band) and presence of the mutated allele (upper band). **b)** Concentration of complement C3 protein in plasma of *α1,3Gt*$^{-/-}$*C3*$^{+/-}$ and *α1,3Gt*$^{-/-}$*C3*$^{-/-}$ mice (n=19-21 mice per group) was determined by C3 ELISA. **c)** Antibody levels of *α1,3Gt*$^{-/-}$*C3*$^{+/+}$ and *α1,3Gt*$^{-/-}$*C3*$^{-/-}$ mice (n=13-20 mice per group) after immunization. Error bars indicate standard deviation.

4.3.2 Protective effect driven by anti-α-gal Abs is complement dependent

We asked whether the protective effect exerted by anti-α-gal Abs was mediated via a mechanism involving complement activation[24,29]. Passive transfer of anti-α-gal IgM Abs and anti-α-gal IgG2b mAb to *α1,3Gt*$^{-/-}$*C3*$^{-/-}$ mice, which lack C3 and cannot activate the complement cascade, failed to confer protection against *Pb*A transmission *vs.* control *α1,3Gt*$^{-/-}$*C3*$^{-/-}$ mice

(Figure 4.4a and 4.4b). Passive transfer of anti-α-gal IgG3 mAb to *α1,3Gt*$^{-/-}$ *C3*$^{-/-}$ mice conferred negligible protection *vs.* control *α1,3Gt*$^{-/-}$*C3*$^{-/-}$ mice **(Figure 4.4c)**. This shows that the protective effect of IgM and IgG2b but not that of IgG3 anti-α-gal Abs acts via a mechanism that is strictly complement-dependent. Once infected, mice developed the same level of blood stage of infection and succumbed to ECM, regardless of genotype or immunization.

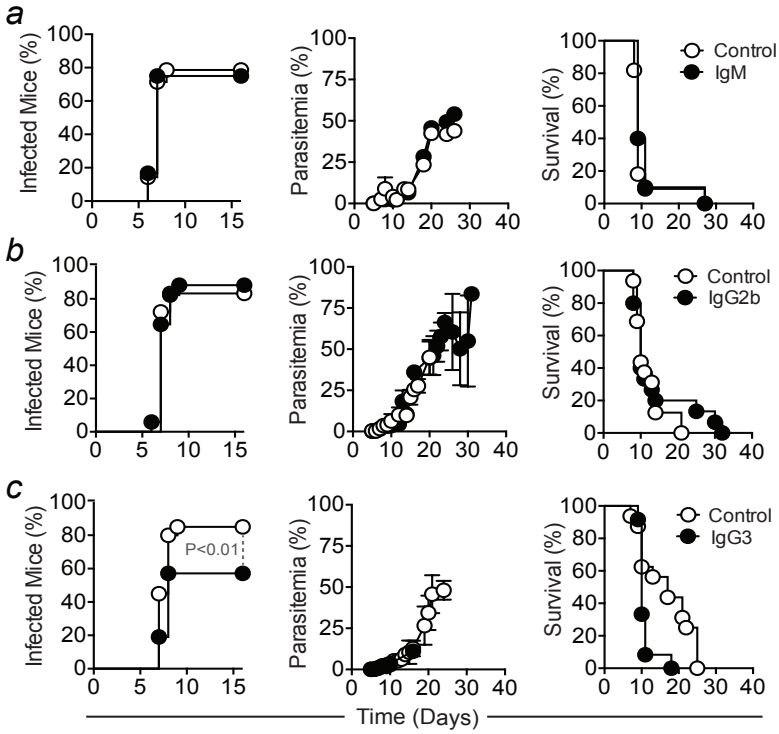

Figure 4.4 Protective effect of anti-α-gal IgM, IgG2b, but not IgG3 Abs occurs via complement activation mechanism. Incidence of blood stage of infection (%), parasitemia (%) and survival (%) in *α1,3Gt*$^{-/-}$*C3*$^{-/-}$ mice receiving anti-α-gal **a)** IgM, **b)** IgG2b and **c)** IgG3 Abs *vs.* controls (Control) not receiving Abs, exposed to *Pb*A$^{EEF1a\text{-}GFP}$ or *Pb*A$^{Hsp70\text{-}GFP}$ infected mosquitoes. Data was pooled from 2-4 independent experiments (n=9-21 mice per group). Error bars indicate standard deviation. Significance between anti-α-gal Abs receiving and controls groups (a-c) were determined by log rank (Mantel-Cox) test.

4.3.3 Protective effect of anti-α-gal Abs involves PMN cells

We asked whether the protective effect of anti-α-gal Abs involves PMN cells. Depletion of PMN cells was performed via the administration of anti-Ly-6G (Gr-1) mAb and assessed by flow cytometry using anti-Gr1 and anti-CD11b Abs **(Figure 4.5)**. Non-depleted control *α1,3Gt*$^{-/-}$ mice have around 5% PMN cells **(Figure 4.5a)** whereas anti-Gr1 administered *α1,3Gt*$^{-/-}$ mice have no or very few PMN cells in the blood circulation **(Figure 4.5b).**

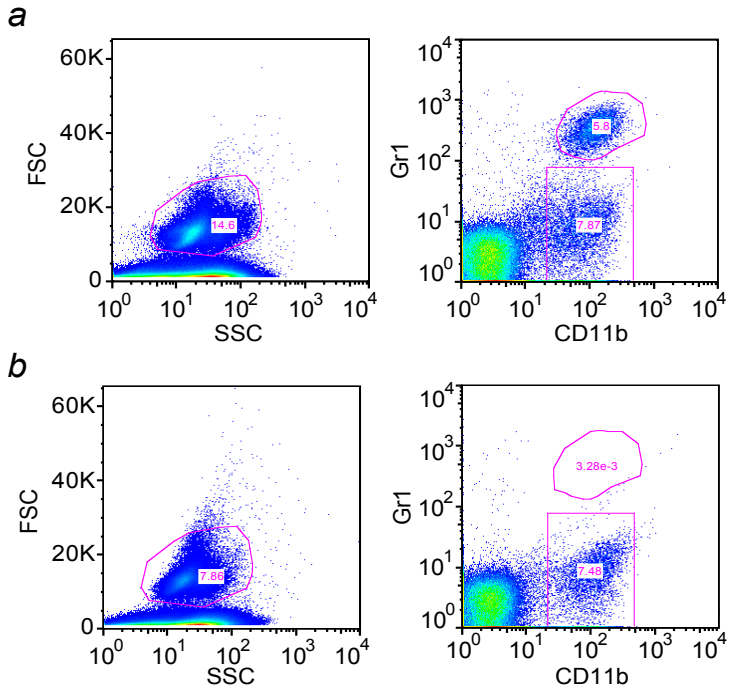

Figure 4.5 Assessment of PMN depletion in mice. Gating strategy for detection of PMN by flow cytometry in control **a)** and **b)** anti-Ly-6G (Gr-1) mAb administered *α1,3Gt*$^{-/-}$ mice blood. Data was representative of 3-4 independent experiments.

Passive transfer of anti-α-gal IgG2b Abs to *α1,3Gt*$^{-/-}$ mice depleted from PMN cells by the administration of anti-Ly-6G (anti-Gr-1) mAb failed to confer protection against *Pb*A infection **(Figure 4.6b)**. In contrast, passive transfer of anti-α-gal IgM Abs and anti-α-gal IgG3 mAb to PMN cells depleted *α1,3Gt*$^{-/-}$ mice conferred a protection against *Pb*A infection **(Figure**

4.6a and 4.6c). This suggests that the protective effect of anti-α-gal IgG2b but not of IgM or IgG3 Abs is dependent on PMN cells. Depletion of PMN cells did not interfere *per se* with the incidence of *Plasmodium* infection[30] while preventing the onset of cerebral malaria **(Figure 4.6)**, consistent with previous findings[31].

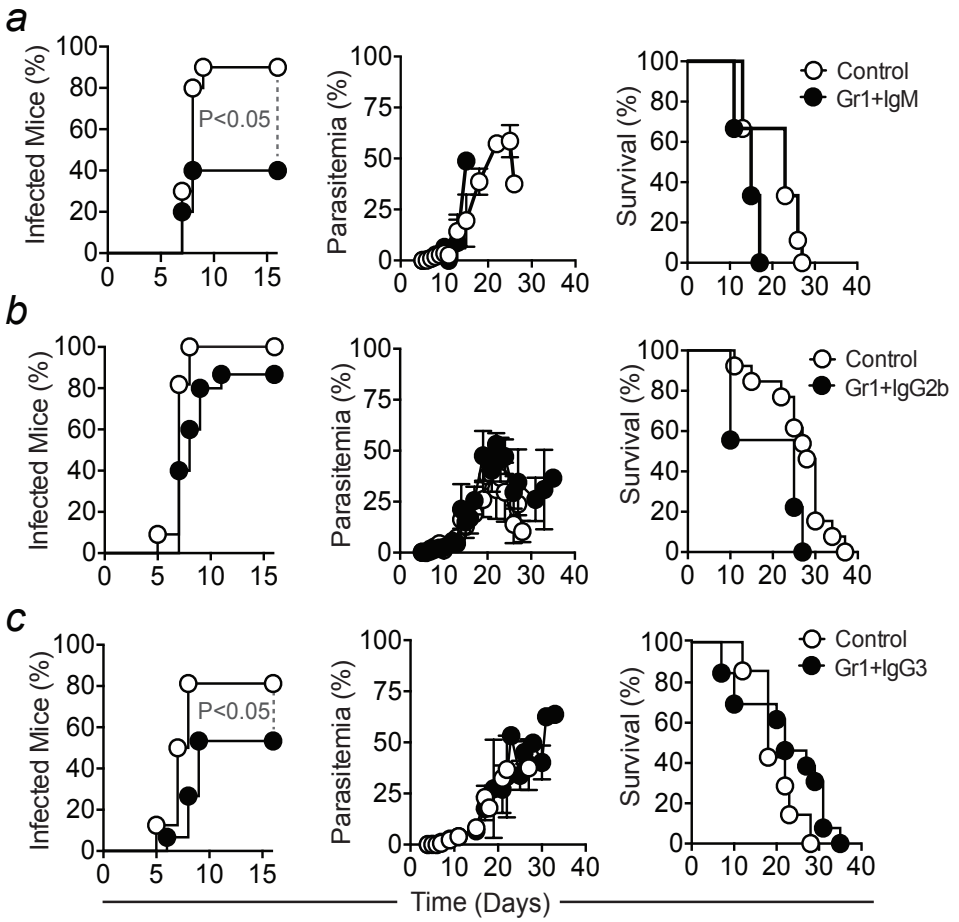

Figure 4.6 Protective effect of anti-α-gal Ig2b Ab, but not IgM and IgG3 Abs, is PMN cells dependent. Incidence of blood stage of infection (%), parasitemia (%) and survival (%) in PMN cells depleted *α1,3Gt*$^{-/-}$ mice receiving anti-α-gal **a)** IgM, **b)** IgG2b and **c)** IgG3 Abs *vs.* controls (Control) not receiving Abs, exposed to *Pb*A$^{EEF1a\text{-}GFP}$ or *Pb*A$^{Hsp70\text{-}GFP}$ infected mosquitoes. Data was pooled from 2-4 independent experiments (n=9-21 mice per group). Error bars indicate standard deviation. Significance between anti-α-gal Abs receiving and control groups (a-c) were determined by log rank (Mantel-Cox) test.

4.3.4 Anti-α-gal Abs are cytotoxic to *Plasmodium* sporozoites

Once bound to the surface of *Plasmodium* sporozoites, anti-α-gal IgM, IgG2b and IgG3 mAbs, activated the classical pathway of complement[24,29], as assessed by C3 deposition **(Figure 4.7b)**. Anti-α-gal IgG1 or IgG2a mAbs failed to activate complement **(Figure 4.7b)**. Complement activation was not observed in the absence of anti-α-gal Abs **(Figure 4.7b)**, showing that the alternative and lectin pathways are not activated by sporozoites.

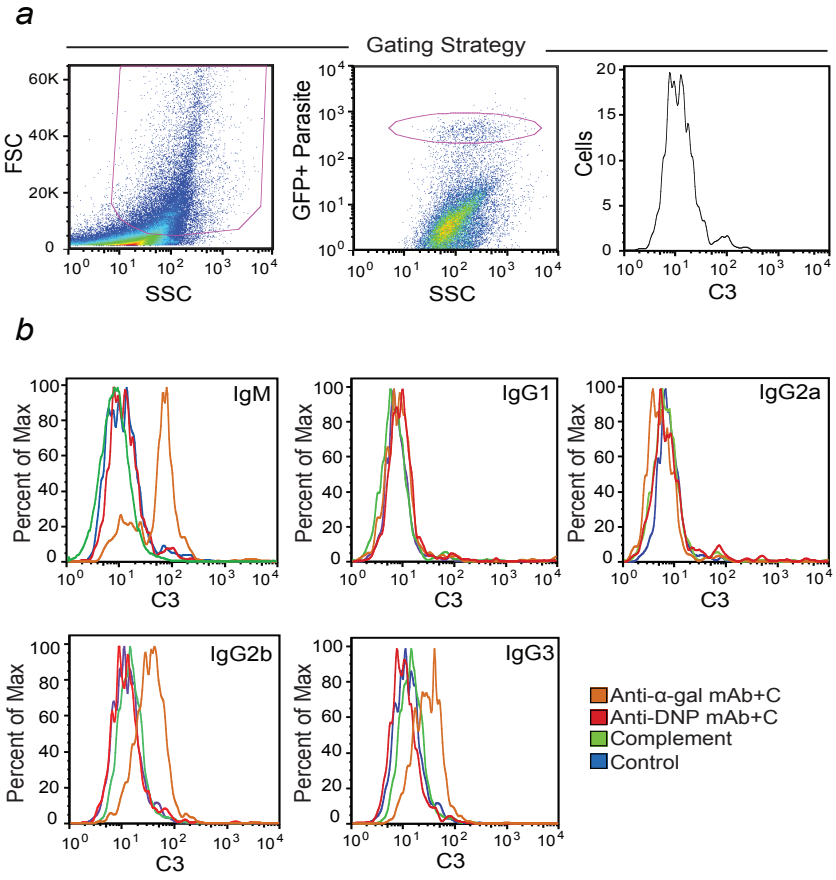

Figure 4.7 Anti-α-gal antibody mediated C3 deposition on *Plasmodium* sporozoites. a) Gating strategy for flow cytometry of GFP^{+} *Pb*A$^{Hsp70\text{-}GFP}$ sporozoites. **b)** Detection of C3 deposition on the surface of *Pb*A$^{Hsp70\text{-}GFP}$ sporozoites, gated as indicated in (a). *Pb*A$^{Hsp70\text{-}GFP}$ sporozoites were incubated *in vitro* with anti-α-gal or control anti-DNP mAbs plus mouse complement (C). Control *Pb*A$^{Hsp70\text{-}GFP}$ sporozoites were incubated with vehicle. C3 was detected using an anti-C3/C3b/iC3b mAb. Histograms are representative of 3 experiments.

Complement activation by anti-α-gal IgM, IgG2b or IgG3 mAb is cytotoxic to sporozoites *in vitro*, as assessed by quantification of GFP^{+} *Pb*$A^{Hsp70\text{-}GFP}$ sporozoites before and after the treatments **(Figure 4.8a)**. Anti-α-gal IgG1 and IgG2a mAbs, which did not activate complement when bound to *Plasmodium* sporozoites, were not cytotoxic **(Figure 4.8a)**. The cytotoxic effect of anti-α-gal IgM, IgG2b and IgG3 was similar when using mouse or rabbit complement, but was strictly dependent on the presence of complement **(Figure 4.8a)**. Moreover, isotype matched Abs against dinitrophenol were not cytotoxic to *Plasmodium* sporozoites **(Figure 4.8a)**.

4.3.5 Anti-α-gal Abs inhibit hepatocytes infection by *Plasmodium*

We asked whether anti-α-gal mAbs inhibit *Pb*A sporozoites migration through hepatocytes (wounding) and/or hepatocyte invasion[32]. In the presence of complement, anti-α-gal IgM, IgG2b and IgG3 Abs, albeit less pronounced, inhibited hepatocyte transmigration and invasion **(Figure 4.8b)**, as assessed *in vitro* for *Pb*$A^{Hsp70\text{-}GFP}$ sporozoites. This inhibitory effect was not observed when using anti-α-gal IgG1 or IgG2a Abs or isotype/subclass matched control anti-DNP Abs **(Figure 4.8b)**. These observations suggest that the recognition of the α-gal glycan by anti-α-gal mAbs on the surface of *Pb*A sporozoites inhibits hepatocyte infection via a complement dependent mechanism.

Lastly, we assessed whether anti-α-gal mAbs inhibit the development of EEFs of *Plasmodium* sporozoites. Complement activation by anti-α-gal IgM, IgG2b and IgG3 Abs reduced the number of EEFs **(Figure 4.9a)** as well as the average EEF size **(Figure 4.9b and 4.9c)** formed *in vitro* by *Pb*$A^{Hsp70\text{-}GFP}$ sporozoites. Anti-α-gal IgG1 Abs did not show this inhibitory effect, while anti-α-gal IgG2a Abs did not reduce the number of EEFs **(Figure 4.9a)** but had a residual inhibitory effect on EEF size **(Figure 4.9b and 4.9c)**.

Isotype/subclass matched control anti-DNP Abs did not modulate EEF numbers **(Figure 4.9a)** or average size **(Figure 4.9b and 4.9c)**, demonstrating that the anti-α-gal Abs are capable of activating complement to limit *Plasmodium* development in the liver.

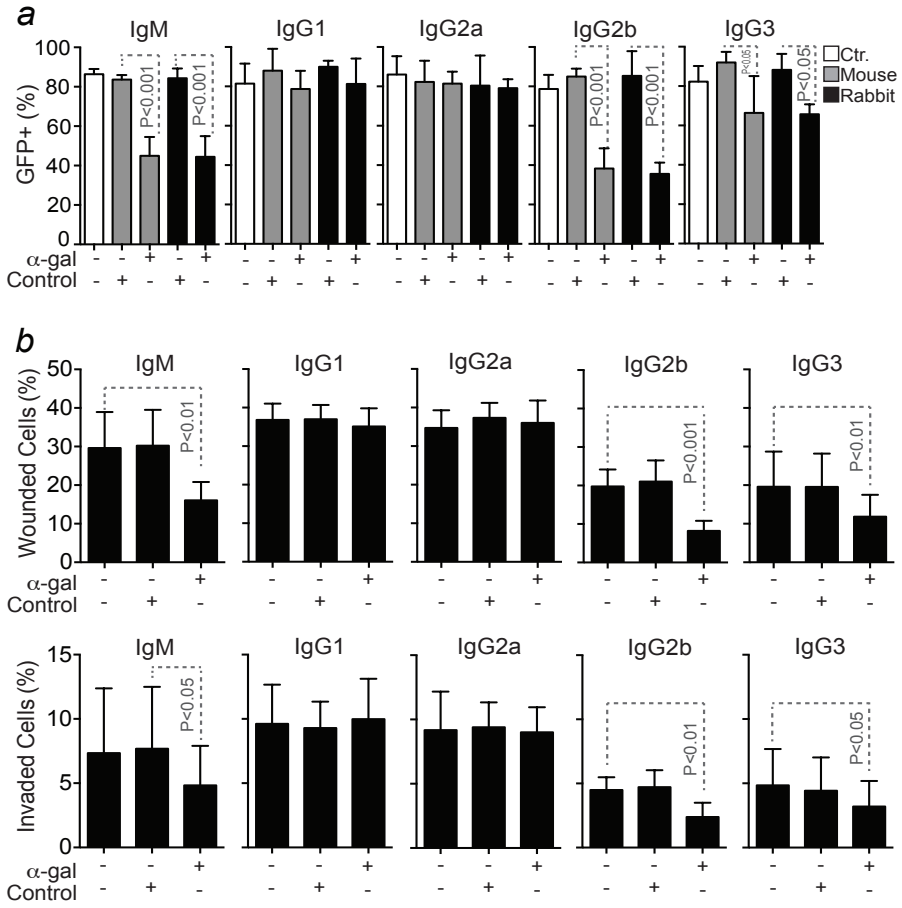

Figure 4.8 Protective effect of anti-α-gal mAbs against hepatocyte infection. a) Mean (%) of viable GFP^{+} *Pb*A$^{Hsp70\text{-}GFP}$ sporozoites incubated with anti-α-gal (α-gal) or anti-DNP mAbs (Control) plus mouse or rabbit complement. **b)** Mean (%) of HepG2 cells wounded (Dextran-Red^{+}) or invaded (GFP^{+}) by *Pb*A$^{Hsp70\text{-}GFP}$ incubated with anti-α-gal or anti-DNP mAbs (Control) plus mouse complement. Data in (a) and (b) were pooled from 3-4 and 6 independent experiments. Graphs show mean values and error bars indicate standard deviation. Differences between anti-α-gal Abs treated groups and control groups in (a and b) were analyzed by repeated measures ANOVA followed by Tukey's multiple comparison post-test.

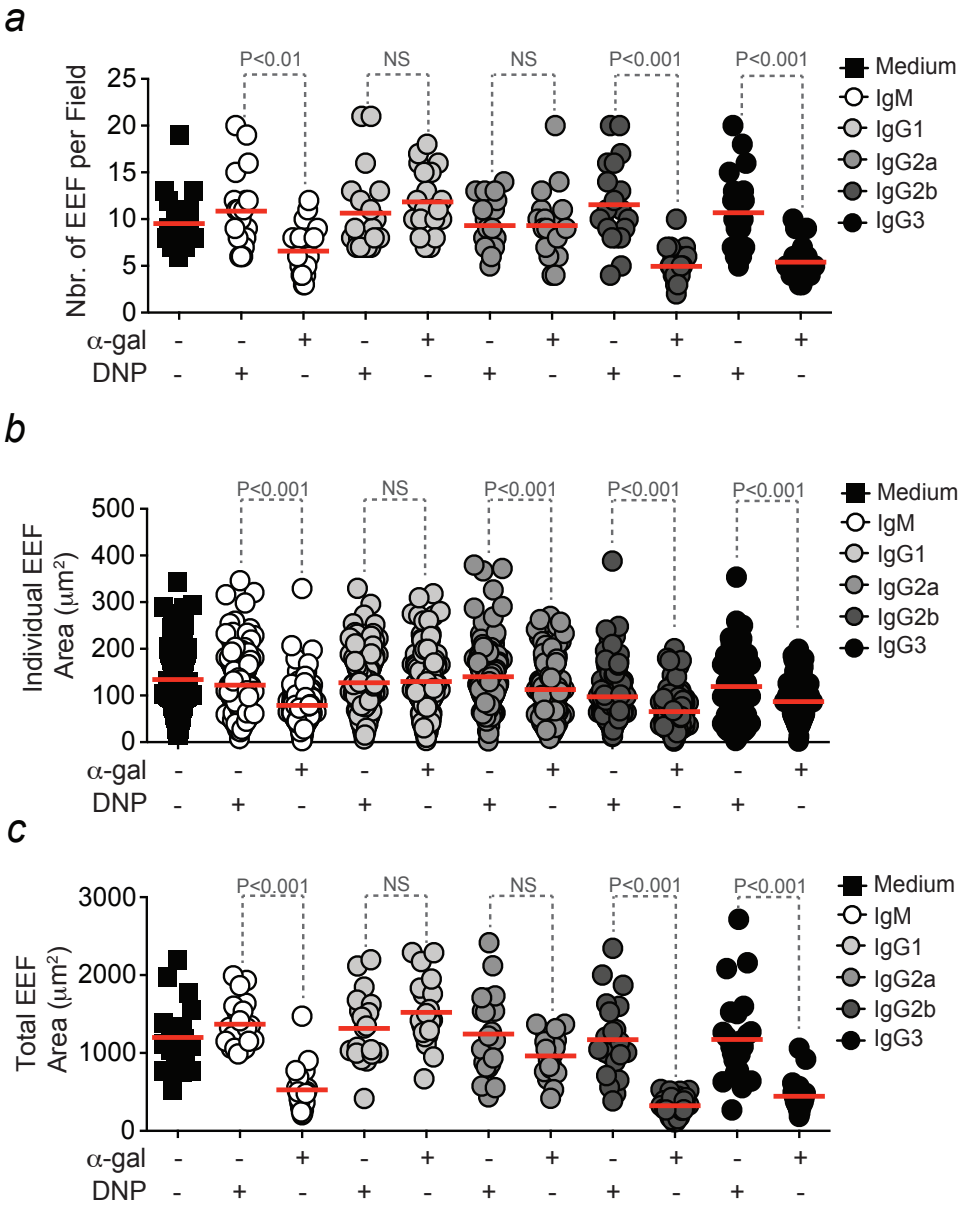

Figure 4.9 Protective effect of anti-α-gal Abs against *Plasmodium* maturation in hepatocytes. a) Number of EEF per field (dots) (20-23 fields). **b)** Area of individual EEF (dots) (n=111-256 EEFs counted in 20-23 fields). **c)** Total area of EEF (dots) per field (20-23 fields). Data is representative of 2 independent experiments with the same trend. All in HepG2 cells after *Pb*A$^{Hsp70\text{-}GFP}$ sporozoites exposure to anti-α-gal or anti-DNP mAbs in the presence of mouse complement.

4.4 Chapter Discussions and Conclusion

In this chapter, we examined whether the complement systems can be activated via anti-α-gal Abs once these recognize *Plasmodium* sporozoites, as assessed by C3 deposition on *Plasmodium* sporozoite surface using flow cytometry analysis **(Figure 4.7 and 4.8)**. We found that this is the case and complement system is critical to support the protective role of anti-α-gal Abs against *Plasmodium* infection **(Figure 4.4)**.

Once bound to the surface of *Plasmodium* sporozoites anti-α-gal IgM, IgG2b and IgG3 Abs induced the deposition of C3b while this was not the case for anti-α-gal IgG1, IgG2a mAbs and control samples **(Figure 4.7b)**. Despite the detectable ability of anti-α-gal IgG3 Abs to induce C3 deposition, complement-mediated lysis of *Plasmodium* sporozoites was less pronounced, as compared to anti-α-gal IgM and IgG2b Abs **(Figure 4.8a)**. Complement-mediated lysis was not observed for anti-α-gal IgG1 and IgG2a. Moreover, *in vivo* experiments performed by administrating the anti-α-gal IgG2b and IgG3 Abs in $\alpha 1,3Gt^{-/-}C3^{+/+}$ mice reflected the same pattern. This data argues that complement activation is strictly required to sustain the protective effect of anti-α-gal IgM and IgG2b Abs but not that of anti-α-gal IgG3 Abs **(Figure 4.4)**.

The chemoattractant role of C3a and C5a promote the biologic activity of anti-α-gal IgG2b[33] and IgG3[34] Abs. In keeping with this notion, the protective effect of anti-α-gal IgG2b is lost in the absence of PMN cells, while PMN cells are not strictly required to sustain the protective effect of anti-α-gal IgM and IgG3 Abs **(Figure 4.5)**. It is well established that binding of different IgG subclasses to FcγR varies significantly[35,36] and that there is a synergistic functional interaction between FcγR-mediated and complement mediated effects. Anti-α-gal IgG3 appears to act predominately via

complement activation while anti-α-gal IgG1, IgG2a and IgG2b Abs acting via both complement activation and presumably FcγR[24]. In the absence of the complement component C3, there is a compensatory mechanism in which thrombin can act as a C5 convertase, generating C5a and activating the complement machinery[37]. This may also help explaining the partial dependency of IgG3 anti-α-gal on C3 for its protective effect against *Plasmodium* infection. Other yet undefined complex regulatory and compensatory mechanisms may also be operational, such as those involving the interactions between FcγR, C5a and thrombin, where C5aR that can promote inflammatory responses and leukocyte chemotaxis. The role of FcγR in protection mediated by anti-α-gal Abs against *Plasmodium* infection needs to be further investigated.

Anti-α-gal IgM, IgG2b and IgG3 Abs suppress *Plasmodium* sporozoite cell traversal activity thus preventing the progression of infection from the dermis into the liver[38]. Activation of complement by anti-α-gal IgM, IgG2b and IgG3 Abs also has an inhibitory effect on sporozoite migration through hepatocytes that is less pronounced for anti-α-gal IgG3 antibody **(Figure 4.8b)**. Anti-α-gal IgM and IgG2b Abs reduced hepatocyte wounding and invasion profoundly, suggesting that complement activation by anti-α-gal Abs damages the surviving sporozoites. These appear to trigger a response in which sporozoites quickly invade hepatocytes without their usual migratory pattern. Presumably, *Plasmodium* sporozoites are damaged by the anti-α-gal Abs, their maturation inside of hepatocytes is also impaired **(Figure 4.9)**.

The positive feedback amplification loop occurring between PMN cells and complement system led us to test the protective role of anti-α-gal Abs in PMN cells deficient conditions. We found that in the absence of PMN cells

the protective effect of anti-α-gal IgG2b Abs was lost whereas the protective effect of anti-α-gal IgM and IgG3 Abs was totally or partially preserved. The interaction between anti-α-gal Abs and PMN leading to protection against *Plasmodium* infection needs to be further characterized.

Contributions

The author of this dissertation performed all experiments described in this chapter. Susana Ramos helped with the detection of C3 deposition on *Plasmodium* sporozoites using flow cytometry.

Acknowledgements

Thanks to Susana Ramos and Birte Blankenhaus for feedback on this chapter of the thesis, Joana Tavares, Rogerio Amino and Robert Ménard (Institute Pasteur, France) for teaching me *in vitro* assays, regarding hepatocyte invasion, past and present member of Flow Cytometry Unit (Instituto Gulbenkian de Ciência, Portugal) for technical support, Rita Carlos for discussions on *in vitro* assay settings. We are indebted to Ana Regelado (Antibody Service, IGC) for producing us anti-Gr1 mAbs.

References

1. Medzhitov, R. & Janeway, C. Decoding the patterns of self and nonself by the innate immune system. *Science (New York, N.Y.)* **296**, 298-300 (2002).
2. Medzhitov, R. & Janeway, C.A., Jr. Innate immunity: the virtues of a nonclonal system of recognition. *Cell* **91**, 295-298 (1997).
3. Medzhitov, R. & Janeway, C.A., Jr. Innate immunity: impact on the adaptive immune response. *Current opinion in immunology* **9**, 4-9 (1997).
4. Dunkelberger, J.R. & Song, W.C. Complement and its role in innate and adaptive immune responses. *Cell research* **20**, 34-50 (2010).

5. Walport, M.J. Complement. First of two parts. *The New England journal of medicine* **344**, 1058-1066 (2001).
6. Walport, M.J. Complement. Second of two parts. *The New England journal of medicine* **344**, 1140-1144 (2001).
7. Noris, M., Mescia, F. & Remuzzi, G. STEC-HUS, atypical HUS and TTP are all diseases of complement activation. *Nature reviews. Nephrology* **8**, 622-633 (2012).
8. Gaboriaud, C., *et al.* The crystal structure of the globular head of complement protein C1q provides a basis for its versatile recognition properties. *The Journal of biological chemistry* **278**, 46974-46982 (2003).
9. Budayova-Spano, M., *et al.* The crystal structure of the zymogen catalytic domain of complement protease C1r reveals that a disruptive mechanical stress is required to trigger activation of the C1 complex. *The EMBO journal* **21**, 231-239 (2002).
10. Collard, C.D., *et al.* Complement activation after oxidative stress: role of the lectin complement pathway. *The American journal of pathology* **156**, 1549-1556 (2000).
11. Brouwer, N., *et al.* Mannan-binding lectin (MBL)-mediated opsonization is enhanced by the alternative pathway amplification loop. *Molecular immunology* **43**, 2051-2060 (2006).
12. Degn, S.E. & Thiel, S. Humoral pattern recognition and the complement system. *Scandinavian journal of immunology* **78**, 181-193 (2013).
13. Crockard, A.D., *et al.* Markers of inflammatory activation: upregulation of complement receptors CR1 and CR3 on synovial fluid neutrophils from patients with inflammatory joint disease. *Clinical immunology and immunopathology* **65**, 135-142 (1992).
14. Camous, L., *et al.* Complement alternative pathway acts as a positive feedback amplification of neutrophil activation. *Blood* **117**, 1340-1349 (2011).

15. Haas, P.J. & van Strijp, J. Anaphylatoxins: their role in bacterial infection and inflammation. *Immunologic research* **37**, 161-175 (2007).
16. Schreiber, A., *et al.* C5a receptor mediates neutrophil activation and ANCA-induced glomerulonephritis. *Journal of the American Society of Nephrology : JASN* **20**, 289-298 (2009).
17. Asberg, A.E., Mollnes, T.E. & Videm, V. Complement activation by neutrophil granulocytes. *Scandinavian journal of immunology* **67**, 354-361 (2008).
18. Trouw, L.A., Blom, A.M. & Gasque, P. Role of complement and complement regulators in the removal of apoptotic cells. *Molecular immunology* **45**, 1199-1207 (2008).
19. Bongoni, A.K., *et al.* Activation of the lectin pathway of complement in pig-to-human xenotransplantation models. *Transplantation* **96**, 791-799 (2013).
20. Schneider, M.K. & Seebach, J.D. Xenotransplantation literature update, November-December 2013. *Xenotransplantation* (2014).
21. Jager, U., Takeuchi, Y. & Porter, C. Induction of complement attack on human cells by Gal(alpha1,3)Gal xenoantigen expression as a gene therapy approach to cancer. *Gene therapy* **6**, 1073-1083 (1999).
22. Xu, H., *et al.* The in vitro and in vivo effects of anti-galactose antibodies on endothelial cell activation and xenograft rejection. *J Immunol* **170**, 1531-1539 (2003).
23. Yin, D., *et al.* Cutting Edge: NK cells mediate IgG1-dependent hyperacute rejection of xenografts. *J Immunol* **172**, 7235-7238 (2004).
24. Ding, J.W., *et al.* Hyperacute rejection by anti-Gal IgG1, IgG2a, and IgG2b is dependent on complement and Fc-gamma receptors. *J Immunol* **180**, 261-268 (2008).
25. Wessels, M.R., *et al.* Studies of group B streptococcal infection in mice deficient in complement component C3 or C4 demonstrate an essential role for complement in both innate and acquired immunity. *Proceedings*

of the National Academy of Sciences of the United States of America **92**, 11490-11494 (1995).

26. Tepper, R.I., Coffman, R.L. & Leder, P. An eosinophil-dependent mechanism for the antitumor effect of interleukin-4. *Science* **257**, 548-551 (1992).
27. Tsiganov, E.N., *et al.* Gr-1dimCD11b+ Immature Myeloid-Derived Suppressor Cells but Not Neutrophils Are Markers of Lethal Tuberculosis Infection in Mice. *J Immunol* **192**, 4718-4727 (2014).
28. Cole, J.G., Fulcher, N.B. & Jerse, A.E. Opacity proteins increase Neisseria gonorrhoeae fitness in the female genital tract due to a factor under ovarian control. *Infection and immunity* **78**, 1629-1641 (2010).
29. Miyatake, T., *et al.* Complement-fixing elicited antibodies are a major component in the pathogenesis of xenograft rejection. *Journal of Immunology* **160**, 4114-4123 (1998).
30. Porcherie, A., *et al.* Critical role of the neutrophil-associated high-affinity receptor for IgE in the pathogenesis of experimental cerebral malaria. *The Journal of experimental medicine* **208**, 2225-2236 (2011).
31. Chen, L., Zhang, Z. & Sendo, F. Neutrophils play a critical role in the pathogenesis of experimental cerebral malaria. *Clinical and experimental immunology* **120**, 125-133 (2000).
32. Mota, M.M., *et al.* Migration of Plasmodium sporozoites through cells before infection. *Science* **291**, 141-144 (2001).
33. Bruhns, P. Properties of mouse and human IgG receptors and their contribution to disease models. *Blood* **119**, 5640-5649 (2012).
34. Gavin, A.L., Barnes, N., Dijstelbloem, H.M. & Hogarth, P.M. Identification of the mouse IgG3 receptor: implications for antibody effector function at the interface between innate and adaptive immunity. *J Immunol* **160**, 20-23 (1998).
35. Kinet, J.P. Antibody-cell interactions: Fc receptors. *Cell* **57**, 351-354 (1989).

36. Ravetch, J.V. & Kinet, J.P. Fc receptors. *Annual review of immunology* **9**, 457-492 (1991).
37. Huber-Lang, M., *et al.* Generation of C5a in the absence of C3: a new complement activation pathway. *Nature medicine* **12**, 682-687 (2006).
38. Amino, R., *et al.* Host cell traversal is important for progression of the malaria parasite through the dermis to the liver. *Cell host & microbe* **3**, 88-96 (2008).

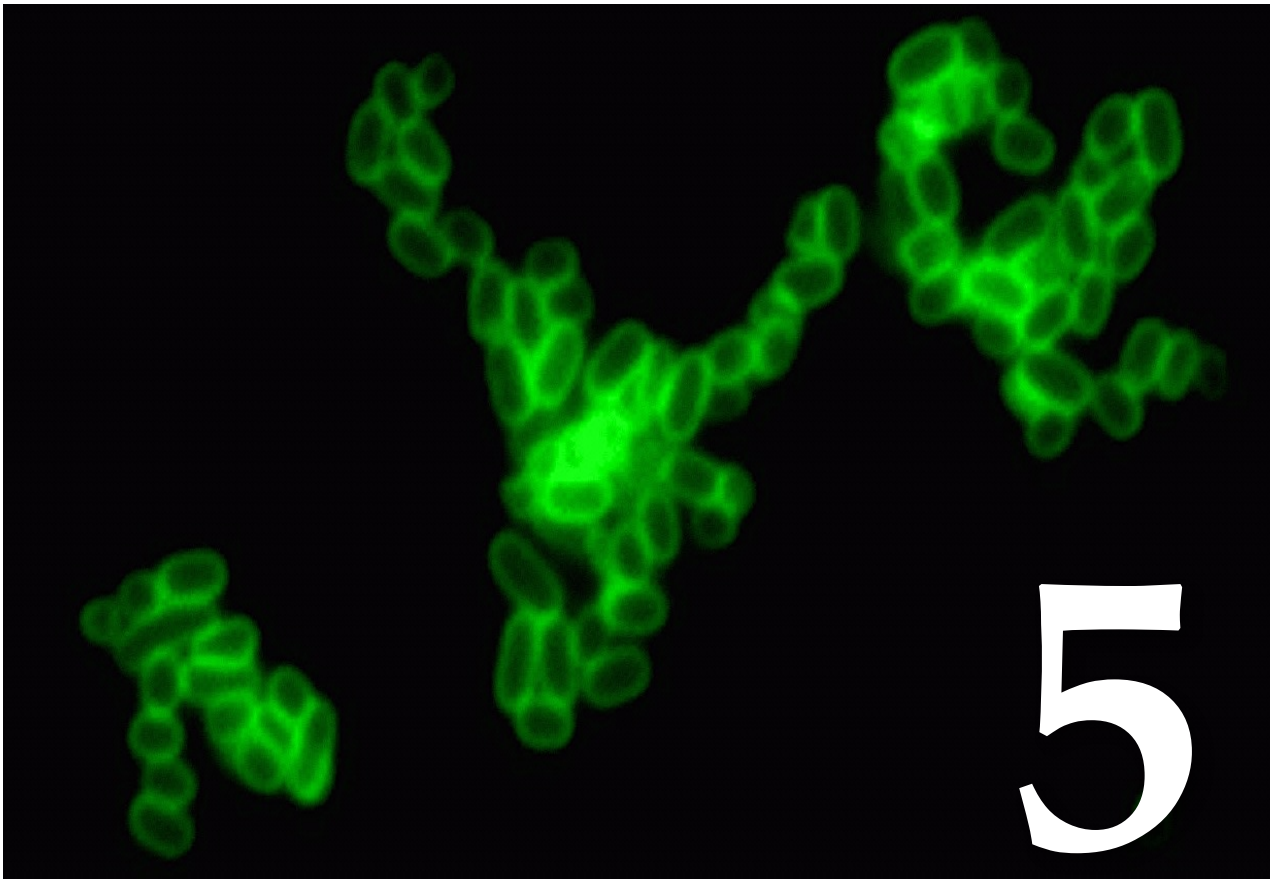

5

Gut Microbiota vs. *Plasmodium*

Abstract

The human anti-glycan Ab repertoire was probably tailored through evolution via natural selective pressure, as illustrated for the inactivation of the *α1,3GT* gene, which suppressed the expression of the α-gal in anthropoid primates and allowed for the production of anti-α-gal NAbs. As for other NAbs, anti-α-gal Abs are found at high levels in the absence of traceable immunization. However, their production may result from ongoing antigenic exposure by specific components of the intestinal microbiota that express α-gal. Here, we tested this hypothesis specifically and asked whether a specific bacterial component of the gut microbiota elicits a protective anti-α-gal Ab response against *Plasmodium* infection. We found that gut colonization as well as systemic infection by an *E. coli* strain expressing α-gal induces the production anti-α-gal Abs, which are protective against *Plasmodium* infection. This chapter demonstrates specific gut pathobiont expressing α-gal can recapitulate the normal etiology of the human anti-α-gal Ab response and be associated with protection against malaria.

5.1 Introduction

Individuals are in continuous interactions with microorganisms starting immediately at birth and throughout life. This results from the colonization of specific niches of the human body by complex communities of microorganisms that contribute crucially to many host physiologic functions. Colonization by microorganisms is particularly prevalent barrier tissues, such as skin, oral cavity, intestinal, respiratory and urogenital tracts[1]. These resident microorganisms constitute the microflora of the host and are called the microbiota. The total number of microorganisms dwelling in human body is estimated at 100 trillion cells, that is 10 times more than the number of host cells. The microbiota contains about 3 million genes, that is, 100 times more than host human genes[2]. The gut microbiota is distributed physically along the gastrointestinal (GI) tract with preferential regions being colonized by specific bacterial strains such as the stomach, e.g., *Lactobacilli*, or colon, e.g. *E.coli*[3]. These have several important roles, which cannot be executed by the host, e.g., breaking down plant carbohydrates or glycans present in mother's milk. While the host establishes a mutualistic interaction with its gut microbiota, in extreme conditions, this interaction can be reverted into a pathogenic relationship reducing host fitness, i.e. disease[3]. The variety of microorganisms in gut is associated with the different type of response by host immune system.

The immune system is extremely effective in preventing the access of gut pathogens to the host inner milieu while providing a delicate balance to host–gut microbiota relationship[5]. Lymphocytes elicit specific responses that are critical to the establishment and maintenance of the microbiota[5]. In healthy individual, mucosal surfaces are the initial site of interactions with microbial population, providing a first line of defense exerted by highly specialized cellular and molecular components such as epithelial cells and gut-associated lymphoid tissues (GALT). These mucosal surfaces can sense specific microbial components and generate anti-microbial peptides as well

as IgA Abs, which are secreted into the lumen where they impact on the composition and biologic activity of specific components of the microbiota **(Figure 5.1)**[4,6,7]. Gut microbiota can play crucial roles in promoting B cell development in local lymph nodes called the Payer's patches and modulate of T or B-cell-mediated immune responses, either locally or systemically **(Figure 5.1)**[8].

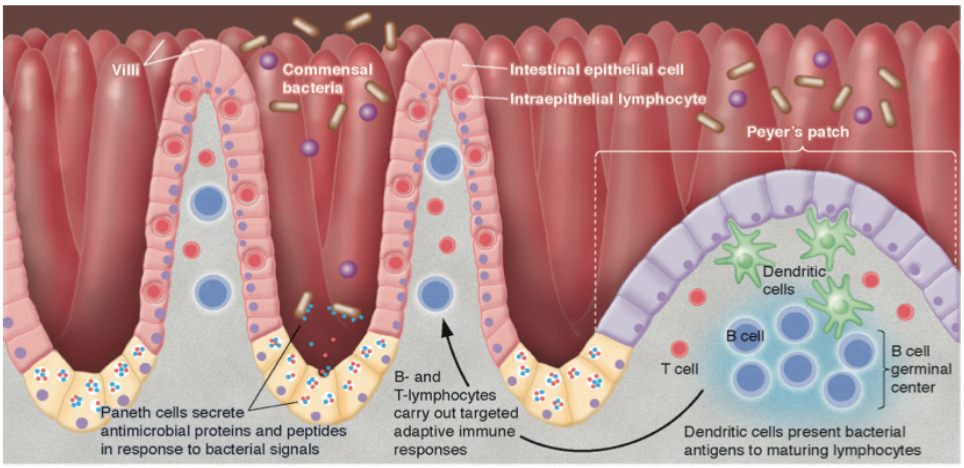

Figure 5.1 Immune response in intestine and role of gut flora. Commensal bacteria shape the immune response in intestine via secretion anti-microbial peptide by Paneth cells and antigen presentation by dendritic cells to lymphocytes to produce Abs. Adapted from[4].

Generally, T and B cell-mediated responses generate a repertoire of Abs that reflects the history of immune response to pathogens and prepare the host to respond to upcoming infections. However, under healthy conditions, where no history of a pathogen was recorded, natural antibodies (NAbs) are apparently produced without prior immunization[9]. NAbs are thought to produced by often auto-reactive B cells subjected to positive selection, and playing an important role on the maintenance of homeostasis while defending the host against a broad spectrum of infections[10-12]. Among other antigens, NAbs can recognize carbohydrate structures, including blood group antigens, do not found during first weeks of life[13]. G.F. Springer showed that anti-glycan NAbs directed

against blood group antigens, may be generated in response to bacterial O-antigens and LPS expressed by components of the gut microbiota[14]. This notion is in keeping with the observation that healthy individuals have high levels of circulating NAbs, directed many other glycan structures, including soluble as well as integral glycoconjugates that act as part of cell membranes attached to proteins or lipids structures[15].

Anti-α-gal Abs are amongst this class of NAbs, present in a considerable amount (1-5% of circulating Igs) under steady state conditions[16,17]. Production of α-gal specific NAbs is thought to be driven mainly by exposure to microbiota expressing α-gal, including *Klebsiella spp*., *Serratia spp*. and *Escherichia coli spp*[18]. These *Enterobacteriaceae* can express galactosyl residues α-linked to LPS, components of the bacterial capsule or cell wall glycoproteins. When present in some of these bacterial components, α-gal glycan acts as a strong immunogen supporting the production of high levels of anti-α-gal Abs production. Presumably expression of α-gal in the outer membrane of enterobacteria in human gut may provide PRR engagement to B cells leading to the production of anti-α-gal T cell independent IgM NAbs, in a similar manner to anti-ABO blood group antigens[18].

Gut colonization by the human pathobiont *E. coli* O86:B7[19] is informative for the etiology of anti-α-gal Ab production. *E. coli* O86:B7, a gram-negative bacteria, presenting α-gal structures on the cell wall or LPS[20] was used as a model bacterial strain to study the generation of anti-blood group NAbs in humans. It was hypothesized that human anti-α-gal NAbs are induced by enteric exposure, in a similar manner to the development of Abs against ABO blood group antigens. In support of this notion, the production of Abs directed against the α-gal related anti-B blood group glycan be induced in

germ-free (GF) chickens upon gut colonization by *E. coli* O86:B7[21]. Moreover, intravenous injection of LPS from *E. coli* O86:B7 can neutralize these Abs. An experimental study performed on sick and healthy humans (from 1 week to 70 years old) by introducing heat-killed *E. coli* O86:B7 administered via nasal inhalation or feeding showed that anti-blood Abs related with α-gal were readily elicit[14]. Afterwards, studies on primates showed that removal of aerobic gram-negative bacteria is associated with a gradual decrease of circulating anti-α-gal Abs, thus suggesting that steady state production of these Abs is modulated by gram-negative bacteria in the gut[22] Lastly, oral inoculation of live *E. coli* O86:B7 leads to gut colonization of streptomycin treated *α1,3Gt*$^{-/-}$ mice elicits the production of cytolytic anti-α-gal Abs[23]. This argues that gut colonization by *E. coli* O86:B7 may be particularly relevant in triggering the production of α-gal specific Abs presumably contributing to the high titers of these circulating Abs in healthy human adult[18]. The production of the Abs is not only triggered upon interaction between host and its gut flora, but it can also occur in pathogenic conditions driven by gram-negative bacteria from *Salmonella spp.* or for protozoan parasites from *Trypanosoma spp.*, as illustrated[24].

In this chapter, we tested whether colonization or systemic infection of *α1,3Gt*$^{-/-}$ mice with *E. coli* O86:B7 can induce the production of anti-α-gal Abs, in a similar manner to induction of natural anti-ABO Abs in humans colonized by this bacterial strain. We used *E. coli* O86:B7, originally isolated from a human infant[14] and *E. coli* K12, isolated from a stool sample of a diphtheria patient[25], to test whether anti-α-gal Abs can be induced by enteric exposure to these bacterial strains and if this was the case whether these Abs can confer protection against *Plasmodium* infection. We demonstrate that gut colonization with α-gal expressing bacteria elicits the production of anti-α-gal IgM Abs and in *α1,3Gt*$^{-/-}$ mice, recapitulating the

normal etiology of human anti-α-gal Abs, thought to be induced by enteric exposure to α-gal expressing bacteria. Importantly, anti-α-gal Abs produced in response to gut colonization by *E. coli* O86:B7, confer protection against malaria transmission.

5.2 Materials and Methods

5.2.1 GF Mice

C57BL/6 *α1,3Gt*$^{-/-}$ mice were re-derived via caesarean section from SPF into GF conditions at the Instituto Gulbenkian de Ciência, as described in detail elsewhere[6]. Briefly, pregnant female *α1,3Gt*$^{-/-}$ mice were euthanized (20 days post-coitum), uteri were immersed in 1% VirkonS, rinsed in sterile water and pups were transferred to surrogate mothers kept in GF isolators (Gettinge-La Calhéne, France). GF status was monitored every third week onwards. For gnotobiotic colonization, 8-12 weeks GF *α1,3Gt*$^{-/-}$ mice were transferred into sterile micro-isolator Ventiracks (Biozone, Margate, UK), fed ad libitum with a standard autoclaved chow diet and water and GF status was monitored every third week onwards.

5.2.2 Bacterial strains and growth conditions

Frozen *E. coli* O86:B7 (ATCC® 12701TM; Rockville, Md.) and *E. coli* K12 (ATCC® 10798) (~10^7 CFU/ml; 50% glycerol solution; -80°C) stocks were inoculated into Luria broth (LB; 50 mL; 37°C; overnight) on a shaker rack. Spectrophotometric absorbance was measured at 600nm (Optical Density-OD_{600}) and adjusted to OD_{600} ~0.2 in order to harvest bacteria during exponential growth corresponding to an OD_{600} of 2. The approximate cell number was determined according to spectrophotometric measurement and confirmed with most probable numbers (MPN) technique, also known as the method of Poisson zeroes[26].

---

[6] http://strains.emmanet.org/protocols/GermFree_0902.pdf

5.2.3 Detection of α-gal on bacterial cultures

E. coli O86:B7 and *E.coli* K12 were cultured (LB; 50 mL; 37°C; overnight), washed (2X; PBS; 4000g; 5min; 4°C) and re-suspended in PBS. Bacteria were fixed (200 µL; 4% PFA in PBS; 20-30 min; RT) and washed (1X; PBS; 4000g; 5min; RT). 10^8-10^9 CFU/mL were stained with BSI-IB4-FITC (200µL; 50µg/mL; 20min; RT) for flow cytometry analysis using FacScan analyzer (BD Biosciences). In parallel, IFA were performed using 10 µL stained samples after air-drying (20 min; RT). Samples were washed (1X; PBS), incubated with 4',6-diamidino-2-phenylindole (DAPI) (200µL; 10 µg/mL; 10min; RT; Molecular Probes®) and washed (1X; PBS). Immunofluorescence images were obtained by Spinning Disk Confocal microscopy Revolution xD (Andor Technology; USA) at 100X magnification and images were processed with ImageJ (NIH) software.

5.2.4 Systemic infection with live bacteria

Bacterial cultures of *E. coli* O86:B7 and *E.coli* K12 were washed (2X; PBS; 4000g; 5min; 4°C) and resuspended (PBS; 10^8 CFU/mL). 10^7 CFU/100 µl of bacterial samples were administered intraperitoneally to *α1,3Gt*$^{-/-}$ mice (3 times at two weeks intervals).

5.2.5 Gut colonization of mice

GF and SPF *α1,3Gt*$^{-/-}$ mice treated with streptomycin sulphate (5g/L in drinking water for 7 days; Gibco), were starved for 12 hours and colonized with *E. coli* O86:B7 (ATCC® 12701TM; Rockville, Md.) or E. coli K12 (ATCC® 10798) (~10^7 CFU/100 µL Luria-Bertani-LB medium) via oral gavage, using a 20-gauge stainless steel animal feeding needle (Cadence Science Inc., Japan). Control mice were inoculated with sterile LB medium. Colonization protocol was administered 3 times at two weeks intervals. Samples were stained to check colonization as described before in Section 5.2.3 to assess colonization.

5.2.6 Anti-α-gal ELISA *See Section 3.2.7*

5.2.7 Parasites maintenance and mosquitoes rearing *See Section 2.2.1*

5.2.8 *Plasmodium* transmission *See Section 3.2.9*

5.2.9 Disease assessment *See Section 3.2.10*

5.2.10 Statistical analysis *See Section 3.2.15*

5.3 Results

5.3.1 Growth of *E. coli* K12 and *E. coli* O86.B7 strains

E. coli O86:B7[14] and *E. coli* K12[25] were cultured and determined the growth kinetics of them. Bacteria were cultured initially with OD_{600} 0.05 in LB medium and followed until reaching to the stationary phase of their growth at 37°C **(Figure 5.2)**. Growth of *E. coli* O86.B7 and *E. coli* K12 cells led to similar final cellular yields **(Figure 5.2)**. Growth curve plots obtained for two independent experiments indicate that doubling under exponential growth corresponding to about 20-30 minutes. Both *E. coli* strains reached stationary phase around 6 hours. Based on these data we decided to harvest bacterial samples for all *in vivo* experiments around 2-3 hours after initial culturing, corresponding to an OD_{600} ~0.2.

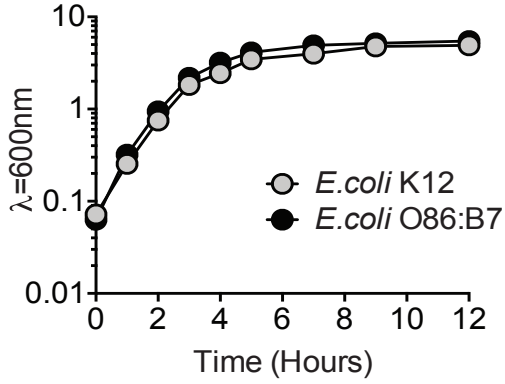

Figure 5.2 Growth kinetics of *E. coli* O86.B7 and *E. coli* K12. Overnight-cultured *E.coli* strains were adjusted to same initial OD and every 1-3h thereafter; a sample was collected to measure OD_{600} over 12 hour. Representative of two independent experiments.

5.3.2 Detecting the α-gal glycan on *E. coli* strains

We asked whether α-gal is expressed on *E. coli* O86.B7 and *E. coli* K12 using BSI-IB_4-FITC. As previously reported[20], *E. coli* O86.B7 expressed high levels of α-gal while expression of α-gal was relatively low or absent on *E. coli* K12, as assessed by flow cytometry **(Figure 5.3a)** and immunofluorescence **(Figure 5.3b)**. These results confirmed the presence of terminal α-gal containing glycoconjugates in *E. coli* O86.B7 and their relative absence on *E. coli* K12.

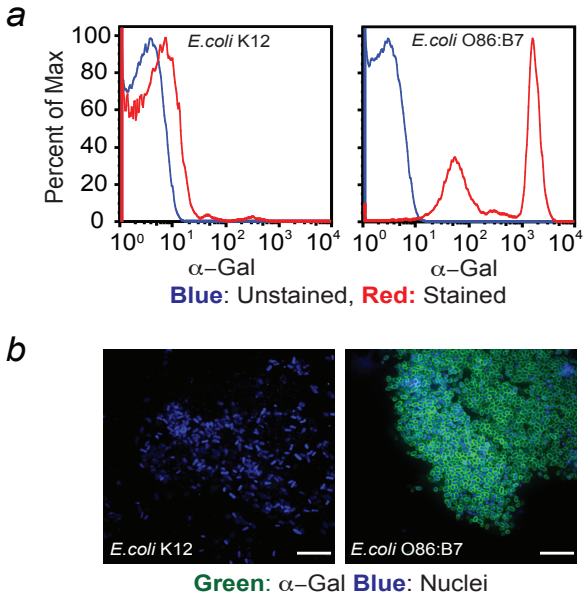

Figure 5.3 Detection of α-gal glycan on *E. coli* O86.B7 but not on *E. coli* K12. The presence of α-gal on *E. coli* strains was detected by **a)** flow cytometry and **b)** IFA. Results are representative of 2-3 independent experiments. Images in (b) represent composite staining, i.e α-gal (green) and DNA (blue) at 100X magnification. Scale bars: 10μm.

5.3.3 Anti-α-gal Abs induced upon systemic infection are protective against *Plasmodium* infection

We used the *E. coli* O86.B7 and *E. coli* K12 strains to infect *α1,3Gt*$^{-/-}$ mice. Initially, we established a sub-lethal dose of inoculation (i.p.; 3 times at two weeks intervals), i.e. infection. Administration of 10^5–10^8 CFU of either *E. coli* strain was not associated with incidence of mortality and selected the 10^7 CFU/mouse. Infection by live *E. coli* O86.B7 but not *E. coli* K12 elicited the production of circulating anti-α-gal IgM and IgG Abs in *α1,3Gt*$^{-/-}$ mice

(Figure 5.4a). Circulating anti-α-gal IgA and IgE Abs were undetectable in the circulation of *α1,3Gt*$^{-/-}$ *(data not shown).*

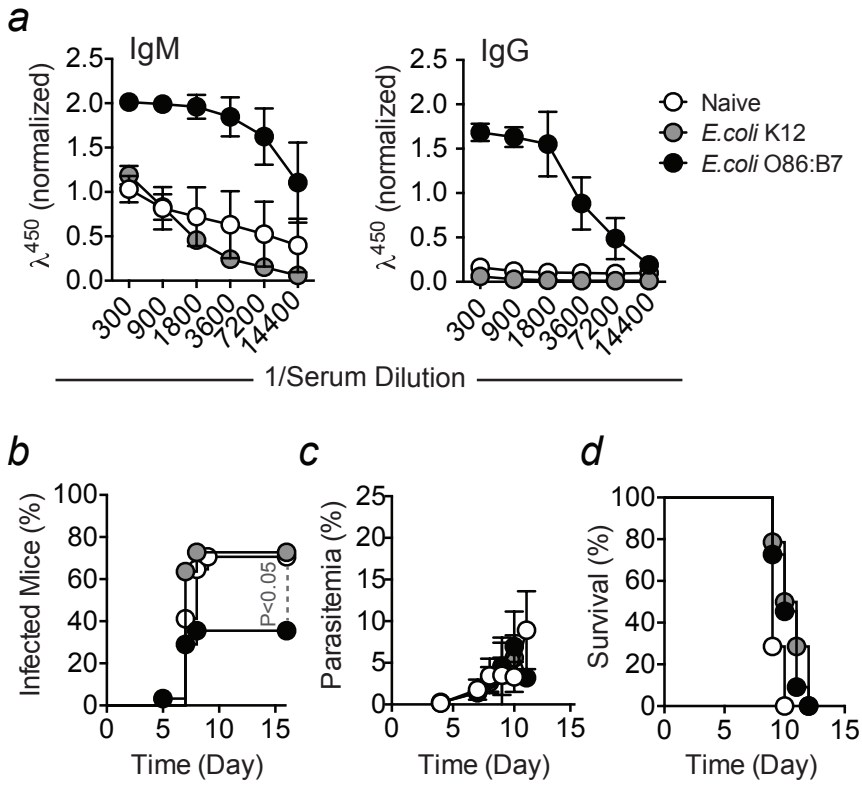

Figure 5.4 Systemic infections by live *E. coli* O86.B7 but not *E. coli* K12, induces anti-α-gal Abs and confers protection against *Plasmodium* infection. a) Mean ± STD of relative absorbance of anti-α-gal Abs from non-infected (Naïve), *E. coli* K12 (*E. coli* K12) or *E. coli* O86.B7 (*E. coli* O86.B7) infected *α1,3Gt*$^{-/-}$ mice. **b)** Incidence of blood stage of *Plasmodium* infection (%) in mice infected with bacteria as in (a) and exposed to *Pb*A$^{EEF1a\text{-}GFP}$ infected mosquitoes, **c)** parasitemia (%) and **d)** survival (%) of the same mice as in (b) infected with *Pb*A$^{EEF1a\text{-}GFP}$. Data shown in (a) is 2-3 independent experiments (n=4-6 mice per group) and (b-d) is from 3 independent experiments (n=11-31 mice per group). Statistical significance among groups in the incidence of infection was determined by log rank (Mantel-Cox) test.

Administration of 10^7 CFU/mouse of *E. coli* K12 or *E. coli* O86.B7 to *α1,3Gt*$^{+/+}$ mice did not induce the production of circulating anti-α-gal Abs *(data not shown).* We then asked whether when infected by *E. coli* K12 or *E.*

coli O86.B7, *α1,3Gt*$^{-/-}$ mice were protected from subsequent *Pb*A infection by *A. stephensi* mosquitoes. Infection with live *E. coli* O86.B7 protected *α1,3Gt*$^{-/-}$ mice from *Pb*A infection vs. naïve *α1,3Gt*$^{-/-}$ mice **(Figure 5.4b)**. This was not the case for *E. coli* K12 infection **(Figure 5.4b)**. When infected by *Pb*A, all mice developed similar levels of parasitemia **(Figure 5.4c)** and succumbed to experimental cerebral malaria, irrespectively of the *E. coli* strain used **(Figure 5.4d)**. These results suggest that systemic infection by a bacterial strain expressing α-gal elicits an anti-α-gal Ab response that is protective against malaria transmission.

5.3.4 Gut colonization with bacteria expressing α-gal elicits protective Ab response against *Plasmodium* infection

The high titer of anti-α-gal NAbs detected in human serum throughout life[27] suggests that the production of these NAbs may be induced by components of the gut flora. To test this hypothesis, we colonized *α1,3Gt*$^{-/-}$ mice with *E. coli* O86.B7 or *E. coli* K12 strains that express α-gal glycan or not, respectively **(Figure 5.3a and 5.3b)**.

In order to eliminate the endogenous gut flora, *α1,3Gt*$^{-/-}$ mice maintained under specific pathogen free (SPF) conditions were treated with streptomycin for 7 days (streptomycin sulphate; 5g/L in drinking water) and colonized thereafter with either *E. coli* O86.B7 or *E. coli* K12. This approach was not associated with discernable morbidity, including weight loss or diarrhea. Colonization of *α1,3Gt*$^{-/-}$ mice by *E. coli* O86:B7, after antibiotic treatment increased the levels of circulating anti-α-gal IgM Abs from 1.4 μg/mL [95% CI: 1.1-1.8 μg/mL] up to 162.9 μg/mL [95% CI: 95.89-230.1 μg/mL] before and after colonization, respectively **(Figure 5.5a)**. Levels of anti-α-gal IgM Abs in *E. coli* O86:B7 colonized *α1,3Gt*$^{-/-}$ mice were in the range of adult individuals from a malaria endemic region **(Figure**

3.2). Levels of circulating anti-α-gal IgG Abs remained at residual levels, i.e. <1 μg/mL **(Figure 5.5b)**, in the range of adult individuals from a malaria endemic region **(Figure 3.2)**. Colonization by *E. coli* K12 did not induce the production of anti-α-gal Abs in *α1,3Gt*$^{-/-}$ mice **(Figure 5.5a and 5.5b)**.

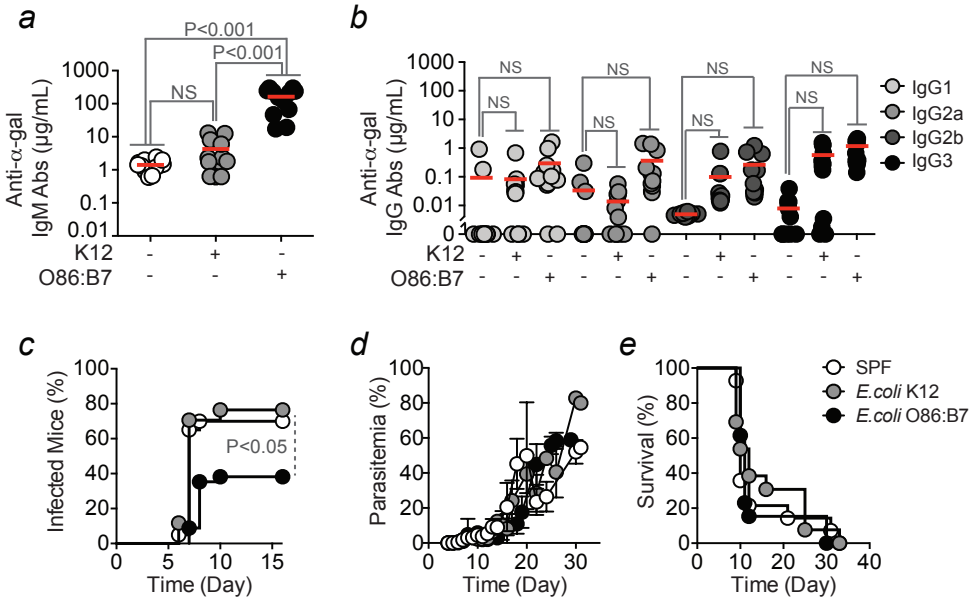

Figure 5.5 Gut colonization using *E. coli* O86.B7, but not *E. coli* K12, triggers anti-α-gal Abs production and confers protection against *Plasmodium* infection. Concentration of anti-α-gal **a)** IgM and **b)** IgG Abs in the serum of SPF *α1,3Gt*$^{-/-}$ mice that are non-colonized (SPF), colonized by *E. coli* K12 or colonized by *E. coli* O86.B7. Bars are mean. **c)** Incidence of blood stage of *Plasmodium* infection (%) in mice colonized as in (a and b) and exposed to *Pb*A$^{EEF1a\text{-}GFP}$ infected mosquitoes (17-34 mice per group). **d)** parasitemia (%) and **e)** survival (%) of *α1,3Gt*$^{-/-}$ mice as in (a and b), infected with *Pb*A$^{EEF1a\text{-}GFP}$ (n=11-14 mice per group). Data shown in (a and b) is 2-3 independent experiments (n=12 mice per group) and (c) is from 3-5 independent experiments (n=17-34 mice per group). Statistically significant correlations among the groups were determined by Kruskal-Wallis test with Dunn's multiple comparison post-test. Statistical significance among groups in the incidence of infection was determined by log rank (Mantel-Cox) test.

We next asked whether anti-α-gal Abs produced in the *E. coli* O86:B7 colonized *α1,3Gt*$^{-/-}$ mice exert a protective effect against *Plasmodium* infection. Colonization by *E. coli* O86.B7 was associated with protection of

$\alpha 1,3Gt^{-/-}$ mice from *Pb*A transmission by infected *A. stephensi* mosquitoes **(Figure 5.5c)**. This was not the case when $\alpha 1,3Gt^{-/-}$ mice were colonized by *E. coli* K12 **(Figure 5.5c)**. Parasitemia was similar among mice that were not protected from *Pb*A infection **(Figure 5.5d)**, succumbing thereafter to experimental cerebral malaria **(Figure 5.5e)**. These results suggest that gut colonization with bacteria expressing α-gal elicits a protective anti-α-gal Ab response against *Plasmodium* infection.

To determine whether the protective effect associated with gut colonization by *E. coli* O86.B7 is mediated by anti-α-gal Abs, similar colonization experiments were performed in $\alpha 1,3Gt^{-/-}J_HT^{-/-}$, $\alpha 1,3Gt^{-/-}\mu S^{-/-}$ or $\alpha 1,3Gt^{-/-}Aid^{-/-}$ mice. Gut colonization by *E. coli* O86.B7 failed to protect $\alpha 1,3Gt^{-/-}J_HT^{-/-}$ **(Figure 5.6a)** and $\alpha 1,3Gt^{-/-}\mu S^{-/-}$ **(Figure 5.6c)** but not $\alpha 1,3Gt^{-/-}Aid^{-/-}$ **(Figure 5.6b)** mice from *Pb*A infected *Anopheles* mosquitoes, as compared to control mice not colonized or colonized by *E. coli* K12. This shows that the protective effect of gut colonization by *E. coli* O86.B7 acts via a mechanism mediated by anti-α-gal IgM Abs that do not undergo somatic hypermutation.

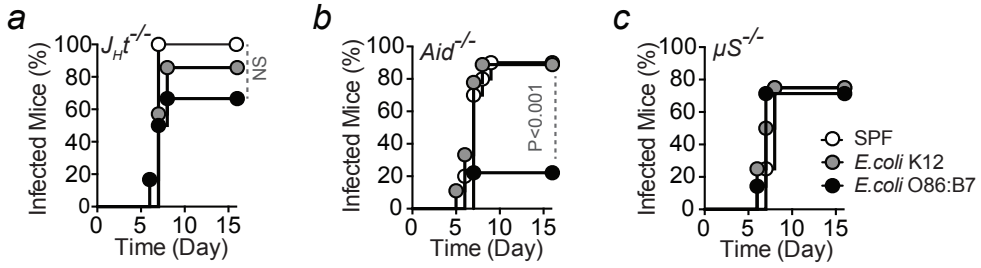

Figure 5.6 Protective effect driven by gut flora against *Plasmodium* infection is antibody dependent. Incidence of blood stage of *Plasmodium* infection (%) in **a)** $\alpha 1,3Gt^{-/-}JHT^{-/-}$, **b)** $\alpha 1,3Gt^{-/-}Aid^{-/-}$ and **c)** $\alpha 1,3Gt^{-/-}\mu S^{-/-}$ mice that are non-colonized (SPF), colonized by *E. coli* K12 or colonized by *E. coli* O86.B7. Data shown in (a-c) is 1-2 experiments (n=4-10 mice per group). Statistical significance among groups in the incidence of infection was determined by log rank (Mantel-Cox) test.

Incoming microorganism do not compete with other microorganism when colonized in germ-free (GF) mice. Colonization of GF mice by a single

bacterial strain is called mono-colonization[28]. GF *α1,3Gt*$^{-/-}$ mice had low but detectable levels of anti-α-gal IgM Abs, i.e. 0.87 μg/mL [95% CI: 0.66-1.1 μg/mL], confirming that these are NAbs since they are produced in the absence of a discernable foreign antigen **(Figure 5.7a)**. This was not the case for anti-α-gal IgG Abs that were almost undetectable **(Figure 5.7b)**. When mono-colonized by either *E. coli* O86.B7 or *E. coli* K12 for three times with 2 weeks intervals mono-colonized GF *α1,3Gt*$^{-/-}$ mice showed no apparent morbidity or mortality. When mono-colonized by *E. coli* O86:B7, the levels of circulating anti-α-gal IgM Abs in *α1,3Gt*$^{-/-}$ mice increased to 96.62 μg/mL [95% CI: 59.32-133.9 μg/mL] **(Figure 5.7a)**, without concomitant induction of anti-α-gal IgG Abs **(Figure 5.7b)**. We then asked whether anti-α-gal Abs induced by mono-colonization of GF *α1,3Gt*$^{-/-}$ mice by *E. coli* expressing α-gal confers protection against *Plasmodium* infection by *A. stephensi* mosquitoes. Mono-colonization by *E. coli* O86:B7 but not by *E. coli* K12 protected *α1,3Gt*$^{+/-}$ mice from *Pb*A transmission by *A. stephensi* mosquitoes **(Figure 5.7c)**. Percentage (%) of infected RBC, i.e. parasitemia, was similar among mice not protected from *Pb*A infection, succumbing thereafter to experimental cerebral malaria **(Figure 5.7d and 5.7e)**. This suggests that mono-colonization by a specific pathobiont expressing α-gal glycan recapitulates the normal etiology of the human anti-α-gal Ab response and is associated with protection against *Plasmodium* infection, such as observed in a malaria endemic region **(Figure 3.2)**.

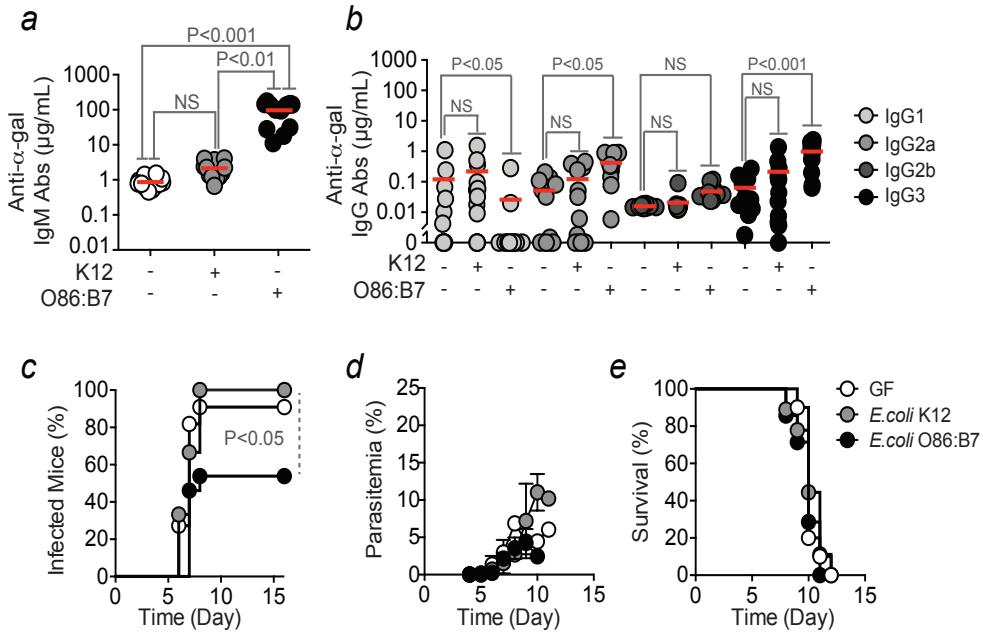

Figure 5.7 Colonization by *E. coli* O86.B7 protects GF mice against *Plasmodium* infection. Concentration of anti-α-gal **a)** IgM and **b)** IgG Abs in the serum of GF *α1,3Gt*$^{-/-}$ mice that are non-colonized (GF), colonized by *E. coli* K12 or colonized by *E. coli* O86.B7. Data is representative of 2-3 independent experiments (12 mice per group) and red bars are mean. **c)** Incidence of blood stage of *Plasmodium* infection (%) in mice colonized as in (*a and b*) and exposed to *Pb*A$^{EEF1a\text{-}GFP}$ or *Pb*A^{HSP70} infected mosquitoes (n=9-13 mice per group). **d)** Parasitemia (%) and **e)** survival (%) of *α1,3Gt*$^{-/-}$ mice as in (a and b), infected with *Pb*A$^{EEF1a\text{-}GFP}$ (n=7-10 mice per group). Data were pooled from 4 independent experiments. Statistically significant correlations among the groups in (a and b) were determined by Kruskal-Wallis test with Dunn's multiple comparison post-test. Statistical significance among groups in the incidence of infection in (c) was determined by log rank (Mantel-Cox) test.

5.4 Chapter Discussions and Conclusion

Mammals have a complex microbiota that starts to be shaped quickly after birth, through colonization by vast number of essentially non-pathogenic or pathobiont microorganism along the body surface. The existence of a highly co-evolved relationship with host immune system has promoted beneficial co-existence and interdependency over millions of years. Host-microbiota interaction can modulate T or B cell mediated immune responses to induce the repertoire of anti-glycan Abs, shaping mammalian

immunity profoundly and regulating immune responses ensuring host-microbial mutualism[29].

In this part of the thesis, we showed that under SPF conditions, *α1,3Gt*$^{-/-}$ mice produce residual levels of circulating IgM anti-α-gal Abs, which are also detected under GF conditions, confirming that these are NAbs **(Figure 5.5a and 5.7a)**. Moreover, anti-α-gal Abs in SPF *α1,3Gt*$^{-/-}$ mice do not increase appreciably over time *(data not shown)* in contrast to adult humans who have high levels of circulating IgM anti-α-gal Abs when compared to newborns **(Figure 3.2a)**. This may be explained by the composition of SPF *α1,3Gt*$^{-/-}$ mice gut flora that does not change much over time as compared to human. Anti-α-gal IgM Abs in humans are relatively low in the first years of their lives and increase with age **(Figure 3.2a)**. The reason for this may relate to lack of gut flora components expressing α-gal glycan[30]. Alternatively, daily dietary intake that alters the composition of the gut flora and may influence gut flora composition and as such as meat-based diet increase the bile-tolerant bacteria and decrease plant polysaccharides metabolizing bacteria[31]. For instance, colonization of *Clostridium* cluster XIVa seems to be established at the age of 4 years after birth, however, composition of *Bacteroidetes*, *Bifidobacteria* and *Clostridium* cluster IV phyla gradually change with age[30]. Moreover, diet consumption composed of animal or plant products could alter the human gut flora and might promote colonization by microbiota expressing α-gal glycan, therefore inducing the production of anti-α-gal NAbs[31]. Presumably, this does not occur in SPF *α1,3Gt*$^{-/-}$ mice which are maintained under a rather control diet and as such should have relatively constant gut as compared to humans. This may explain why the levels of anti-α-gal Abs in plasma of SPF *α1,3Gt*$^{-/-}$ mice fail to increase gradually over time *(data not shown)*. Assuming that the production of anti-α-gal Abs arises from enteric

exposure to bacteria expressing α-gal, then specific components of the gut microbiota may be sufficient to induce protective mechanisms against pathogens expressing α-gal, such as *Plasmodium*. Our studies showed that this is the case in *α1,3Gt*$^{-/-}$ mice colonized by *E. coli* O86:B7 **(Figure 5.5a and 5.7a)**. This suggests that continuous or intermittent antigenic stimulation by components of the gut microbiota expressing α-gal is necessary for the life-long production of anti-α-gal Abs.

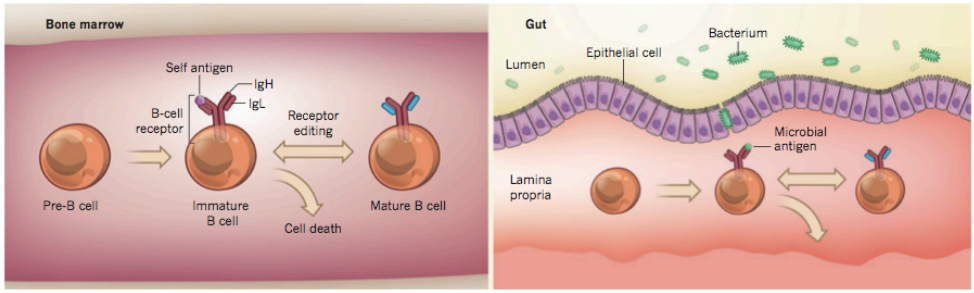

Figure 5.8 B cell development in bone marrow and in gut. B cell development occurs in the bone marrow and regulated by interactions with self-antigens. In contrast, it was shown that B cell receptor editing can occur in lamina propria of the gut, which induce B-cell tolerance to these resident microorganisms, and diversification of B cell receptors repertoire. Adapted from[32].

While B cells arise from the bone marrow and are activated in secondary lymphoid organs to produce Abs, B-cell development can also occur in the lamina propria of gut via a process involving BCR editing driven by gut microbiota[33] **(Figure 5.8)**. It is still unclear whether the NAbs that are generally low in the serum are produced by this population of B cells in the lamina propria of gut. In a similar manner, we showed that gut colonization with *E. coli* O86.B7 triggers the production of anti-α-gal IgM Abs produced most probably by B1 cells in the gut[34]. Local physical trauma or inflammation associated with the gavage process may promote inflammation and/or allow low numbers of microbes to infiltrate into the mucosal surface, and induce further the production of anti-α-gal Abs by B1 cells, in the peritoneal cavity. Moreover, there may be a yet undefined

mechanism in which B cells can sample antigens from the gut without breaching the mucosal barrier and act as a link between innate and adaptive immune systems to provide defense mechanisms against microbial invasion.

Gut colonization by *E. coli* O86.B7 triggers the production of anti-α-gal Abs of the IgM but not the IgG isotypes, suggesting that *E. coli* O86.B7 fails to induce Ig class switch, usually associated with B2 cell responses and assisted by T cells after colonization with commensal bacteria[34]. This suggests that *E. coli* O86.B7 may not be efficient in inducing B2 cells to produce anti-α-gal IgG Abs. Our work also demonstrates that gut colonization by specific strains of microbiota can contribute to the pool of circulating anti-α-gal IgM Abs. However, the levels of anti-α-gal Abs IgM Abs produced upon gut colonization are lower than those produced via immunization against α-gal glycan, but in similar concentration when compared to human adults **(Figure 3.3, 3.12, 5.5a and 5.7a)**. This is sufficient however, to confer protection against *Plasmodium* infection **(Figure 5.4b and 5.5b)**. This suggests that gut colonization with bacteria expressing α-gal is the main source of anti-α-gal Ab production but not the only one. When naïve *α1,3Gt*$^{-/-}$ mice are immunized against the α-gal glycan **(Figure 3.3 and 3.12)**, the protective effect against *Plasmodium* transmission is higher than *α1,3Gt*$^{-/-}$ mice colonized with *E. coli* O86.B7.

In conclusion, host can encounter many different types of pathogens expressing α-gal such as *S. pneumoniae, H. influenza, S. aureus, E. coli, Salmonella or Clostridium*. These can lead to inflammation and trigger activation of the immune system and subsequently, the production of anti-α-gal Abs that are protective against *Plasmodium* infection. Other anti-glycan Abs, that need to be further investigated, may have a similar protective role against several pathogens including *Plasmodium*.

Additionally, anti-α-gal Abs induced by the gut flora may also play a role against other vector borne protozoan parasites expressing α-gal, such as *Leishmania spp.* and *Trypanosoma spp.*, the causative agents of Leishmaniasis and Trypanosomiasis, respectively[24].

Contributions

The author of this dissertation performed all experiments described in this chapter.

Acknowledgements

I'd like to thank to Ana Rita Carlos for revising this chapter. Thanks to Karina Xavier (IGC) for providing us the *E.coli* K12 strain, the Animal Facility Members (IGC), specifically Karen Berman de Ruiz, for generating and taking care of GF $\alpha 1,3Gt^{-/-}$ mice, past and present member of the Flow Cytometry Unit (IGC) for technical support, Marie Louise Bergman (IGC) for helping to setup flow cytometry to detect α-gal in *E. coli* strains, Jessica Thompson (IGC) for providing me the protocol for antibiotic treatment, culturing bacteria and fruitful discussions on gut flora colonization.

References

1. Belkaid, Y. & Naik, S. Compartmentalized and systemic control of tissue immunity by commensals. *Nature immunology* **14**, 646-653 (2013).
2. Belkaid, Y. Tailored immunity at mucosae. *Immunological reviews* **60**, 5–7 (2014).
3. Hooper, L.V. & Gordon, J.I. Glycans as legislators of host-microbial interactions: spanning the spectrum from symbiosis to pathogenicity. *Glycobiology* **11**, 1R-10R (2001).
4. Cash, H.L.H., V. L. Commensal Bacteria Shape Intestinal Immune System Development. *ASM News* **71**, 77 - 83 (2005).

5. Kato, L.M., Kawamoto, S., Maruya, M. & Fagarasan, S. The role of the adaptive immune system in regulation of gut microbiota. *Immunological reviews* **260**, 67-75 (2014).
6. Macpherson, A.J., *et al.* A primitive T cell-independent mechanism of intestinal mucosal IgA responses to commensal bacteria. *Science* **288**, 2222-2226 (2000).
7. Hill, D.A. & Artis, D. Intestinal bacteria and the regulation of immune cell homeostasis. *Annual review of immunology* **28**, 623-667 (2010).
8. Jiang, H.Q., *et al.* Interactions of commensal gut microbes with subsets of B- and T-cells in the murine host. *Vaccine* **22**, 805-811 (2004).
9. Coutinho, A., Kazatchkine, M.D. & Avrameas, S. Natural autoantibodies. *Current opinion in immunology* **7**, 812-818 (1995).
10. Gronwall, C., Vas, J. & Silverman, G.J. Protective Roles of Natural IgM Antibodies. *Frontiers in immunology* **3**, 66 (2012).
11. Hayakawa, K., *et al.* Positive selection of natural autoreactive B cells. *Science* **285**, 113-116 (1999).
12. Ochsenbein, A.F., *et al.* Control of early viral and bacterial distribution and disease by natural antibodies. *Science* **286**, 2156-2159 (1999).
13. Wiener, A.S. Origin of naturally occurring hemagglutinins and hemolysins; a review. *J Immunol* **66**, 287-295 (1951).
14. Springer, G.F. & Horton, R.E. Blood group isoantibody stimulation in man by feeding blood group-active bacteria. *The Journal of clinical investigation* **48**, 1280-1291 (1969).
15. Wong, S.Y.C. & Arsequell, G. *Immunobiology of Carbohydrates*, (KLUWER ACADEMIC / PLENUM PUBLISHERS, USA, 2003).
16. Galili, U., Anaraki, F., Thall, A., Hill-Black, C. & Radic, M. One percent of human circulating B lymphocytes are capable of producing the natural anti-Gal antibody. *Blood* **82**, 2485-2493 (1993).
17. Galili, U., Buehler, J., Shohet, S.B. & Macher, B.A. The human natural anti-Gal IgG. III. The subtlety of immune tolerance in man as

demonstrated by crossreactivity between natural anti-Gal and anti-B antibodies. *The Journal of experimental medicine* **165**, 693-704 (1987).

18. Galili, U., Mandrell, R.E., Hamadeh, R.M., Shohet, S.B. & Griffiss, J.M. Interaction between human natural anti-alpha-galactosyl immunoglobulin G and bacteria of the human flora. *Infection and immunity* **56**, 1730-1737 (1988).
19. Pal, S.C., *et al.* An extensive community outbreak of enteropathogenic Escherichia coli O86: B7 gastroenteritis. *Bulletin of the World Health Organization* **41**, 851-858 (1969).
20. Yi, W., *et al.* Two different O-polysaccharides from Escherichia coli O86 are produced by different polymerization of the same O-repeating unit. *Carbohydrate research* **341**, 100-108 (2006).
21. Springer, G.F., Horton, R.E. & Forbes, M. [Origin of anti-human blood group B agglutinins in white Leghorn chicks]. *The Journal of experimental medicine* **110**, 221-244 (1959).
22. Manez, R., *et al.* Removal of bowel aerobic gram-negative bacteria is more effective than immunosuppression with cyclophosphamide and steroids to decrease natural alpha-galactosyl IgG antibodies. *Xenotransplantation* **8**, 15-23 (2001).
23. Posekany, K.J., Pittman, H.K., Bradfield, J.F., Haisch, C.E. & Verbanac, K.M. Induction of cytolytic anti-Gal antibodies in alpha-1,3-galactosyltransferase gene knockout mice by oral inoculation with Escherichia coli O86:B7 bacteria. *Infection and immunity* **70**, 6215-6222 (2002).
24. Avila, J.L., Rojas, M. & Galili, U. Immunogenic Gal alpha 1----3Gal carbohydrate epitopes are present on pathogenic American Trypanosoma and Leishmania. *J Immunol* **142**, 2828-2834 (1989).
25. Bachmann, B.J. Pedigrees of some mutant strains of Escherichia coli K-12. *Bacteriological reviews* **36**, 525-557 (1972).

26. Oblinger, J.L. & Koburger, J.A. Understanding and Teaching the Most Probable Number Technique. *Journal of Milk Food Technology* **38**, 540-545 (1975).
27. Galili, U., Rachmilewitz, E.A., Peleg, A. & Flechner, I. A unique natural human IgG antibody with anti-alpha-galactosyl specificity. *The Journal of experimental medicine* **160**, 1519-1531 (1984).
28. Schaedler, R.W., Dubs, R. & Costello, R. Association of Germfree Mice with Bacteria Isolated from Normal Mice. *The Journal of experimental medicine* **122**, 77-82 (1965).
29. Rhee, K.J., Sethupathi, P., Driks, A., Lanning, D.K. & Knight, K.L. Role of commensal bacteria in development of gut-associated lymphoid tissues and preimmune antibody repertoire. *J Immunol* **172**, 1118-1124 (2004).
30. Ringel-Kulka, T., *et al.* Intestinal microbiota in healthy U.S. young children and adults--a high throughput microarray analysis. *PloS one* **8**, e64315 (2013).
31. David, L.A., *et al.* Diet rapidly and reproducibly alters the human gut microbiome. *Nature* **505**, 559-563 (2014).
32. Schlissel, M. Immunology: B-cell development in the gut. *Nature* **501**, 42-43 (2013).
33. Wesemann, D.R., *et al.* Microbial colonization influences early B-lineage development in the gut lamina propria. *Nature* **501**, 112-115 (2013).
34. Thurnheer, M.C., Zuercher, A.W., Cebra, J.J. & Bos, N.A. B1 cells contribute to serum IgM, but not to intestinal IgA, production in gnotobiotic Ig allotype chimeric mice. *J Immunol* **170**, 4564-4571 (2003).

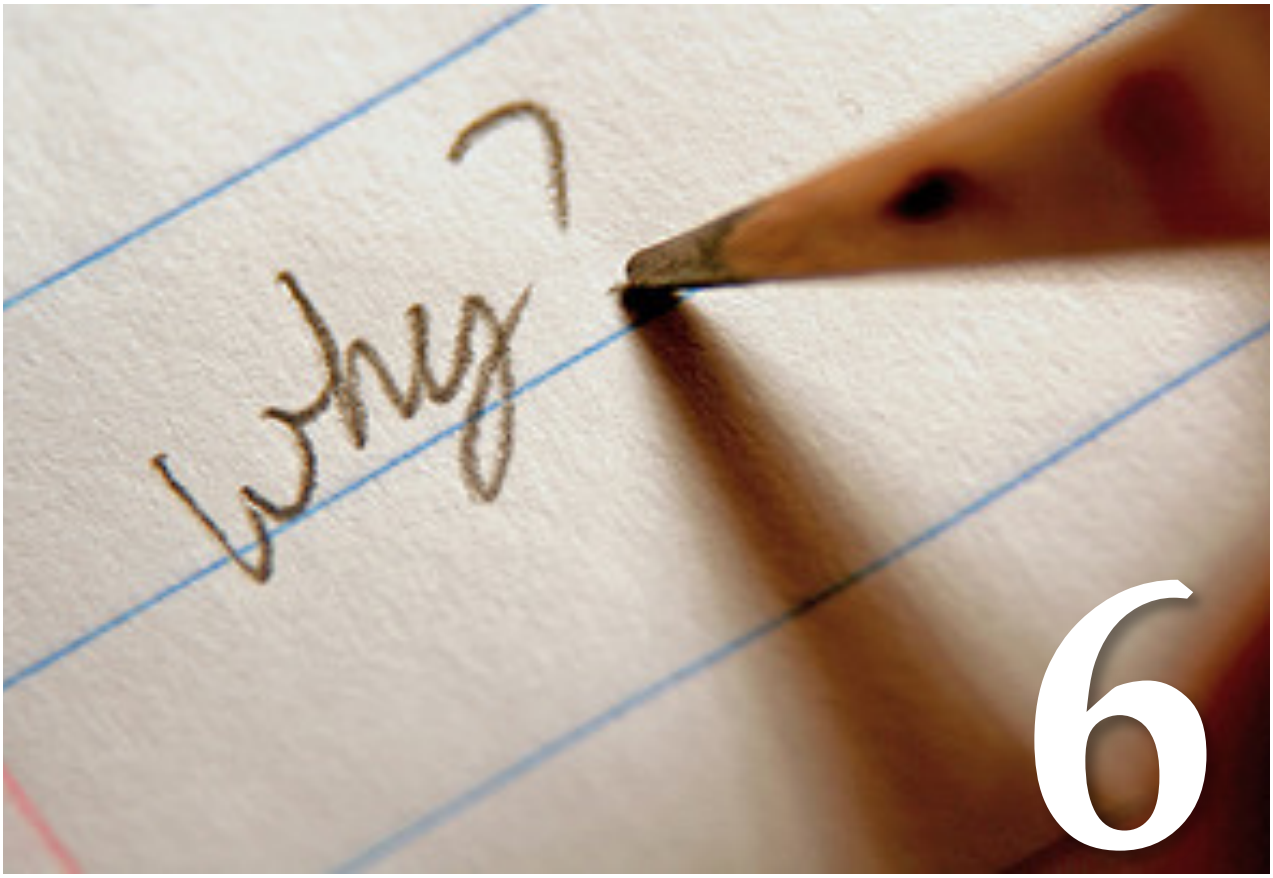

Discussion - Concluding Remarks And Ideas for Future Studies

Plasmodium infection is still a major global threat to mankind. Despite recent progresses in reducing the global burden imposed by malaria, *Plasmodium* infection kills around 700.000 people per year, mostly children under the age of 3-4 years living in sub-Saharan Africa and South East Asia[1]. Moreover, over 200 million malaria cases are reported per year worldwide, mostly affecting children, to whom malaria imposes mortality or major sequels over life[1]. The recent breakthroughs provided by malaria control interventions (i.e. insecticide-impregnated bed nets, indoor insecticide spraying and anti-malarial drugs) managed to reduce malaria morbidity and mortality but there are still no available vaccines conferring sterile protection against *Plasmodium* infection. Phase III trials with what is considered as the most promising vaccine candidate, i.e. RTS,S/AS01, in infants and children from malaria endemic areas show only modest protection with 50% efficacy in the first 3–4 months after immunization that decreases with exposure to *Plasmodium* infected mosquitoes. Therefore, the protective effect provided by this vaccine is too low to be used clinically[2].

The reason why children under the age of 3-4 years are more susceptible to this deadly disease seems to rely on a defective adaptive immunity against *Plasmodium*. The increasing knowledge about the biological features of *Plasmodium* infection and the immune system of its human host should allow to develop a better preventive and protective vaccine in children. This PhD thesis is centered around one such solution: to define a natural protective mechanism against this vector borne protozoan parasite, which is relatively absent in children, while innately present in adults. We found that Abs directed against α-gal and present at high levels in adults but not in children under the age of 3-4 years, effectively prevent *Plasmodium* infection. Presumably, this contributes to explain why children are more susceptible to *Plasmodium* infection as compared to adults. As a final touch of this study, we showed that the host gut flora can shape the generation of these NAbs and confer protection against *Plasmodium* infection.

In the final synthesis of this thesis, the main findings will be briefly reviewed focusing on the questions we asked since the beginning of this project:

"Do we have a natural immune mechanism of defense against Plasmodium infection and if it is the case, can we enhance its effect to achieve the maximum level of protection?"

6.1 Brief Overview and Conclusions of the Thesis

Glycans associated with intracellular proteins as well as extracellular proteins/lipids on the cell surface, have a variety of essential biologic functions[3]. Regulation/distribution of glycan expression in mammals is under the control of glycosyltransferases that produce di-, tri-, oligo- and polysaccharides. Organisms can differ in the classes of glycans, with most organisms expressing *N*-glycans, while others are restricted to the expression of specific glycans, as is the case for hyaluronic acid in vertebrates and sialic acids in deuterostomes. Moreover, specific glycans are absent from very constrained taxa, e.g. α-gal and N-glycolylneuraminic acid (Neu5Gc) that are expressed by most vertebrates except humans[4]. The biologic relevance of some glycans has been probed by the deletion of specific galactosyltransferase genes, indicating that some of these are essential for development and other vital biologic processes.

Loss of function mutations in genes encoding specific glycosyltransferases lead to the elimination of the end product glycan generated by these enzymes and are probably under natural selective pressure. As such, the complete loss of a particular glycan might occur in an attempt to restrain pathogen invasion. In this case, host interaction with glycan-expressing pathogens promotes immune recognition of that glycan, as illustrated for the production of anti-glycan Abs. Therefore, an evolutionary process is

thought to have provided acquired resistance against pathogens expressing such glycans, as illustrated in this thesis for the α-gal glycan[5,6].

Much of the attention related to anti-α-gal NAbs has been framed in the context of on xenotransplantation, that is, the transplantation of cells, tissues or organs across different specifies. In particular, pig organs have been argued to be suitable for transplantation into humans. However, pig cells express high levels of α-gal glycan at their surfaces, leading to hyperacute rejection of pig to human xenografts via a cytotoxic mechanism mediated by anti-α-gal NAbs. While many studies have addressed methodologies to overcome this type of rejection, relatively few studies asked what is the physiologic role, if any, of these anti-α-gal Abs[7-11]. Several studies also identified the presence of the α-gal glycan in pathogens including *Serratia spp.*[12], *Leishmania spp.*[13], *Trypanosoma spp.*[14] and *Plasmodium spp.*[15,16]. Others studies have also associated infections by these pathogens with increasing anti-α-gal Abs[17] levels and analyzed whether these anti-α-gal Abs targets these pathogens *in vitro*[13,18-20]. However, whether anti-α-gal Abs confer resistance to infection by these pathogens has never been tested *in vivo*. In this thesis, we tested this hypothesis in the context of *Plasmodium* infection, the causative agent of malaria and a major driving force that shaped the evolution of anthropoid primates, including humans[21,22].

Under Chapter 2, we demonstrated that *Plasmodium spp*. express the α-gal glycan in the exo-erythrocytic stages. However, bioinformatics tools did not give any hit for candidate genes in *Plasmodium* genome encoding enzymes that may transfer α-gal to proteins or lipids. As such, we reasoned that *Plasmodium* obtains α-gal from its vector. Therefore, we asked whether α-gal is expressed by *Anopheles* mosquitoes. We detected the glycan in the

salivary glands of non-infected *Anopheles* mosquitoes, which led us to hypothesize that *Plasmodium* may be coated by mosquito components containing α-gal. Presumably, this may enable *Plasmodium* ookinetes or sporozoites to avoid the mosquito's immune system as they emerge from the epithelial cells of the midgut. One candidate protein that could coat *Plasmodium* ookinetes or sporozoites during its development in the mosquito is laminin, a ubiquitous non-collagenous connective tissue glycoprotein expressed by insects as well as by mammalian, avian, reptilian, and amphibian cells and known to be decorated with α-gal[23]. The notion that laminin may confer avoidance from mosquito's immunity is supported by the following observation: when injected into the hemocoel of *A. aegypti* female mosquitoes, negatively charged carboxymethyl (CM)-Sephadex beads are usually not melanized as they become coated with mosquito-derived laminin[24]. In reverse, electrically neutral G-Sephadex beads are easily melanized. Since mosquito laminin prevents melanization, the melanization of mouse laminin coated-beads was tested in the mosquito abdominal body cavity and found to be significantly reduced. This suggests that mouse laminin prevents melanization in mosquitoes and that perhaps other insect-derived proteins expressing α-gal may also interact with *Plasmodium spp.* and mask them to avoid the immune system of the mosquito[24-26]. Thus, the α-gal detected on *Plasmodium spp.* surface might be derived from the *Anopheles* mosquito. However, we cannot exclude the possibility that there may be a yet unidentified homologue of the *α1,3Gt* gene in *Plasmodium* sporozoites presenting alternative mechanisms to utilize the host UDP-Gal and add it to the non-reducing termini of oligosaccharide chains of its own proteins or lipids.

We confirmed that α-gal is also expressed during the erythrocytic stage of *Plasmodium spp.* infection[27], as demonstrated in RBC from *α1,3Gt*$^{-/-}$ mice as well as in human RBC that inherently lack the expression of α-gal. It is

possible therefore that while *Plasmodium spp.* do not express an active enzyme capable of producing α-gal glycoconjugates, it may obtain those from its host. In support of this notion, Vanderberg and co-workers have shown that *Plasmodium* sporozoites extracted from salivary glands of *A.* mosquitoes are not recognized by lectins detecting D-glucose (SBA, RCA I and PNA), α-methyl-D-mannoside (ConA), *N*-acetyl-D-glucosamine (WGA), *N*-acetyl-D-galactosamine (DBA), fucose (UEA) or *N*-acetyl-neuraminic acid (LPA)[28]. However, when sporozoites were incubated with mammalian host serum, host plasma glycoproteins or host glycolipids absorbed by sporozoites that were then positively stained for ConA and RCA I[28], suggesting that *Plasmodium* are able to integrate host glycoconjugates into their cell surface structures. However, this was never tested for lectin BSI-IB_4 that detects the α-gal glycan.

The α-gal glycan was detected in *Plasmodium* infected RBC of *α1,3Gt*$^{-/-}$ mice or human. This shows that since *α1,3Gt*$^{-/-}$ mice and human do not express α-gal in RBCs, parasites can retain α-gal from host serum component and utilized in a way that can be conjugated in α-1,3-gal form if *Plasmodium* does not constitutively express α-gal glycan. Additionally, the hepatocyte membranes have galactose detecting receptors, which help to uptake glycoproteins with terminal galactose residues. Therefore, upon liver invasion, glycoproteins containing terminal galactose coating the parasites would assist them to invade hepatocytes[29]. As mentioned before, *Plasmodium* sporozoite surface is a highly active and dynamic structure. If by any chance, *Plasmodium* sporozoites lose the α-gal glycan through the capping process when deposited into dermis, an interaction with host serum might provide them with terminal galactose residues. However, this needs to be further characterized.

We can argue that *Plasmodium* transmission, which is rather inefficient is hinting at a natural mechanism of protection, presumably targeting the initial phases of the *Plasmodium* life-cycle[30-32]. In Chapter 3, we demonstrated that anti-α-gal Abs are a natural defense mechanism, reducing malaria transmission by *Anopheles* mosquitoes. When inoculated into the dermis via mosquito bite, *Plasmodium* sporozoites are confronted with high levels of cytotoxic anti-α-gal IgM Abs that prevent malaria transmission, as demonstrated by three independent lines of evidence. First, individuals from malaria endemic areas that show evidence of decreased *P. falciparum* infection risk have higher levels of circulating anti-α-gal IgM Abs, compared to individuals susceptible to *P. falciparum* infection. Second, anti-α-gal IgM Abs -when present in *α1,3Gt*$^{-/-}$ mice at levels similar to those observed in individuals from a malaria endemic area- are associated with protection from malaria transmission. Third, passive transfer of anti-α-gal IgM Abs protects *α1,3Gt*$^{-/-}$ mice from *Plasmodium* infection. This suggests that relative absence of anti-α-gal IgM Abs in children under the age of 3-4 years compared to adults may help explain higher susceptibility malaria[33].

In contrast, the levels of circulating anti-α-gal IgG Abs found in individuals from a malaria endemic region as well as in *α1,3Gt*$^{-/-}$ mice colonized with the α-gal glycan expressing *E. coli* O86:B7 are ~30 fold and ~40-70-fold, respectively, lower than levels of anti-α-gal IgM Abs. This may help to explain why anti-α-gal IgG Abs are not associated with decreased risk of *P. falciparum* infection in this study. This also suggests that infection by *P. falciparum* in malaria endemic regions fails to induce class switch for the production of anti-α-gal IgG Abs. However, when present above a certain threshold level, anti-α-gal IgG Abs are also protective against malaria transmission as shown in the murine model. We found that this protective effect can be further enhanced by immunization protocols favoring the

production of complement-fixing subclasses of anti-α-gal IgG Abs. In this regard, immunization of *α1,3Gt*$^{-/-}$ mice with rRBCM emulsified in complete Freund´s adjuvant (CFA) supplemented with the Toll like receptor 9 agonist CpG, enhanced the anti-α-gal IgG2b and IgG3 Ab response 2-3 fold *vs.* immunization without adjuvant and with association of 88% reduction in the relative risk of infection *vs.* 61% reduction upon immunization without adjuvant. Immunization of *α1,3Gt*$^{-/-}$ mice using several different adjuvants also enhanced the anti-α-gal IgG Ab response (Chapter 3). However, this was not associated with increased protection against *Plasmodium* infection, suggesting that the protective effect of α-gal immunization can be enhanced in the presence of specific adjuvants, e.g. CpG, that favor the production of anti-α-gal Abs from specific IgG subclasses, i.e. IgG2b and IgG3.

While anti-α-gal Abs can provide sterile protection against malaria in mice (Chapter 3), this is not commonly observed in malaria endemic regions where, despite adult individuals have circulating anti-α-gal Abs, possibly these Abs are present at levels below a threshold level required to provide sterile protection. Nonetheless, we showed that this natural mechanism of protection can be enhanced via immunization using adjuvants that favor the production of T cell-dependent complement fixing anti-α-gal IgG Abs. Moreover, when coupled to other *Plasmodium* antigens, this approach should increase the immunogenicity[34] of such antigens. Furthermore, this approach should be useful in preventing not only individual infections as well as disease transmission[35].

It is important to emphasize that anti-α-gal Abs are not protective once *Plasmodium* sporozoites reach the bloodstream or during the later erythrocytic stage of the infection. The lack of protection against

Plasmodium sporozoites in the bloodstream might be related with the short time frame required to reach the liver[36], which may not allow for the efficient detection and targeting by anti-α-gal Abs. Additionally, when *Plasmodium* sporozoites invade hepatocytes, they become covered with PV membrane, which is derived from the host hepatocyte plasma membrane and forms a barrier between the host cell cytosol and the parasite surface[37], thus protecting the parasite against the antagonistic environment of the host. Therefore, PV membrane might block the interaction of anti-α-gal Abs with *Plasmodium*, making Abs ineffective against parasites. In the same extent, during erythrocytic stage of the infection when *Plasmodium* infects RBCs, both PV membrane and the RBC membrane also protect the parasite. Two layers of membrane might contribute to render *Plasmodium* inaccessible for anti-α-gal Abs and hence, to abrogate protection at this stage of infection.

Complement-mediated cytotoxicity was shown to be the prevalent mechanism mediating the protective effect of anti-α-gal Abs against *Plasmodium* infection (Chapter 4). When bound to *Plasmodium* sporozoites, anti-α-gal Abs activate the complement system, which is cytotoxic to sporozoites and inhibits *Plasmodium* migration through hepatocytes and the establishment of intracellular hepatocyte infection.

These observations led us to propose the following model: when inoculated in the dermis via the bite of a female *Anopheles* mosquitoe[38] *Plasmodium* sporozoites migrate to the liver in a matter of 15 minutes to a few hours[39,40]. As the *Anopheles* mosquitoes probes for a blood meal, it leads to the formation of edema and eventually micro-hematomas, i.e. a collection of blood outside of a blood vessel, inside the skin[41]. This might contribute to the mobilization of anti-α-gal Abs and complement components from blood circulation into the skin, allowing for sporozoites to be tagged by

anti-α-gal Abs that in turn activate the complement system and as a consequence, *Plasmodium* sporozoites lose their ability to reach the liver to establish a successful hepatocyte infection. For those sporozoites that spend very little time (only a couple of minutes) in the skin and rapidly reach to blood circulation, they are able to succeed an infection in the host.

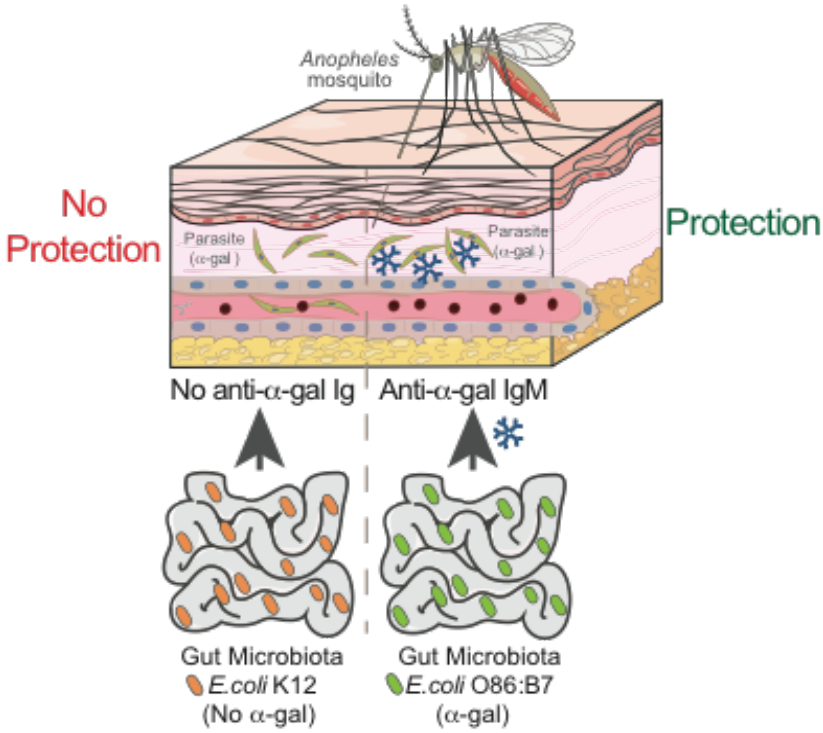

Figure 6.1 Protective effect of anti-α-gal Abs at the skin level is driven by the gut flora. An *Anopheles* mosquito deposits *Plasmodium* sporozoites into the dermis of the mammalian host. When sporozoites encounter anti-α-gal IgM Abs, induced upon gut colonization, they lose their infectivity and are not able to infect the host. Gut colonization with bacteria do not express α-gal does not induce anti-α-gal Abs production and hence, *Plasmodium* is able to successfully infect the host.

Under Chapter 5, we examined the connection between anti-α-gal Abs and the gut flora. The presence of high levels of circulating anti-α-gal Abs throughout life, as seen in malaria endemic areas, has led us to ask whether these Abs could arise from a continuous exposure to specific components

of the gut flora, as enteric bacteria expressing α-gal[42]. We initially observed that, when kept under specific pathogen-free conditions, *α1,3Gt*$^{-/-}$ mice can produce only residual levels of circulating anti-α-gal Abs, below 0.01-1μg/mL (Chapter 3)[43]. These mice are exposed to strict controlled food and environmental conditions that apparently maintain the gut flora of mice at a constant steady state of composition over time. Presumably, these mice have low number of bacteria expressing α-gal in their gut flora allowing for the production of anti-α-gal Abs. However, in this study the gut flora of *α1,3Gt*$^{-/-}$ mice was not characterized for the presence of bacteria expressing α-gal. Additionally, a microbial imbalance of the intestinal gut flora, i.e. dysbiosis, could promote the growth of pathobiont bacterial strains such as *Proteobacteria* or adherent/invasive *E. coli* that could in turn influence the production of circulating anti-α-gal Abs. However, dysbiosis is not likely to occur under these controlled conditions in mice[44,45] when it is induced there is no effect on levels of anti-α-gal Abs. In contrast, the situation in humans is quite different. Humans are continuously exposed to a complex consortia of bacteria (pathogenic or non-pathogenic) that form the microbiota that can quickly change depending on the daily diet, a major factor influencing the composition and metabolism of the colonic microbiota[46].

To test whether specific components of human enteric α-gal expressing bacteria can induce the production of anti-α-gal Abs, we introduced an α-gal expressing pathobiont into the gut of *α1,3Gt*$^{-/-}$ mice, which resulted in the effective production of anti-α-gal IgM Abs. This shows that specific components of the human gut microbiota expressing α-gal can trigger the production of anti-α-gal Abs. It should be noted that circulating anti-α-gal IgM Abs are detected in non-colonized *α1,3Gt*$^{-/-}$ mice maintained under GF conditions, confirming that these are natural Abs. Interestingly, the levels

of anti-α-gal IgM NAbs, presumably produced by the natural Abs producing B1 cells, are significantly higher in SPF *vs.* GF *α1,3Gt*$^{-/-}$ mice. This suggests that specific stimulation driven by the gut flora is required for further stimulation of B1 cells to mount additional IgM responses and that this stimulation can depend on gut colonization by specific strains of bacteria. However, this is not the case for anti-α-gal IgG Abs, as these antibodies are not produced upon gut colonization by bacteria expressing α-gal.

We then asked whether the gut flora could control the activation of anti-α-gal B cells to afford protection against *Plasmodium* infection **(Figure 6.1)**. We found that the anti-α-gal IgM Abs produced upon gut colonization by *E. coli* O86.B7 confers protection against *Plasmodium* infection in antibiotic treated SFP as well as in GF mono-colonized mice. Our results are consistent with previous findings on oral inoculation of *E. coli* O86.B7 and indicate that *α1,3Gt*$^{-/-}$ mice may be useful to elucidate the role of these Abs, mainly of the IgM subclass, in human resistance mechanisms to pathogens that expresses α-gal. Gut colonization by α-gal expressing bacteria thus leads to the production of anti-α-gal IgM Abs, comparable in titer and cytolytic activity to that of human serum, conferring protection against *Plasmodium* infection in GF or antibiotic treated SPF groups. This suggests that *E. coli* O86.B7 colonization in *α1,3Gt*$^{-/-}$ mice can recapitulate the normal etiology of anti-α-gal IgM Ab production in humans.

6.2 Some Ideas for the Future Studies

The main finding in this dissertation was that anti-α-gal Abs confer protection against *Plasmodium* infection. However, we believe that this study will largely assist to future studies investigating other vector-borne protozoan parasites expressing α-gal such as *Leishmania spp.* and

Trypanosoma spp., the causative agents of Leishmaniasis and Trypanosomiasis, respectively[13]. Similar vaccination approaches as the ones developed under this PhD thesis may be considered against these infectious diseases. In a similar manner, other naturally occurring anti-glycan Abs should be considered to test the protective role against pathogens including bacteria, viruses and protozoan parasites.

While detected on the *Plasmodium* surface the mechanism responsible for introducing α-gal glycan in *Plasmodium* proteins or lipids was not determined. Although we have speculated that the expression of α-gal in *Plasmodium* could be inherited from mosquito's components the origin of α-gal glycan in *Plasmodium* needs to be further characterized.

The protective effect associated with immunization against α-gal was enhanced using protocols of immunization that incorporate adjuvants such as the CpG, a TLR9 agonist. This shows that the Abs response driven by α-gal immunization can be enhanced, paving the way for the generation of an improved vaccine against *Plasmodium* infection via modulation of the natural anti-α-gal Ab response. This will promise to profoundly enhance the protective immune response currently obtained via immunization with protein/sub-unit vaccine formulations such as CSP, the core antigenic components of the RTS,S vaccine. This type of immunization protocol can enhance the generation of a robust, long-lasting, T cell-dependent, complement fixing, cytotoxic anti-α-gal and anti-CSP Abs targeting *Plasmodium* sporozoites in the skin as well as the generation of T_H and T_C cells targeting the liver stage of infection, supporting the notion of α-gal epitopes can increase the protective effect of the RTS,S vaccine, which is initially very low[2,47,48]. The relative efficacy of this approach can be tested in murine models as well as in humans. Moreover, the inhibiting capacity of

anti-α-gal Abs from rodents as well as from protected volunteers can also be tested functionally with *in vitro* assays.

Protection against *Plasmodium* infection, as driven by anti-α-gal Abs, is complement and/or PMN cell dependent. It is likely that Fc receptors expressed by PMN cells may be involved in the mechanism via which anti-α-gal Abs confer protection against *Plasmodium* infection. Accordingly, studies related to xenotransplantation revealed that anti-α-gal Abs can mediate xenograft rejection via mechanisms involving Fcγ receptor[49]. Our results showed that anti-α-gal IgG3 Abs are partially protective in the absence of complement or PMN cells in contrast to a study that reported anti-α-gal IgG3 Abs to be strictly complement dependent. Nevertheless, this result led us to think that there might be other immune cells, i.e. NK cells, providing a partial protection against *Plasmodium* infection in presence of anti-α-gal IgG3 Abs. Therefore, investigating the role of NK cells and FcγR in context of anti-α-gal IgG3 mediated protection should be considered as a next step.

Our comprehension of dynamics of the gut microbiota is still scarce and its physiological action and its role in certain diseases have been neglected until recently. However, today, scientists attempt to resolve it by many leading works on the interaction of the microflora with its host. In this context, one of the mysteries that require more attention is the role of the gut flora on the production of NAbs. Here, we showed that gut colonization by one specific strain of bacteria is able to induce the production of anti-α-gal NAbs that in turn elicit protective mechanisms against infection by a protozoan parasite. Other bacterial strains may also induce the generation of NAbs, apart from anti-α-gal Abs, and confer protection against different pathogens. This should be further explored.

In sum, this thesis provides original experimental evidence on the protective role of NAbs elicited by the gut flora against an infectious agent. It opens new doors to be explored in the light of biological science. Similar vaccination approaches as the one proposed hereby for malaria may be tested against other vector-borne protozoan parasites expressing α-gal, such as *Leishmania spp.* and *Trypanosoma spp.*

References

1. WHO, W.H.O. World Malaria Report. 284 (2013).
2. Rts, S.C.T.P., *et al.* A phase 3 trial of RTS,S/AS01 malaria vaccine in African infants. *The New England journal of medicine* **367**, 2284-2295 (2012).
3. Varki, A. Biological roles of oligosaccharides: all of the theories are correct. *Glycobiology* **3**, 97-130 (1993).
4. Springer, S.A. & Gagneux, P. Glycan evolution in response to collaboration, conflict, and constraint. *The Journal of biological chemistry* **288**, 6904-6911 (2013).
5. Bishop, J.R. & Gagneux, P. Evolution of carbohydrate antigens--microbial forces shaping host glycomes? *Glycobiology* **17**, 23R-34R (2007).
6. Cywes-Bentley, C., *et al.* Antibody to a conserved antigenic target is protective against diverse prokaryotic and eukaryotic pathogens. *Proc Natl Acad Sci U S A* **110**, E2209-2218 (2013).
7. Collins, B.H., *et al.* Cardiac xenografts between primate species provide evidence for the importance of the alpha-galactosyl determinant in hyperacute rejection. *J Immunol* **154**, 5500-5510 (1995).
8. Cooper, D.K., Koren, E. & Oriol, R. Oligosaccharides and discordant xenotransplantation. *Immunological reviews* **141**, 31-58 (1994).

9. Galili, U., Tibell, A., Samuelsson, B., Rydberg, L. & Groth, C.G. Increased anti-Gal activity in diabetic patients transplanted with fetal porcine islet cell clusters. *Transplantation* **59**, 1549-1556 (1995).
10. Good, A.H., *et al.* Identification of carbohydrate structures that bind human antiporcine antibodies: implications for discordant xenografting in humans. *Transplantation proceedings* **24**, 559-562 (1992).
11. Sandrin, M.S., Vaughan, H.A., Dabkowski, P.L. & McKenzie, I.F. Anti-pig IgM antibodies in human serum react predominantly with Gal(alpha 1-3)Gal epitopes. *Proceedings of the National Academy of Sciences of the United States of America* **90**, 11391-11395 (1993).
12. Hamadeh, R.M., *et al.* Human natural anti-Gal IgG regulates alternative complement pathway activation on bacterial surfaces. *The Journal of clinical investigation* **89**, 1223-1235 (1992).
13. Avila, J.L., Rojas, M. & Galili, U. Immunogenic Gal alpha 1----3Gal carbohydrate epitopes are present on pathogenic American Trypanosoma and Leishmania. *J Immunol* **142**, 2828-2834 (1989).
14. Couto, A.S., Goncalves, M.F., Colli, W. & de Lederkremer, R.M. The N-linked carbohydrate chain of the 85-kilodalton glycoprotein from Trypanosoma cruzi trypomastigotes contains sialyl, fucosyl and galactosyl (alpha 1-3)galactose units. *Molecular and biochemical parasitology* **39**, 101-107 (1990).
15. Ramasamy, R. Studies on glycoproteins in the human malaria parasite Plasmodium falciparum--lectin binding properties and the possible carbohydrate-protein linkage. *Immunology and cell biology* **65 (Pt 2)**, 147-152 (1987).
16. Ramasamy, R. & Reese, R.T. Terminal galactose residues and the antigenicity of Plasmodium falciparum glycoproteins. *Molecular and biochemical parasitology* **19**, 91-101 (1986).
17. Ravindran, B., Satapathy, A.K. & Das, M.K. Naturally-occurring anti-alpha-galactosyl antibodies in human Plasmodium falciparum

infections--a possible role for autoantibodies in malaria. *Immunology letters* **19**, 137-141 (1988).

18. Almeida, I.C., Milani, S.R., Gorin, P.A. & Travassos, L.R. Complement-mediated lysis of Trypanosoma cruzi trypomastigotes by human anti-alpha-galactosyl antibodies. *J Immunol* **146**, 2394-2400 (1991).
19. Gazzinelli, R.T., *et al.* Anti-Trypanosoma cruzi and anti-laminin antibodies in chagasic patients after specific treatment. *Journal of clinical microbiology* **26**, 1795-1800 (1988).
20. Avila, J.L. alpha-Galactosyl-bearing epitopes as potent immunogens in Chagas' disease and leishmaniasis. *Sub-cellular biochemistry* **32**, 173-213 (1999).
21. Shinkel, T.A., *et al.* Changes in cell surface glycosylation in alpha1,3-galactosyltransferase knockout and alpha1,2-fucosyltransferase transgenic mice. *Transplantation* **64**, 197-204 (1997).
22. Tearle, R.G., *et al.* The alpha-1,3-galactosyltransferase knockout mouse. Implications for xenotransplantation. *Transplantation* **61**, 13-19 (1996).
23. Towbin, H., *et al.* Circulating antibodies to mouse laminin in Chagas disease, American cutaneous leishmaniasis, and normal individuals recognize terminal galactosyl(alpha 1-3)-galactose epitopes. *The Journal of experimental medicine* **166**, 419-432 (1987).
24. Warburg, A., Shtern, A., Cohen, N. & Dahan, N. Laminin and a Plasmodium ookinete surface protein inhibit melanotic encapsulation of Sephadex beads in the hemocoel of mosquitoes. *Microbes and infection / Institut Pasteur* **9**, 192-199 (2007).
25. Angrisano, F., Tan, Y.H., Sturm, A., McFadden, G.I. & Baum, J. Malaria parasite colonisation of the mosquito midgut--placing the Plasmodium ookinete centre stage. *International journal for parasitology* **42**, 519-527 (2012).
26. Nacer, A., Walker, K. & Hurd, H. Localisation of laminin within Plasmodium berghei oocysts and the midgut epithelial cells of Anopheles stephensi. *Parasites & vectors* **1**, 33 (2008).

27. Ramasamy, R. & Field, M.C. Terminal galactosylation of glycoconjugates in Plasmodium falciparum asexual blood stages and Trypanosoma brucei bloodstream trypomastigotes. *Exp Parasitol* **130**, 314-320 (2012).
28. Schulman, S., Oppenheim, J.D. & Vanderberg, J.P. Plasmodium berghei and Plasmodium knowlesi: serum binding to sporozoites. *Exp Parasitol* **49**, 420-429 (1980).
29. Ashwell, G. & Morell, A.G. The role of surface carbohydrates in the hepatic recognition and transport of circulating glycoproteins. *Advances in enzymology and related areas of molecular biology* **41**, 99-128 (1974).
30. Verhage, D.F., *et al.* Clinical outcome of experimental human malaria induced by Plasmodium falciparum-infected mosquitoes. *Neth J Med* **63**, 52-58 (2005).
31. Sauerwein, R.W., Roestenberg, M. & Moorthy, V.S. Experimental human challenge infections can accelerate clinical malaria vaccine development. *Nat Rev Immunol* **11**, 57-64 (2011).
32. Rickman, L.S., *et al.* Plasmodium falciparum-infected Anopheles stephensi inconsistently transmit malaria to humans. *The American journal of tropical medicine and hygiene* **43**, 441-445 (1990).
33. Modiano, D., *et al.* Different response to Plasmodium falciparum malaria in west African sympatric ethnic groups. *Proc Natl Acad Sci U S A* **93**, 13206-13211 (1996).
34. Benatuil, L., *et al.* The influence of natural antibody specificity on antigen immunogenicity. *Eur J Immunol* **35**, 2638-2647 (2005).
35. Olotu, A., *et al.* Four-year efficacy of RTS,S/AS01E and its interaction with malaria exposure. *N Engl J Med* **368**, 1111-1120 (2013).
36. Shin, S.C., Vanderberg, J.P. & Terzakis, J.A. Direct infection of hepatocytes by sporozoites of Plasmodium berghei. *The Journal of protozoology* **29**, 448-454 (1982).

37. Lingelbach, K. & Joiner, K.A. The parasitophorous vacuole membrane surrounding Plasmodium and Toxoplasma: an unusual compartment in infected cells. *Journal of cell science* **111 (Pt 11)**, 1467-1475 (1998).
38. Menard, R., *et al.* Looking under the skin: the first steps in malarial infection and immunity. *Nature reviews. Microbiology* **11**, 701-712 (2013).
39. Amino, R., *et al.* Quantitative imaging of Plasmodium transmission from mosquito to mammal. *Nature medicine* **12**, 220-224 (2006).
40. Gueirard, P., *et al.* Development of the malaria parasite in the skin of the mammalian host. *Proceedings of the National Academy of Sciences of the United States of America* **107**, 18640-18645 (2010).
41. Jin, Y., Kebaier, C. & Vanderberg, J. Direct microscopic quantification of dynamics of Plasmodium berghei sporozoite transmission from mosquitoes to mice. *Infection and immunity* **75**, 5532-5539 (2007).
42. Galili, U., Mandrell, R.E., Hamadeh, R.M., Shohet, S.B. & Griffiss, J.M. Interaction between human natural anti-alpha-galactosyl immunoglobulin G and bacteria of the human flora. *Infection and immunity* **56**, 1730-1737 (1988).
43. Chiang, T.R., *et al.* Anti-Gal antibodies in humans and 1, 3alpha-galactosyltransferase knock-out mice. *Transplantation* **69**, 2593-2600 (2000).
44. Craven, M., *et al.* Inflammation drives dysbiosis and bacterial invasion in murine models of ileal Crohn's disease. *PloS one* **7**, e41594 (2012).
45. Martinez-Medina, M., *et al.* Western diet induces dysbiosis with increased E coli in CEABAC10 mice, alters host barrier function favouring AIEC colonisation. *Gut* **63**, 116-124 (2014).
46. David, L.A., *et al.* Diet rapidly and reproducibly alters the human gut microbiome. *Nature* **505**, 559-563 (2014).
47. Agnandji, S.T., *et al.* First results of phase 3 trial of RTS,S/AS01 malaria vaccine in African children. *The New England journal of medicine* **365**, 1863-1875 (2011).

48. Rts, S.C.T.P. Efficacy and safety of the RTS,S/AS01 malaria vaccine during 18 months after vaccination: a phase 3 randomized, controlled trial in children and young infants at 11 African sites. *PLoS medicine* **11**, e1001685 (2014).
49. Ding, J.W., *et al.* Hyperacute rejection by anti-Gal IgG1, IgG2a, and IgG2b is dependent on complement and Fc-gamma receptors. *J Immunol* **180**, 261-268 (2008).

Appendix

Article

Cell

Gut Microbiota Elicits a Protective Immune Response against Malaria Transmission

Bahtiyar Yilmaz,[1] Silvia Portugal,[2] Tuan M. Tran,[2] Raffaella Gozzelino,[1] Susana Ramos,[1] Joana Gomes,[1,3] Ana Regalado,[1] Peter J. Cowan,[4,5] Anthony J.F. d'Apice,[4,5] Anita S. Chong,[6] Ogobara K. Doumbo,[7] Boubacar Traore,[7] Peter D. Crompton,[2] Henrique Silveira,[3] and Miguel P. Soares[1,*]

[1]Instituto Gulbenkian de Ciência, Rua da Quinta Grande, 6, 2780-156 Oeiras, Portugal

[2]Laboratory of Immunogenetics, National Institute of Allergy and Infectious Diseases, National Institutes of Health, Twinbrook II, Room 125, 12441 Parklawn Drive, Rockville, MD 20852-8180, USA

[3]Centro de Malaria e Outras Doenças Tropicais, Instituto de Higiene e Medicina Tropical, Universidade Nova de Lisboa, Rua da Junqueira, 100, 1349-008 Lisboa, Portugal

[4]Immunology Research Centre, St. Vincent's Hospital, Fitzroy, Melbourne, VIC 3065, Australia

[5]Department of Medicine, University of Melbourne, Parkville, VIC 2900, Australia

[6]Section of Transplantation, Department of Surgery, University of Chicago, 5841 South Maryland Avenue, Chicago, IL 60637, USA

[7]Mali International Center of Excellence in Research, University of Sciences, Techniques and Technologies of Bamako, 1805 Bamako, Mali

*Correspondence: mpsoares@igc.gulbenkian.pt

http://dx.doi.org/10.1016/j.cell.2014.10.053

This is an open access article under the CC BY-NC-ND license (http://creativecommons.org/licenses/by-nc-nd/3.0/).

SUMMARY

Glycosylation processes are under high natural selection pressure, presumably because these can modulate resistance to infection. Here, we asked whether inactivation of the UDP-galactose:β-galactoside-α1-3-galactosyltransferase (*α1,3GT*) gene, which ablated the expression of the Galα1-3Galβ1-4GlcNAc-R (α-gal) glycan and allowed for the production of anti-α-gal antibodies (Abs) in humans, confers protection against *Plasmodium spp.* infection, the causative agent of malaria and a major driving force in human evolution. We demonstrate that both *Plasmodium spp.* and the human gut pathobiont *E. coli* O86:B7 express α-gal and that anti-α-gal Abs are associated with protection against malaria transmission in humans as well as in *α1,3GT*-deficient mice, which produce protective anti-α-gal Abs when colonized by *E. coli* O86:B7. Anti-α-gal Abs target *Plasmodium* sporozoites for complement-mediated cytotoxicity in the skin, immediately after inoculation by *Anopheles* mosquitoes. Vaccination against α-gal confers sterile protection against malaria in mice, suggesting that a similar approach may reduce malaria transmission in humans.

INTRODUCTION

Humans have relatively high levels of circulating antibodies (Abs) recognizing xeno-glycans expressed by pathogens (Oyelaran et al., 2009). As for other antigens, xeno-glycans cannot be targeted by the immune system when also expressed as self-glycans. This limitation can be bypassed by natural selection of mutations that inactivate the expression of self-glycans (Bishop and Gagneux, 2007). Presumably, natural selection of such loss-of-function mutations tailored the human anti-glycan immune repertoire through evolution (Bishop and Gagneux, 2007). This notion is supported by the inactivation of the cytidine monophosphate-N-acetylneuraminic acid hydroxylase-like (*CMAH*) gene in humans, which suppressed the expression of N-glycolylneuraminic acid (Neu5Gc) (Hayakawa et al., 2001) and allowed for immune reactivity against Neu5Gc (Tangvoranuntakul et al., 2003). In a similar manner, inactivation of the *α1,3GT* gene, which suppressed the expression of the Galα1-3Galβ1-4GlcNAc-R (α-gal) carbohydrate in ancestral anthropoid primates that gave rise to humans (Galili and Swanson, 1991), also allowed for immune reactivity against α-gal (Galili et al., 1984). While it has been argued that this evolutionary process is driven to a large extent by the acquisition of immune-resistance against pathogens expressing such glycans (Bishop and Gagneux, 2007; Cywes-Bentley et al., 2013), this was never tested experimentally.

Humans do not express α-gal and up to 1%–5% of the repertoire of circulating immunoglobulin M (IgM) and immunoglobulin G (IgG) in healthy adults is directed against this glycan (Macher and Galili, 2008). Production of α-gal-specific Abs is thought to be driven by exposure to bacterial components of the microbiota expressing α-gal (Macher and Galili, 2008), including specific members of the *Klebsiella spp.*, *Serratia spp.*, and *Escherichia coli spp.* (Galili et al., 1988). Expression of α-gal by these *Enterobacteriaceae* is associated with the bacterial capsule and cell wall glycoproteins, as well as with lipopolysaccharide (LPS) (Galili et al., 1988). Gut colonization by the human pathobiont *E. coli* O86:B7 (Pal et al., 1969) recapitulates the etiology of anti-α-gal Ab production in mice (Posekany et al., 2002) and in primates (Mañez et al., 2001), as well as the production of Abs directed against the α-gal-related anti-B blood group glycan in chickens

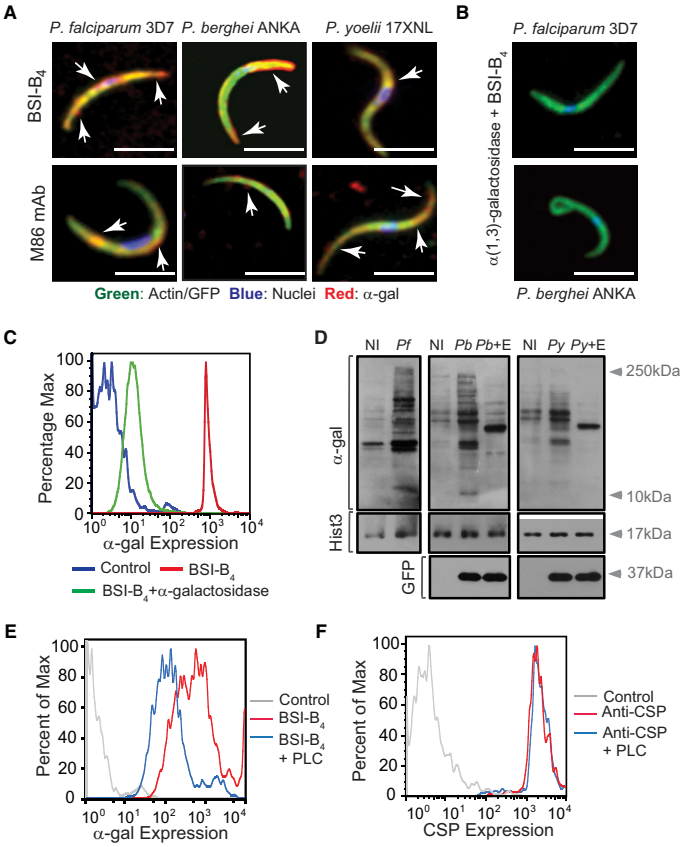

Figure 1. Detection of α-Gal in *Plasmodium* Sporozoites

(A) Composite images of GFP/actin (green), α-gal (red; white arrows), and DNA (blue) in *Plasmodium* sporozoites.

(B) Same staining as (A), after removal of α-gal by α-galactosidase. Images are representative of 2–3 independent experiments. Scale bar, 5 μm.

(C) Detection of α-gal in *Pb*A$^{Hsp70\text{-}GFP}$ sporozoites by flow cytometry, representative of three independent experiments.

(D) Detection of α-gal in proteins extracted from salivary glands of noninfected (NI), *P. falciparum* 3D7 (*Pf*), *Pb*A$^{Hsp70\text{-}GFP}$ (*Pb*), or *P. yoelii* 17XNL (*Py*)-infected *A.* mosquitoes. Histone H3 (Hist3) and GFP were detected as loading controls. When indicated, α-gal was digested using α-galactosidase (E).

(E and F) Detection of α-gal (E) and CSP (F) in *Pb*A$^{Hsp70\text{-}GFP}$ sporozoites treated or not with phospholipase C (+PLC). Control is not stained. Data representative of 2–4 independent experiments.

See also Figure S1.

Malaria is transmitted to humans by the inoculation of *Plasmodium* sporozoites via the bite of female *Anopheles* (*A.*) mosquitoes (Ménard et al., 2013). While transmission may be rather efficient, only a fraction of the inoculated parasites manage to progress toward the establishment of infection (Rickman et al., 1990; Sauerwein et al., 2011; Verhage et al., 2005), hinting at a natural mechanism of protection that presumably targets the initial phases of the *Plasmodium* life cycle. Here, we demonstrate that production of anti-α-gal Abs in response to the gut *E. coli* O86:B7 pathobiont contributes critically to this natural defense mechanism, reducing malaria transmission by *A.* mosquitoes.

(Springer et al., 1959) and humans (Springer and Horton, 1969). This argues that gut colonization by *E. coli* O86:B7 may be particularly relevant in triggering the production of α-gal-specific Abs, presumably contributing to the high titers of these circulating Abs in healthy adult humans (Galili et al., 1988). Moreover, anti-α-gal Abs may also be produced in response to infection by pathogens expressing α-gal, such illustrated for gram-negative bacteria from *Salmonella spp.* or for protozoan parasites from *Trypanosoma spp.* (Avila et al., 1989).

Anti-α-gal Abs are cytotoxic toward α-gal-expressing pathogens, as demonstrated in vitro for bacteria (Galili et al., 1988), protozoan parasites (Avila et al., 1989), and viruses enveloped by xenogeneic α-gal-expressing cell membranes (Takeuchi et al., 1996). Whether anti-α-gal Abs confer resistance to these and/or other pathogens in vivo has, to the best of our knowledge, not been established. Here, we tested this hypothesis specifically for *Plasmodium spp.* infection, the causative agent of malaria and a major driving force that shaped the evolution of anthropoid primates, including humans.

RESULTS

Plasmodium spp. Express the α-Gal Glycan

The α-gal glycan was detected on the surface of *Plasmodium* sporozoites, as assessed by immunofluorescence for the human pathogen *Plasmodium falciparum* 3D7, as well as for the transgenic GFP-expressing strains of the rodent pathogens *Plasmodium berghei* ANKA (*Pb*A) or *Plasmodium yoelii* 17XNL, using the lectin *Bandeiraea* (*Griffonia*) *simplicifolia*-I isolectin IB$_4$ (BSI-B$_4$) (Galili et al., 1985) or an anti-α-gal monoclonal antibody (M86 mAb) (Galili et al., 1998) (Figure 1A; Figures S1A and S1B available online). Specificity of α-gal detection was confirmed by its enzymatic removal using α-galactosidase (Figures 1B and 1C). Expression of α-gal was associated with proteins, as assessed by western blot in whole-cell extracts from *P. falciparum* 3D7, *Pb*A, or *P. yoelii* 17XNL sporozoites

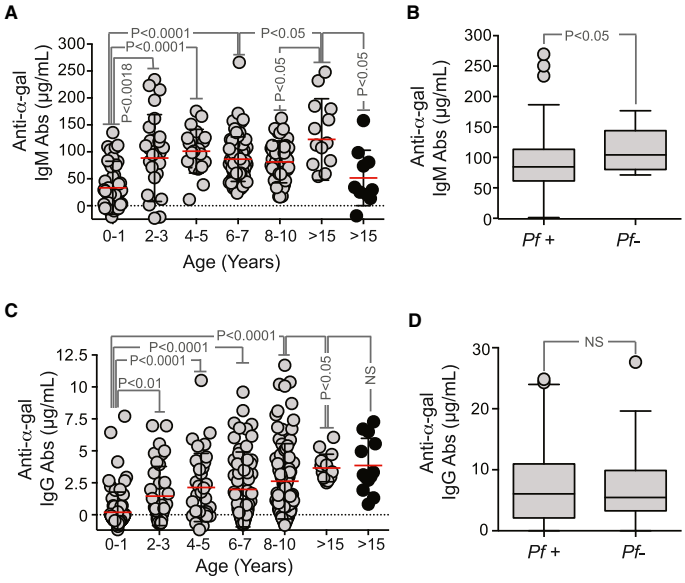

Figure 2. Anti-α-Gal IgM Abs Are Associated with Protection against Malaria Transmission in Individuals from a Malaria Endemic Region

(A) Anti-α-gal IgM Abs in individuals from a malaria endemic region in Mali (gray dots) or from the United States (black dots). Mean (red bars) ± SD.

(B) Levels of anti-α-gal IgM Abs in *P. falciparum*-infected (*Pf*+) versus noninfected (*Pf*−) children >4 years of age are shown as box plots in the same population as in (A).

(C) Anti-α-gal IgG Abs in individuals from a malaria endemic region in Mali (gray dots) or from the United States (black dots). Mean (red bars) ± SD.

(D) Levels of anti-α-gal IgG Abs in *P. falciparum*-infected (*Pf*+) versus noninfected (*Pf*−) children >4 years of age are shown as box plots in the same population as in (C).

(Figure 1D) and confirmed by enzymatic removal of α-gal (Figure 1D). Residual levels of α-gal were detected in the salivary glands of noninfected mosquitoes, suggesting that this glycan may be generated, at least partially, by *A.* mosquitoes (Figure 1D).

Expression of α-gal by *Pb*A sporozoites was reduced by ~4-fold when the glycosylphosphatidylinositol (GPI) anchor was cleaved by phospholipase C (PLC), as assessed by flow cytometry (Figure 1E). In contrast, GPI cleavage failed to reduce the expression of circumsporozoite protein (CSP), the main protein expressed at the surface of *Plasmodium* sporozoites (Figure 1F). This suggests that α-gal is bound to GPI-anchored surface proteins, including or not CSP, which despite being GPI-anchored (Moran and Caras, 1994) is resistant to PLC cleavage (Kimmel et al., 2003) (Figure 1F).

α-Gal-Specific IgM Abs Are Associated with Protection from *P. falciparum* Infection in Humans

We investigated whether a correlation exists between the levels of anti-α-gal Abs in healthy uninfected children and adults before the malaria season (n = 330 for IgG; n = 229 for IgM) and subsequent risk of *P. falciparum* infection (determined by biweekly PCR analysis of fingerprick blood samples) and febrile malaria (determined by weekly physical examination), during the ensuing 6 month malaria season in a cohort study in Mali, where this season is predictable and intense (Tran et al., 2014). In children <2 years, the average level of anti-α-gal IgM Abs was 33.4 μg/ml (95% confidence interval [CI]: 18.4–48.3 μg/ml) (Figure 2A), similar to that reported in children with no history of malaria exposure (Avila et al., 1992; Doenz et al., 2000; Galili et al., 1984; Parker et al., 1999). However, anti-α-gal IgM Abs increased with age, reaching an average of 123.03 μg/ml (95% CI: 79.3–166.7 μg/ml) in adults— more than twice the level reported in adults with no malaria exposure, i.e., 51.6 μg/ml (95% CI: 14.9–88.3 μg/ml) (Figure 2A) (Avila et al., 1992; Doenz et al., 2000; Galili et al., 1984; Parker et al., 1999). The average level of anti-α-gal IgM Abs in children >4 years of age who had no *P. falciparum* infections detected during the 6-month malaria season (n = 13) was higher than those who became infected (n = 141) (Figure 2B). This suggests that there is a positive correlation between the levels of anti-α-gal IgM Abs and incidence of *P. falciparum* infection.

The average level of anti-α-gal IgG Abs in children <2 years was 1.46 μg/ml (95% CI: 0.22–0.69 μg/ml) and increased in adults to 3.66 μg/ml (95% CI: 3.04–4.28 μg/ml) (Figure 2C). In contrast to IgM, the levels of circulating α-gal-specific IgG were similar between malaria-exposed and nonexposed adults, suggesting that *P. falciparum* infection fails to drive an IgG response directed against α-gal (Figure 2D). This also suggests that there is no correlation between anti-α-gal IgG Abs and incidence of *P. falciparum* infection. Time-to-event analysis did not show a correlation between α-gal-specific IgM and IgG levels before the malaria season and subsequent risk of *P. falciparum* infection (p = 0.76 and p = 0.08, respectively) or febrile malaria (p = 0.35 and p = 0.18, respectively).

Gut Colonization by *E. coli* O86:B7 Elicits a Protective α-Gal-Specific IgM Ab Response against Malaria Transmission

To test whether anti-α-gal IgM Abs are protective against malaria transmission, we took advantage of "human-like" *α1,3Gt*-deficient mice. Unlike humans, wild-type mice have a functional *α1,3Gt* gene and express α-gal on secreted and cell-surface glycoconjugates, suppressing the development of anti-α-gal immunity (Yang et al., 1998). Deletion of *α1,3Gt* gene eliminates α-gal (Tearle et al., 1996), allowing for anti-α-gal Ab production in *α1,3Gt*$^{-/-}$ mice (Chiang et al., 2000; Tearle et al., 1996; Yang

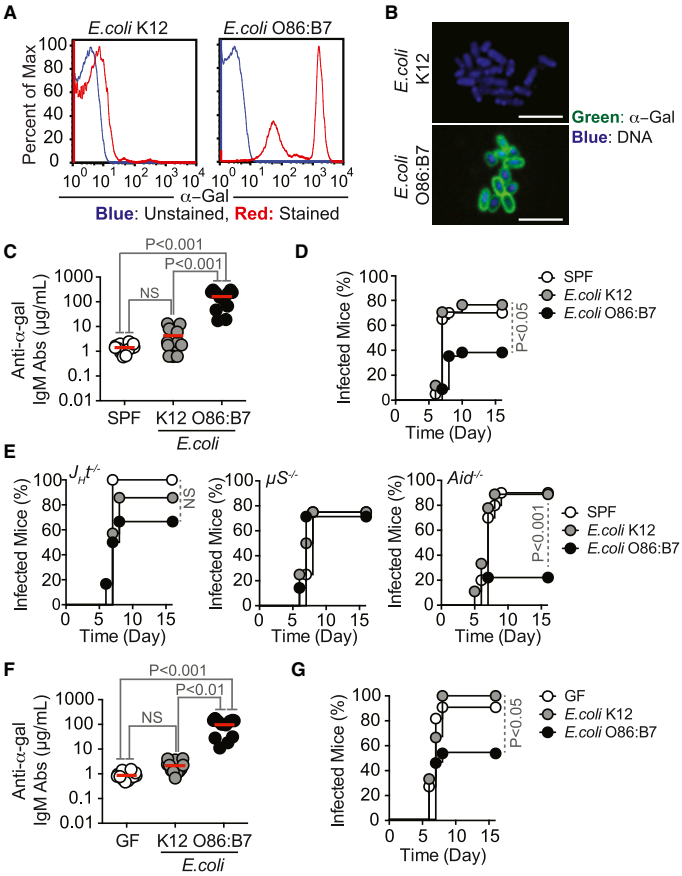

Figure 3. Gut Colonization by *E. coli* Expressing α-Gal Protects against *Plasmodium* Infection

(A and B) Detection of α-gal in *E. coli* strains by (A) flow cytometry and (B) immunofluorescence. Representative of 2–3 independent experiments. Composite images in (B), i.e., α-gal (green) and DNA (blue) at 100× magnification. Scale bar, 10 μm.

(C and D) $\alpha 1,3Gt^{-/-}$ mice maintained under SPF were treated with streptomycin for 7 days. (C) Anti-α-gal IgM Abs levels were measured in $\alpha 1,3Gt^{-/-}$ mice not colonized (SPF), colonized with *E. coli* K12, or colonized with O86.B7 strains (2–3 experiments; n = 12). (D) Incidence of blood stage of *Plasmodium* infection (%) in mice colonized as in (C) and exposed to *Pb*A$^{EEF1a\text{-}GFP}$-infected *A. stephensi* mosquitoes (four experiments; n = 17–34).

(E) Incidence of blood stage of *Plasmodium* infection (%) in $\alpha 1,3Gt^{-/-}J_HT^{-/-}$, $\alpha 1,3Gt^{-/-}Aid^{-/-}$, and $\alpha 1,3Gt^{-/-}\mu S^{-/-}$ mice colonized as in (C) and exposed to *Pb*A$^{Hsp70\text{-}GFP}$-infected *A. stephensi* mosquitoes (1–2 experiments; n = 4–10).

(F) Anti-α-gal IgM Abs were measured in GF $\alpha 1,3Gt^{-/-}$ mice not colonized (GF), colonized with *E. coli* K12, or colonized with O86.B7 strains (2–3 experiments; n = 12). (G) Incidence of blood stage of *Plasmodium* infection (%) in mice colonized as in (F) and exposed to *Pb*A$^{EEF1a\text{-}GFP}$-infected *A. stephensi* mosquitoes (four experiments; n = 9–13).

Mean (red bars).

See also Figure S2.

et al., 1998). However, $\alpha 1,3Gt^{-/-}$ mice are known to produce only residual levels of circulating anti-α-gal Abs when maintained under specific pathogen-free (SPF) conditions (Chiang et al., 2000). Production of anti-α-gal Abs can be enhanced upon enteric exposure to *E. coli* O86:B7 (Posekany et al., 2002). We confirmed that *E. coli* O86:B7 expresses high levels of α-gal (Yi et al., 2006), which is not the case for the *E. coli* K12 strain (Figures 3A and 3B). Colonization of $\alpha 1,3Gt^{-/-}$ mice by *E. coli* O86:B7 after antibiotic treatment (streptomycin sulfate; 5 g/l in drinking water for 7 days prior to colonization) increased the levels of circulating anti-α-gal IgM Abs from 1.4 μg/ml (95% CI: 1.1–1.8 μg/ml) to 162.9 μg/ml (95% CI: 95.89–230.1 μg/ml) before and after colonization, respectively (Figure 3C). Levels of anti-α-gal IgM Abs in colonized $\alpha 1,3Gt^{-/-}$ mice were in the range of adult individuals from a malaria endemic region (Figure 2A). In contrast, the levels of circulating anti-α-gal IgG Abs remained at residual levels, i.e., <1 μg/ml (Figure S2A), again in the range of adult individuals from a malaria endemic region (Figure 2C). Colonization by *E. coli* K12 did not induce the production of circulating anti-α-gal Abs (Figure 3C). Gut colonization by *E. coli* O86.B7 was associated with protection of $\alpha 1,3Gt^{-/-}$ mice from *Pb*A transmission by infected *Anopheles stephensi* mosquitoes (Figure 3D). This was not the case when $\alpha 1,3Gt^{-/-}$ mice were or were not colonized by *E. coli* K12 (Figure 3D).

To determine whether the protective effect associated with gut colonization by *E. coli* O86.B7 is mediated by anti-α-gal Abs, we performed similar colonization experiments in $\alpha 1,3Gt^{-/-}J_HT^{-/-}$ lacking B cells (Gu et al., 1993), $\alpha 1,3Gt^{-/-}\mu S^{-/-}$ mice lacking circulating IgM (Ehrenstein et al., 1998) or $\alpha 1,3Gt^{-/-}Aid^{-/-}$ mice that fail to undergo Ig class switch recombination or somatic hypermutation (Muramatsu et al., 2000). Gut colonization by *E. coli* O86.B7 failed to protect $\alpha 1,3Gt^{-/-}J_HT^{-/-}$ and $\alpha 1,3Gt^{-/-}\mu S^{-/-}$, but not $\alpha 1,3Gt^{-/-}Aid^{-/-}$ mice from *Pb*A-infected mosquitoes, as compared to genetic-matched control mice colonized or not by *E. coli* K12 (Figure 3E). This shows that the protective effect of gut colonization by *E. coli* O86.B7 acts via a mechanism mediated by anti-α-gal IgM Abs that do not undergo somatic hypermutation.

Germ-free (GF) $\alpha 1,3Gt^{-/-}$ mice had low but detectable levels of anti-α-gal IgM Abs, i.e., 0.87 μg/ml (95% CI: 0.66–1.1 μg/ml),

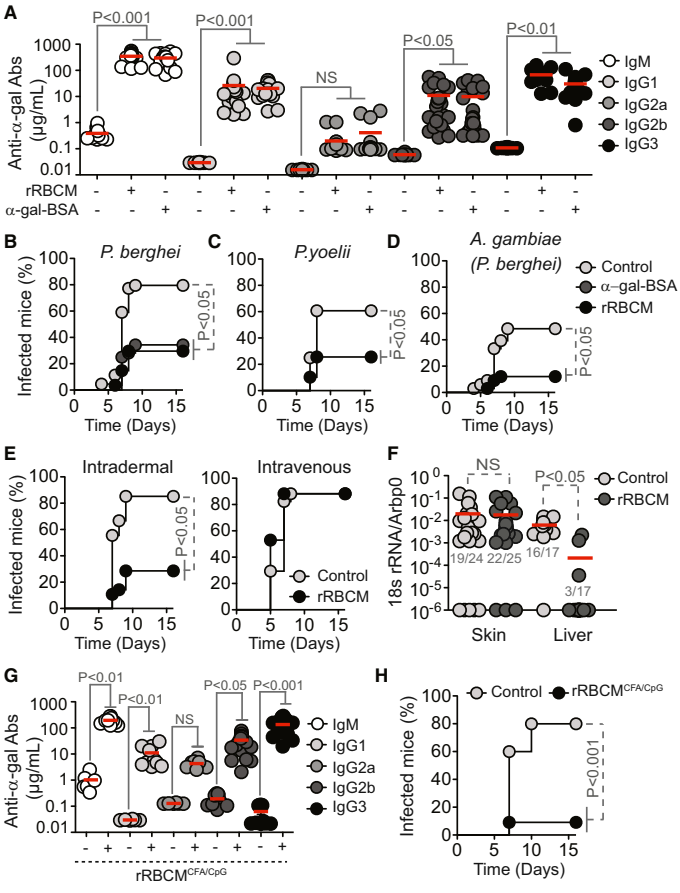

Figure 4. Protective Effect of α-Gal Immunization

(A) Anti-α-gal Abs in the serum of control (–) versus rRBCM (+) or α-gal-BSA (+) immunized *α1,3Gt*$^{-/-}$ mice (2–3 experiments; n = 12–29).

(B–D) Incidence of blood stage of infection (%) in *α1,3Gt*$^{-/-}$ mice treated as in (A) and exposed to (B) *Pb*A$^{EEF1a\text{-}GFP}$-infected *A. stephensi* mosquitoes (seven experiments; n = 27–44), (C) *P. yoelii* 17XNL-infected *A. stephensi* mosquitoes (five experiments; n = 28–39), or (D) *Pb*A$^{EEF1a\text{-}GFP}$-infected *A. gambiae* mosquitoes (four experiments; n = 27–34).

(E) Incidence of blood stage of infection (%) in nonimmunized (control) versus immunized (rRBCM) *α1,3Gt*$^{-/-}$ mice receiving *Pb*A$^{EEF1a\text{-}GFP}$ sporozoites (3–4 experiments; n = 17–28).

(F) *Plasmodium* 18 s rRNA/*Arbp0* mRNA in skin and liver of nonimmunized (control) versus immunized (rRBCM) *α1,3Gt*$^{-/-}$ mice exposed to *Pb*A$^{EEF1a\text{-}GFP}$-infected *A. stephensi* mosquitoes (3–5 experiments). Infected/total mice (gray nbrs).

(G) Same as (A) in control (–) versus immunized (+; rRBCM emulsified in CFA+CpG) *α1,3Gt*$^{-/-}$ mice (two experiments; n = 6–23).

(H) Incidence of blood stage of infection (%) in *α1,3Gt*$^{-/-}$ mice treated as in (G) and infected as in (B) (three experiments; n = 16–19). In (A), (F), and (G), dots are individual mice and mean (red bars). See also Figures S3 and S4.

suggesting that these are natural Abs (Figure 3F). The production of anti-α-gal IgM Abs in GF *α1,3Gt*$^{-/-}$ mice being driven by expression of these glycans in food components is possible, but this has not been tested. GF *α1,3Gt*$^{-/-}$ mice did not produce anti-α-gal IgG Abs (Figure S2C). Susceptibility to *Pb*A transmission by infected *A.* mosquitoes was similar in SPF versus GF *α1,3Gt*$^{-/-}$ mice (Figures 3D and 3G). When GF *α1,3Gt*$^{-/-}$ mice were monocolonized by *E. coli* O86:B7, the levels of circulating anti-α-gal IgM Abs increased to 96.62 μg/ml (95% CI: 59.32–133.9 μg/ml) (Figure 3F), which is the range in which adult individuals from a malaria endemic region (Figure 2A), without concomitant induction of anti-α-gal IgG Abs (Figure S2C). Monocolonization by *E. coli* O86:B7, but not by *E. coli* K12, protected *α1,3Gt*$^{-/-}$ mice from *Pb*A transmission by *A.* mosquitoes (Figure 3F). This suggests that gut colonization by a specific pathobiont expressing α-gal recapitulates to a large extent the normal etiology of the human anti-α-gal Ab response (Figure 2) and induces protection against *Plasmodium* infection, such as observed in a malaria endemic region (Figure 2).

It should be noted that the percentage of infected red blood cell (RBC), i.e., parasitemia, and incidence of mortality were similar among those *α1,3Gt*$^{-/-}$ mice that were infected by *Pb*A regardless of colonization (Figures S2B and S2D). This suggests that gut colonization by *E. coli* O86:B7 protects against *Plasmodium* transmission, but not against disease once the erythrocytic stage of infection is established.

Immunization against α-Gal Protects from *Plasmodium* Transmission

Immunization of *α1,3Gt*$^{-/-}$ mice against α-gal, using rabbit RBC membranes (rRBCM) expressing high levels of α-gal or synthetic α-gal conjugated to BSA (α-gal-BSA) elicited the production of circulating anti-α-gal IgM and IgG Abs (Figure 4A). Control *α1,3Gt*$^{+/+}$ mice failed to produce anti-α-gal Abs (Chiang et al., 2000; Tearle et al., 1996; Yang et al., 1998) (Figure S3A). Circulating anti-α-gal immunoglobulin A (IgA) and immunoglobulin E (IgE) Abs were undetectable in control or immunized *α1,3Gt*$^{-/-}$ and *α1,3Gt*$^{+/+}$ mice (data not shown). The concentration of anti-α-gal IgM Abs in the plasma of immunized *α1,3Gt*$^{-/-}$ mice was in the range of adult individuals from malaria endemic regions (Figure 2A). Circulating anti-α-gal IgG Abs in immunized

$\alpha 1,3Gt^{-/-}$ mice, predominantly from IgG1, IgG2b, and IgG3 subclasses, were present at higher concentrations, as compared to total IgG in adult individuals from malaria endemic regions. Little or no circulating IgG2a (Figure 4A) or IgG2c (data not shown) were detected in immunized $\alpha 1,3Gt^{-/-}$ mice.

Immunization against α-gal protected $\alpha 1,3Gt^{-/-}$ mice from *Pb*A (Figure 4B) and *P. yoelli* 17XNL (Figure 4C) transmission by infected *A. stephensi* mosquitoes, as well as from *Pb*A transmission by *A. gambiae* mosquitoes (Figure 4D) versus control nonimmunized $\alpha 1,3Gt^{-/-}$ mice. Control immunized $\alpha 1,3Gt^{+/+}$ mice were neither protected from *Pb*A (Figure S3B) nor *P. yoelli* 17XNL (Figure S3C) transmission by *A. stephensi* mosquitoes nor against *Pb*A transmission by *A. gambiae* mosquitoes (Figure S3D) versus naive $\alpha 1,3Gt^{+/+}$ mice.

Immunized $\alpha 1,3Gt^{-/-}$ mice were protected from artificial transmission of *Pb*A sporozoites via intradermal inoculation versus control nonimmunized $\alpha 1,3Gt^{-/-}$ mice (Figure 4E) or control immunized or nonimmunized $\alpha 1,3Gt^{+/+}$ mice (Figure S3E). Protection was no longer observed when sporozoites were inoculated intravenously (Figures 4E and S3E). This suggests that the protective effect of α-gal immunization is exerted in the dermis, presumably via an anti-α-gal Ab driven mechanism that is no longer effective once sporozoites reach the blood.

*Pb*A transmission was associated with accumulation of *Plasmodium* 18S rRNA at the site of inoculation, as quantified in the ear pinna by qRT-PCR (Figure 4F). The relative amount of *Plasmodium* 18S rRNA was similar in immunized versus control nonimmunized $\alpha 1,3Gt^{-/-}$ mice (Figure 4F) or control immunized or nonimmunized $\alpha 1,3Gt^{+/+}$ mice (Figure S3F). Immunized $\alpha 1,3Gt^{-/-}$ mice did not accumulate *Plasmodium* 18S rRNA in the liver, when compared to control nonimmunized $\alpha 1,3Gt^{-/-}$ mice (Figure 4F) or control nonimmunized or immunized $\alpha 1,3Gt^{+/+}$ mice (Figure S3F). This suggests that α-gal immunization arrests the transit of inoculated sporozoites from the skin into the liver, without interfering with sporozoite inoculation by *A.* mosquitoes.

TLR9 Agonist Adjuvant Enhances the Protective Effect of α-Gal Immunization

Immunization of $\alpha 1,3Gt^{-/-}$ mice with rRBCM emulsified in complete Freund's adjuvant (CFA), supplemented with toll-like receptor 9 agonist CpG, enhanced anti-α-gal IgG2b and IgG3 Ab response by 2- to 3-fold (Figure 4G) versus immunization without adjuvant (Figure 4A). This was associated with 88% reduction in the relative risk of transmission of *Pb*A infection by *A.* mosquitoes (95% CI: 0.032–0.452) versus 61% reduction upon immunization without adjuvant (95% CI: 0.209–0.726) (Figures 4B and 4H). This protective effect was not observed in control $\alpha 1,3Gt^{+/+}$ mice (Figures S3G and S3H).

Parasitemias were similar in immunized $\alpha 1,3Gt^{-/-}$ mice not protected from *Pb*A infection versus control nonimmunized $\alpha 1,3Gt^{-/-}$ mice as well as control nonimmunized or immunized $\alpha 1,3Gt^{+/+}$ mice (data not shown). Moreover, when infected, all mice succumbed to experimental cerebral malaria. This suggests that while protective against malaria transmission, α-gal immunization is not protective against the development of severe disease if *Plasmodium* manages to establish infection. In keeping with this notion, when inoculated with *Pb*A-infected RBC, immunized $\alpha 1,3Gt^{-/-}$ mice developed similar levels of parasitemia and disease severity, as compared to control nonimmunized $\alpha 1,3Gt^{-/-}$ mice as well as to control nonimmunized or immunized $\alpha 1,3Gt^{+/+}$ mice (Figure S4A).

We tested further whether the protective effect conferred by α-gal immunization is associated with sterile protection, i.e., inability of *Plasmodium* to establish blood stage of infection. Passive transfer of RBCs harvested from protected immunized $\alpha 1,3Gt^{-/-}$ mice at day 8–9 post-*Pb*A transmission by *A.* mosquitoes failed to transmit disease to naive $\alpha 1,3Gt^{-/-}$ mice (Figure S4B). In contrast, passive transfer of RBC harvested from nonprotected immunized $\alpha 1,3Gt^{-/-}$ mice, readily transmitted disease to naive $\alpha 1,3Gt^{-/-}$ mice (Figure S4B). This demonstrates that the protective effect of immunization against α-gal is associated with sterile protection against malaria.

Anti-α-Gal IgM and IgG Abs Produced in Response to α-Gal Immunization Confer Protection against Malaria Transmission

We asked whether the protective effect of α-gal immunization is mediated by anti-α-gal IgM and/or IgG Abs. Immunized $\alpha 1,3Gt^{-/-}J_HT^{-/-}$ mice failed to produce anti-α-gal IgM or IgG Abs versus naive $\alpha 1,3Gt^{-/-}J_HT^{-/-}$ mice or immunized $\alpha 1,3Gt^{-/-}$ mice (Figure 5A). Moreover, immunized $\alpha 1,3Gt^{-/-}J_HT^{-/-}$ mice were not protected against *Pb*A transmission by *A.* mosquitoes versus control nonimmunized $\alpha 1,3Gt^{-/-}J_HT^{-/-}$ mice (Figure 5B). This shows that the protective effect of α-gal immunization is mediated via a B cell-dependent mechanism.

Immunization of $\alpha 1,3Gt^{-/-}Aid^{-/-}$ mice failed to induce the production of anti-α-gal IgG, but not IgM Abs, versus naive $\alpha 1,3Gt^{-/-}Aid^{-/-}$ or immunized $\alpha 1,3Gt^{-/-}$ mice (Figure 5A). Immunized $\alpha 1,3Gt^{-/-}Aid^{-/-}$ mice were nevertheless protected against *Pb*A transmission by *A.* mosquitoes versus nonimmunized $\alpha 1,3Gt^{-/-}Aid^{-/-}$ mice (Figure 5B). This confirms that anti-α-gal IgM Abs can confer protection against malaria transmission (Figure 2B) and that the protective effect of α-gal-specific IgM Abs does not require somatic hypermutation.

Immunization of $\alpha 1,3Gt^{-/-}\mu S^{-/-}$ mice failed to induce anti-α-gal IgM Abs, without interfering with anti-α-gal IgG Ab response versus naive $\alpha 1,3Gt^{-/-}\mu S^{-/-}$ mice or immunized $\alpha 1,3Gt^{-/-}$ mice (Figure 5A). Immunized $\alpha 1,3Gt^{-/-}\mu S^{-/-}$ mice were nevertheless protected from *Pb*A transmission by *A.* mosquitoes versus control naive $\alpha 1,3Gt^{-/-}\mu S^{-/-}$ mice (Figure 5B). Immunized $\alpha 1,3Gt^{-/-}$ mice did not produce circulating anti-α-gal IgA or IgE Abs (data not shown) and a putative protective effect for these Ig isotypes was excluded. This demonstrates that anti-α-gal IgG Abs produced in response to immunization confer protection against malaria transmission.

Immunization of $\alpha 1,3Gt^{-/-}Tcr\beta^{-/-}$ mice lacking mature αβ T cells (Mombaerts et al., 1992) compromised anti-α-gal IgM and IgG response versus control immunized $\alpha 1,3Gt^{-/-}$ mice (Figure 5A). Immunized $\alpha 1,3Gt^{-/-}Tcr\beta^{-/-}$ mice were not protected from *Pb*A transmission by *A.* mosquitoes versus control naive $\alpha 1,3Gt^{-/-}Tcr\beta^{-/-}$ mice (Figure 5B). This shows that anti-α-gal Abs produced in response to immunization are T cell-dependent (Cretin et al., 2002) and so is their protective effect.

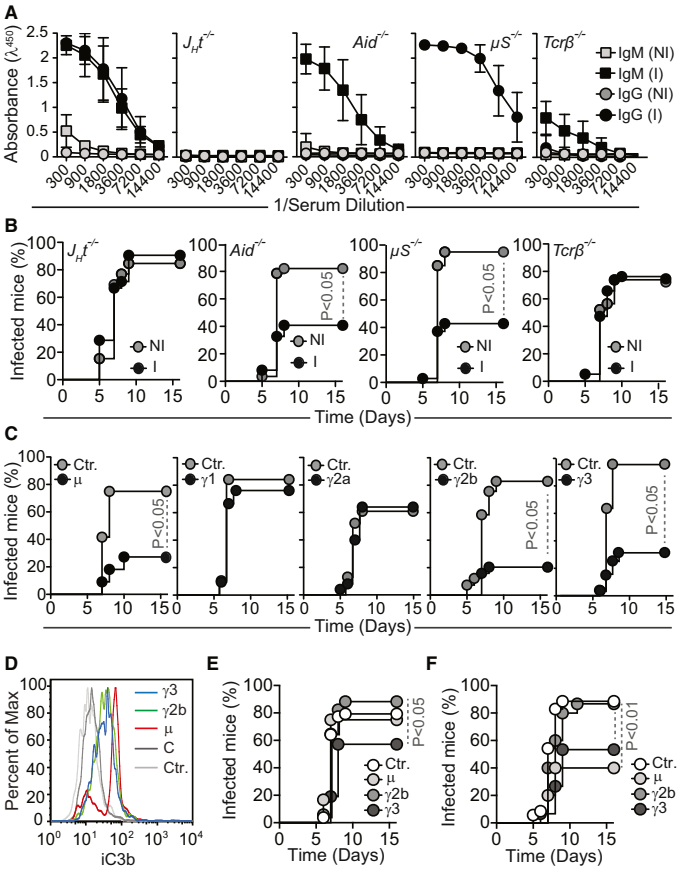

Figure 5. Protective Effect of Anti-α-Gal Abs

(A) Relative absorbance of anti-α-gal Abs (Mean ± SD) in serial serum dilutions from nonimmunized (NI) or rRBCM-immunized (I) *α1,3Gt*$^{-/-}$ mice (two experiments; n = 10).

(B) Incidence of blood stage infection (%) in specific immune component-deleted *α1,3Gt*$^{-/-}$ mice immunized (I) or not (NI) as in (A) and exposed to *Pb*A$^{EEF1a\text{-}GFP}$-infected mosquitoes (3–7 experiments; n = 13–41).

(C) Incidence of blood stage of infection (%) in *α1,3Gt*$^{-/-}$ mice after passive transfer of anti-α-gal Abs versus controls (no passive transfer; ctr.) exposed to *Pb*A$^{EEF1a\text{-}GFP}$-infected mosquitoes (4–7 experiments; n = 19–32).

(D) C3 deposition in *Pb*A$^{Hsp70\text{-}GFP}$ sporozoites not exposed (ctr.) or exposed to anti-α-gal Abs plus mouse complement (C). Representative of three independent experiments.

(E) Incidence of blood stage of infection (%) in *α1,3Gt*$^{-/-}$*C3*$^{-/-}$ mice after passive transfer of anti-α-gal IgM (μ), IgG2b (γ2b), or IgG3 (γ3) Abs versus controls (ctr.; no passive transfer) not receiving Abs, exposed to *Pb*A$^{EEF1a\text{-}GFP}$-infected mosquitoes (four experiments; n = 21–37).

(F) Same as (E) in PMN-depleted *α1,3Gt*$^{-/-}$ mice (four experiments; n = 15–25).

See also Figures S5 and S6.

face of *Plasmodium* sporozoites (Figure S6C). IgG2a, IgG2b, and IgG3 mAbs are class-switched mutants derived from the original anti-α-gal IgG1 clone and as such have similar affinities for α-gal (Ding et al., 2008). These data reveal that while IgM anti-α-gal Abs are sufficient per se to confer protection against malaria transmission, this protective effect can be enhanced when specific subclasses anti-α-gal IgG Abs are present at sufficient high levels.

Naive and immunized *α1,3Gt*$^{-/-}$*J*$_H$*T*$^{-/-}$ (Figure S5A), *α1,3Gt*$^{-/-}$*Aid*$^{-/-}$, (Figure S5B) and *α1,3Gt*$^{-/-}$*μS*$^{-/-}$ (Figure S5C) mice, not protected from *Pb*A transmission, developed similar levels of parasitemia and succumbed to experimental cerebral malaria. This was not the case for *α1,3Gt*$^{-/-}$*Tcrβ*$^{-/-}$ mice (Figure S5D), consistent with the involvement of T cells in the pathogenesis of experimental cerebral malaria (Belnoue et al., 2002).

Passive transfer of anti-α-gal IgM to naive *α1,3Gt*$^{-/-}$ mice conferred protection against *Pb*A transmission by *A. mosquitoes* (Figure 5C). This was also the case for passive transfer of anti-α-gal Abs from specific IgG subclasses, namely, IgG2b and IgG3 (Figure 5C), but not IgG1 or IgG2a (Figure 5C). Relative binding to α-gal was similar for all mAbs tested, as assessed by ELISA using α-gal-BSA as a solid-phase antigen (Figure S6A) or by immunofluorescence using *Pb*A sporozoites (Figure S6B). Specificity of anti-α-gal binding to *Plasmodium* sporozoites was assessed by enzymatic removal of α-gal, confirming that these mAbs recognize specifically and only the α-gal glycan on the sur-

Once bound to the surface of *Plasmodium* sporozoites, anti-α-gal IgM, IgG2b, and IgG3 mAbs activated the classical pathway of complement, as assessed by C3 deposition (Figure 5D). Anti-α-gal IgG1 or IgG2a mAbs failed to activate complement (data not shown), and complement activation was also not observed in the absence of anti-α-gal Abs (Figures 5D and S7), showing that the alternative and lectin pathways of complement are not activated by *Plasmodium* sporozoites.

We then asked whether the protective effect exerted by anti-α-gal Abs is mediated via a mechanism involving the activation of the complement cascade (Figure 5D) (Ding et al., 2008; Miyatake et al., 1998). Passive transfer of anti-α-gal IgM Abs or anti-α-gal IgG2b mAb to *α1,3Gt*$^{-/-}$*C3*$^{-/-}$ mice, which lack C3 and cannot activate the complement cascade, failed to confer protection against *Pb*A transmission versus control *α1,3G*$^{-/-}$*C3*$^{-/-}$ mice (Figure 5E). Passive transfer of anti-α-gal IgG3 mAb to *α1,3Gt*$^{-/-}$*C3*$^{-/-}$ mice conferred residual but significant protection versus control *α1,3G*$^{-/-}$*C3*$^{-/-}$ mice (Figure 5E). This

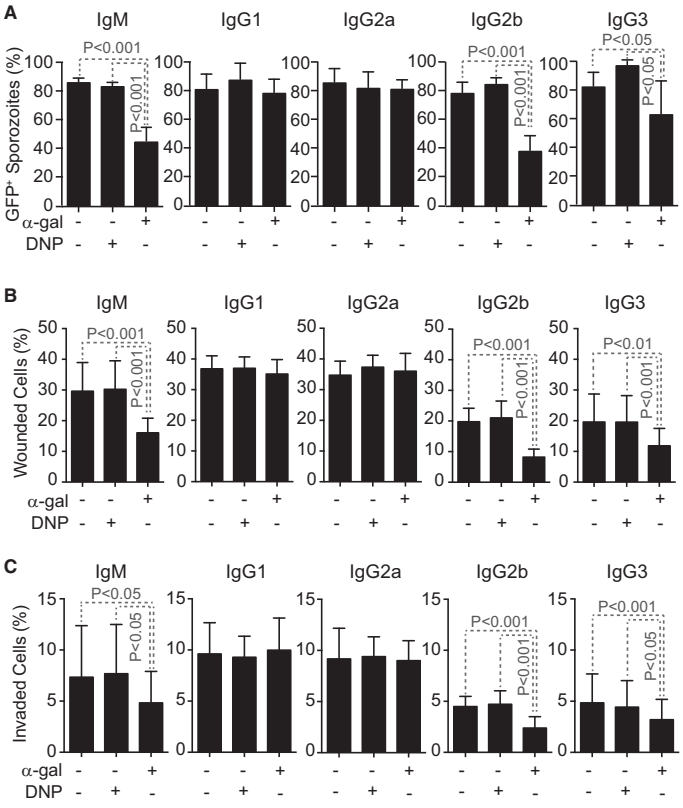

Figure 6. Protective Effect of Anti-α-Gal Abs against Hepatocyte Infection

(A) Mean percentage (%) of viable GFP$^+$ *Pb*A$^{Hsp70\text{-}GFP}$ sporozoites ± STD (3–4 experiments) after exposure in vitro to anti-α-gal or control anti-DNP mAbs in the presence of mouse complement. (B and C) Mean percentage (%) of HepG2 cells (B) wounded (Dextran-Red$^+$) or (C) invaded (GFP$^+$) by *Pb*A$^{Hsp70\text{-}GFP}$ sporozoites treated as in (A) ± SD (six experiments).

suggests that the protective effect exerted by anti-α-gal IgM and IgG2b Abs acts via a mechanism that is strictly complement dependent, whereas the protective effect of anti-α-gal IgG3 Abs is partially but probably not strictly dependent on complement activation. Infection incidence was similar in control $\alpha 1,3Gt^{-/-}C3^{-/-}$ versus $\alpha 1,3Gt^{-/-}C3^{+/+}$ mice (Figures 5C and 5E).

Complement activation generates C3a and C5a chemoattractants that promote IgG-dependent polymorphonuclear (PMN) cell cytotoxicity (Ding et al., 2008; Nimmerjahn and Ravetch, 2008; Yin et al., 2004). Therefore, we asked whether the protective effect of anti-α-gal Abs involves PMN cells. Passive transfer of anti-α-gal IgG2b Abs to $\alpha 1,3Gt^{-/-}$ mice, depleted from PMN cells by the administration of anti-Ly-6G (Gr-1) (Porcherie et al., 2011), failed to confer protection against *Pb*A transmission by *A.* mosquitoes, whereas passive transfer of anti-α-gal IgM or IgG3 Abs conferred protection (Figure 5F). This suggests that the protective effect exerted by anti-α-gal IgM and IgG2b Abs acts via a mechanism strictly dependent on PMN cells, whereas the protective effect of anti-α-gal IgG3 Abs is partially but probably not strictly dependent on PMN cells. Depletion of PMN cells per se did not interfere with *Plasmodium* infection (Figure 5F) while preventing the onset of cerebral malaria (data not shown), consistent with previous findings (Chen et al., 2000).

Anti-α-Gal Abs Are Cytotoxic to *Plasmodium* Sporozoites

Complement activation by anti-α-gal IgM, IgG2b, or IgG3 mAb was cytotoxic to *Pb*A sporozoites in vitro, as assessed by sporozoite GFP expression (Figure 6A). Anti-α-gal IgG1 and IgG2a mAbs, which did not activate complement when bound to *Plasmodium* sporozoites (data not shown), were not cytotoxic (Figure 6A). The cytotoxic effect of anti-α-gal IgM, IgG2b, and IgG3 was similar when using mouse (Figure 6A) or rabbit (Figure S7A) complement but was strictly dependent on the presence of complement (Figure S7B). A similar cytotoxic effect was observed when quantifying viable "crescent-shaped" sporozoites (Figure S7C), an independent readout for sporozoite viability (Hegge et al., 2010). Isotype-matched control anti-dinitrophenyl (DNP) Abs were not cytotoxic to *Pb*A sporozoites in vitro (Figures 6A and S7A–S7C).

Anti-α-Gal Abs Inhibit Hepatocyte Invasion by *Plasmodium* Sporozoites

We asked whether anti-α-gal Abs inhibit hepatocyte transmigration (wounding) and/or hepatocyte invasion by *Plasmodium* sporozoites (Mota et al., 2001). Complement activation by anti-α-gal IgM, IgG2b, and IgG3 Abs inhibited hepatocyte transmigration (Figure 6B) and invasion (Figure 6C), as assessed in vitro for *Pb*A sporozoites. This inhibitory effect was not observed when using anti-α-gal IgG1 or IgG2a Abs or isotype/subclass-matched control anti-DNP Abs (Figures 6B and 6C).

We then assessed whether anti-α-gal Abs inhibit the development of exoerythrocytic forms (EEF) of *Plasmodium*. Complement activation by anti-α-gal IgM, IgG2b, and IgG3 Abs reduced the number of EEF (Figure 7A), as well as the average EEF size (Figures 7B and 7C) formed in vitro by *Pb*A sporozoites. Anti-α-gal IgG1 Abs did not show this inhibitory effect, while anti-α-gal IgG2a Abs did not reduce the number of EEF (Figure 7A) but had a residual inhibitory effect on EEF size (Figures 7B and

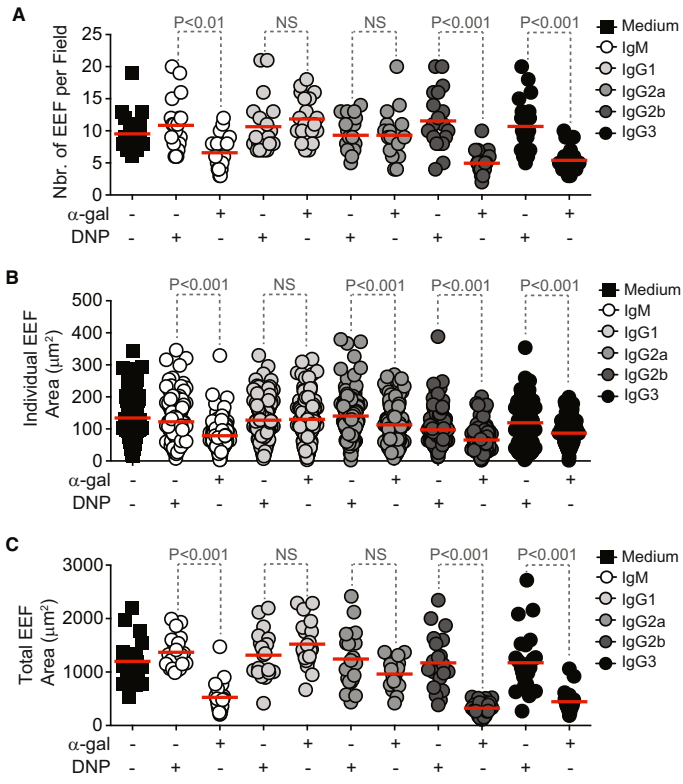

Figure 7. Protective Effect of Anti-α-Gal Abs against *Plasmodium* Maturation in Hepatocytes

(A) Number of EEF per field (dots; 20–23 fields).

(B) Area of individual EEF (dots) (n = 111–256 EEFs counted in 20–23 fields).

(C) Total area of EEF (dots) per field (20–23 fields). HepG2 cells were incubated with *Pb*A$^{Hsp70\text{-}GFP}$ sporozoites, previously exposed to anti-α-gal or control anti-DNP mAbs in the presence of complement (A–C).

See also Figure S7.

7C). Isotype/subclass-matched control anti-DNP Abs did not modulate EEF numbers (Figure 7A) or average size (Figures 7B and 7C).

DISCUSSION

When inoculated in humans through the bite of an *A.* mosquito, *Plasmodium* sporozoites are confronted with relatively high levels of cytotoxic anti-α-gal IgM Abs (Figure 2A). That these Abs are protective against malaria transmission is supported by three independent lines of evidence. First, individuals from a malaria endemic region that show evidence of decreased *P. falciparum* infection risk have higher levels of circulating α-gal-specific IgM Abs, as compared to individuals who are susceptible to *P. falciparum* infection (Figure 2B). Second, when present at levels similar to those observed in individuals from a malaria endemic region—in *α1,3Gt*$^{-/-}$ mice colonized by human gut pathobiont *E. coli* O86:B7 expressing α-gal (Figure 3) or in immunized *α1,3Gt*$^{-/-}$ mice (Figures 4A and 4B)—anti-α-gal IgM Abs confer protection against malaria transmission. Third, passive transfer of anti-α-gal IgM Abs is sufficient per se to protect *α1,3Gt*$^{-/-}$ mice from malaria transmission (Figure 5C).

The protective effect exerted by anti-α-gal IgM Abs should be relevant to understand why malaria incidence is higher in children versus adults from malaria endemic regions (Modiano et al., 1996). Relative absence of these antibodies in children under the age of 2–3 years should favor malaria transmission, as compared to adults that have higher levels of circulating anti-α-gal IgM Abs (Figure 2A). This relative absence of anti-α-gal IgM in children may be explained by the (1) kinetics of establishment of an adult-like gut microbiota (Ringel-Kulka et al., 2013), (2) requirement of environmental and dietary exposure in the establishment of an adult-like gut microbiota, and/or (3) the kinetics of the establishment of adult-like B cell repertoire, including anti-α-gal B cells.

The protective effect exerted by anti-α-gal IgM Abs might also contribute to explain why only a small fraction of *Plasmodium* sporozoites inoculated by mosquitoes manage to progress toward the establishment of infection in humans. This is true even when *Plasmodium* sporozoites are inoculated under controlled experimental conditions in adults (Rickman et al., 1990; Sauerwein et al., 2011; Verhage et al., 2005). Presumably, when present at sufficient high levels in adults, circulating anti-α-gal IgM Abs prevent the large majority of *Plasmodium* sporozoites from establishing a successful infection. However, infection is established if as few as a couple of *Plasmodium* sporozoites manage to escape this natural mechanism of protection.

Whether α-gal detected at the surface of *Plasmodium* sporozoites (Figure 1) is produced by *Plasmodium* and/or by the mosquito is not clear. The salivary glands of noninfected mosquitoes express low levels of α-gal, as detected by western blot (Figure 1) and immunostaining (data not shown). *Plasmodium* sporozoites are masked by mosquito laminin (Warburg et al., 2007), an evolutionary conserved glycoprotein that in other species contains α-gal (Takahashi et al., 2014). It is possible therefore that anti-α-gal Abs recognize laminin or another mosquito-derived protein expressing α-gal, masking *Plasmodium* sporozoites (Warburg et al., 2007).

It is now well established that specific components of the gut microbiota can modulate immunity and resistance to infection (Belkaid and Hand, 2014; Honda and Littman, 2012). In support of this notion, resistance to viral and bacterial (Fagundes et al., 2012) infections is impaired in GF mice (Dolowy and Muldoon, 1964) or mice subjected to antibiotic-driven dysbiosis (Ichinohe et al., 2011). We reasoned that xeno-glycans expressed by specific components of the gut microbiota might trigger a protective immune response against pathogens expressing the same xeno-glycans. We show that this is the case for α-gal, a xeno-glycan expressed by the human gut pathobiont *E. coli* O86:B7, as well by *Plasmodium spp.* (Figures 1, 3A, and 3B). When colonized by *E. coli* O86:B7, $\alpha 1,3Gt^{-/-}$ mice produce an anti-α-gal IgM Ab response (Figures 3C and 3F) that confer protection against *Plasmodium* infection (Figures 3D, 3E, 3G, and 5C) via a lytic mechanism mediated by complement activation (Figures 5E and 6A). It is worth noticing that in a similar manner to other microbiota-driven resistance mechanisms, the protective effect exerted by *E. coli* O86:B7 acts at the level of a tissue barrier, i.e., the skin, to prevent *Plasmodium* transmission (Figures 4E and 4F).

Levels of circulating anti-α-gal IgG Abs in individuals from a malaria endemic region (Figure 2C), as well as in $\alpha 1,3Gt^{-/-}$ mice colonized with *E. coli* O86:B7 (Figures S2A and S2C), are ~30-fold and ~40 to 70-fold, respectively, lower than levels of IgM anti-α-gal Abs. This may explain why basal levels anti-α-gal IgG Abs in individuals from a malaria endemic region are not associated with decreased risk of *P. falciparum* infection (Figure 2D). This also suggests that *P. falciparum* infection fails to induce class switch of the anti-α-gal Ig Ab response in those individuals. It is possible therefore that *P. falciparum* represses Ig class-switch recombination, explaining the residual levels of circulating anti-α-gal IgG Abs (Figure 2C).

While anti-α-gal Abs can provide sterile protection against malaria in mice (Figures 5B, 5C, and S4B), this is not commonly observed in malaria endemic regions in which adult individuals have circulating anti-α-gal IgM Abs, possibly because the levels of these Abs are below a threshold level required to provide sterile protection (Figure 2). However, we show that this natural mechanism of protection can be enhanced via immunization using adjuvants that favor the production of T cell-dependent complement fixing anti-α-gal IgG Abs (Figures 4G and 4H). Moreover, when coupled to *Plasmodium* antigens, this approach should enhance the immunogenicity of such antigens (Benatuil et al., 2005) and boost the protective efficacy of candidate malaria vaccines based on such antigens (Olotu et al., 2013). This approach should be useful in preventing not only individual infections but also disease transmission given the protective effect of anti-α-gal Abs.

It is possible that the protective effect of "attenuated" sporozoite vaccine trials against malaria (Seder et al., 2013) is driven to some extent by an anti-α-gal Ab response, given the expression of α-gal by *Plasmodium falciparum* sporozoites (Figure 1). Whether a correlation can be established between the effectiveness of such candidate vaccines and a putative anti-α-gal IgG Ab response has not been established but may be useful to consider as a retrospective analyzes.

As a final note, we predict that in a similar manner to anti-α-gal Abs other anti-glycan Abs may confer protection against malaria as well as other vector-borne protozoan parasites (Huflejt et al., 2009; Lacroix-Desmazes et al., 1995; Nagele et al., 2013). Moreover, anti-α-gal Abs may also target other vector-borne protozoan parasites expressing α-gal, such as *Leishmania spp.* and *Trypanosoma spp.*, the causative agents of Leishmaniasis and Trypanosomiasis, respectively (Avila et al., 1989). As such, vaccination approaches similar to the one proposed here for malaria may be considered against these diseases as well.

EXPERIMENTAL PROCEDURES

Cohort Study

For detailed analysis, see the Extended Experimental Procedures.

Immunization against α-Gal

Eight- to ten-week-old mice received 3 × 10^8 rabbit rRBCM equivalents (100 μl; PBS; intraperitoneal [i.p.]). Adjuvants are described in the Extended Experimental Procedures. Mouse serum was collected 2 weeks after last immunization, and circulating anti-α-gal Abs were quantified by ELISA. See the Extended Experimental Procedures for details on anti-α-gal ELISA.

Passive Transfer of Anti-α-Gal mAbs

$\alpha 1,3Gt^{-/-}$ mice received anti-α-gal IgG1, IgG2a, IgG2b, and IgG3 mAbs (Ding et al., 2008; Yin et al., 2004) (150 μg; 100 μl per mouse) or polyclonal IgM (150 μg; 300–400 μl per mouse) via a single intravenous (i.v.) injection 24 hr prior to mosquito exposure.

Plasmodium Strains

Transgenic *P. berghei* ANKA (*Pb*A) strains expressing GFP under the *eef1α* promoter, i.e., *Pb*$A^{EEF1a\text{-}GFP}$ (259cl1; MR4; MRA-865) (Franke-Fayard et al., 2004), or under the *hsp70* promoter (Ishino et al., 2006), i.e., *Pb*$A^{Hsp70\text{-}GFP}$ (kindly provided by Robert Menard, Institut Pasteur), transgenic *P. yoelii* 17XNL strain expressing GFP under the *PbA eef1α* promoter (MR4; MRA-817; kindly provided by Robert Menard, Institut Pasteur) (Weiss et al., 1989). For sporozoite production, see the Extended Experimental Procedures.

Plasmodium Transmission

A. stephensi or *gambiae* mosquitoes were allowed to feed on anesthetized mice (i.p.; 125 mg/kg ketamine; 12.5 mg/kg xylazine) placed on a warming tray. Two mosquitoes were allowed to probe and feed independently (90–100 s) on restricted to the edge of the mouse ear (10–12/3–4 mm) and dissected thereafter for confirmation of sporozoites in salivary glands. If negative, infection was repeated.

Sporozoites Inoculation

Pb$A^{EEF1a\text{-}GFP}$ sporozoites were inoculated (i.d.) in the ear pinna (750 sporozoites in 20–30 μl; 1% BSA in PBS) or i.v. in the retro-orbital vein (150 sporozoites in 50 μl; 1% BSA in PBS) using a microsyringe (Nanofil 100 μl; 33G beveled needle; World Precision Instruments).

Detection of α-Gal in *Plasmodium* Sporozoites

Sporozoites were stained with Alexa Fluor 647-conjugated BSI-IB_4 or Alexa Fluor 647-conjugated anti-α-gal mAbs and detected by confocal microscope or flow cytometer. For detection of α-gal in *Pb*$A^{Hsp70\text{-}GFP}$ by western blotting, see the Extended Experimental Procedures. Green coffee bean α-galactosidase (50–200 μl; 5 U/ml; 60–90 min; 25°C; Sigma Chemical) was used to hydrolyze terminal α-galactosyl moieties from glycolipids and glycoproteins (Luo et al., 1999).

Statistical Analysis

All tests (except human cohort studies) were performed using the GraphPad Prism (v. 6.0) (GraphPad Software). Human analyses were performed in R (v. 3.0.2). Detailed analyses are described in the Extended Experimental Procedures.

Mice

Experiments in mice were performed in accordance with protocols approved by the Ethics Committee of the Instituto Gulbenkian de Ciência and the Portuguese National Entity (DGAV-Direção Geral de Alimentação e Veterinária). Experiments in mice were performed in accordance with the Portuguese (Decreto-Lei no. 113/2013) and European (directive 2010/63/EU) legislation related to housing, husbandry, and animal welfare. C57BL/6 $J_HT^{-/-}$ (Gu et al., 1993), $Tcr\beta^{-/-}$ (Mombaerts et al., 1992), $Aid^{-/-}$ (Muramatsu et al., 2000), $\mu S^{-/-}$ (Ehrenstein et al., 1998), and $C3^{-/-}$ (Circolo et al., 1999) mice were crossed with C57BL/6 $\alpha 1,3Gt^{-/-}$ mice (Shinkel et al., 1997; Tearle et al., 1996). For the details on genotyping, see the Extended Experimental Procedures.

SUPPLEMENTAL INFORMATION

Supplemental Information includes Extended Experimental Procedures and seven figures and can be found with this article online at http://dx.doi.org/10.1016/j.cell.2014.10.053.

AUTHOR CONTRIBUTIONS

B.Y. contributed to study design, performed, and/or contributed critically to all experiments, analyzed data, and contributed to writing of the manuscript. In some experiments, B.Y. was assisted by S.R., S.P., T.M.T., and P.D.C. designed, performed, and analyzed the human studies. R.G. performed the western blot experiments. H.S. supervised J.G. in the establishment and maintenance of *Plasmodium*-infected *A.* mosquitoes. A.R. produced and troubleshooted all mAb production. P.J.C. and A.J.F.A. generated $\alpha 1,3Gt^{-/-}$ mice. A.S.C. provided anti-α-gal hybridomas. O.K.D. and B.T. organized the human studies and provided the human serum samples. M.P.S. formulated the original hypothesis, drove the study design, and wrote the manuscript with B.Y. All authors read and approved the manuscript.

ACKNOWLEDGMENTS

The authors thank the Inflammation Group (IGC) for insightful discussions and review of the manuscript, Sofia Rebelo and Silvia Cardoso for mouse breeding and genotyping, Pedro Almada and Nuno Pimpão Martins (IGC Imaging Facility) for technical support, Karen Berman de Ruiz and Joana Bom (IGC Animal Facility) for germ-free breeding, Joana Tavares, Rogerio Amino, and Robert Ménard (Institute Pasteur) for technical support, Alekos Athanasiadis and Jocelyne Demengeot for insightful discussions, Pascal Gagneaux (University of California San Diego), and Daniel Mucida (Rockefeller University) for critical review of the initial version of the manuscript. Financial support from the Bill and Melinda Gates Foundation (OPP1024563), Fundação para a Ciência e Tecnologia (RECI-IMI-IMU-0038-2012), and European Research Council (ERC-2011-AdG 294709-DAMAGECONTROL) (to M.P.S.) and Fundação para a Ciência e a Tecnologia (SFRH/BD/51176/2010) within the PhD Program of Integrative Biomedical Science of the Instituto Gulbenkian de Ciência (to B.Y.) is gratefully acknowledged. The Division of Intramural Research, National Institute of Allergy and Infectious Diseases, and NIH supported the Mali cohort study. Mouse axenization was supported by the EMMA, EU FP7 Capacities Specific Program.

Received: August 8, 2014
Revised: September 26, 2014
Accepted: September 30, 2014
Published: December 4, 2014

REFERENCES

Avila, J.L., Rojas, M., and Galili, U. (1989). Immunogenic Gal alpha 1——3Gal carbohydrate epitopes are present on pathogenic American Trypanosoma and Leishmania. J. Immunol. *142*, 2828–2834.

Avila, J.L., Rojas, M., and Velazquez-Avila, G. (1992). Characterization of a natural human antibody with anti-galactosyl(alpha 1-2)galactose specificity that is present at high titers in chronic Trypanosoma cruzi infection. Am. J. Trop. Med. Hyg. *47*, 413–421.

Belkaid, Y., and Hand, T.W. (2014). Role of the microbiota in immunity and inflammation. Cell *157*, 121–141.

Belnoue, E., Kayibanda, M., Vigario, A.M., Deschemin, J.C., van Rooijen, N., Viguier, M., Snounou, G., and Rénia, L. (2002). On the pathogenic role of brain-sequestered alphabeta CD8+ T cells in experimental cerebral malaria. J. Immunol. *169*, 6369–6375.

Benatuil, L., Kaye, J., Rich, R.F., Fishman, J.A., Green, W.R., and Iacomini, J. (2005). The influence of natural antibody specificity on antigen immunogenicity. Eur. J. Immunol. *35*, 2638–2647.

Bishop, J.R., and Gagneux, P. (2007). Evolution of carbohydrate antigens—microbial forces shaping host glycomes? Glycobiology *17*, 23R–34R.

Chen, L., Zhang, Z., and Sendo, F. (2000). Neutrophils play a critical role in the pathogenesis of experimental cerebral malaria. Clin. Exp. Immunol. *120*, 125–133.

Chiang, T.R., Fanget, L., Gregory, R., Tang, Y., Ardiet, D.L., Gao, L., Meschter, C., Kozikowski, A.P., Buelow, R., and Vuist, W.M. (2000). Anti-gal antibodies in humans and 1, 3alpha-galactosyltransferase knock-out mice. Transplantation *69*, 2593–2600.

Cretin, N., Bracy, J., Hanson, K., and Iacomini, J. (2002). The role of T cell help in the production of antibodies specific for Gal alpha 1-3Gal. J. Immunol. *168*, 1479–1483.

Cywes-Bentley, C., Skurnik, D., Zaidi, T., Roux, D., Deoliveira, R.B., Garrett, W.S., Lu, X., O'Malley, J., Kinzel, K., Zaidi, T., et al. (2013). Antibody to a conserved antigenic target is protective against diverse prokaryotic and eukaryotic pathogens. Proc. Natl. Acad. Sci. USA *110*, E2209–E2218.

Ding, J.W., Zhou, T., Zeng, H., Ma, L., Verbeek, J.S., Yin, D., Shen, J., and Chong, A.S. (2008). Hyperacute rejection by anti-Gal IgG1, IgG2a, and IgG2b is dependent on complement and Fc-gamma receptors. J. Immunol. *180*, 261–268.

Doenz, U., Nydegger, U.E., Kueng, A., Carrel, T., and Mohacsi, P. (2000). Anti-Galalpha1-3Gal IgM/IgG antibody levels in infants: do they have a clinical relevance in pediatric xenotransplantation? J. Heart Lung Transplant. *19*, 1108–1113.

Dolowy, W.C., and Muldoon, R.L. (1964). Studies of germfree animals. I. Response of mice to infection with influenza A virus. Proc. Soc. Exp. Biol. Med. *116*, 365–371.

Ehrenstein, M.R., O'Keefe, T.L., Davies, S.L., and Neuberger, M.S. (1998). Targeted gene disruption reveals a role for natural secretory IgM in the maturation of the primary immune response. Proc. Natl. Acad. Sci. USA *95*, 10089–10093.

Fagundes, C.T., Amaral, F.A., Vieira, A.T., Soares, A.C., Pinho, V., Nicoli, J.R., Vieira, L.Q., Teixeira, M.M., and Souza, D.G. (2012). Transient TLR activation restores inflammatory response and ability to control pulmonary bacterial infection in germfree mice. J. Immunol. *188*, 1411–1420.

Franke-Fayard, B., Trueman, H., Ramesar, J., Mendoza, J., van der Keur, M., van der Linden, R., Sinden, R.E., Waters, A.P., and Janse, C.J. (2004). A Plasmodium berghei reference line that constitutively expresses GFP at a high level throughout the complete life cycle. Mol. Biochem. Parasitol. *137*, 23–33.

Galili, U., and Swanson, K. (1991). Gene sequences suggest inactivation of alpha-1,3-galactosyltransferase in catarrhines after the divergence of apes from monkeys. Proc. Natl. Acad. Sci. USA *88*, 7401–7404.

Galili, U., LaTemple, D.C., and Radic, M.Z. (1998). A sensitive assay for measuring alpha-Gal epitope expression on cells by a monoclonal anti-Gal antibody. Transplantation *65*, 1129–1132.

Galili, U., Rachmilewitz, E.A., Peleg, A., and Flechner, I. (1984). A unique natural human IgG antibody with anti-alpha-galactosyl specificity. J. Exp. Med. *160*, 1519–1531.

Galili, U., Macher, B.A., Buehler, J., and Shohet, S.B. (1985). Human natural anti-alpha-galactosyl IgG. II. The specific recognition of alpha (1——3)-linked galactose residues. J. Exp. Med. *162*, 573–582.

Galili, U., Mandrell, R.E., Hamadeh, R.M., Shohet, S.B., and Griffiss, J.M. (1988). Interaction between human natural anti-alpha-galactosyl immunoglobulin G and bacteria of the human flora. Infect. Immun. *56*, 1730–1737.

Gu, H., Zou, Y.R., and Rajewsky, K. (1993). Independent control of immunoglobulin switch recombination at individual switch regions evidenced through Cre-loxP-mediated gene targeting. Cell *73*, 1155–1164.

Hayakawa, T., Satta, Y., Gagneux, P., Varki, A., and Takahata, N. (2001). Alu-mediated inactivation of the human CMP- N-acetylneuraminic acid hydroxylase gene. Proc. Natl. Acad. Sci. USA *98*, 11399–11404.

Hegge, S., Kudryashev, M., Barniol, L., and Frischknecht, F. (2010). Key factors regulating Plasmodium berghei sporozoite survival and transformation revealed by an automated visual assay. FASEB journal *24*, 5003–5012.

Honda, K., and Littman, D.R. (2012). The microbiome in infectious disease and inflammation. Annu. Rev. Immunol. *30*, 759–795.

Huflejt, M.E., Vuskovic, M., Vasiliu, D., Xu, H., Obukhova, P., Shilova, N., Tuzikov, A., Galanina, O., Arun, B., Lu, K., and Bovin, N. (2009). Anti-carbohydrate antibodies of normal sera: findings, surprises and challenges. Mol. Immunol. *46*, 3037–3049.

Ichinohe, T., Pang, I.K., Kumamoto, Y., Peaper, D.R., Ho, J.H., Murray, T.S., and Iwasaki, A. (2011). Microbiota regulates immune defense against respiratory tract influenza A virus infection. Proc. Natl. Acad. Sci. USA *108*, 5354–5359.

Ishino, T., Orito, Y., Chinzei, Y., and Yuda, M. (2006). A calcium-dependent protein kinase regulates Plasmodium ookinete access to the midgut epithelial cell. Mol. Microbiol. *59*, 1175–1184.

Kimmel, J., Ogun, S.A., de Macedo, C.S., Gerold, P., Vivas, L., Holder, A.A., Schwarz, R.T., and Azzouz, N. (2003). Glycosylphosphatidyl-inositols in murine malaria: Plasmodium yoelii yoelii. Biochimie *85*, 473–481.

Lacroix-Desmazes, S., Mouthon, L., Coutinho, A., and Kazatchkine, M.D. (1995). Analysis of the natural human IgG antibody repertoire: life-long stability of reactivities towards self antigens contrasts with age-dependent diversification of reactivities against bacterial antigens. Eur. J. Immunol. *25*, 2598–2604.

Luo, Y., Wen, J., Luo, C., Cummings, R.D., and Cooper, D.K. (1999). Pig xenogeneic antigen modification with green coffee bean alpha-galactosidase. Xenotransplantation *6*, 238–248.

Macher, B.A., and Galili, U. (2008). The Galalpha1,3Galbeta1,4GlcNAc-R (alpha-Gal) epitope: a carbohydrate of unique evolution and clinical relevance. Biochim. Biophys. Acta *1780*, 75–88.

Mañez, R., Blanco, F.J., Díaz, I., Centeno, A., Lopez-Pelaez, E., Hermida, M., Davies, H.F., and Katopodis, A. (2001). Removal of bowel aerobic gram-negative bacteria is more effective than immunosuppression with cyclophosphamide and steroids to decrease natural alpha-galactosyl IgG antibodies. Xenotransplantation *8*, 15–23.

Ménard, R., Tavares, J., Cockburn, I., Markus, M., Zavala, F., and Amino, R. (2013). Looking under the skin: the first steps in malarial infection and immunity. Nat. Rev. Microbiol. *11*, 701–712.

Miyatake, T., Sato, K., Takigami, K., Koyamada, N., Hancock, W.W., Bazin, H., Latinne, D., Bach, F.H., and Soares, M.P. (1998). Complement-fixing elicited antibodies are a major component in the pathogenesis of xenograft rejection. J. Immunol. *160*, 4114–4123.

Modiano, D., Petrarca, V., Sirima, B.S., Nebié, I., Diallo, D., Esposito, F., and Coluzzi, M. (1996). Different response to Plasmodium falciparum malaria in west African sympatric ethnic groups. Proc. Natl. Acad. Sci. USA *93*, 13206–13211.

Mombaerts, P., Clarke, A.R., Rudnicki, M.A., Iacomini, J., Itohara, S., Lafaille, J.J., Wang, L., Ichikawa, Y., Jaenisch, R., Hooper, M.L., et al. (1992). Mutations in T-cell antigen receptor genes alpha and beta block thymocyte development at different stages. Nature *360*, 225–231.

Moran, P., and Caras, I.W. (1994). Requirements for glycosylphosphatidylinositol attachment are similar but not identical in mammalian cells and parasitic protozoa. J. Cell Biol. *125*, 333–343.

Mota, M.M., Pradel, G., Vanderberg, J.P., Hafalla, J.C., Frevert, U., Nussenzweig, R.S., Nussenzweig, V., and Rodríguez, A. (2001). Migration of Plasmodium sporozoites through cells before infection. Science *291*, 141–144.

Muramatsu, M., Kinoshita, K., Fagarasan, S., Yamada, S., Shinkai, Y., and Honjo, T. (2000). Class switch recombination and hypermutation require activation-induced cytidine deaminase (AID), a potential RNA editing enzyme. Cell *102*, 553–563.

Nagele, E.P., Han, M., Acharya, N.K., DeMarshall, C., Kosciuk, M.C., and Nagele, R.G. (2013). Natural IgG autoantibodies are abundant and ubiquitous in human sera, and their number is influenced by age, gender, and disease. PLoS ONE *8*, e60726.

Nimmerjahn, F., and Ravetch, J.V. (2008). Fcgamma receptors as regulators of immune responses. Nat. Rev. Immunol. *8*, 34–47.

Olotu, A., Fegan, G., Wambua, J., Nyangweso, G., Awuondo, K.O., Leach, A., Lievens, M., Leboulleux, D., Njuguna, P., Peshu, N., et al. (2013). Four-year efficacy of RTS,S/AS01E and its interaction with malaria exposure. N. Engl. J. Med. *368*, 1111–1120.

Oyelaran, O., McShane, L.M., Dodd, L., and Gildersleeve, J.C. (2009). Profiling human serum antibodies with a carbohydrate antigen microarray. J. Proteome Res. *8*, 4301–4310.

Pal, S.C., Rao, C.K., Kereselidze, T., Krishnaswami, A.K., Murty, D.K., Pandit, C.G., and Shrivastav, J.B. (1969). An extensive community outbreak of enteropathogenic Escherichia coli O86: B7 gastroenteritis. Bull. World Health Organ. *41*, 851–858.

Parker, W., Lin, S.S., Yu, P.B., Sood, A., Nakamura, Y.C., Song, A., Everett, M.L., and Platt, J.L. (1999). Naturally occurring anti-alpha-galactosyl antibodies: relationship to xenoreactive anti-alpha-galactosyl antibodies. Glycobiology *9*, 865–873.

Porcherie, A., Mathieu, C., Peronet, R., Schneider, E., Claver, J., Commere, P.H., Kiefer-Biasizzo, H., Karasuyama, H., Milon, G., Dy, M., et al. (2011). Critical role of the neutrophil-associated high-affinity receptor for IgE in the pathogenesis of experimental cerebral malaria. J. Exp. Med. *208*, 2225–2236.

Posekany, K.J., Pittman, H.K., Bradfield, J.F., Haisch, C.E., and Verbanac, K.M. (2002). Induction of cytolytic anti-Gal antibodies in alpha-1,3-galactosyltransferase gene knockout mice by oral inoculation with Escherichia coli O86:B7 bacteria. Infect. Immun. *70*, 6215–6222.

Rickman, L.S., Jones, T.R., Long, G.W., Paparello, S., Schneider, I., Paul, C.F., Beaudoin, R.L., and Hoffman, S.L. (1990). Plasmodium falciparum-infected Anopheles stephensi inconsistently transmit malaria to humans. Am. J. Trop. Med. Hyg. *43*, 441–445.

Ringel-Kulka, T., Cheng, J., Ringel, Y., Salojärvi, J., Carroll, I., Palva, A., de Vos, W.M., and Satokari, R. (2013). Intestinal microbiota in healthy U.S. young children and adults—a high throughput microarray analysis. PLoS ONE *8*, e64315.

Sauerwein, R.W., Roestenberg, M., and Moorthy, V.S. (2011). Experimental human challenge infections can accelerate clinical malaria vaccine development. Nat. Rev. Immunol. *11*, 57–64.

Seder, R.A., Chang, L.J., Enama, M.E., Zephir, K.L., Sarwar, U.N., Gordon, I.J., Holman, L.A., James, E.R., Billingsley, P.F., Gunasekera, A., et al.; VRC 312 Study Team (2013). Protection against malaria by intravenous immunization with a nonreplicating sporozoite vaccine. Science *341*, 1359–1365.

Springer, G.F., and Horton, R.E. (1969). Blood group isoantibody stimulation in man by feeding blood group-active bacteria. J. Clin. Invest. *48*, 1280–1291.

Springer, G.F., Horton, R.E., and Forbes, M. (1959). [Origin of anti-human blood group B agglutinins in white Leghorn chicks]. J. Exp. Med. *110*, 221–244.

Takahashi, H., Chinuki, Y., Tanaka, A., and Morita, E. (2014). Laminin γ-1 and collagen α-1 (VI) chain are galactose-α-1,3-galactose-bound allergens in beef. Allergy *69*, 199–207.

Takeuchi, Y., Porter, C.D., Strahan, K.M., Preece, A.F., Gustafsson, K., Cosset, F.L., Weiss, R.A., and Collins, M.K. (1996). Sensitization of cells and retroviruses to human serum by (alpha 1-3) galactosyltransferase. Nature *379*, 85–88.

Tangvoranuntakul, P., Gagneux, P., Diaz, S., Bardor, M., Varki, N., Varki, A., and Muchmore, E. (2003). Human uptake and incorporation of an immunogenic nonhuman dietary sialic acid. Proc. Natl. Acad. Sci. USA *100*, 12045–12050.

Tearle, R.G., Tange, M.J., Zannettino, Z.L., Katerelos, M., Shinkel, T.A., Van Denderen, B.J., Lonie, A.J., Lyons, I., Nottle, M.B., Cox, T., et al. (1996). The alpha-1,3-galactosyltransferase knockout mouse. Implications for xenotransplantation. Transplantation *61*, 13–19.

Tran, T.M., Ongoiba, A., Coursen, J., Crosnier, C., Diouf, A., Huang, C.Y., Li, S., Doumbo, S., Doumtabe, D., Kone, Y., et al. (2014). Naturally acquired antibodies specific for Plasmodium falciparum reticulocyte-binding protein homologue 5 inhibit parasite growth and predict protection from malaria. J. Infect. Dis. *209*, 789–798.

Verhage, D.F., Telgt, D.S., Bousema, J.T., Hermsen, C.C., van Gemert, G.J., van der Meer, J.W., and Sauerwein, R.W. (2005). Clinical outcome of experimental human malaria induced by Plasmodium falciparum-infected mosquitoes. Neth. J. Med. *63*, 52–58.

Warburg, A., Shtern, A., Cohen, N., and Dahan, N. (2007). Laminin and a Plasmodium ookinete surface protein inhibit melanotic encapsulation of Sephadex beads in the hemocoel of mosquitoes. Microbes Infect. *9*, 192–199.

Weiss, W.R., Good, M.F., Hollingdale, M.R., Miller, L.H., and Berzofsky, J.A. (1989). Genetic control of immunity to Plasmodium yoelii sporozoites. J. Immunol. *143*, 4263–4266.

Yang, Y.G., deGoma, E., Ohdan, H., Bracy, J.L., Xu, Y., Iacomini, J., Thall, A.D., and Sykes, M. (1998). Tolerization of anti-Galalpha1-3Gal natural antibody-forming B cells by induction of mixed chimerism. J. Exp. Med. *187*, 1335–1342.

Yi, W., Bystricky, P., Yao, Q., Guo, H., Zhu, L., Li, H., Shen, J., Li, M., Ganguly, S., Bush, C.A., and Wang, P.G. (2006). Two different O-polysaccharides from Escherichia coli O86 are produced by different polymerization of the same O-repeating unit. Carbohydr. Res. *341*, 100–108.

Yin, D., Zeng, H., Ma, L., Shen, J., Xu, H., Byrne, G.W., and Chong, A.S. (2004). Cutting edge: NK cells mediate IgG1-dependent hyperacute rejection of xenografts. J. Immunol. *172*, 7235–7238.

EXTENDED EXPERIMENTAL PROCEDURES

Material

Synthetic α-gal linked to bovine serum albumin (BSA) or human serum albumin (HSA; Dextra Labs; Reading, UK), α-galactosidase from green coffee beans (Sigma Chemical Co), Fluorescein isothiocyanate (FITC)-conjugated (Sigma-Aldrich Co) and Alexa Fluor 647-conjugated (Invitrogen) *Bandeiraea simplicifolia* lectin (BSI-IB_4; *Griffonia simplicifolia*) (Kisailus and Kabat, 1978), rabbit RBC (Patricell Ltd.; Nottingham, UK), incomplete Freund's Adjuvant (IFA) (BD Difco), inactivated and dried *M. tuberculosis* H37 Ra (BD Difco), Dextran, Tetramethylrhodamine, 10,000 MW, Lysine Fixable (fluoro-Ruby; Life Technologies), mouse anti-α-gal IgM (M86; EnzoLife Sciences or kindly provided by Uri Galili, University of Massachusetts Medical School, Worcester, MA, USA) (Galili et al., 1998), IgG1 (GT6-27), IgG2a, IgG2b and IgG3 (GT4-31) mAbs (Ding et al., 2008; Yin et al., 2004), mouse anti-dinitrophenyl IgM (MADNP-5), IgG1 (MADNP-1), IgG2a (MADNP-2), IgG2b (MADNP-3) and IgG3 (MADNP-4) mAbs (kindly provided Hérve Bazin, University of Louvain, Belgium) (Platteau et al., 1990). Mouse IgM, IgG1, IgG2a, IgG2b, IgG3, IgA and IgE were detected using horse-radish peroxidase (HRP)-conjugated goat anti-mouse IgM, IgG1, IgG2a, IgG2b, IgA and IgE or a rat mAb anti-mouse IgG3 (Southern Biotechnology Associates). Anti-CSP 3D11 (Yoshida et al., 1980) hybridoma (IgG1 mAb directed against the repeat region of *P. berghei* CSP) was kindly provided by Ana Rodriguez (New York Medical School).

Cohort Study

The Ethics Committee of the Faculty of Medicine, Pharmacy and Dentistry at the University of Sciences, Technique and Technology of Bamako, and the Institutional Review Board of NIAID-NIH approved the cohort study. In May 2011, 695 individuals aged 3 months to 25 years were enrolled in a cohort study in the rural village of Kalifabougou, Mali. Individuals were followed during the malaria season for 7 months. Individuals were invited to participate after random selection from an age-stratified census of the entire village population (n = 4394). Written, informed consent was obtained from adult participants and the parents or guardians of participating children. Enrollment exclusion criteria were hemoglobin level < 7 g/dL, axillary temperature ≥ 37.5°C, acute systemic illness, use of anti-malarial or immunosuppressive medications in the past 30 days and pregnancy. Clinical malaria was detected prospectively by self-referral and weekly active clinical surveillance. All individuals with signs and symptoms of malaria and any level of *Plasmodium* parasitemia detected by light microscopy were treated according to the National guidelines in Mali. The research definition of malaria was parasitemia ≥ 2500 parasites/μL, temperature ≥ 37.5°C and no other cause of fever discernible by physical exam. During scheduled clinic visits, blood was collected by finger prick every two weeks on filter paper. Detection of asymptomatic *Plasmodium* infection by PCR was done retrospectively at the end of the surveillance period. For each participant, PCR was performed on blood samples in chronological order from enrollment onward until the first *P. falciparum* infection was detected. Detailed methods for *P. falciparum* PCR detection have been described (Tran et al., 2013). α-gal-specific IgM and IgG Ab levels were determined using ELISA on plasma collected at enrollment from the subset of individuals. Statistical analyses were described in the Statistical analysis' section.

Genotyping

Mice were genotyped by PCR using tail genomic DNA and the following primers: i) $\alpha 1,3Gt^{-/-}$: 5′-TCTTGACGAGTTCTTCTGAG-3′, 5′-TCAGCATGATGCGCATGAAGA-3′, 5′-TGGCCGCGTGGTAGTAAAAA-3′; ii) $J_\mu T^{-/-}$: 5′-CAGTGAATGACAGATGGACCTCC-3′, 5′-GCAGAAGCCACAACC ATACATTC-3′, 5′-ACAGTAACTCGTTCTTCTCTGC-3′; iii) $Aid^{-/-}$: 5′-GGCCAGCTCATTCCTCCACT-3′, 5′-CACTGAGCGCACCTGTAGCC-3′, 5′-CCTAGTGGCCAAGGTGCAGT-3′, 5′-TCAGGCTGAGGTTAGGGTTCC-3′; iv) $Tcr\beta^{-/-}$: 5′-TGTCTGAAGGGCAATGACTG-3′, 5′-GCTGATCCGTGGCATCTATT-3′, 5′-CTTGGGTGGAGAGGCTATTC-3′, 5′-AGGTGAGATGACAGGAGATC-3′; v) $C3^{-/-}$: 5′-ATCTTGAGTGCACCAAGCC-3′, 5′-GGTTGCAGCAGTCTATGAAGG-3′, 5′-GCCAGAGGCCACTTGTGTAG-3′. $\mu S^{-/-}$ mice were phenotyped by ELISA, as described (Ehrenstein et al., 1998). Total genomic DNA was isolated from the tail using a standard protocol. Briefly, tails (0,5 to 1 cm) were obtained and submerged into DirectPCR Lysis Reagent (200-300 μL; Viagen Biotech) containing Proteinase K (100 μg/ml) and incubated (overnight; 55°C) under vigorous agitation. Next day, samples were centrifuged (16,000 g; 5-10 s; RT) and supernatant (1 μl) was amplified by PCR: 95°C (15 min), 30 cycles of 94°C (45 s), 60°C (90 s) (except $Aid^{-/-}$ genotyping; 63°C), 72°C (90 s) and 72°C (15 min). Visualizations of PCR results were done on 1.5%–2% agarose gel (80-100V; 1-2 hr).

Extraction of Rabbit RBC Membranes

Rabbit RBC membranes (rRBCM) expressing high levels of α-gal (Eto et al., 1968) were prepared from lyzed RBC (50 mM sodium phosphate buffer pH 8), washed (5-7X; sodium phosphate buffer; 10,000 g; 20 min, 4°C) until supernatant was hemoglobin-free, essentially as described (Matsuzawa and Ikarashi, 1979). Membranes were collected by centrifugation (20,000 g; 20 min, 4°C), re-suspended in PBS and stored (−80°C) until used.

Immunization

rRBCM were emulsified in Complete Freund's Adjuvant (CFA; Incomplete Freund's Adjuvant (IFA) plus *Mycobacterium tuberculosis* H37 RA; 4 mg/ml; DIFCO) with CpG (50 μg/mouse; ODN M362; Invivogen) and administered subcutaneously (s.c.). Two subsequent immunizations were emulsified in IFA+rRBC+CpG. Emulsions were administered at 200 μl per mouse, 3 times at two weeks intervals.

Mice were also immunized (s.c.) with α-gal-BSA (75 μg/mouse) emulsified in CFA with two subsequent immunizations, 2 and 4 weeks thereafter with α-gal-BSA emulsified in IFA.

Anti-α-Gal ELISA

Mouse serum was collected two weeks after immunization and circulating anti-α-gal antibodies were quantified by ELISA, as described (Galili et al., 1998; LaTemple and Galili, 1998). Briefly, 96-well plates (PolySorp; Nunc) were coated with α-gal (α-gal-HSA or α-gal-BSA; 50 μl; 10 μg/ml in 0.5 M carbonate bicarbonate buffer; pH 9.5; 2 hr at 37°C or overnight at 4°C), blocked with BSA (100 μl; 1% w/v in PBS; 1 hr; RT) and washed (5X; PBS/0.05% Tween-20). Plates were incubated (1 hr; RT) with serum serial dilutions in PBS, 1% BSA and washed (5X; PBS/0.05% Tween-20). Anti-α-gal antibodies were detected using HRP-conjugated anti-mouse IgM, total IgG, IgG1, IgG2a, IgG2b or IgG3 (50 μl, 1:1-2,000 dilution, 1 hr, RT) and washed (5X; PBS/0.05% Tween-20). Purified anti-α-gal IgM (Galili et al., 1998), IgG1 (GT6-27), IgG2a and IgG2b and IgG3 (GT4-31) mAb (Ding et al., 2008; Yin et al., 2004) were used as standards. TMB Substrate Reagent Set (BD Biosciences) was used to reveal peroxidase activity (15-30 min; RT) and the reaction was stopped using 2N sulfuric acid. Optical densities (OD) were reported at λ = 450 nm and normalized by subtracting background OD values (λ = 600 nm) (Victor 3; PerkinElmer). Concentration of each anti-α-gal IgG subclass was determined, as described (Spalter et al., 1999). Concentration of anti-α-gal antibodies in human plasma was analyzed using a similar assay and a standard curve to transform absorbance into immunoglobulin concentration was obtained by coating 8 duplicate wells in every plate with purified human IgG and IgM (500 to 1.5 ng/ml) and performing the protocol described above in the absence of diluted serum.

Anti-α-Gal mAbs

Anti-α-gal hybridomas were cultured in RPMI 1640 (Invitrogen Life Technologies) supplemented with 0.1 mM Sodium Pyruvate, 0.01 M HEPES, 0.05 mM 2-mercaptoethanol and 2% FBS (IgG depleted). Anti-α-gal IgG2a, IgG2b and IgG3 hybridomas were derived by sub-cloning of the original IgG1 (GT6-27) hybridoma and as such have similar affinities for α-gal, as described (Ding et al., 2008; Yin et al., 2004). Antibodies were purified by affinity chromatography using HiTrap Protein G columns (GE Healthcare Life Sciences). Anti-α-gal IgG3 purification was carried out by a nonchromatographic method taking advantage of its euglobulin properties, as described (García-González et al., 1988). Purified mAbs were extensively dialyzed against PBS. Protein concentration was determined using NanoDrop ND-1000 spectrophotometer (λ = 280 nm; Thermo Scientific) and purity confirmed by SDS-PAGE analysis. When indicated, mAbs were labeled with Alexa Fluor 647 Protein Labeling Kit (A20173), as per manufacturer recommendations (Molecular Probes, Invitrogen). Anti-mouse IgM total-A647 (Clone: R33.24.12) was used to reveal anti-α-gal IgM mAb in immunofluorescence assay.

Passive Anti-α-Gal mAbs Transfer

$\alpha 1,3Gt^{-/-}$ mice received anti-α-gal IgG1, IgG2a, IgG2b or IgG3 mAbs via a single i.v. injection (150 μg; 100 μl per mouse), 24 hr prior to mosquito exposure. Passive anti-α-gal IgM transfer was performed using polyclonal IgM. Briefly, eight to ten weeks old $\alpha 1,3G^{-/-}Aid^{-/-}$ mice received $3x10^8$ RBC equivalents of rRBCM in PBS (100 μl; i.p.). Serum was collected two weeks after the last immunization and concentration of anti-α-gal IgM was determined by ELISA (Galili et al., 1998; LaTemple and Galili, 1998). Serum collected from naive $\alpha 1,3G^{-/-}Aid^{-/-}$ mice was used as control. $\alpha 1,3Gt^{-/-}$ mice received the polyclonal IgM via a single i.v. (150 μg; 300-400 μl per mouse), 24 hr prior to mosquito exposure.

Plasmodium Strains

For sporozoite production, *P. berghei* ANKA infected RBC ($1x10^6$) were administered i.p. to BALB/c mice and the presence of gametocyte-stage parasites capable of exflagellation was monitored in fresh blood preparations. Infected BALB/c mice were used to feed 3 to 4-day-old female mosquitoes (~1 hr), which were used 18-25 days postinfection for subsequent infections. When infected with *P. berghei* ANKA mosquitoes were maintained at 21°C (IHMT) whereas mosquitoes infected with *P. yoelii* 17XNL-GFP(Ono et al., 2007) were maintained (24-25°C; Centre for Production and Infection of *Anopheles*; CEPIA, Pasteur Institute, France). Alternatively, *P. yoelii* 17XNL (MR4; MRA-593) (Weiss et al., 1989) infected mosquitoes were purchased from Radboud University Nijmegen Medical Centre (Nijmegen, Netherlands). *P. falciparum* 3D7 strain (kindly provided by Robert Menard, Institut Pasteur, France) (Walliker et al., 1987) were used for α-gal detection in infected RBC by immunofluorescence assay.

Sporozoites Isolation and Inoculation

Mosquitoes were narcotized (−20°C; 3-5 min), washed in 70% ethanol (1X; 10-20 s) and PBS (3X; 10-20 s; Ambion). Salivary glands were obtained by dissection under a zoom stereomicroscope (3X magnification; Nikon SMZ800, Japan) and preserved in RPMI 1640 medium (GIBCO BRL) or PBS. Salivary glands were smashed using Pellet pestles cordless motor (10-15 s; Sigma) to release sporozoites and centrifuged (100 g; 5 min) in LoBind microfuge tubes (Eppendorf). Supernatant was filtered (100 μm cell strainers; BD Falco) to exclude debris. Sporozoites were counted using KOVA Glasstic Slide 10 with quantitative grid (Fisher Scientific GMBH). $PbA^{EEF1a\text{-}GFP}$ sporozoites were inoculated i.d. in the ear pinna (750 sporozoites in 20-30 μl; 1% BSA in PBS) or i.v. (retro-orbital; 150 sporozoites in 50 μl; 1% BSA in PBS) using a microsyringe (Nanofil 100 μl; 33G beveled needle; World Precision Instruments).

Passive RBCs Transfer

$\alpha 1,3Gt^{-/-}$ mice immunized with rRBCM and age matched naive $\alpha 1,3Gt^{-/-}$ mice were exposed to *Pb*A$^{EEF1a\text{-}GFP}$ infected mosquitoes, as described above. Parasitemia was monitored by flow cytometry in FacScan analyzer (BD Biosciences). Nine days post-mosquito feeding, blood was collected and injected i.p. (100-200 μl) to naive $\alpha 1,3Gt^{-/-}$ mice. Infection was monitored daily for parasitemia and clinical symptoms, starting from day 3–4 postinfection RBC administration.

Quantification of Sporozoite mRNA

The mouse ear was excised immediately after and the whole liver was harvested 40 hr after mosquito biting. Samples were frozen in liquid nitrogen, tissues were homogenized in TRIzol (Life Technologies), total RNA isolated according to manufacturer's instructions (RNeasy Mini kit; QIAGEN). Briefly, RNA (2 μg; 10 μl) was mixed to random primers (1 μl) and dNTPs (10 mM; 1 μl), incubated (65°C; 5 min.), placed on ice and incubated in PCR Buffer (0.1 M DTT; 40 units/μl RNaseOU; 2 min.; 42°C). Superscript RT (SSIIRT) was added (1 μl; 50 min. 42°C) and samples were heated to finalize synthesis (70°C; 15 min). qRT-PCR was performed using *Pb*A 18S rRNA specific primers (5′-AAGCATTAAATAAAGCGAATACATCCTTAC-3′ and 5′-GGAGA TTGGTTTTGACGTTTATGTG-3′). Mouse housekeeping *Arbp0* gene (5′-CTTTGGGCATCACCACGAA-3′ and 5′-GCTGGCTCCCACCTTGTCT-3′) was amplified as control. Applied Biosystems' Power SYBR Green PCR Master Mix was used as per manufacturer's instructions (ABI Prism 7000 system; Applied Biosystems). Data are presented as relative expression of *P. berghei* ANKA 18S rRNA normalized to mouse *Arbp0* mRNA.

Detection of α-Gal in *Plasmodium* Sporozoites

*Pb*A$^{EEF1a\text{-}GFP}$, *Pb*A$^{Hsp70\text{-}GFP}$, *P. falciparum* 3D7 or *P. yoelii* 17XNL-GFP sporozoites, isolated from the salivary glands of *Anopheles stephensi* or *Anopheles gambiae* mosquitoes, 18-25 days postinfection were allowed to attach to Teflon printed (10 wells, 8 mm; no-adherent surface; Immuno-Cell Int.) or to diagnostic glass slides. Sporozoites were fixed (20-50 μl; 4% PFA; 20-30 min; RT or 37°C) and washed gently (1X; PBS). Sporozoites were stained with Alexa Fluor 647 conjugated BSI-IB_4 (100 μl; 200 μg/ml; 2 hr, RT), Alexa Fluor 647 conjugated anti-α-gal IgG1, IgG2a, IgG2b, IgG3 mAb (100 μl; 50 μg/ml; overnight; 4°C) or with nonconjugated anti-α-gal IgM (M86) mAb (100 μl; 50 μg/ml; overnight; 4°C) and washed (1X; PBS). Nonconjugated IgM antibodies were detected using Alexa Fluor 647 conjugated goat anti-mouse IgM (100 μl; 10 μg/ml; overnight, 4°C) (Molecular Probes, Invitrogen). After washing (1X; PBS), slides were incubated with 4',6-diamidino-2-phenylindole (DAPI) (100 μl; 10 μg/ml; 10 min; RT) (Molecular Probes, washed (1X; PBS) and dried in dark room without covering with coverslip (RT). Images of *Pb*A sporozoites were obtained by DeltaVision Core immunofluorescence microscopy (Applied Precision/Olympus) or Spinning Disk Confocal microscopy Revolution xD (Andor Technology) at 100 × magnification. Actin was detected using Alexa Fluor 488 Phalloidin (Molecular Probes; 100 μl; 3 units/ml; 1 hr; RT) in *P. falciparum* 3D7 and *P. yoelii* 17XNL-GFP sporozoites to which was added ProLong Gold Antifade Reagent (Invitrogen) and wells were covered with coverslips. Slides were visualized with Axiovert II fluorescence microscope (Zeiss). Images were analyzed using bicubic interpolation and rescaling with ImageJ software (NIH).

For detection of α-gal by flow cytometry, *Pb*A$^{Hsp70\text{-}GFP}$ sporozoites were isolated from the salivary glands of *A. stephensi* mosquitoes 19-25 days postinfection (10^5; 30-40ul; PBS; ice cold: 30 min), fixed (30-40 μl; 4% PFA in PBS; 20-30 min; 37°C) and washed (1 × ; PBS; 9,300 g; 2 min). Staining was performed with Alexa Fluor 647 conjugated BSI-IB_4 (100 μg/ml; 1 hr; 37°C). Sporozoites were washed (1 × ; PBS; 9,300 g; 2 min) and Alexa Fluor 647 BSI-IB_4 signal was detected in CyAn^{TM} ADP flow cytometry (Beckman Coulter; USA) with Summit Software (v4.3; Beckman Coulter), gating on FITC (for sporozoite detection) and APC (for α-gal detection).

For detection of α-gal by western blotting *Pb*A$^{Hsp70\text{-}GFP}$, *P. falciparum* 3D7 and *P. yoelii* 17XNL-GFP sporozoites were isolated from the salivary glands of 40-70 mosquitoes, 21-25 days after infection. Briefly, salivary glands were collected into the LoBind microfuge tubes (PBS; on ice), smashed using pellet pestles cordless motor (10-15 s; 2X) and a short spin was applied to pellet debris. Supernatant (30-50 μl; 1-2.5 × 10^5 sporozoites) was transferred into LoBind microfuge tube and aliquots were stored at −80°C until used. Number of *Plasmodium* sporozoites (equivalent to 10^5 per sample) was normalized to corresponding number of salivary glands from noninfected mosquitoes. Samples were lysed (50 mM Tris/HCl pH 7.5, 150 mM NaCl, 1% Triton X-100, Roche complete EDTA-free protease inhibitor cocktail; 1 hr; on ice) and centrifuged (16,000 g, 10 min.; 4°C). Samples (supernatant) were denatured with Laemmli buffer (1% β-mercaptoethanol; 2%SDS; 95°C; 2 min) and separated in SDS-PAGE gradient gel (12% acrylamide/bisacrylamide gel, 29:1; 100V; 2 hr). Proteins were transferred into a PVDF membrane (90 min; 12V), blocked (3% BSA) and incubated overnight with anti-α-gal IgG2b mAb (1 μg/ml; 20 ml). Membrane was washed with 20 mM Tris/HCl pH7.5, 150 mM NaCl and 0.1% Tween-20 buffer (TBST, 3 × ; 5 min; RT) and incubated with horseradish peroxidase (HRP)-conjugated goat anti-mouse IgG2b-HRP (SouthernBiotech, 20 ng/ml; 1 hr; 50 ml; RT). Membrane was washed (TBST; 1 hr; RT) and developed (SuperSignal Chemiluminescent detection kit; West Pico, Thermo Scientific).

GPI Anchor Cleavage from *Plasmodium* Sporozoites

*Pb*A$^{Hsp70\text{-}GFP}$ sporozoites were fixed (4% PFA in PBS; 20-30 min; 37°C) and treated with phosphatidylinositol-specific phospholipase C (from *Bacillus cereus*; 5U/ml; 14-16 hr; 37°C). Detection of α-gal is described above and CSP was detected using anti-CSP conjugated to Alexa Fluor 647 in CyA ADP Analyzer (Beckman Coulter).

Bacterial Strains and Growth Conditions

Frozen *E. coli* O86:B7 (ATCC 12701^{TM}; Rockville, Md.) and *E. coli* K12 (ATCC 10798) (~10^7 CFU/ml; 50% glycerol solution; −80°C) stocks were inoculated into Luria broth (LB; 50 ml; 37°C; overnight) on a shaker rack. Spectrophotometric absorbance was measured

at 600 nm (Optical Density-OD_{600}) and adjusted to OD_{600} ~0.2 in order to harvest bacteria during exponential growth corresponding to a OD_{600} of 2. The approximate cell number was determined according to spectrophotometric measurement and confirmed with most probable numbers (MPN) technique, also known as the method of Poisson zeroes (Oblinger and Koburger, 1975).

Detection of α-Gal on Bacterial Cultures

E. coli O86:B7 and *E.coli* K12 were cultured (LB; 50 ml; 37°C; overnight), washed (2 × ; PBS; 4,000 g; 5 min; 4°C) and re-suspended in PBS. Bacteria were fixed (200 μl; 4% PFA in PBS; 20-30 min; RT) and washed (1X; PBS; 4000 g; 5 min; RT). 10^8-10^9 CFU/ml were stained with BSI-IB_4-FITC (200 μl; 50 μg/ml; 2 hr, RT) for flow cytometry analysis using FacScan analyzer (BD Biosciences). In parallel, immunofluorescence assays were performed using 10 μl stained samples after air-drying (10-20 min; RT). Samples were washed (1x; PBS), incubated with 4',6-diamidino-2-phenylindole (DAPI) (200 μl; 10 μg/ml; 10 min; RT; Molecular Probes) and washed (1 × ; PBS). Immunofluorescence images were obtained by Spinning Disk Confocal microscopy Revolution xD (Andor Technology; USA) at 100 × magnification and images were processed with ImageJ (NIH) software.

Rederivation of GF $\alpha 1,3Gt^{-/-}$ Mice

Briefly, pregnant female $\alpha 1,3Gt^{-/-}$ mice were euthanized (20 days postcoitum), uteri were immersed in 1% VirkonS, rinsed in sterile water and pups were transferred to surrogate mothers kept in GF isolators (Gettinge-La Calhéne, France). GF status was monitored every third week onward.

Gnotobiotic and SPF-Colonized Mice

$\alpha 1,3Gt^{-/-}$ mice were re-derived via caesarean section from SPF into GF conditions at the Instituto Gulbenkian de Ciência, as described (http://strains.emmanet.org/protocols/GermFree_0902.pdf). For gnotobiotic colonization, 8-12 weeks GF $\alpha 1,3Gt^{-/-}$ mice were transferred into sterile micro isolator Ventiracks (Biozone, Margate, UK), fed *ad libitum* with a standard autoclaved chow diet and water and GF status was monitored every third week onward. GF and SPF $\alpha 1,3Gt^{-/-}$ mice treated with streptomycin sulfate (5 g/l in drinking water for 7 days; GIBCO), were starved for 12 hr and colonized with *E. coli* O86:B7 or *E. coli* K12 (~10^7 CFU/100 μl Luria-Bertani - LB - medium) via oral gavage, using a 20-gauge stainless steel animal feeding needle (Cadence Science, Japan). Control mice were inoculated with sterile LB medium. Colonization protocol was administered 3 times at two weeks intervals.

Complement Activation

Pb$A^{Hsp70\text{-}GFP}$ sporozoites were exposed to anti-α-gal mAbs (150 μg/ml; in 50 μl DMEM; 60 min; 4°C) and subsequently to naive C57BL/6 mouse plasma (1:5 in 0.1% gelatin in Veronal Buffer $(VB)^{2+}$; 50 μl; 60 min; 37°C) (Lonza), used as a source of complement. Samples were washed (1 × ; PBS). C3 was detected using APC labeled anti-C3/C3b/iC3b (Clone: 6C9; 1:100; 50 μl; 45 min; 4°C) and analyzed in CyA ADP Analyzer (Beckman Coulter).

Sporozoite Cytotoxicity Assays

Pb$A^{Hsp70\text{-}GFP}$ sporozoites (10-50x10^3) were incubated with anti-α-gal or isotype matched anti-DNP mAbs (150 μg/ml mAb in 10 μl DMEM GlutaMA; 60 min; 4°C). Naive C57BL/6 mouse plasma (1:5) or baby rabbit complement (1:10; Cedarlane Laboratories) was added (0.1% gelatin in VB^{2+}) as a source of complement (60 min; 37°C). Cytotoxicity was quantified according to GFP expression in Andor Spinning Disk Confocal Microscopy (Andor Technology). Alternatively, *Pb*$A^{EEF1a\text{-}GFP}$ sporozoites (10-30 × 10^3) were isolated from the salivary glands of *Anopheles stephensi* mosquitoes, 19-25 days postinfection and incubated with anti-α-gal or isotype matched anti-DNP mAbs (150 μg/ml mAb in 10 μl PBS, Life Technologies) (60 min; on ice). Plasma from C57BL/6 mice (1:5) or baby rabbit complement (bRC; 1:10; Cedarlane Laboratories) was added (0.1% gelatin in VB^{2+} buffer; Lonza) as a source of complement (60 min; 37°C). Alternatively, sporozoite cytotoxicity was evaluated according to loss of crescent-shaped morphology (%).

Invasion Assay

Human hepatoma cells (HepG2; kindly provided from Robert Menard, Institut Pasteur, France) were cultured (4x10^4/well; 200 μl in 96-well plates) in DMEM (GlutaMA, 10% FBS, 100U/ml penicillin/streptomycin; Life Technologies) (37°C; 5%CO^2; 2 days). *Pb*$A^{Hsp70\text{-}GFP}$ sporozoites (19-25 days postinfection) were preincubated with anti-α-gal or isotype matched control anti-DNP mAbs (150 μg/ml in 20-50 μl; 60 min; 4°C). Plasma from C57BL/6 mice (1:5 in 20-50 μl 0.1% gelatin in VB^{2+} buffer; Lonza) was added (60 min.; 37°C) as a source of complement and sporozoites were immediately transferred onto HepG2 cells at a 1:4 parasite/cell ratio. Cocultures were incubated (120 min; 37°C) with Tetramethylrhodamine-Dextran (10,000 MW, 1:1; 2 mg/ml; Molecular Probes), washed (2X; PBS) and trypsinized (30-50 μl; 0.05% Trypsin-EDTA (1X), phenol red (GIBCO). Percentage of wounded and parasite-invaded cells was determined by flow cytometry analysis (FACScan, BD Biosciences), gating on FL1 (GFP; invasion) and FL2 (Dextran-Red; wounding). Sporozoite maturation was determined by quantifying the number of EEFs per field and EEF area after 40 hr coculture in 15 μ-Slide 8 well (ibiTreat; IBIDI; Germany) using fluorescence microscopy (Screening Microscopy; Nikon Eclipse TE2000-S). Images were obtained at 20x magnification. Pictures were analyzed using Image J software (NIH).

PMN Cell Depletion

Anti-Gr1 mAb (Clone: RB6-8C5; RB6-8C5 hybridoma) was produced at the IGC under serum-free conditions using a CELLine (Integra, Switzerland) (Tepper et al., 1992). Neutrophils were depleted in $\alpha 1,3Gt^{-/-}$ mouse by a single intravenous anti-Gr1 mAb injection (250 μg), 48 hr prior to mosquito biting. PMN depletion was confirmed by staining for CD11b-FITC (Integrin α[M] chain, Mac-1 α chain, CR3, BD PharMingen™) and Anti-Gr1-PE (1A8, BD PharMingen™) and analyzed in flow cytometry(Tsiganov et al., 2014) (CyA ADP Analyzer, Beckman Coulter).

Statistical Analysis

All tests (except human cohort studies) were performed using the GraphPad Prism v6.0 (GraphPad Software). Human analyses were performed in R version 3.0.2 (http://www.R-project.org). Ab levels between groups were compared with the Kruskal-Wallis test. The relationship between Ab levels and time to *P. falciparum* infection and febrile malaria was determined by Kaplan-Meier survival analysis and the log-rank test. Age dependent differences in anti-α-gal IgM and IgG antibody concentrations in human serum were determined using nonparametric Mann-Whitney test. Differences in anti-α-gal antibody concentration in mouse serum were determined using nonparametric Kruskal-Wallis test with Dunn's multiple comparison posttest. Incidence of infection was compared using log rank (Mantel-Cox) test. Survival curves were plotted using Kaplan-Meier plot and significant differences among experimental groups were determined using the Log-Rank (Mantel-Cox) test. Data corresponding to relative amount of *Plasmodium* in the skin and liver obtained from qRT-PCR was analyzed using nonparametric Mann–Whitney test. Cytotoxic effect of anti-α-gal antibodies was analyzed using repeated-measures ANOVA followed by Tukey's multiple comparison posttest. A p value equal to or below 0.05 was considered statistically significant.

SUPPLEMENTAL REFERENCES

Circolo, A., Garnier, G., Fukuda, W., Wang, X., Hidvegi, T., Szalai, A.J., Briles, D.E., Volanakis, J.E., Wetsel, R.A., and Colten, H.R. (1999). Genetic disruption of the murine complement C3 promoter region generates deficient mice with extrahepatic expression of C3 mRNA. Immunopharmacology *42*, 135–149.

Eto, T., Ichikawa, Y., Nishimura, K., Ando, S., and Yamakawa, T. (1968). Chemistry of lipid of the posthemyolytic residue or stroma of erythrocytes. XVI. Occurrence of ceramide pentasaccharide in the membrane of erythrocytes and reticulocytes of rabbit. J. Biochem. *64*, 205–213.

García-González, M., Bettinger, S., Ott, S., Olivier, P., Kadouche, J., and Pouletty, P. (1988). Purification of murine IgG3 and IgM monoclonal antibodies by euglobulin precipitation. J. Immunol. Methods *111*, 17–23.

Kisailus, E.C., and Kabat, E.A. (1978). A study of the specificity of Bandeiraea simplicifolia lectin I by competitive-binding assay with blood-group substances and with blood-group A and B active and other oligosaccharides. Carbohydr. Res. *67*, 243–255.

LaTemple, D.C., and Galili, U. (1998). Adult and neonatal anti-Gal response in knock-out mice for alpha1,3galactosyltransferase. Xenotransplantation *5*, 191–196.

Matsuzawa, T., and Ikarashi, Y. (1979). Haemolysis of various mammalian erythrocytes in sodium chloride, glucose and phosphate-buffer solutions. Lab. Anim. *13*, 329–331.

Oblinger, J.L., and Koburger, J.A. (1975). Understanding and teaching the most probable number technique. J. Milk Food Technol. *38*, 540–545.

Ono, T., Tadakuma, T., and Rodriguez, A. (2007). Plasmodium yoelii yoelii 17XNL constitutively expressing GFP throughout the life cycle. Exp. Parasitol. *115*, 310–313.

Platteau, B., Ritz, M., Cormont, F., Wauters, D., and Bazin, H. (1990). Production and Characterization of Rat-Rat Hybridomas against the DNP Hapten (Boca Raton, FL: CRC Press).

Shinkel, T.A., Chen, C.G., Salvaris, E., Henion, T.R., Barlow, H., Galili, U., Pearse, M.J., and d'Apice, A.J. (1997). Changes in cell surface glycosylation in alpha1,3-galactosyltransferase knockout and alpha1,2-fucosyltransferase transgenic mice. Transplantation *64*, 197–204.

Spalter, S.H., Kaveri, S.V., Bonnin, E., Mani, J.C., Cartron, J.P., and Kazatchkine, M.D. (1999). Normal human serum contains natural antibodies reactive with autologous ABO blood group antigens. Blood *93*, 4418–4424.

Tepper, R.I., Coffman, R.L., and Leder, P. (1992). An eosinophil-dependent mechanism for the antitumor effect of interleukin-4. Science *257*, 548–551.

Tran, T.M., Li, S., Doumbo, S., Doumtabe, D., Huang, C.Y., Dia, S., Bathily, A., Sangala, J., Kone, Y., Traore, A., et al. (2013). An intensive longitudinal cohort study of Malian children and adults reveals no evidence of acquired immunity to Plasmodium falciparum infection. Clin. Infect. Dis. *57*, 40–47.

Tsiganov, E.N., Verbina, E.M., Radaeva, T.V., Sosunov, V.V., Kosmiadi, G.A., Nikitina, I.Y., and Lyadova, I.V. (2014). Gr-1dimCD11b+ immature myeloid-derived suppressor cells but not neutrophils are markers of lethal tuberculosis infection in mice. J. Immunol. *192*, 4718–4727.

Walliker, D., Quakyi, I.A., Wellems, T.E., McCutchan, T.F., Szarfman, A., London, W.T., Corcoran, L.M., Burkot, T.R., and Carter, R. (1987). Genetic analysis of the human malaria parasite Plasmodium falciparum. Science *236*, 1661–1666.

Yoshida, N., Nussenzweig, R.S., Potocnjak, P., Nussenzweig, V., and Aikawa, M. (1980). Hybridoma produces protective antibodies directed against the sporozoite stage of malaria parasite. Science *207*, 71–73.

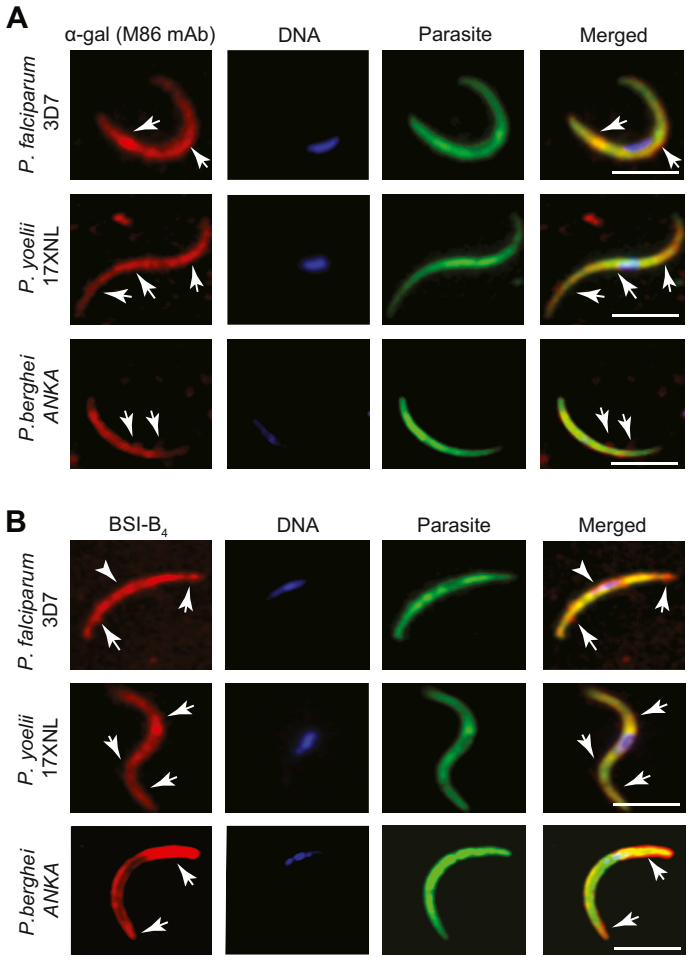

Figure S1. Detection of α-Gal in *Plasmodium* Sporozoites, Related to Figure 1

(A and B) Expression of GFP (*P. berghei* ANKA) and actin (*P. falciparum* 3D7 and *P. yoelli* 17XNL) shown in green, α-gal shown in red and DNA (DAPI) shown in blue. The α-gal epitope was detected with (A) anti-α-gal mAb (M86) or (B) the BSI-B_4 lectin. Representative of 2-3 experiments. Arrows indicate α-gal staining. Scale bar, 5 μm.

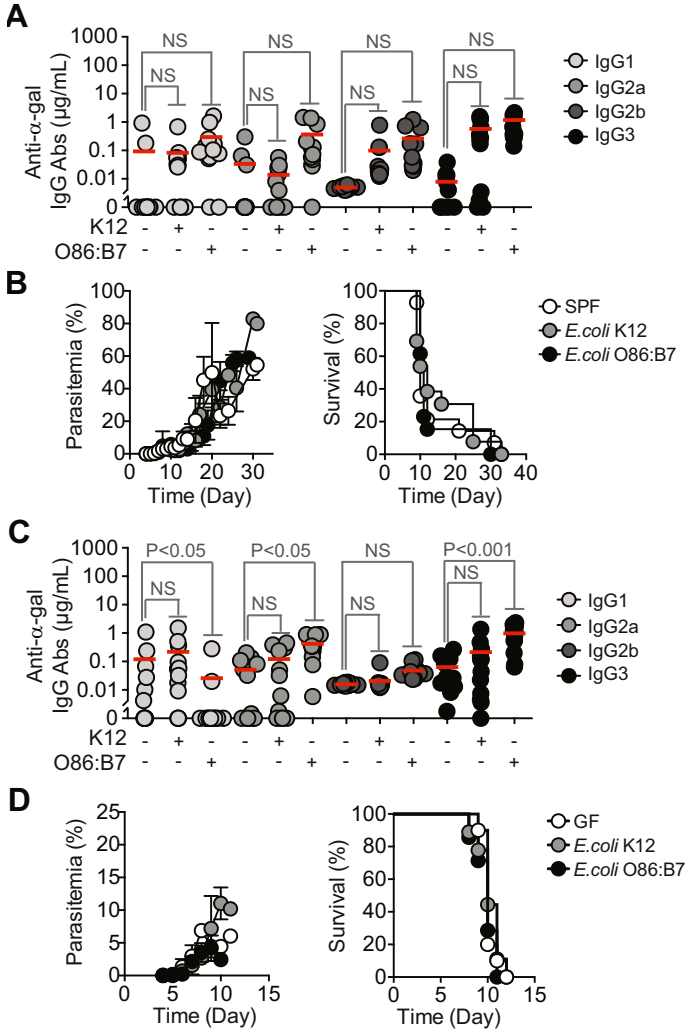

Figure S2. Anti-α-Gal IgG Abs in Gut-Colonized $\alpha 1,3Gt^{-/-}$ Mice and Disease Assessment after Exposure to Infected Mosquitoes, Related to Figure 3

(A) Anti-α-gal IgG subclass Ab levels in $\alpha 1,3Gt^{-/-}$ mice not-colonized (SPF), colonized with *E. coli* K12 or O86.B7 strains after streptomycin treatment (2-3 experiments; n = 12).

(B) Parasitemia (%) and survival (%) in same mice as (A) after exposure to *Pb*A$^{EEF1a\text{-}GFP}$ infected *A. stephensi* mosquitoes (4 experiments; n = 17-34).

(C) Anti-α-gal IgG subclass Ab levels in GF $\alpha 1,3Gt^{-/-}$ mice not colonized (GF), colonized with *E. coli* K12 or O86.B7 strains (2-4 experiments; n = 12).

(D) Parasitemia (%) and survival (%) in same mice as (C) after exposure to *Pb*A$^{EEF1a\text{-}GFP}$ infected *A. stephensi* mosquitoes (4 experiments; n = 7-10 per group). Mean (red bars).

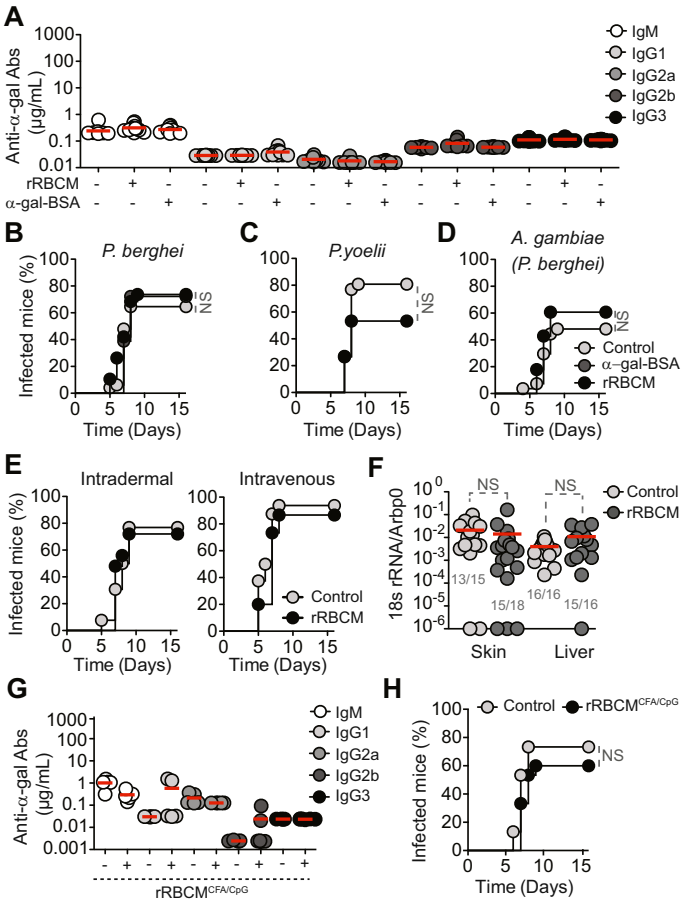

Figure S3. $\alpha 1,3Gt^{+/+}$ Mice Are Not Protected against Malaria Transmission, Related to Figure 4

(A) Anti-α-gal antibodies in the serum of control (-) versus rRBCM (+) or α-gal-BSA (+) immunized $\alpha 1,3Gt^{+/+}$ mice (2-3 experiments; n = 12-16).

(B–D) Incidence of blood stage of infection (%) in $\alpha 1,3Gt^{+/+}$ mice treated as in (A) and exposed to (B) *Pb*A$^{EEF1a\text{-}GFP}$ infected *A. stephensi* mosquitoes (7 experiments; n = 19-48), (C) *P. yoelii* 17XNL infected *A. stephensi* mosquitoes (5 experiments; n = 26-30) or (D) *Pb*A$^{EEF1a\text{-}GFP}$ infected *A. gambiae* mosquitoes (4 experiments; n = 27-28).

(E) Incidence of blood stage of infection (%) in nonimmunized (Control) versus immunized (rRBCM) $\alpha 1,3Gt^{+/+}$ mice receiving *Pb*A$^{EEF1a\text{-}GFP}$ sporozoites (3-4 experiments; n = 15-26).

(F) *Plasmodium* 18 s rRNA/*Arbp0* mRNA in skin and liver of nonimmunized (Control) versus immunized (rRBCM) $\alpha 1,3Gt^{+/+}$ mice exposed to *Pb*A$^{EEF1a\text{-}GFP}$ infected *Anopheles stephensi* mosquitoes (3-5 experiments). Infected/total mice (gray Nbrs).

(G) Same as (A) in control (-) versus immunized (+; rRBCM emulsified in CFA plus CpG) $\alpha 1,3Gt^{+/+}$ mice (2 experiments; n = 5).

(H) Same as (B) in mice treated as in (G) (3 experiments; n = 15). In (A, F and G) dots are individual mice and mean (red bars).

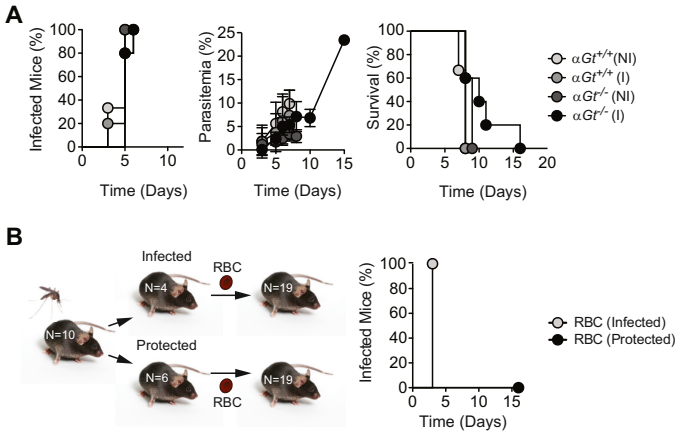

Figure S4. Immunization against α-Gal Is Ineffective in Protecting against Blood Stage of Infection but Confers Sterile Protection against Malaria Transmission, Related to Figure 4

(A) Incidence of blood stage of infection (%; left panel), parasitemia (%; middle panel) and survival (%; right panel) upon inoculation of *Pb*A$^{EEF1a\text{-}GFP}$ infected RBC. Mice were either immunized (I) with rRBCM or not immunized (NI) (One experiment; n = 3-5).

(B) Schematic representation of infection protocol (left panel) and incidence of blood stage of infection (%; right panel) in $\alpha 1,3Gt^{-/-}$ mice transferred with RBC from $\alpha 1,3Gt^{-/-}$ mice infected *Pb*A$^{EEF1a\text{-}GFP}$ or protected from transmission of *Pb*A$^{EEF1a\text{-}GFP}$ infection by *A. stephensi* mosquitoes (2 experiments; n = 19).

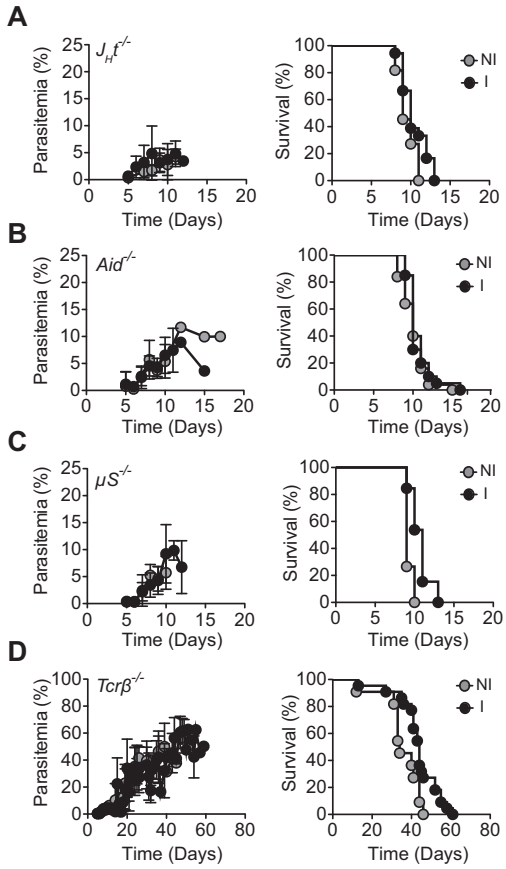

Figure S5. Blood Stage Infection and Lethality, Related to Figure 5

(A–D) Parasitemia (%; left panels) and survival (%; right panels) are shown for infected (A) *α1,3Gt*$^{-/-}$*Jht*$^{-/-}$, (B) *α1,3Gt*$^{-/-}$*Aid*$^{-/-}$, (C) *α1,3Gt*$^{-/-}$*μS*$^{-/-}$ and (D) *α1,3Gt*$^{-/-}$*Tcrβ*$^{-/-}$ mice immunized with rRBCM (I) *vs.* control nonimmunized (NI) (3-7 experiment; n = 11-22).

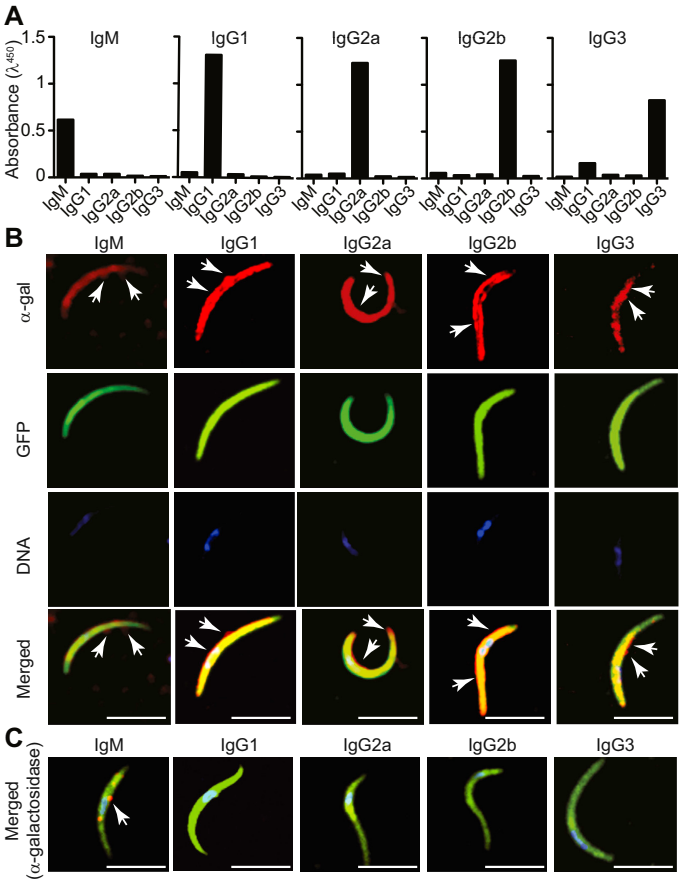

Figure S6. Specificity of Anti-α-Gal mAbs, Related to Figure 5

(A) Comparison of relative binding of anti-α-gal mAbs (125 ng/ml of mAb) determined by ELISA using α-gal-BSA as a solid phase antigen.

(B) Comparison of relative binding capacity of anti-α-gal mAbs (50 μg/ml of mAb) determined by immunofluorescence using *Pb*A$^{EEF1a\text{-}GFP}$ sporozoites as an antigen. mAb (red), GFP (green) and DNA (blue) staining. Merged images show composite of the three staining. Representative of 2-3 experiments.

(C) Similar staining as in (*B*) for *Pb*A$^{EEF1a\text{-}GFP}$ sporozoites treated with α-galactosidase. Composite images are shown with mAb (red), GFP (green) and DNA (blue) staining. White arrows in (B) and (C) indicate binding of different mAb to the α-gal epitope. Scale bar, 5 μm.

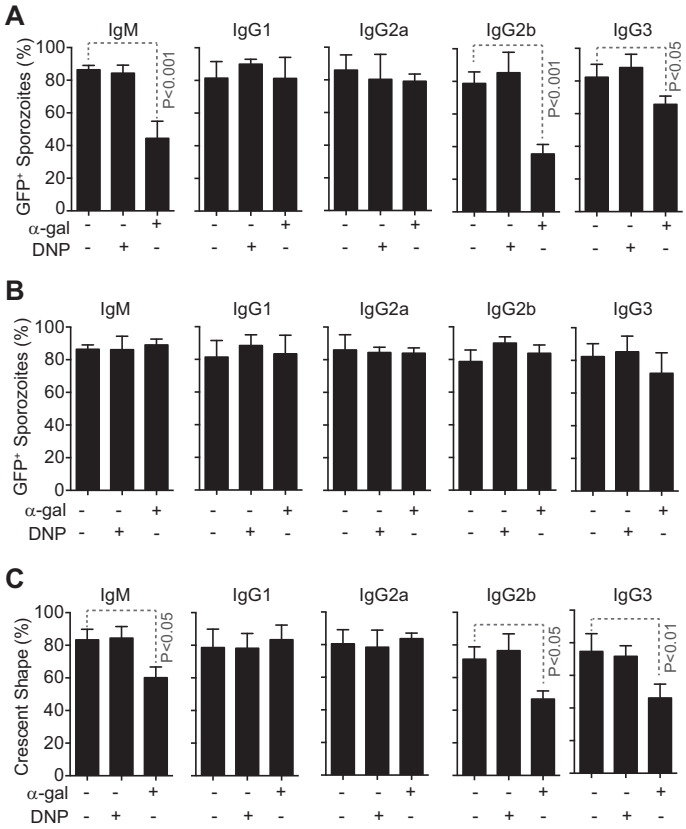

Figure S7. Cytotoxic Effect of Anti-α-Gal Antibodies, Related to Figure 7

(A) Mean percentage (%) of viable GFP$^+$ *Pb*A$^{Hsp70\text{-}GFP}$ sporozoites ± STD (3-4 experiments) after in vitro exposure to anti-α-gal (α-gal) or anti-DNP mAbs in the presence of rabbit complement.

(B) Mean percentage (%) of viable GFP$^+$ *Pb*A$^{Hsp70\text{-}GFP}$ sporozoites ± STD (3-4 experiments) after in vitro exposure to anti-α-gal (α-gal) or anti-DNP mAbs in the absence of complement.

(C) Mean percentage (%) of viable crescent shaped *Pb*A$^{EEF1a\text{-}GFP}$ sporozoites ± STD (3 experiments) after in vitro exposure to anti-α-gal (α-gal) or anti-DNP (DNP) mAb in the presence of mouse complement.